DSPACE

https://dspace.org/

An investigation of Westonaria formation lavas (WAF) and it's influence on the rock engineering design at Goldfield's No.4 (Ya Rona) shaft pillar extraction

Durapraj, Shyandra

2015-04-28
http://hdl.handle.net/10539/17545

Downloaded from a DSpace repository. https://dspace.org/

AN INVESTIGATION OF WESTONARIA FORMATION LAVAS (WAF) AND ITS INFLUENCE ON THE ROCK ENGINEERING DESIGN AT GOLDFIELD'S NO. 4 (YA RONA) SHAFT PILLAR EXTRACTION

Shyandra Durapraj

A research submitted to the Faculty of Engineering and the Built Environment, of the University of the Witwatersrand, in partial fulfilment of the requirements for the degree of Master of Science in Engineering.

February 2015

Johannesburg

DECLARATION

I, Shyandra Durapraj, declare that this research report is my own unaided work. Where use has been made of the work of others, it has been duly acknowledged. It is being submitted for the Master of Science Engineering in the University of the Witwatersrand, Johannesburg. It has not been submitted before in any form for any degree or examination at any other University.

.....

Shyandra Durapraj

19th day of February 2015

Synopsis

Geological complexity has always been a large contributor to instabilities at the mines on the Far West Rand. Part of the problem lies in the unknown nature of many of the rock types and formations that overlie or underlie the conglomerate reef bands within the rockmass. One of these little known rock types is the highly altered Westonaria Formation Lavas (WAF), which has impacted significantly on the stability, production sustainability and the rock engineering designs at many of the mines in the area.

The Ya Rona Shaft Pillar Extraction is one of the mining operations where WAF has determined the course of many interventions. Failure of the WAF has occurred at mines that had not identified it as a potential hazard, which has led to large-scale fall-outs, significant damage to excavations, particularly shafts, and more importantly, operational downtime. Under this risk profile, Ya Rona shaft would not be able to sustain a profitable production profile should failure of the WAF occur.

This research report investigates the WAF rock type, why it poses such a threat to stability, and how it influences rock engineering design where it is encountered. Using the available literature, rockmass rating systems and numerical modelling of the Ya Rona Shaft Pillar Extraction, classification of WAF will be attempted. Moreover, the research report will show what mitigation measures may be required to achieve stability under the WAF conditions, and also provide a guideline for rock engineering design under WAF conditions within a shaft pillar extraction.

Table of Content

1 General introduction 1

1.1. Definition of the problem 3

1.2. Research objectives 4

1.3. Scope and limitations 6

1.4. Facilities 7

1.5. Content of the report 7

1.6. Expectations and conclusions of the report 8

2 Literature review 9

2.1. Introduction 9

2.2. Available literature on 'soft' lava materials 9

2.3. Available literature on the WAF material 10

2.3.1. Case study 1: South Deep SV1 11

2.3.2. Case study 2: Ezulwini Main and Ventilation shafts 15

2.3.3. Case study 3: KDC Kloof Main Shaft 16

2.3.4. Case study 4: KDC West (Driefontein) Ya Rona (4) Sub-Vertical Shaft 17

2.3.4.1. Input data used in the inelastic numerical modelling 18

2.3.4.2. Conclusions from the numerical modelling 19

2.4. WAF – weakness in view of lithostratigraphy and chemical composition 21

2.4.1. WAF lithostratigraphy 21

2.4.2. Mineral composition of WAF 24

2.5. Review of failure criteria and critical conditions for excavations in WAF 26

2.5.1. Ya Rona Sub-Vertical Shaft failure criteria and critical conditions 26

2.5.2. Large displacement regional geological structures failure criterion 28

2.5.3. LOM2012 mining plan failure criteria 28

2.5.3.1. Average Pillar Stress 28

2.5.3.2. Energy Release Rate 29

2.6. Summary and lessons learnt 30

3 Selection of appropriate rockmass rating system/s for WAF 32
3.1. Introduction 32
3.2. Limitations of the Q, RMR and RCF rockmass rating systems 32
3.3. Classification of WAF using available rockmass rating systems 34
3.3.1. Data used in the classification 34
3.3.2. Rockmass rating of WAF 36
3.4. Selection of the most appropriate system/s for the WAF 37

4 Consolidation of the WAF rockmass data and the selection of input parameters for numerical modelling 39
4.1. Introduction 39
4.2. The consolidation of WAF data for use in the numerical modelling 39
4.2.1. Stress regime at Ya Rona Shaft Pillar 40
4.2.2. WAF strength data 42
4.2.3. The calibration of Young's Modulus for use in the elastic modeling 46
4.2.4. Rock test data 48
4.2.5. Geological structures 49
4.3. Selection of input parameters for the numerical modeling 53

5 The effect of WAF in the numerical modeling 55
5.1. Introduction 55
5.2. Objectives of the numerical models 56
5.3. Overview of the numerical models 56
5.3.1. The BesolMS model 57
5.3.2. The 3DEC model 60
5.4. Stability assessments 62
5.5.1. Shaft stability assessment 63
5.5.1.1. Stress imposed on the shaft 63
5.5.1.2. Vertical and horizontal displacement of the shaft 65
5.5.1.2.1. Vertical displacement 66
5.5.1.2.2. Horizontal displacement 68
5.5.1.3. Ride in stoping excavations near the shaft 70
5.5.1.4. Rockwall Condition Factor (RCF) 74

5.5.1.5. Concluding remarks on the shaft barrel stability 75
5.5.2. Large displacement regional geological structures' assessment 75
5.5.2.1. Calibration of ESS with respect to different Young's Moduli 76
5.5.2.2. ESS analyses of the geological structures 77
5.5.2.2.1. ESS assessment of the Syncline Axis 79
5.5.2.2.2. ESS assessment of Kate's Fault 80
5.5.2.2.3. ESS assessment of Murray Fault 81
5.5.2.2.4. ESS assessment of Smith Fault 82
5.5.2.2.5. ESS assessment of Shane's Fault 83
5.5.3. LOM12 mining plan assessment 84
5.5.3.1. Regional Stability Pillar assessment 85
5.5.3.1.1. Calibration of the model to show the effect that WAF has on APS 85
5.5.3.1.2. Pillar XX APS assessment 86
5.5.3.1.3. Pillar ZZ APS assessment 87
5.5.3.2. Energy Release Rate (ERR) 88
5.6. Conclusions with regard to the WAF influence in the numerical models 89
5.7. Revised mining layout using WAF properties 90
5.7.1. Change in Vertical and Radial cumulative closure at Shaft Barrel 90
5.7.2. Change in ride at the Shaft 94
5.7.3. Change in RCF 94
5.7.4. Change in ESS of the Syncline Axis and Murray Fault 95
5.7.5. Change in Average Pillar Stress 96
5.7.6. Change in ERR 99
5.8. Conclusions from the optimized mining sequence 100

6 Mitigation strategies to reduce the impact of WAF 101
6.1. Introduction 101
6.2. Instrumentation and monitoring 101
6.3. Current WAF mitigation strategies to reduce the impact of WAF 105
6.3.1. Ya Rona Shaft WAF mitigation strategy 106
6.3.1.1. The Alberton Lava Zone (ALZ) 107

6.3.1.2. The WAF Zone (WZ) 108
6.3.1.3. The Shale WAF Zone (SWZ) 109
6.3.1.4. The Shale Zone (SZ) 111
6.3.1.5. The siting of the inner pillar extraction in the footwall 111
6.3.2. The Syncline Axis mitigation strategy 112
6.3.3. The Murray Fault mitigation strategy 112
6.3.4. WAF mitigation strategies in the stoping horizon 113
6.3.4.1. Closure assessments 113
6.3.4.2. Backfill selection 114
6.3.4.3. Pre-stressed Elongates and Pack considerations 115
6.3.4.4. Rock Consolidation 116
6.3.4.5. Proposed Mining Guidelines in WAF 117
6.3.4.5.1. Mining Sequence and Extraction Rate in WAF 117
6.3.4.5.2. Wide-Raising as opposed to Raise Development 119
6.3.5. Regional stability 120

7 **Guidelines and Conclusions** 121
7.1. A guideline for mining under WAF conditions in a Shaft Pillar Extraction 124
7.2. Conclusions from the research 123
7.2.1. The WAF ‘understood’ 123
7.2.2. Numerical modeling – toward understanding the input parameters for modeling of the WAF rockmass 124
7.2.3. Shaft Pillar Extraction Design Revision 125
7.2.4. WAF mitigation 125
7.3. Concluding remarks 126

8 **Recommendations for further research** 127

References 128

Appendices 134

Appendix A – Rockmass Rating 134

Appendix B – WAF Rock Test and Rock Fracture Data 153

Appendix C – Support Units' Data 159

List of Figures

Chapter 1

Figure 1-1 Location of KDCWest (formally known as Driefontein Gold Mine, Gold Fields Mining South Africa)

Figure 1-2 Gold Fields Limited: KDCWest (Driefontein Division) GME plan showing the location of the various shafts

Figure 1-3 Simplified cross section showing location of shafts relative to the conglomerate reef bands (KDCWest, 2012)

Figure 1-4 Geological model showing position of shaft relative to Syncline Axis, and multiple faulted blocks (Durapraj, et al, 2005)

Chapter 2

Figure 2-1 Closure profiles for low and high strength rock materials at a remnant mining stope within a Klerksdorp gold mine (Rangasamy, et al, 2003)

Figure 2-2 Diagram of South Deep SV1 failure in WAF (Petho, et al, 2004)

Figure 2-3 Plan of South Deep SV1 extent of failure as well as potential zone (red) of failure (edited from Petho, et al, 2004)

Figure 2-4 South Deep SV1 barrel movement as a function of time (Petho, et al, 2004)

Figure 2-5 Isometric sketch of the 3DEC numerical model showing the location of the shaft relative to large geological structures (Leach, 2006)

Figure 2-6 FLAC3D model showing barrel sidewall failure modes using strong WAF properties (edited from Leach, 2006)

Figure 2-7 FLAC3D model showing barrel sidewall failure modes using weak WAF properties (edited from Leach, 2006)

Figure 2-8 Section of WAF zone mineralogy at South Deep SV1 (Rangasamy, et al, 2006)

Figure 2-9 Graphical representation of rock types immediately overlying the VCR conglomerate reef (edited from KDCWest, 2012)

Figure 2-10 Section looking east and plan view of Ya Rona Sub-Vertical Shaft during the development phase showing WAF intersection (edited from Castelyn, et al, 2007)

Figure 2-11 Photograph showing multiple planes of weakness and shearing of the WAF rockmass

Figure 2-12 Photograph in stope showing WAF laminations

Chapter 3

Figure 3-1 N-S (J1) and E-W (J2) joint directions at Ya Rona sub-vertical shaft (Durapraj, 2006b)

Figure 3-2 Photograph, looking east, showing 3rd joint set at Ya Rona sub-vertical shaft (Durapraj, 2006b)

Chapter 4

Figure 4-1 Simulation process in numerical modelling (Karabin, et al, 1999)

Figure 4-2 Measured in-situ stress profile at Ya Rona shaft showing k-ratio profile (Leach, 2006)

Figure 4-3 Orientation of stresses relative to the Ya Rona shaft barrel and reef dip (Leach, 2006)

Figure 4-4 Drill core from Alberton Lava hangingwall geotechnical hole at Ya Rona

Figure 4-5 Drill core from WAF hangingwall geotechnical hole at Ya Rona shaft

Figure 4-6 Figure 4-6 Graphical representation of WAF strength under increasing confinement at Ya Rona shaft (compilation of data from Appendix B, Table B-1 (Yilmaz, 2006); and Table 4-1 (Van der Heever, 2007))

Figure 4-7 Comparison between actual and modelled convergences for different values of Young's Modulus (after Van der Heever, 2007)

Figure 4-8 Comparison between measured closure and modelled convergences for different values of Young's Modulus (after Van der Heever, 2007)

Figure 4-9 CadsMine plan showing location of geological structures within the shaft pillar at Ya Rona and shaft pillar boundary (yellow solid line)

Figure 4-10 CADSMine isometric view of Ya Rona shaft pillar area (yellow border) showing location of shaft barrel, reef dip and the Syncline Axis

Figure 4-11 Sketch showing folded nature of Syncline Axis (Wilson, 2010)

Figure 4-12 Photograph of the Syncline exposed in the lower parking lot of Calico Ghost Town near Barstow, California (Wilson, 2010)

Chapter 5

Figure 5-1 Besol simulation of mining plan showing the mining steps 1-12

Figure 5-2 Besol simulation of mining plan showing the mining steps 11-15

Figure 5-3 Section, looking north, of 4SV (Ya Rona) shaft excavation showing WAF zones above reef contacts and Murray Fault through shaft barrel

Figure 5-4 Isometric view of the 3DEC numerical modelling showing planes representing geological structures (Leach, 2003)

Figure 5-5 Plan view of mining sequence in the 3DEC numerical modelling (Leach, 2003)
Figure 5-6 Sketch indicating hangingwall and footwall of reef at Ya Rona, as well as Section A-B showing line of analysis for RCF, Vertical and Horizontal displacements at Ya Rona Shaft
Figure 5-7 Vertical stress along the Ya Rona shaft for the unfilled BESOL model
Figure 5-8 Vertical stress along the Ya Rona barrel for unfilled and filled 3DEC models (after Leach, 2003)
Figure 5-9 Plan section of Ya Rona Sub-Vertical Shaft showing true north, X and Y directions (after Leach, 2006)
Figure 5-10 Cumulative closure in the Z-direction as a function of distance to reef through 15 mining steps at Ya Rona shaft barrel
Figure 5-11 Figure 5-11 Sketch showing exaggerated radial displacement of Ya Rona shaft
Figure 5-12 Cumulative closure in the Y-direction as a function of distance to reef
Figure 5-13 Cumulative closure in the X-direction as a function of distance to reef
Figure 5-14 X-and-Y-Ride at the Ya Rona Shaft
Figure 5-15 Displacement in the Y-direction of the Ya Rona shaft for unfilled models (after Leach, 2003)
Figure 5-16 Displacement in the Y-direction of the Ya Rona shaft for filled models (after Leach, 2003)
Figure 5-17 Displacement in the X-direction of the Ya Rona shaft for unfilled models (after Leach, 2003)
Figure 5-18 Displacement in the X-direction of the Ya Rona shaft for filled models (after Leach, 2003)
Figure 5-19 Plot of RCF as a function of distance from reef at the Ya Rona Sub-vertical shaft through 15 mining steps
Figure 5-20 Comparison of ESS value using 70GPa and 20GPa Young's Modulus at steps 1 and 12 of the BesolMS numerical model at the Syncline Axis
Figure 5-21 Plan view of the modelled geological features showing positions at which ESS data of faulting was analysed for the Ya Rona SV Pillar Extraction
Figure 5-22 Isometric view of the modelled plane views of geological features at the Ya Rona SV Pillar Extraction
Figure 5-23 Plot of Kate's Fault ESS value (section C-D) as a function of distance from reef over 15 mining steps

Figure 5-24 Plot of Murray Fault ESS value (section E-F) as a function of distance from reef over 15 mining steps
Figure 5-25 Plot of Smith Fault ESS value (section G-H) as a function of distance from reef over 15 mining steps
Figure 5-26 Plot of Shane's Fault ESS value (section J-K) as a function of distance from reef over 15 mining steps
Figure 5-27 Besol MSPrep model showing the regional stability pillars (XX and ZZ) with the sections N-P and R-S used for pillar analysis
Figure 5-28 Graph showing APS of Pillar XX (Figure 5-27, section N-P)
Figure 5-29 Graph showing APS of Pillar ZZ (Figure 5-27, section R-S)
Figure 5-30 ERR Plot of mining blocks over time at Ya Rona pillar extraction
Figure 5-31 Revised Besol simulation of mining plan showing the mining steps 1-12
Figure 5-32 Revised Besol simulation of mining plan showing the mining steps 13-15
Figure 5-33 Revised Model: Cumulative Vertical Displacement of Block A showing the superimposed shaft
Figure 5-34 Revised Model: Ya Rona Shaft Cumulative Y-Direction displacement
Figure 5-35 Current vs Revised Model: X-and-Y-Ride plot at the Ya Rona Shaft
Figure 5-36 Revised Model: Syncline Axis ESS as a function of distance from the reef plane
Figure 5-37 Revised Model: Murray Fault ESS as a function of distance from reef plane
Figure 5-38 Pillar Stress vs Pillar Strength Criteria at final stage of mining of Pillar 1
Figure 5-39 Pillar Stress vs Pillar Strength Criteria at final stage of mining of Pillar 2
Figure 5-40 Pillar Stress vs Pillar Strength Criteria at final stage of mining of Pillar 3
Figure 5-41 Pillar Stress vs Pillar Strength Criteria at final stage of mining of Pillar 4
Figure 5-42 ERR Plot of revised mining sequence at Ya Rona pillar extraction

Chapter 6

Figure 6-1 Section of Ya Rona shaft showing planned network of geotechnical instruments
Figure 6-2 Collage of photographs (from left – multipoint rod extensometer, calcification of rod extensometer, laser sight, wire extensometer) showing the geotechnical monitoring instruments installed at Ya Rona shaft
Figure 6-3 East laser plot of cumulative deformation over time (2007-2013) at Ya Rona shaft
Figure 6-4 Section of Ya Rona shaft and photographs showing theodolite multipoint survey instruments and prisms installed in 2009 at Ya Rona shaft

Figure 6-5 East and West lasers' plot of cumulative deformation over time (2009-2013) at the Ya Rona Sub-Vertical shaft showing WAF creep behaviour
Figure 6-6 Graphical representation showing the Murray Fault wedge, the two WAF intersections and the zones of potential failure in the Ya Rona Shaft
Figure 6-7 Graphical representation of SP1 standard at Ya Rona SV (amended from Durapraj, 2002)
Figure 6-8 Graphical representation of SP2 standard at Ya Rona SV (amended from Durapraj, 2002)
Figure 6-9 Photographs showing comparison of fracture angle for concrete lining and rock specimen (Durapraj, 2007)
Figure 6-10 Graphical representation of SP3 standard at Ya Rona SV (amended from Durapraj, 2002)
Figure 6-11 Plan (simulation) and section (stoping footwall slot) views of the inner pillar extraction at the Ya Rona Sub-Vertical shaft
Figure 6-12 Photograph showing multiple failure surfaces of WAF which resulted in a significant fall of ground
Figure 6-13 Graph of roof span vs Stand-up Time for WAF using Q
Figure 6-14 Modelled mining sequence at Ya Rona Shaft pillar extraction (Tkloweni, 2007)
Figure 6-15 Photograph showing a development raise with WAF hangingwall before the production blast
Figure 6-16 Photograph showing the same development raise in figure 6-15 after the production blast
Figure 6-17 Photograph showing tensile crack failure after the ledging blast in the raise featured in figure 6-15

Chapter 7

Figure 7-1 Design process methodology when mining WAF in a Shaft Pillar Extraction at depth

List of Tables

Table 2-1 Comparison of major input data for numerical modelling (Leach, 2006)

Table 2-2 WAF zone mineralogy at South Deep SV1 (Rangasamy, et al, 2006)

Table 2-3 Failure criteria for the shaft (edited from Tkloweni, 2007)

Table 2-4 Failure criteria for analyses of mining layouts and geological formations

Table 4-1 Summary of WAF raw geotechnical data from different sources (edited from van der Heever, 2007 - (a & c) Petho, et al, 2004; (b) Durapraj, 2006; Leach, 2006; (d) Ortlepp, et al, 2008; (e) van der Heever, 2007)

Table 4-2 Comment on input parameters for WAF as summarised in table 4-1

Table 4-3 List of major geological structures within the Ya Rona shaft pillar (KDCWest, 2012)

Table 4-4 List of rockmass stress and material properties used as input parameters in the Ya Rona shaft pillar numerical model

Table 5-1 Input parameters used in the 3DEC model (Leach, 2003; Tkloweni, 2007)

Table 5-4 LOM12 ERR values for mining blocks over the 15 mining steps

Table 5-5 ERR values for optimised mining sequence over the 15 mining steps

Table 6-1 Zones of weakness at the Ya Rona Sub-Vertical Shaft Barrel

Table 6-2 Comparison of closures modeled in LOM12 and Optimized plan for Ya Rona Shaft Pillar Extraction

List of Abbreviations

ΔA	Change in Area (used to quantify area being enlarged by mining)
ΔV	Change in Volume (used in volumetric convergence)
σ_{cr}	Critical strength
E	Young's Modulus
F	F-factor used in the RCF equation to indicate the quality of the rockmass
G	Shear Modulus
υ	Poisson's Ratio

ALZ	Alberton Lava Zone
AMMSA	Association of Mine Managers of South Africa
APS	Average Pillar Stress
BLOI	Bottom Line of Intersection
B.S.	Below Surface
CLR	Carbon Leader Reef
COP	Code of Practice
DZ	Closure in the Z-direction
ERR	Energy Release Rate – typically measured in MJ/m^2
ESS	Excess Shear Stress – measured in MPa
et al	Denotes additional authors
E-W	East-West
Exto.	Extensometer
EZZ	Strain in the Z-direction
FOS	Factor of Safety
GSI	Geological Strength Index
KDCEast	Kloof-Driefontein East, also known as Kloof Gold Mine
KDCWest	Kloof-Driefontein West, also known as Driefontein Gold Mine
LOM12	KDCWest C2012 Life of Mine Extraction Sequence
LVDT	Linear Variable Displacement Transformer
M_{max}	Maximum Magnitude
MRMR	Mining Rock Mass Rating
MVR	Middelvlei Reef

N	North
N-S	North-South
PW	Pull wire extensometers
RCF	Rock Condition Factor
RMR	Rock Mass Rating
RQD	Rock Quality Designation
SBDS	Shaft Barrel Deformation System
SP1	Support Procedure 1
SP2	Support Procedure 2
SP3	Support Procedure 3
SP4	Support Procedure 4
SRP	Seismic Response to Production
SV	Sub-Vertical
SV1	Sub-Vertical 1
SWZ	Shale WAF Zone
SZ	Shale Zone
TLOI	Top Line of Intersection
Tuff	Tuffaceous Lava
TXX	Minor Stress acting in the Y-plane
TYY	Minor Stress acting in the Y-plane
TZZ	Major Stress perpendicular (Z-direction) to the reef plane
UCS	Uniaxial Compressive Strength
VCR	Ventersdorp Contact Reef
WAF	Westonaria Formation Lavas
W:H	Width to Height ratio
WZ	WAF Zone
X	X direction
Y	Y direction
Z	Z direction

Units of Measure - Abbreviations

kPa	kiloPascals	mm	millimetre
MPa	MegaPascals	kg/m^3	kilogram per cubic metre
GPa	GigaPascals	hrs	hours
m^2/km^2	square metre per square kilometre	MJ/m^2	MegaJoules/square metre
km	kilometre	kN	kiloNewton
m	metre	^{0}	degree
%	percent		

Chemical Element - Abbreviations

Ca	Calcium	Si	Silicon
C	Carbon	H	Hydrogen
O	Oxygen	Fe	Iron
Mg	Magnesium		

Acknowledgements

The author would like to acknowledge the contributions of the following persons and companies in the compilation of this research report:

Dr. H. Yilmaz – Supervisor, Project Mentor and Senior Lecturer at University of Witwatersrand.
Dr. B.P. Watson – External Supervisor, Motivator and Chief Rock Engineer at South Deep Mine: Goldfields International: South African region.
Dr. D.F. Malan – Mentor and Senior Rock Engineering Consultant: Goldfields International: South Africa Region.
Mr. F.J. Castelyn – Rock Engineering Manager (retired).
Mr. G.A. Wienand – Rock Engineering Manager: Goldfields.
Mr. P. S. Piper – Managing Director, Groundwork Consulting (Pty) Ltd.
The rock engineering design team, management and staff at Ya Rona shaft for their contribution to the research including ***Mr. B. Du Plessis and Mr. L. Louw***.
The senior management team at KDC West including ***Mr. J.J. Barnard***.
The senior leadership staff, especially ***Mr. V.P. Pillay***, at Goldfields International Mining: South African Operations: Head Office, for affording me the opportunity to present this work.

Special thanks go to my wife and my son for their continued support.

For my dog

Cody

1. General introduction

The Kloof-Driefontein West Complex (KDCWest Gold Mine), formally known as Driefontein Gold Mine (Figure 1-1), is located approximately 10 km south of the town of Westonaria, 2km east of Carletonville and 60km west of Johannesburg, in the province of Gauteng, South Africa.

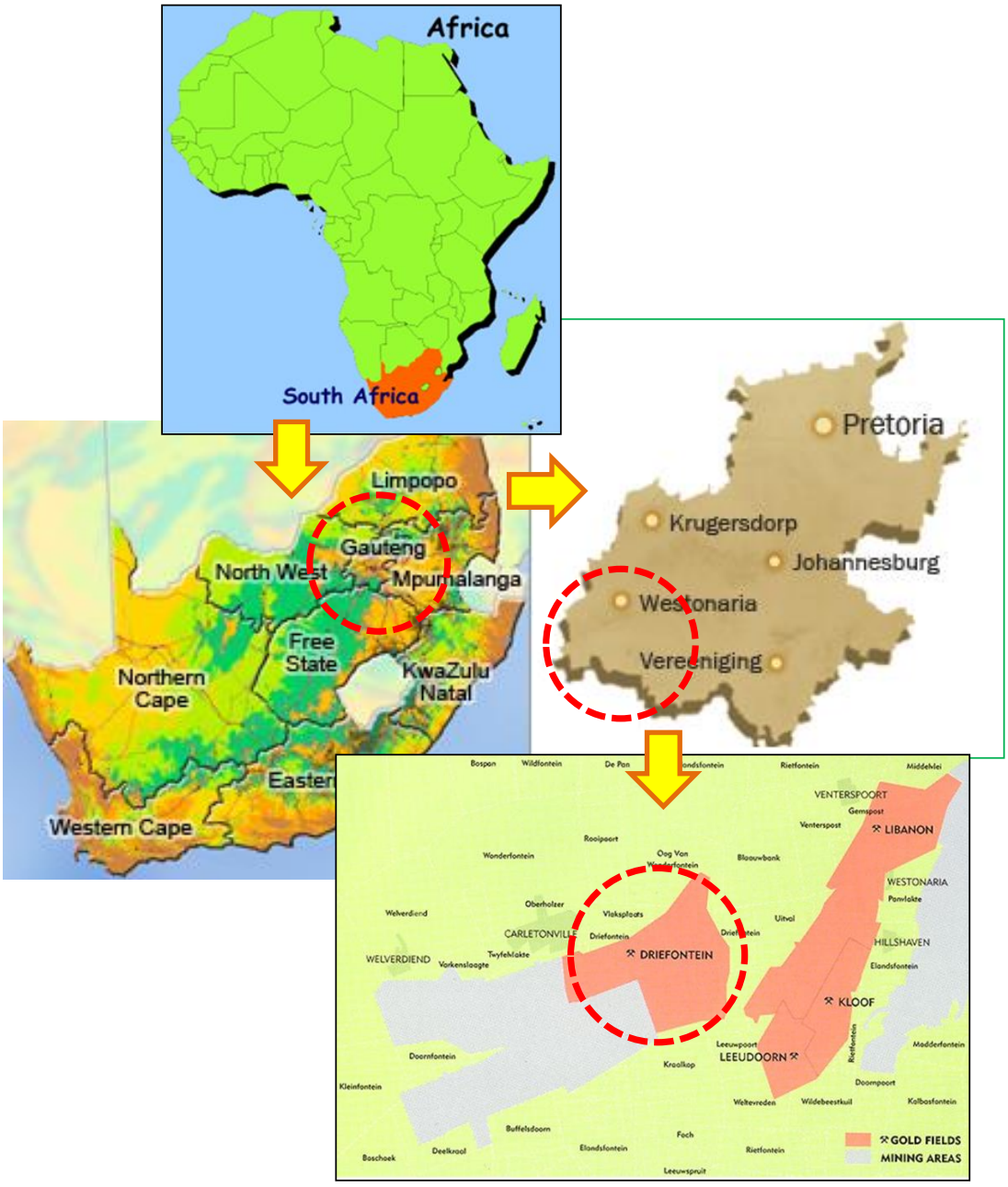


Figure 1-1 Location of KDCWest (formally known as Driefontein Gold Mine, Gold Fields Mining South Africa)

Nine shaft systems (Figure 1-2) are operational within the Driefontein mining lease area. These exploit three reef bands. They are the Ventersdorp Contact Reef (VCR), the Middelvlei Reef (MVR) and the Carbon Leader Reef (CLR). The vertical distance, or middling, between these conglomerates vary from 0m at the sub-crops, to a maximum of 100m. Apart from the depositional aspects of each type of conglomerate, each has unique geophysical characteristics, one of which is variable reef dip. These range from 10^0 to 70^0 and are often combined in undulating layers with variations in reef strike. The rockmass, that incorporate these reef packages, is further broken up by large displacement faults and dykes, which typically impact on the ability to mine the ore reserve successfully.

Toward the eastern limb of the Driefontein lease area, lies the Ya Rona Shaft system (Figure 1-2). All analyses, described in this research report, prior to the year 2010, will reflect the 4 Shaft nomenclature, rather than the current name of Ya Rona Shaft. The complex consists of two shaft systems, namely, the Ya Rona Main Shaft, and the Ya Rona (4) Sub-Vertical Shaft (Figure 1-3), which extends vertically from 1784m to 2897m below surface.

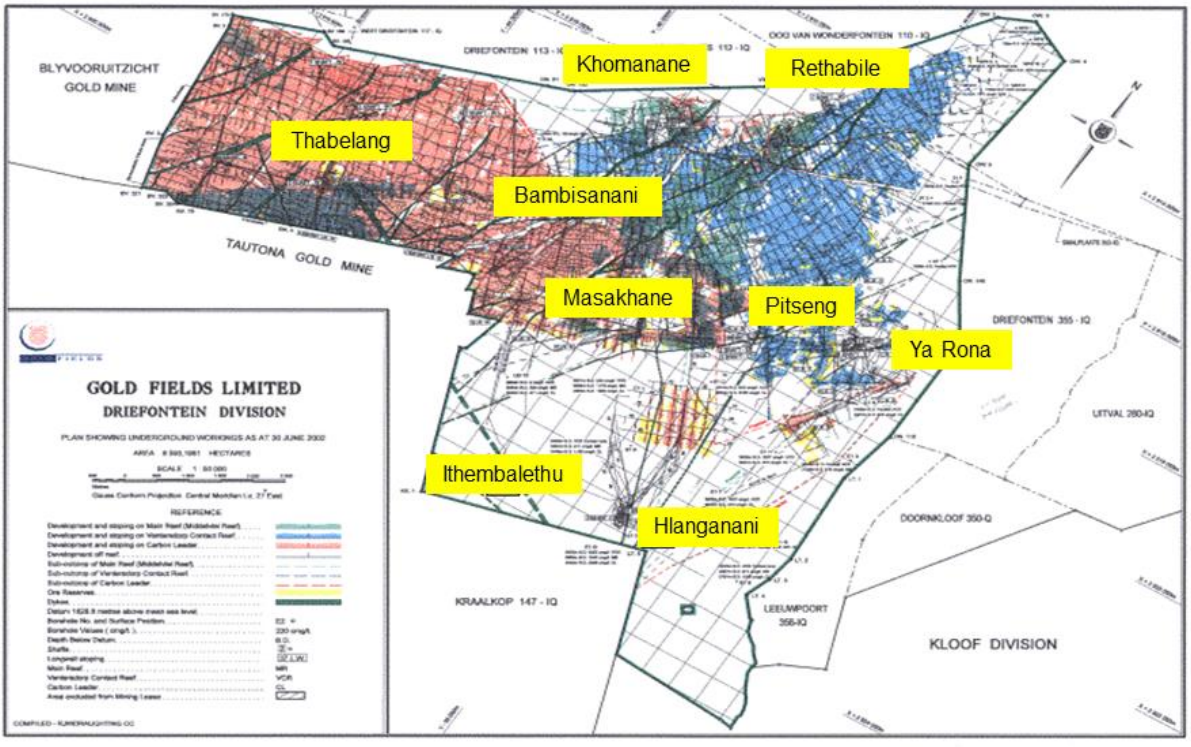


Figure 1-2 Gold Fields Limited: KDCWest (Driefontein Division) GME plan showing the location of the various shafts

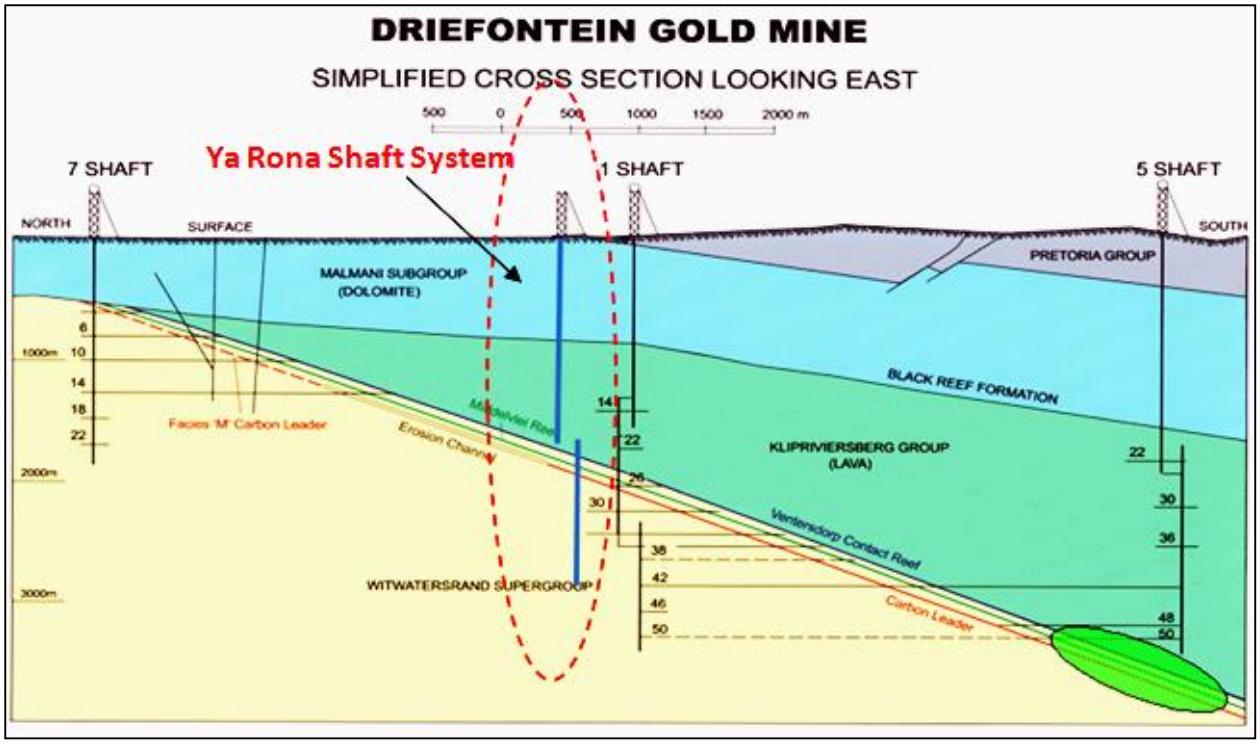


Figure 1-3 Simplified cross section showing location of shafts relative to the conglomerate reef bands (KDCWest, 2012)

1.1. Definition of the problem

Since 1998, Ya Rona has been preparing and executing aspects of the shaft pillar extraction at depths between 2237m and 2485m below surface. Geological complexity (Figure 1-4) has always been a large contributor to instability at this operation. Through extensive literature reviews and geological drilling programmes, the interpretation of these structures, have been enhanced. Paradoxically, however, as the re-interpretation continued, revisions to the shaft pillar extraction strategy became necessary, which raised more concerns about stability within the shaft pillar extraction.

On a regional scale, the rock engineering design process had to take into account that the mining had to occur within a rockmass which included large blocks of ground truncated by major geological weaknesses, reef planes with different strike and dip orientations, and a rockmass impaled with multiple joint and fracture planes. On a local scale, the design had to consider the presence of a weak, highly altered, Westonaria Formation Lava (WAF), which directly overlay the high value VCR conglomerate within the shaft pillar extraction. WAF has proven to be a significant contributor to instability, posing an

immediate risk to shaft barrel stability, as well as a medium to long term risk to continued ore extraction within the stoping environment. The presence of this layer poses a significant risk to mining operations, and is, therefore, the primary focus and subject of this research report.

In this context, the impact and contribution of WAF, to the rock engineering design, within the Ya Rona Shaft Pillar Extraction, needs to be clearly understood.

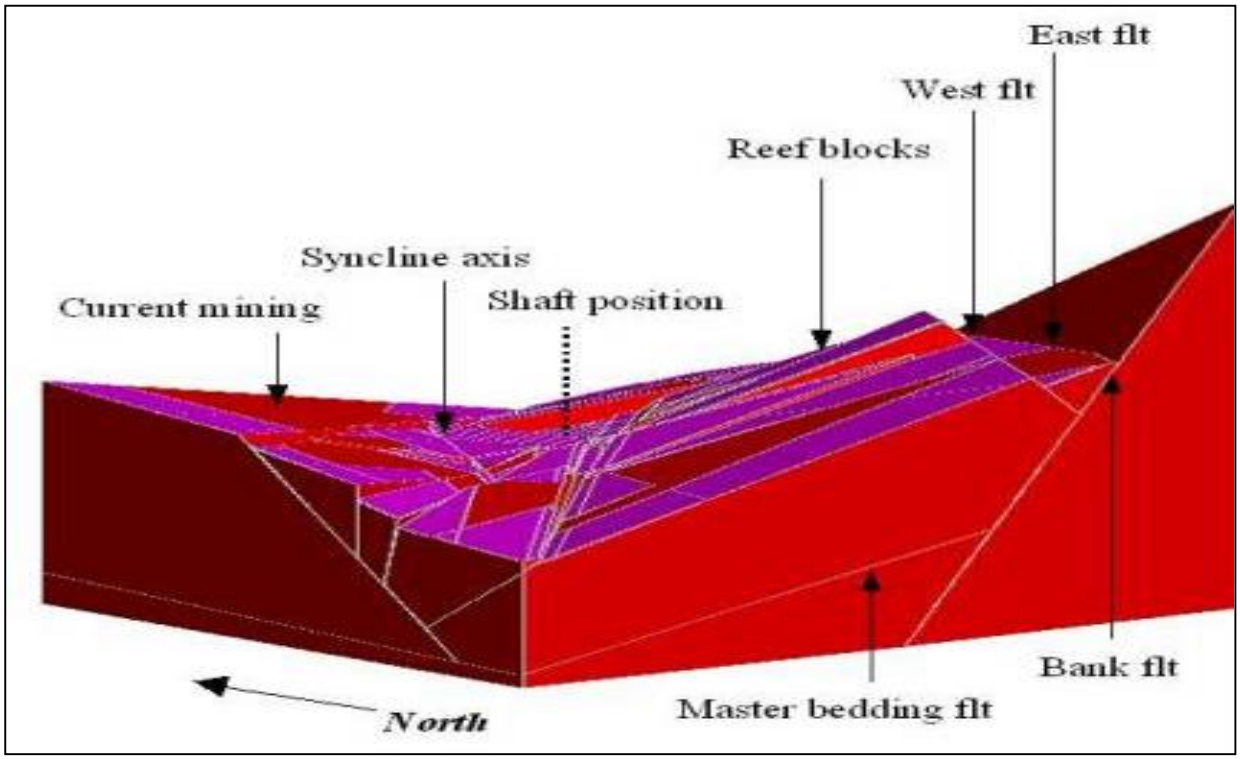


Figure 1-4 Geological model showing position of shaft relative to Syncline Axis, and multiple faulted blocks (Durapraj, et al, 2005)

1.2. Research objectives

As there were no significant failures of WAF prior to 2005, specific research and literature on the subject, prior to that time, is limited. However, early in 2004, a significant event in the history of WAF occurred. The incident involved catastrophic failure of a large portion of the sidewall of the ventilation shaft at the South Deep Gold Mine (SV1 Shaft). The failure damaged the shaft infrastructure, rendering the shaft unusable. This episode was a turning point in the understanding of WAF, more so with regard to the mitigation strategies that had to be explored when WAF is encountered.

Prior to this failure, a conventional approach to shaft pillar extraction design was followed by the rock engineering team at the Ya Rona Pillar Extraction. The SV1 failure impacted on both the timeline and the financing of the additional WAF mitigation measures at Ya Rona shaft. Where the South Deep accident occurred at a ventilation shaft, which serviced mining operations further away from the shaft, and consequently, did not impact directly on the mining production, the Ya Rona Shaft case occurs within an operational shaft system, where primary production activities access the ore reserve. In this context, the understanding of WAF, and the WAF relationship to the stability of the Ya Rona Sub-Vertical Shaft system, is critical to both the design and the extraction process.

The primary objective of this research report is to establish how the WAF has contributed to the rock engineering design at the Ya Rona Shaft Pillar Extraction. Only the behaviour and impact of WAF on the design will be the primary consideration for this research report. To achieve the objective:

- WAF rockmass properties are investigated;
- The available WAF literature is perused and analysed;
- Rock test data and rockmass monitoring information is interrogated;
- Rock engineering design tools including numerical modelling techniques, rockmass rating systems and rock engineering risk assessment processes are used to simulate mining sequences using good quality rockmass input data as well as WAF case study data;
- The numerical models are calibrated using underground observations to compare what aspects of the numerical model are similar to the in-situ WAF rockmass characteristics – the back analysis approach;
- Results from the WAF numerical modelling are used to quantify the risks to the shaft, geological structures and mining sequences using information from both elastic and inelastic numerical models; and,
- Improvements to the rock engineering design, and strategies thereto, are then tabled.

Although the WAF information has been instrumental in determining the guidelines for mine design and shaft stability at the Ya Rona Pillar Extraction in the past, the application of the interrogated WAF data to the process of selection has not been previously rigorously applied. This research report outlines the application of this technique to the current mine layout, with

a view to establishing areas within the design which have a significant hazard, and high instability risk potential. It is envisaged that these risks could be mitigated, having being identified, through the rigorous application of the WAF information, in the rock engineering design process.

1.3. Scope and limitations

Any shaft pillar extraction has many rock engineering design elements, each of which have a particular bearing on the implementation phase of such extraction. However, all of these aspects cannot be discussed as part of the scope of the study. Therefore, the research report will only establish how the behaviour of the WAF contributes to the rock engineering design process.

Another limitation relates to the way in which the numerical modelling is conducted. The elastic modelling codes are used to simulate the pseudo-plastic behaviour of WAF. Although the research report will show how this is done, the simulation will only suggest areas of potential risk using WAF as the driving factor. These focal points could then be further articulated using an inelastic code. Although 3DEC numerical modelling had been completed for specific areas, the intention in this research report was to provide a platform for future inelastic numerical modelling.

Moreover, input parameters for the numerical models are based on the test data procured from small scale intact rock. Even though downgrading of the data is required to replicate the in-situ conditions, the degree to which this downgrade is valid and acceptable, is often subjective.

Although the rock engineering design process presented a case to limit the consequential effects of the dynamic ground motion of WAF by using backfill, in-depth analyses of this strategy is not undertaken. Moreover explicit data with regard to the seismic catalogue at Ya Rona Shaft is not analysed in this report as it would detract from the focus of thereof.

1.4. Facilities

In addition to the research material, the primary resource utilised to simulate the mining layouts in the research is the use of the numerical modelling code BesolMS which is a suite of programs used by rock engineering practitioners to quantify stress and deformation in tabular mining environments. It is particularly suited to deep level mining environments of which Ya Rona is an example. Information was also used from the inelastic code 3DEC to provide inelastic data and simulate those aspects that the BesolMS numerical model could not.

Data gathered from monitoring devices operational at Ya Rona shaft, was used to quantify actual deformation in excavations containing WAF. Underground investigations also provided information on stope closure and WAF rockmass deformation.

1.5. Content of the report

The initial chapter reviews some soft lava rock geotechnical literature before exploring the current available WAF case studies. Thereafter, in chapter three, WAF rock strength data is used in rockmass rating systems to provide a range of values that are used in chapter four as input parameters into the numerical models. The association of WAF to geological complexity within the Ya Rona shaft pillar extraction is outlined in chapter four.

Chapter five focuses on the impact of WAF in the numerical modelling and how the numerical modelling data has contributed to the rock engineering design. Results obtained from the numerical model for the geological features, the shaft barrel and the mining sequence are discussed. The chapter plays a pivotal role in that it provides insight as to whether the WAF rockmass can promote the stability within the mining plan and what mitigation measures, including changes in the rock engineering design, which may be required to address the identified hazards.

Chapter six outlines the mitigation measures introduced at the Ya Rona shaft pillar extraction, through the rock engineering design process, to reduce the impact of WAF. The research report is concluded, in chapter seven, with a design process methodology when mining WAF

in a shaft pillar extraction. A guideline is provided outlining what key aspects need to be considered when mining in WAF.

1.6. Expectations and conclusions of the report

The benefits of this research report extend to ensuring that the unique geotechnical characteristics of the WAF are outlined, that potential areas of improvement when conducting numerical modeling are understood, and that the timeous mitigation strategies, required to limit the consequences of instability, become industry accepted practice. Since shaft pillar extractions, underscored by low strength rocks like WAF, are likely to increase in the future, a guideline based on the experiences at Ya Rona shaft may be invaluable to other similar extractions.

2. Literature review

2.1. Introduction

Although there are very few case studies on WAF, the standard of information available is of a high quality, and has been procured from leading rock engineering practitioners. This chapter consists of:

- A brief discussion on the relevant 'soft' lava literature,
- The presentation and learning points from the known WAF case studies,
- A discussion on the lithostratigraphy and chemical composition of the WAF, highlighting the weak zones that constitute the rockmass,
- A summary of the salient points that characterise the WAF, and,
- As the study will include a significant amount of numerical modeling analyses, a review of failure criteria to be used in the analyses is also reviewed here.

2.2. Available literature on 'soft' lava materials

A broad classification of WAF would put in the category of 'soft' lava materials. Typically these materials exhibit geomechanical properties and lithologies that are weaker (Rangasamy, et al, 2006) than the rock types that overlay or underlay them. Their presence results in highly fragmented hangingwall conditions (Schweitzer, 1997). Furthermore, in a study (Rangasamy, et al, 2003) conducted in a remnant mining area of a deep level gold mine in the Klerksdorp region, closure profiles (Figure 2-1) indicated that low strength rock materials exhibited higher closure rates than those of high strength rock materials.

The study (Rangasamy, et al, 2003) also presented data with regard to the closure ratio of 'soft' lava rock materials. Closure ratio (CR) is defined as the ratio of the instantaneous blast closure to total daily closure and was accepted in the study as *"a good measure to identify different geotechnical conditions and possible hazards"*. In soft lava rock conditions low values of closure ratio indicate poor ground conditions whereas high values of closure ratio show those areas that are prone to face bursting (Malan & Napier, 1999). In the Ya Rona Shaft Pillar Extraction, the research data will compare high closure rates of stoping

excavations with WAF material (Durapraj, 2006b) in the hangingwall, with typical closure and convergence rates (Jager &Ryder, 1999) in more competent but fractured rockmasses.

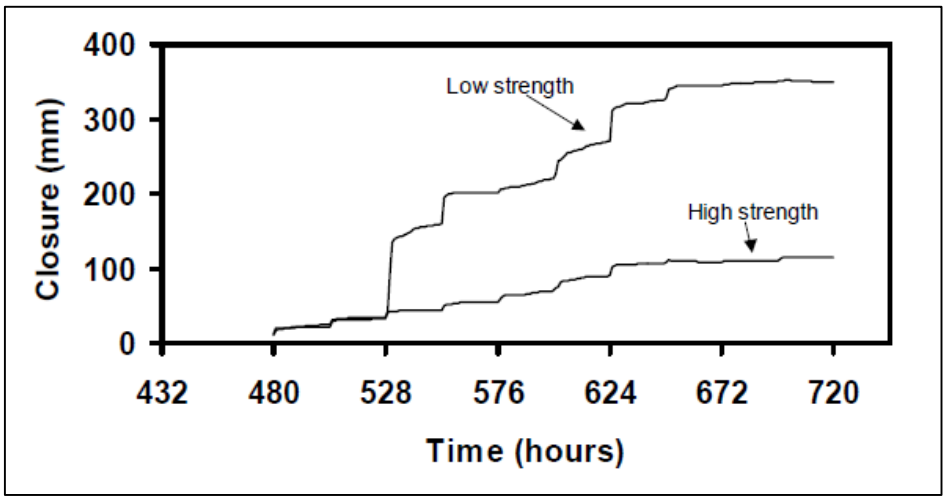


Figure 2-1 Closure profiles for low and high strength rock materials at a remnant mining stope within a Klerksdorp gold mine (Rangasamy, et al, 2003)

2.3. Available literature on the WAF material

Although there are many sources where 'soft' lava rock material has featured, there are only four case studies that the author could identify, where the influence of WAF has been adequately extrapolated and analysed as a feature that posed a significant hazard:

- Gold Field's South Deep SV1 (Petho, et al, 2004),
- First Uranium's Ezulwini Main and Ventilation Shaft (Ortlepp, et al, 2008)
- Gold Field's KDC East (Kloof Gold Mine) Main Shaft (van der Heever, 2007), and,
- Gold Field's KDC West (Driefontein Gold Mine) Ya Rona Sub-Vertical Shaft (Olivier, 2002; Leach, et al, 2003; Leach, 2006; Durapraj, 2006a,b,c; Castelyn, et al, 2007; Durapraj, 2010).

Many of these are consulting reports, not available in the public domain, but form the basis of the rock engineering design at the Ya Rona Shaft Pillar Extraction. A brief summary of each of these reports follow; the emphasis being on the WAF characteristics and how the WAF contributed to the rock engineering design at Ya Rona.

2.3.1. Case study 1: South Deep SV1

The first accident where failure of the WAF was reported occurred in January 2004 when a large WAF section of the South Deep SV1 shaft sidewall collapsed into the shaft. The collapse provided crucial information in the understanding of WAF behaviour as well as consequences associated with WAF failure. As the failure of the WAF had been significant, a team of rock engineering industry professionals were required to investigate the causes of the event, provide a formal geotechnical and geological evaluation of the problem, and formulate failure mechanisms for the WAF (Petho, et al, 2004).

The failure resulted in significant shaft infrastructure damage from approximately 1690m below surface to the shaft bottom. The position and dimensions of the initial collapse are indicated on figure 2-2.

Key features of the investigation were that the hazard assessment process had not considered WAF as a threat to stability, had not quantified the magnitude of the potential damage if the WAF failed, and had not determined what rehabilitation methods would be required in the event of catastrophic failure.

Due to the unstable nature of the accident site, observations and measurements could only be taken from about 10m above the top contact of the sidewall collapse (Figure 2-2, 1680m below surface). Therefore, some measurements had to be inferred from the actual observations. It is important to note that many of the recommendations and conclusions were based on this “inferred” information.

The radial extent of the collapse is depicted on figure 2-3 and the mass of the fall out was estimated at 607 tons. Of note is the geometry of the collapse, or “dog-earing”, relative to the direction of the reef dip. The area marked in red, identified by the investigation team, is an “inferred” unstable block of potential failure (Figure 2-3: quadrants 2 and 3), approximately 1215 tons in mass.

In deep level gold mines under a normal stress gradient with a k-ratio of 0.5 (Jager, & Ryder, 1999), a collapse of the sidewall of a shaft would mimic a high vertical component of stress, which would typically manifest as radial failure around the shaft barrel.

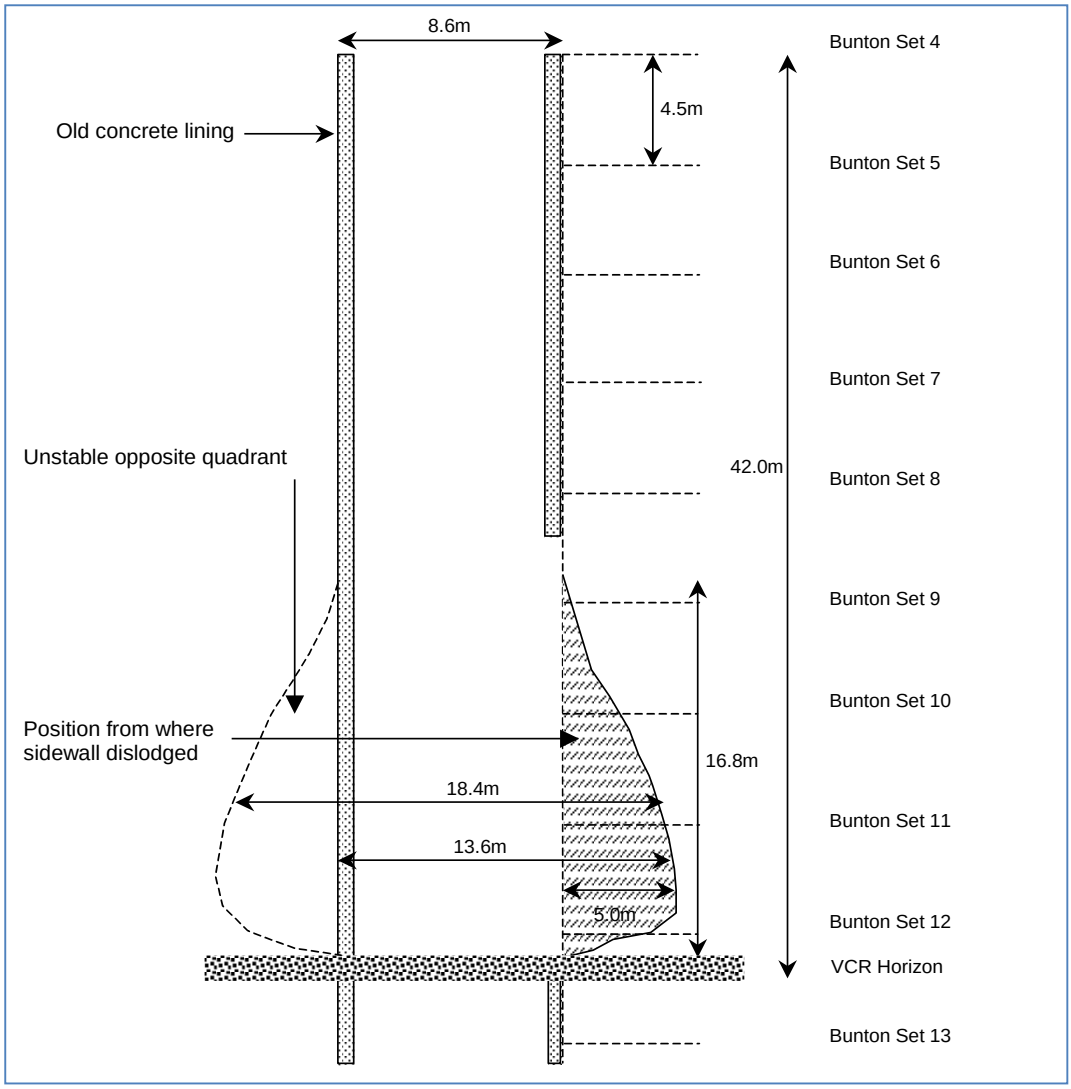


Figure 2-2 Diagram of South Deep SV1 failure in WAF (Petho, et al, 2004)

However, from figure 2-3, the failure zone is along a specific axis of symmetry. This indicates that, prior to the failure, the stress gradient was not 'normal' (k-ratio =0.5). Furthermore, although the shaft was lined with 300mm concrete with a design strength >30MPa, the cured strength was found to be between 10-20MPa, which was up to 66% lower than design strength (Petho, et al, 2004). This impacted negatively on the ability of the shaft sidewall to restrain the WAF rockmass.

This was an important facet in the rock engineering design in Ya Rona example in that the team had to realise that specific zones of weakness in WAF occur when subjected to anomalous stress regimes, and that if the shaft concrete lining was not according to the designed strengths, the concrete may not be able to restrain the WAF rockmass in post-failure mode.

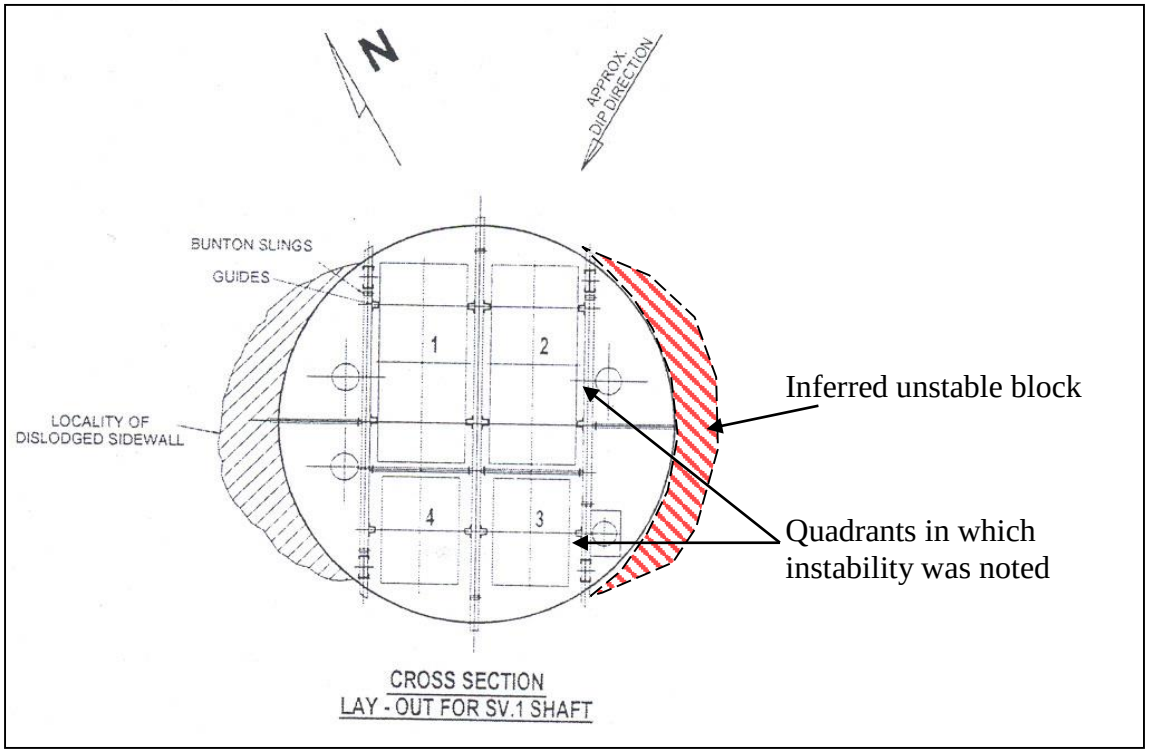


Figure 2-3 Plan of South Deep SV1 extent of failure as well as potential zone (red) of failure (edited from Petho, et al, 2004)

Figure 2-4 shows a graph of WAF deformation over time at the SVI shaft (Petho, et al, 2004) where:

- The WAF had been in creep mode from 1967 when the shaft was sunk,
- WAF had been exposed to air and water during that time,
- Significant WAF deterioration had commenced in 1994 therewith indicating a timeline for the onset of secondary creep, and,
- Tertiary creep and an increased rate of creep could have occurred in the four years prior to the major collapse.

Prior to the collapse, geological evaluations (Petho, et al, 2004) of the areas around the shaft had revealed that there had been a *"high intensity of geological structures, surrounding, passing through and close to the shaft…"*, that the WAF was characterised with a dense pattern of weaknesses emanating from regional stresses impacting on the rock, and that the deformation had been *"a metamorphic effect where rocks become chemically and physically altered"*.

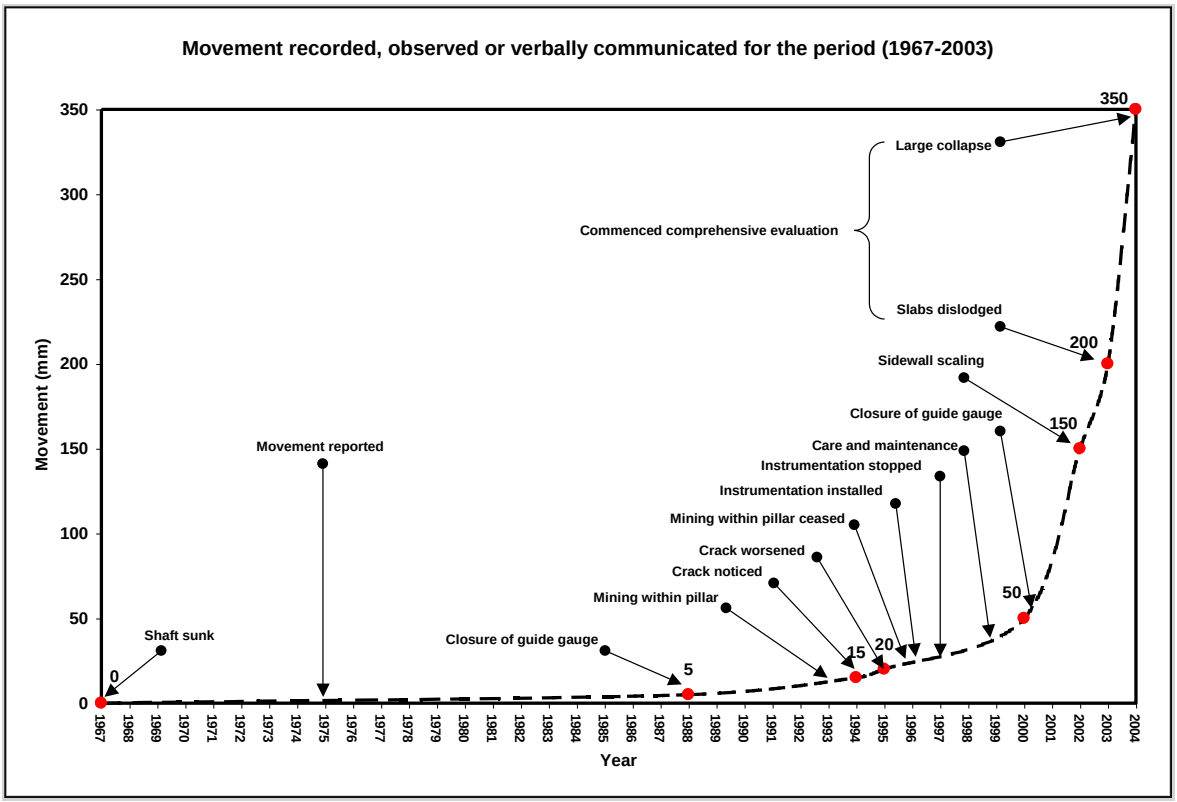


Figure 2-4 South Deep SV1 barrel movement as a function of time (Petho, et al, 2004)

Conclusions in the report (Petho, et al, 2004) suggest that the:

- Mechanisms causing the instability were the *"inherent incompetence"* of the lava directly overlying the Ventersdorp Contact Reef (VCR). It is probable, that, unsupported it may not be able to withstand the virgin stress field at that depth. Small changes in stress will cause it to fail;
- Rockmass material, WAF, above the VCR was *"susceptible to visco-plastic deformation".* Even though the WAF can be restrained and supported, time dependant deformation will result if the material is stressed too close to the compressive strength thereof;
- The area of instability had already been through all typical stages of rock mass creep;
- Inappropriate support applications and the presence of water led to the inability of the support to curtail movement and collapse, and,
- *"Detection and management of this type of deformation can only be accomplished by a dedicated programme of rock engineering instrumentation and monitoring".*

Therefore, for the rock engineering design team at Ya Rona, this information was invaluable. It was now imperative that a proper instrumentation protocol be invoked; that support strategies had to cater for the expected WAF conditions and consequences; that even though appropriate support measures were instituted, the WAF would still deform; the WAF had already been in creep mode at Ya Rona since the sub-vertical shaft was sunk in 1983; and that the risk assessment process had to outline the risks adequately and comprehensively to ensure that if failure did occur, the consequences would not be catastrophic.

2.3.2. Case study 2: Ezulwini Main and Ventilation shafts

The case study at Ezulwini Main and ventilation shaft (Ortlepp, et al, 2008) was commissioned to determine what interventions were necessary to restrict movement of the WAF rockmass. WAF had been intersected at 1030 and 1060m below surface and as part of preparations for the extraction of the shaft pillar area, the shaft barrel had to remain operational during the extraction process. Instead of repeating all the WAF interventions listed in the Ezulwini report, which had considered all of the South Deep SV1 observations, conclusion and recommendations, the author has concentrated on just those issues not covered by the SV1 accident:

- The study did not consider the mining sequence, volumetric extraction rates and layout on WAF which intersected the shaft barrel;
- WAF failure was primarily time dependant 'creep' behaviour as opposed to WAF deformation as a result of stress related changes. For this reason, the conventional classical engineering design (load versus capacity) approach was not adopted by the team. Their approach (Ortlepp, et al, 2008) was based on installing "*...as much capacity as practically possible, in as dense a pattern of holes as can be drilled economically...to overcome the uncertainty"*.
- The variables of WAF strength, load-demand, mining induced stress changes on WAF, the flow characteristics of WAF and a suitable Factor of Safety when designing to mitigate the effects of WAF, could only be, at best, assumed or estimated;

- Material RMR had to be downgraded by 36% (45 to 33) based on in-situ data that did correlate well with the data obtained from the borehole core logging and rock testing;
- As location of the geotechnical drilling proceeded away from reef, the strength of the WAF increased. The team identified three zones, namely; Very Poor WAF, Poor WAF and Good WAF;
- The cost of the support system is *"negligible"* if the designed and installed support system is effective at accomplishing the long term sustainability of operations at Ezulwini.

This study showed the rock engineering design team at Ya Rona that the appropriate support designs had to consider downgraded rock strengths; that the mining sequence, extraction rates and layout were imperative to the stability of the WAF rockmass, and that because much of the rockmass characteristics had to be estimated, a dense support regime would be required to negate the uncertainty.

2.3.3. Case study 3: KDC Kloof Main Shaft

At the Goldfield's Kloof Main Shaft, in preparation for the shaft pillar extraction, a rock engineering investigation (Van der Heever, 2007) was undertaken to characterize the WAF rockmass. The comprehensive program included rock testing, geotechnical drilling, borehole core logging, petrographic analyses, underground investigations and literature reviews.

In view of not repeating WAF characteristics, only the points that have not been considered are articulated in the Kloof report (Van der Heever, 2007):

- Incomplete knowledge of and *"appreciation of the role of geological features"* led to shaft sidewall failures,
- WAF UCS varies between 30 MPa and 75 MPa, with a thickness of 9m, at Kloof Gold Mine. There are zones within the WAF of varying strength,
- The Q-system of rockmass classification confirmed the *'Very Poor'* rating,
- Elastic and strength properties need to be significantly downgraded to compare the modelled and actual stope closures,

- Petrographic analyses revealed that WAF is a highly altered volcanic rock. Degradation and foliation of the rockmass decreases with increasing distance from the conglomerate VCR reef,
- Over time, support units corrode and approach the end of their yield range which renders them ineffective at containing WAF rockmass movement, and,
- Because of the variation in the WAF over very short distances, it is not advisable to extrapolate information about WAF behavior and properties from other mines and shafts.

Aspects from this case study allowed the Ya Rona rock engineering design team to focus on support elements that would not degrade over time; to focus on mimicking inelastic closures in elastic models through back analyses of closure measurements, and use rockmass rating systems to quantify WAF so that appropriate support interventions could be executed. WAF, depending on location, may have different strengths that would need to be tested and not extrapolated from other mines.

2.3.4. Case study 4: KDC West (Driefontein) Ya Rona (4) Sub-Vertical Shaft

The WAF case study at Ya Rona sub-vertical shaft was initiated with the inclusion of the Ya Rona shaft pillar into the Driefontein ore reserve in 1998. To ensure objectivity in the decision making process, rock engineering industry consultants completed most of the inelastic numerical modelling for this pillar extraction.

Since 2006, further inelastic numerical modelling has not been initiated, as work was being executed according to the rock engineering design team's recommendations. The purpose of this report, therefore, was to ascertain those areas that may be susceptible to damage during the mining phases. This assessment would utilise elastic modelling software and provide a basis for future inelastic numerical modelling.

Three reports (Olivier, 2002; Dlokweni, at al, 2003; Leach, 2006) and a formal presentation (Castelyn & Durapraj, 2007) to the Association of Mine Managers of South Africa (AMMSA) were produced for the Ya Rona Shaft Pillar Extraction. The timeline in these reports would indicate the increasing awareness of the WAF hazard. The initial

analyses only investigated how mining toward or away from the shaft would affect the Ya Rona shaft. The report (Olivier, 2002) concluded that mining away from the shaft would be safer than mining toward it. Thereafter, the rock engineering design team indicated that the large throw faults (Figure 2-5) would be the driving mechanism for instability. As with the South Deep SV1 accident, the WAF was not perceived as a particularly weak rockmass, or that the weakness would negatively affect workings to a large extent if failure occurred. However, after the SV1 accident, the understanding and characterisation of WAF gained prominence and downgraded rock strength data was used in the 2006 iteration of the 3DEC model.

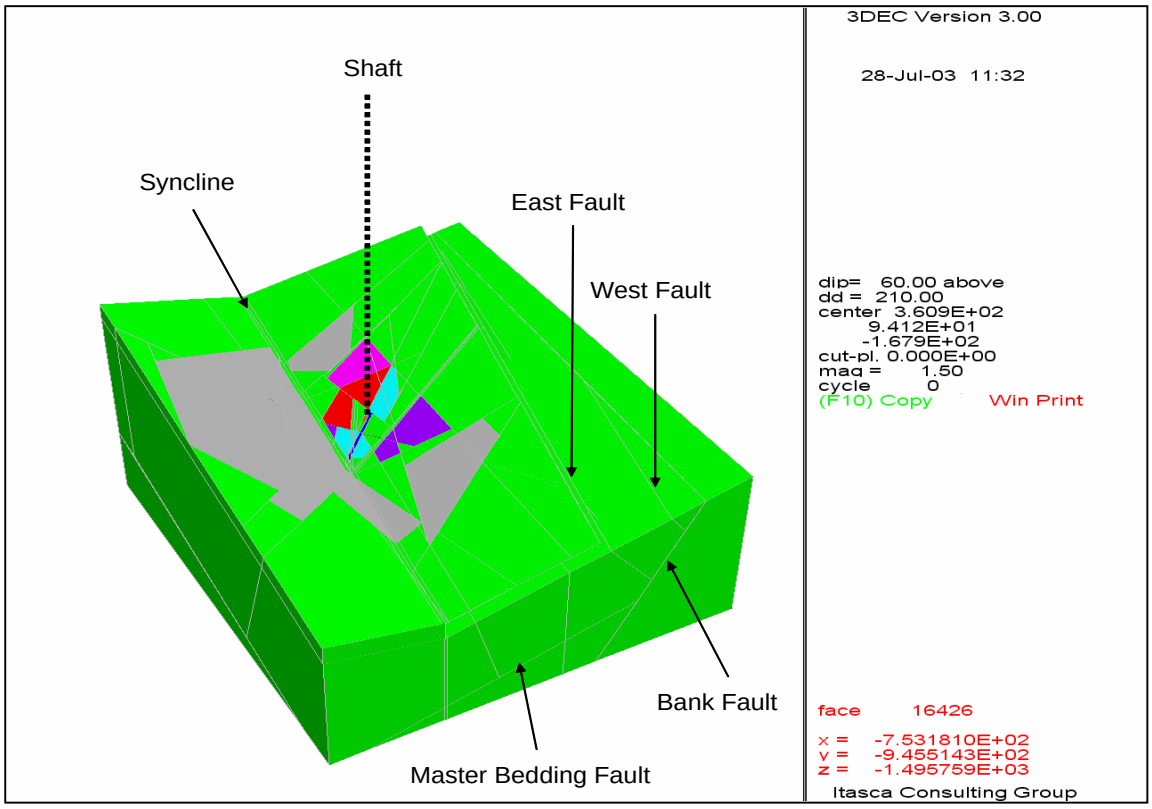


Figure 2-5 Isometric sketch of the 3DEC numerical model showing the location of the shaft relative to large geological structures (Leach, 2006)

2.3.4.1. Input data used in the inelastic numerical modelling

The numerical model (Leach, et al, 2003) was aimed at quantifying the impact of mining steps on the stability of the shaft (Figure 2-5) and used a WAF UCS value of 150MPa (Table 2-1). In contrast, the WAF downgraded rock strength, used in the 2006 numerical model, was 30MPa (Table 2-1). This value was regarded as the lower limit for the UCS of WAF and

when used as an input parameter in the numerical model, it would, hypothetically, produce conservative results.

	(Leach, 2003)	**(Leach, 2006)**
UCS	150 MPa	30 MPa
RMR	55	50
Hoek-Brown m_i	10	5

Table 2-1 Comparison of major input data for numerical modelling (Leach, 2006)

Although inelastic (Leach, 2003) numerical modeling was used, the analysis failed to replicate the in-stope closures being experienced at the time. The model used a high UCS value for WAF and did not simulate the inelastic components of closure characteristic of the WAF rockmass. Furthermore routine underground investigations continued to indicate high closure rates (Durapraj, 2006b) of 50% in 12-15 months in an area with a span of 22m on strike and 40m on dip. Initial closure rates exceeded 50mm per metre of face advance with backfill, in contrast to measured closure rates (Jager and Ryder, 1999) of 25-30mm/m with backfill. However, as mining progressed, the support system which included classified tailings, started to restrain the inelastic deformation of the rockmass and, consequently, lower closure rates were measured.

2.3.4.2. Conclusions from the numerical modelling

The inelastic numerical models showed that:

- The WAF rockmass rock blocks failed in tension (Figure 2-7) and then squeezed into shaft.
- A localized, deeply weathered/deformed area is present around the shaft,
- Water ingress into the rockmass and possible oxidation the WAF had led to the significant alteration of the WAF,
- During the sinking of the shaft, a zone of fractured rockmass had already been created. Further fracture propagation had occurred due to mining induced stresses. Continued deformation is possible in the WAF zone, particularly during the early stages of mining, and that,
- Neither property set (strong or weak WAF) was applicable to the entire rock mass (Table 2-1, Figures 2-6 and 2-7). WAF strength is variable and therefore, it is

understandable if the more conservative property set is used for the entire rockmass. This will produce a more conservative estimate and signify the lower end of the variability.

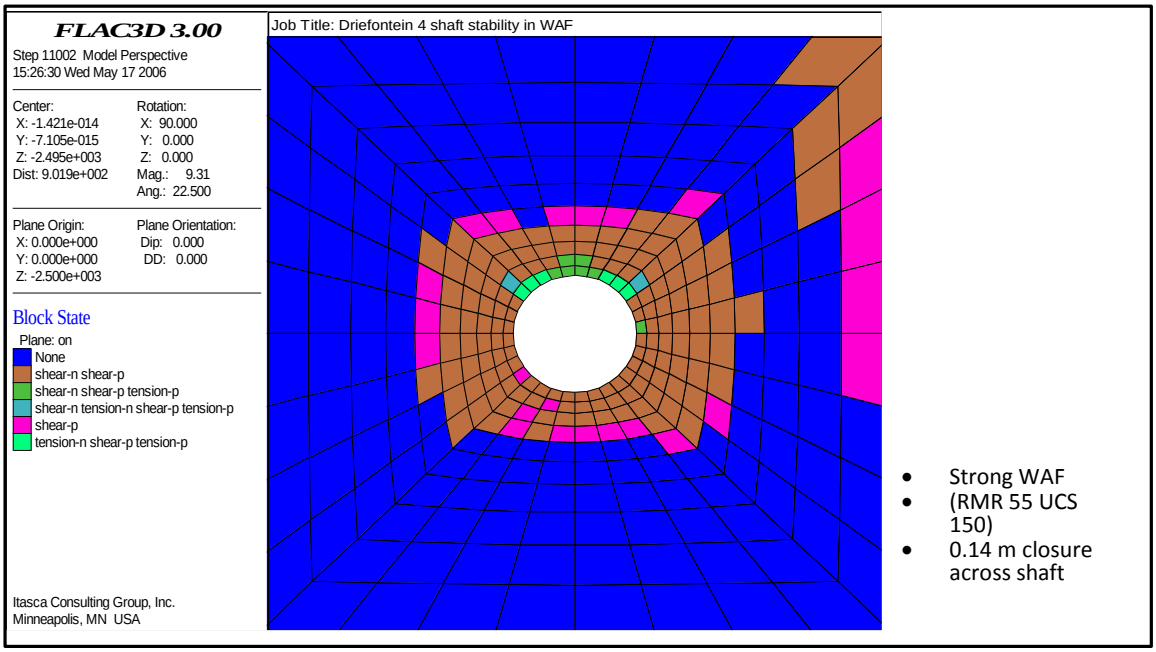


Figure 2-6 FLAC3D model showing barrel sidewall failure modes using strong WAF properties (edited from Leach, 2006)

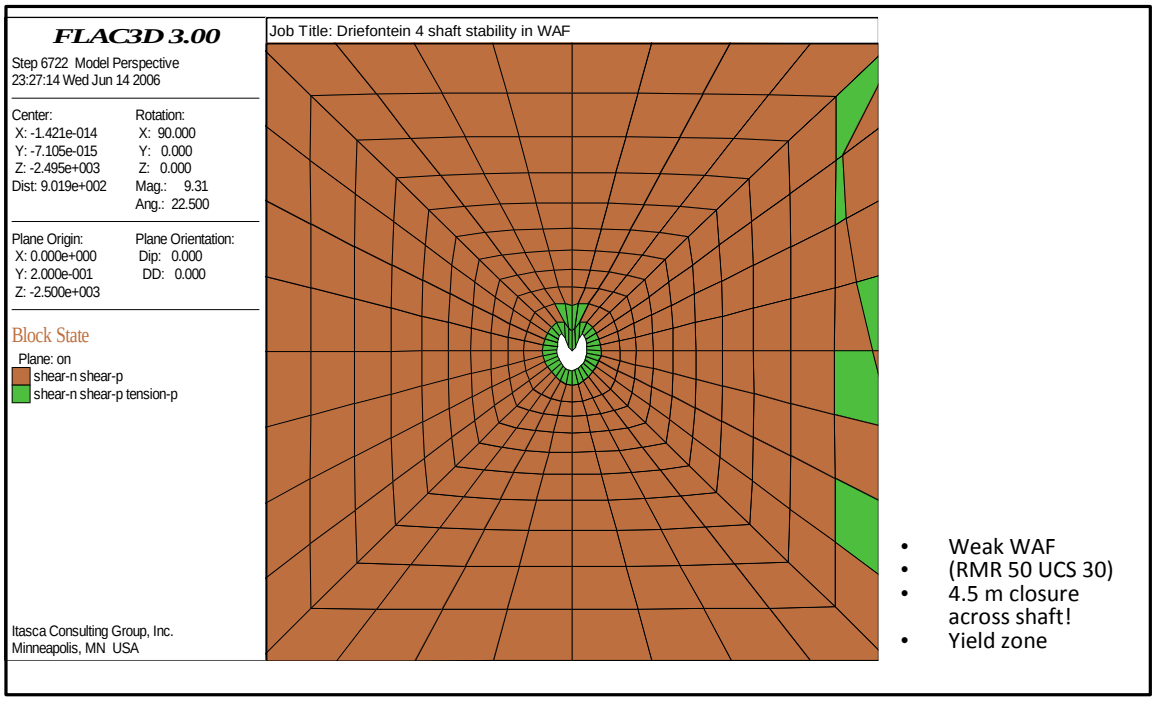


Figure 2-7 FLAC3D model showing barrel sidewall failure modes using weak WAF properties (edited from Leach, 2006)

This recommendation formed the basis for the use of a single downgraded Young's Modulus for the entire rockmass in the elastic modelling,

2.4. WAF – weakness in view of lithostratigraphy and chemical composition

The case studies show that WAF is a weak rock material which is susceptible to failure when exposed to water and air. Therefore, the understanding of the mineralogy and geomechanical characteristics of WAF is imperative for the rock engineering design.

2.4.1. WAF lithostratigraphy

The lithostratigraphy of the South Deep SV1 shaft (Rangasamy, 2006) as well as that of the KDCWest operation (KDCWest, 2012) are depicted in a graphical representation in figures 2-8 and 2-9 respectively. The mineralogy (Table 2-2) of the WAF components in the stratigraphic column of South Deep SV1 show combinations of talcose, calcite and olivine minerals within the tuffaceous basalt lava (approximately 69m thick), whilst the stratigraphy at KDCWest reflects only tuff and tuffaceous quartzite with a combined thickness of 40m.

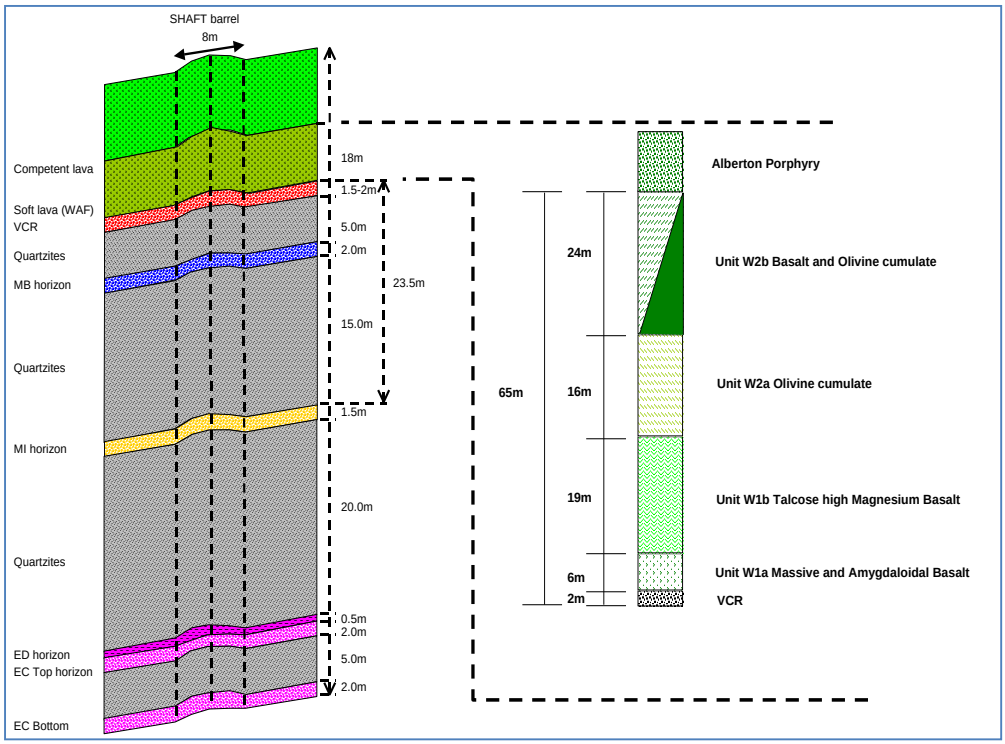


Figure 2-8 Section of WAF zone mineralogy at South Deep SV1 (Rangasamy, et al, 2006)

UNIT	DESCRIPTION	THICKNESS (m)	RQD	SPACING OF LAVA FLOW BOUNDARIES (m)
W1a	A basal massive and amygdaloidal mottled zone. The dominant mineral phases are chlorite and quartz with minor to abundant talc/tremolite	6	28-74	< 0.05
W1b	A massive amorphous or highly contorted talcose zone. Talc and chlorite are the predominant mineral phases with tremolite as a minor constituent. Extremely fined grained with 0.5 cm wide carbonate veins	19	< 49	0.05-0.3
W2a	A massive, amorphous, mottled, olive-pale green, very fine to coarse grained rock comprising chlorite, quartz and carbonate with minor to abundant dolomite. Most striking feature is its olivine cumulate texture.	16	53-87	0.3-1
W2b	A dark homogeneous extremely fine grained massive mottled amygdaloidal and talcose basalt with thin bands of olivine cumulate flow. No volcani-clastic sediments	24	60-80	> 3

Table 2-2 WAF zone mineralogy at South Deep SV1 (Rangasamy, et al, 2006)

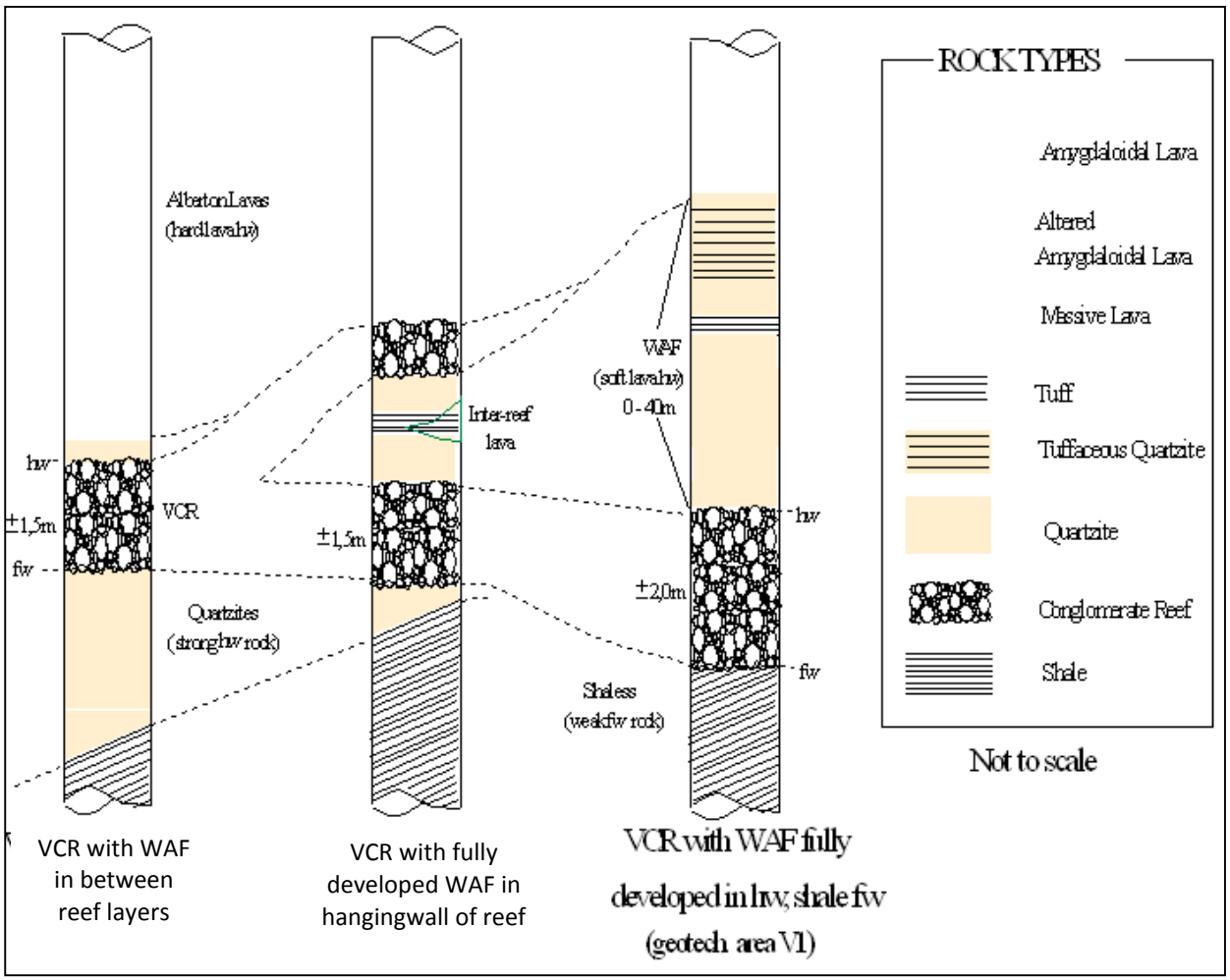


Figure 2-9 Graphical representation of rock types immediately overlying the VCR conglomerate reef (edited from KDCWest, 2012)

However, at the Ya Rona shaft pillar the vertical extent has been measured to 19m. Core drilling to estimate the lithology at Ya Rona shaft, similar to the South Deep example, has been difficult due to the blocky nature of the ground surrounding the shaft barrel. However it has been noted (Durapraj, 2010) that a zone of extremely poor rock within the 19m thick WAF, is located between 11m and 15m from the top contact of the WAF (Figure 2-10). Unfortunately the minerology of the WAF at Ya Rona has not been determined, but if Figure 2-8 data is applied, the WAF W2a Olivine cumulate seems to be the zone of poor ground in Figure 2-10. Dolomite, olivine, chlorite and quartz feature within this zone.

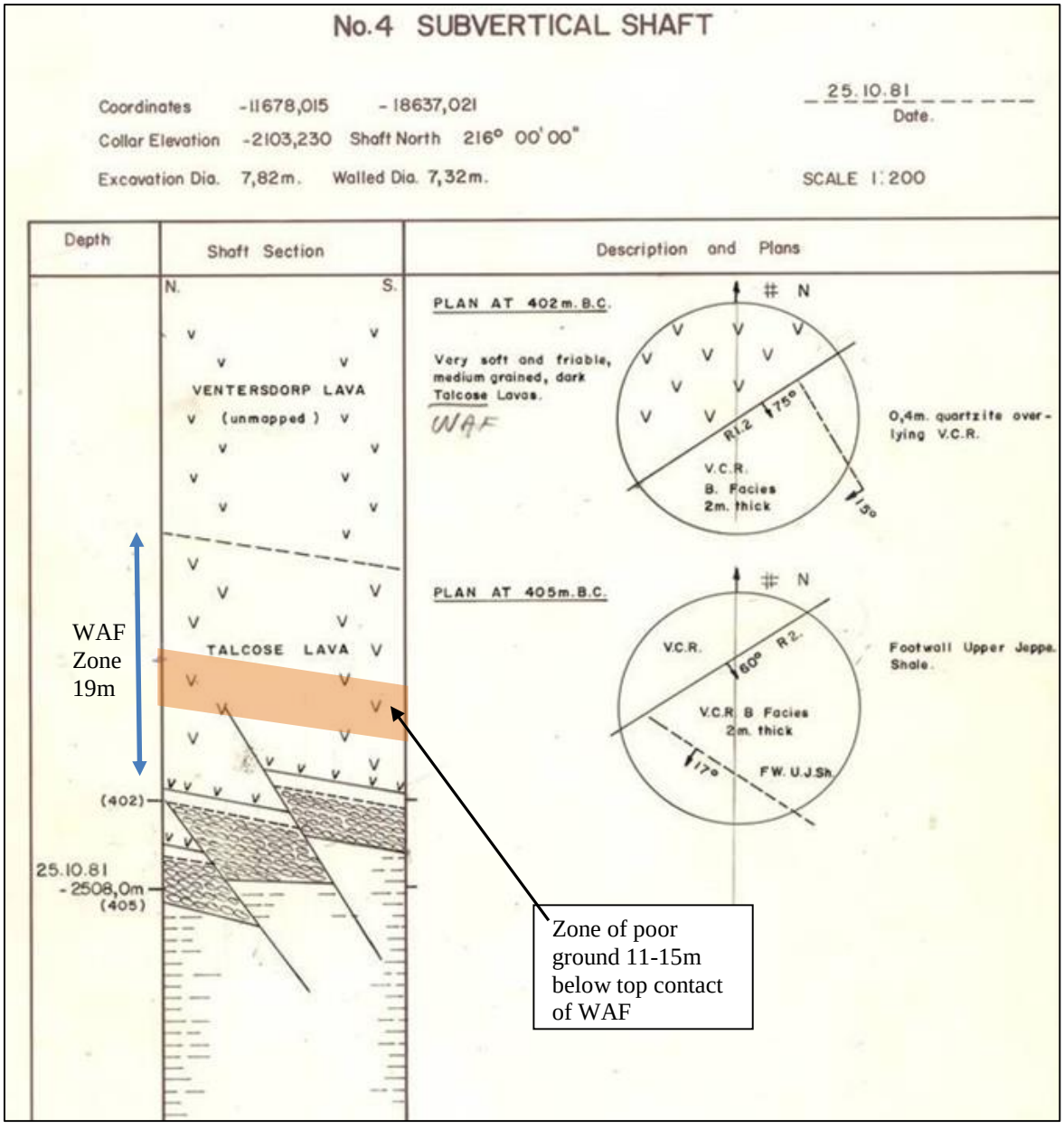


Figure 2-10 Section looking east and plan view of Ya Rona Sub-Vertical Shaft during the development phase showing WAF intersection (edited from Castelyn, et al, 2007)

2.4.2. Mineral composition of WAF

To illustrate how WAF is susceptible to degradation, some of the known mineral components are analysed. The definitions of some of the WAF geologic mineral terms (Parker, 1994), include:

- Tuffaceous or Welded Lava is formed from ejected volcanic rock, formed by the fusing together of small rock fragments through action of heat, gas or weight of overburden.
- Basalt is a dark dense, fine grained, crystalline type igneous rock of a lava flow or minor intrusion, composed essentially of labrodonite, olivine and pyroxene, often displaying a columnar structure.
- Calcite is usually a white, clear, pale-yellow or blue mineral occurring in many different forms, found in sedimentary and metamorphic rocks. Formula: $Ca\,CO_3$.
- Talc/talcose is a white, grey, brown or pale green mineral found in metamorphic rocks. It is crystalline, soft and soapy in nature and composed of hydrated magnesium silicate. Formula: $Mg_3\,Si_4\,O_{10}\,(OH)_2$.
- Tremolite is a magnesium rich, white or grayish variety of long-bladed crystals. Formula: $Ca_2\,Mg_5\,Si_8\,O_{22}\,(OH)_2$.
- Olivine, also called chrysolite, is an olive-green mineral of the olivine group found in igneous and metamorphic rocks. Formula: $(MgFe)_2\,Si\,O_4$.

From the definitions and chemical formulae listed above, it is clear that the degree and manner of degradation is linked to the way the WAF was formed, as well as the degree of mineralization of the WAF rockmass. In particular, the inherent high levels of hydrogen and oxygen within the rockmass, will ensure that WAF degrades when it comes into contact with air and water. Van der Heever (2007) indicates that WAF *"has undergone severe mineral alteration and low grade metamorphism and has been subjected to structural episodes that are manifested as shear zones, localised low angle and bedding plane faulting, foliation and extensive micro and regional jointing".*

Figures 2-11 and 2-12 are photographs taken on the reef plane at Ya Rona shaft. These highlight foliation, shearing and lamination of the WAF rockmass.



Figure 2-11 Photograph showing multiple planes of weakness and shearing of the WAF rockmass



Figure 2-12 Photograph in stope showing WAF laminations

2.5. Review of failure criteria and critical conditions for excavations in WAF

A large proportion of the research report will be dedicated to the results obtained from the numerical models. Therefore, for the analyses of these results, a review of failure criteria, as well as critical conditions for stability, at Ya Rona shaft, is presented in this section. For the rock engineering design team, it was envisaged that WAF would impact on three critical aspects:

- The stability of the Ya Rona Shaft – if WAF deformed to a point which rendered the shaft inoperable, production losses could occur;
- The potential for slip on the large displacement geological structures; and,
- The WAF impact on the LOM2012 mining plan – if WAF deformed on the reef horizon, production losses could also occur.

Therefore, from a design point of view, the need to incorporate the results from the numerical modeling into the design, was crucial.

2.5.1. Ya Rona Sub-Vertical Shaft failure criteria and critical conditions

To analyse the effect of WAF on the Ya Rona Shaft, literature on the five failure criteria listed below, was sourced:

- Stress imposed on the shaft,
- Horizontal and vertical displacement of the shaft as a result of the reef mining,
- The mining-induced vertical strain,
- Tilt of the shaft, and,
- Ride of excavations near the shaft that may impact on shaft stability.

In addition, the Rockwall Condition Factor (RCF) analysis is also viewed as critical to the design at the shaft, as it has been used successfully to determine support design (Jager & Ryder, 2002) in this environment because it employs failure criteria using stress and strength.

Table 2-3 (edited from Tlokweni, 2007) shows the recognized tolerances, for each of the criteria listed above, when shaft numerical modeling analyses, are being investigated.

Aspect	Failure/Tolerance criteria	Reference	Comment
Stress	σ_{cr}< 100MPa for good quality quartzite; σ_{cr}< 29MPa for WAF	Ryder and Jager (1999)	According to Ryder and Jager (2002) good quality quartzite = 200MPa, so the σ_{cr} level is approximately half of the UCS of the rockmass. Therefore, for poorer quality WAF at 57MPa UCS, the failure criterion will be 29MPa, but the analyses of the numerical models will consider a range of values between 29MPa and 57 MPa.
Strain Steelwork damage and increased shaft maintenance	0.2millistrain -0.4millistrain 0.4millistrain 0.4millistrain	Leach (2003) siting works by: Wilson (1971) van Emmenis & More O'Ferrall (1971), Esterhuizen (1980), and Jager and Ryder (1999)	Summary of suggested empirical maximum vertical strain tolerances for shaft pillar design. Strain values are in millistrains and positive values are compressive. Based on the summary compiled by McKinnon (1990).
Tilt Deviation from the vertical calculated as horizontal displacement per unit vertical length	1 millistrain	Leach (2003)	McKinnon (1990) - one millistrain of tilt can be tolerated by shaft steelwork without any adjustment. Spearing (1995) states that the rate of change of tilt is more important than the absolute value. 3 forms of tilt – tilt, kink and rotation
Ride	None		
Rock Condition Factor (RCF)	1.4	Jager & Ryder (1999)	RCF beyond this limit are not catered for in the current research
Horizontal (radial) displacement	0.02% (0.15m)	Leach (2006)	The design of the steelwork would only tolerate 0.02% (0.15m) radial displacement before mitigation measures would be required.
Vertical displacement	1.5m total displacement	Steelwork design (Durapraj, 2005)	Maximum vertical displacement allowed for shaft suspended steelwork, 130m long with tower on 31 level above WAF zone

Table 2-3 Failure criteria for the shaft (edited from Tkloweni, 2007)

2.5.2. Large displacement geological structures' failure criterion

For the geological structures, the review contains analyses of Excess Shear Stress (ESS). Table 2-4 shows acceptable ESS failure criteria when geological features are being investigated in numerical modeling analyses. For analyses and evaluation of ESS in a given mining scenario, Ryder and Jager (2002) show that:

- If a positive ESS >2MPa for a fault is calculated, a prior event would have probably occurred;
- If ESS <0.1MPa, no significant event is likely;
- If ESS <0MPa, no event is theoretically possible;
- Seismic events related to faults have average inferred stress drops of 2MPa;
- Weak planes cannot sustain ESS levels higher than 2MPa;
- ESS values greater than the criterion would indicate slip on the feature as opposed to those of a lower value than the criterion;
- An average inferred stress drop of greater than 2MPa would also indicate a propensity for slip (ride) on that feature at that point in time.

2.5.3. LOM2012 mining plan failure criteria

For the mining plan, analyses of Stress, Average Pillar Stress (APS) and Energy Release Rate (ERR) will be provided. Table 2-4 shows the recognized failure criterion for each when mining sequences are being investigated.

2.5.3.1. Average Pillar Stress

Ryder and Jager (2002) indicate that for high levels of Average Pillar Stress (APS), *"extensive fracturing of the pillar periphery and…through-going fracturing into the pillar core"* may occur. The authors also cite that *"foundation failure… can take the form of a series of seismic events involving rupture along quasi-planes of previously intact rock in the foundations of the pillar"*. Ryder and Jager (2002) also indicate that the failure criterion should be set at 2.5 x the UCS of the rock type that the stability pillar is comprised of. In the soft WAF environment, the numerical modeling results will be interrogated against a range. The lower limit will be 2.5 x UCS of the lower limit of WAF at Ya Rona, which is 57MPa

(Chapter 4, Table 4-1). This indicates that the lower limit of APS should be 143MPa. As the upper limit of the range, the author used the average UCS (89MPa – Chapter 4, Table 4-1), which results in an APS of 223MPa. The reason for using these two UCS values to indicate the failure criterion range is that the small-scale rock testing was biased toward higher values of WAF, a limitation described in the introduction of this research report.

Aspect	Failure/Tolerance criteria	Reference	Comment
Excess Shear Stress (ESS)	2MPa Cohesion of 3.25MPa and angle of internal friction of 23^0 (Chapter 4, Table 4-1).	Ryder and Jager (2002); Ryder (1998)	As per 2.5.2. above
Average Pillar Stress (APS)	143 – 223 MPa	Chapter 4, Table 4-1	As per 2.5.3.1. above
Energy Release Rate (ERR)	$30MJ/m^2$	KDCWest (2012); Jager & Ryder (1999)	As per 2.5.3.2. below

Table 2-4 Failure criteria for analyses of mining layouts and geological formations

2.5.3.2. Energy Release Rate

In a tabular mining environment, the volumetric extraction of rock results in energy changes and energy redistributions. A valuable measure of this change is Energy Release Rate (ERR) which takes into account the effects of mining geometry and depth.

Average ERR (Jager, & Ryder, 1999) is*….a descriptive measure of the mining environment,"* and is not *"a direct expression of seismic energy releases due to mining."* A further implication when contemplating use of ERR as a criterion, is that it is a guide in the design of mining layouts, particularly, deep geologically-undisturbed environments. The authors' recommend that an analysis of seismic events in different mining environments be conducted as a measure to *"set appropriate values of ERR"* at a particular mine. Based on this requirement, the criterion was set as $30MJ/m^2$ (KDCWest, 2012). The ERR for a fully open stope is given by equation 1:

$$\mathbf{ERR = 0.5\ q_v\ \Delta V/\Delta A} \qquad \text{(Eqn. 1)}$$

Where q_v is the virgin vertical stress,
ΔV is the change in volumetric convergence, and,
ΔA is the area being enlarged by mining.

Industry accepted norm (Ryder and Jager, 2002) indicate that values above 30MJ/m^2 result in poorer ground conditions than those below this threshold. The Driefontein COP (KDCWest, 2012) also requires that under normal mining conditions, average ERR be limited (failure criterion) to below this value.

2.6. Summary and lessons learnt

WAF characterisation would include facts that:

- Instabilites arise due to the incompetency of the rock type,
- The material is susceptible to visco-plastic deformation,
- Failure is primarily time dependant 'creep' behaviour,
- Alteration of the WAF over time is usually the result of water and air entering the rock interfaces,
- Rotation of WAF blocks are promoted by a high horizontal stress field,
- WAF strength is low and varied in different zones within the rockmass,
- Input parameters have had to be significantly downgraded to achieve the recorded closures recorded in WAF,
- Over time, support may be inadequate to prevent failure of the WAF,
- WAF strength increases under increasing confinement – deeper into the rockmass, away from the excavation periphery, the WAF will be less exposed, less deformation will occur and therefore the rock will be able to carry higher loads, and,
- Due to the variation in the properties and deformation characteristics of the WAF over very short distances, WAF strength and deformation information should not be extrapolated across mines. Each mine should formulate a strategy to characterize their own WAF rockmass and WAF behaviour profile.

Furthermore, the review at the conclusion of this chapter indicates that the low strength WAF material will be subjected to rigorous failure criteria in the numerical modelling section of this research report.

In the chapters that follow, much of the information gathered in this chapter will be used to categorise the WAF, serve as input data into rockmass rating systems, utilise the inherent characteristics to analyse the numerical models, quantify requirements for ground motion monitoring and review mitigation strategies to reduce the consequences of WAF failure.

3. Selection of appropriate rockmass rating system/s for WAF

3.1. Introduction

Empirical rockmass rating and classification systems have been developed in an effort to characterise rock. In this chapter, read together with appendix A:

- A brief discussion on the limitations of some rockmass rating systems (Q, RMR and RCF) will be provided,
- The appropriate rock mass rating system/s will be selected for the WAF, and,
- The WAF rock type will be quantified within the selected rockmass rating system/s.

3.2. Limitations of the Q, RMR and RCF rockmass rating systems

Most rockmass rating systems try to characterise the rockmass according to a set criteria so that the information can be used to provide support requirements for the tunnelling and ancillary excavations to ensure safe and sustainable production. These systems also estimate the deformation probabilities of the rockmasses, especially under mining and stress loading conditions.

Authors (Pells, 2008; Pells, et al, 2011; Palmstrom, et al, 2006) highlight that although rockmass classification systems are widely used, easy to use, have been successfully used, and are applicable to many environments, they have their limitations. Moreover, many of the earlier systems utilise only the available joint information, which were regarded as the primary contributor to instability. However, when dealing with a heterogeneous rockmass, there are a number of potential sources of instability and therefore, joint information cannot be used as the sole quantification measure of instability in deep level mining. Pells, et al (2011) further comments that:

- Palmstrom, et al (2006), reflect that, in the Q-system RQD/Jn ratio does not *"provide a meaningful measure of relative block size"*,
- That the ratio Jw/*SRF "is not a meaningful measure of stresses acting on the rockmass to be supported"*,
- The Q-system and RMR is a good checklist and should only be used for planning and not for final design purposes,

- The systems do not adequately quantify rockmass behaviour, and,
- There have been instances in the Australia where collapses have occurred as a result of insufficient primary support being installed as a result of poor support design based on the Q-system.

Rockwall Condition Factor (RCF) attributes higher weighting to field stresses in the characterisation of deep level rockmasses. In equation 2, only the F-factor quantifies the intrinsic qualities (faulting, foliation) of the rockmass, describing only a range from F=1 for good quality rock, to F=0.5 for highly discontinuous rock (Jager and Ryder, 1999). For the calculation of RCF (equation 2), σ_1 and σ_3 refer to the major principal stress and minor principal stress acting on the shaft whereas σ_c refers to the uniaxial compressive strength of small scale WAF rocks.

$$RCF = \frac{3\sigma_1 - \sigma_3}{F\sigma_c} \qquad \text{(Eqn. 2)}$$

This is an extremely subjective approach to rock characterisation. In deep level mining, stresses play a large role in how excavations are designed and supported. Rockmass response to such stress plays a pivotal, if not more important, role than stress in a particular environment. The type of rock is also crucial to understanding how it may behave under elevated stress conditions. Therefore, attributing greater importance to stress, in the RCF calculation for a particular excavation, than the type of rock that such stress may impact on, will inherently produce a flawed design. Furthermore, RCF is mainly used for support system design, rather than rock characterisation, with an equally limited design range of between 0.0 and 1.4. Values that exceed 1.4 do not have set design criteria. Therefore, the rock engineering practitioner is charged with articulating his/her own support system for excavations exceeding the 1.4 criteria. This, unfortunately, is not an engineering approach to design.

Therefore, the context of the original classification system should be considered when support design is required. It should not replace the "engineering" in rock engineering design. Failure criterion should be set based on proper in-situ information, experiential evidence and sound rock engineering practice. If a rockmass rating system is favoured to enhance the

design process, cognisance should be taken of the fact that the systems are biased in the weighting of their parameters. To fully appreciate the risk, and the mitigation strategies required, several rating systems need to be applied to the same data. This is the approach taken in this report.

3.3. Classification of WAF using available rockmass rating systems

3.3.1. Data used in the classification

Chapter 2 contains much of the information that is used as input data in the rockmass rating systems. However, there are two crucial elements that are needed to complete the ratings. As many of the systems utilise joint data, these have to be considered. Moreover, when calculating RCF, a value for the F-factor has to be determined.

With regard to the joint information in the calculations, 3 major joint sets were observed (Durapraj, 2006b). Figures 3-1and 3-2 show their orientation and dips. These joint directions were projected from several geology reports, and from actual underground observations (Durapraj, 2006b).

Figure 3-2 is a photograph taken approximately 580m north-west of the shaft barrel where WAF was exposed. Whereas figure 3-1 shows the N-S and E-W trending joint set (Durapraj, 2006b), dipping between 75-80^0 to the horizontal plane, figure 3-2 shows the third joint set, which is flat dipping, sub-parallel to the reef dip. Extensive jointing is not a feature that characterises the WAF rockmass, but where jointing is visible, these joints are undulating, calcite-rich, and in some cases open.

Jointing was also extensively characterised, at the Kloof Mine (Van der Heever, 2007), through borehole and underground in-situ observations. Ortlepp, et al (2008) and Petho, et al, (2004), also used borehole data to establish joint properties for use in the classification systems. The joint information is summarised in table 3-1.

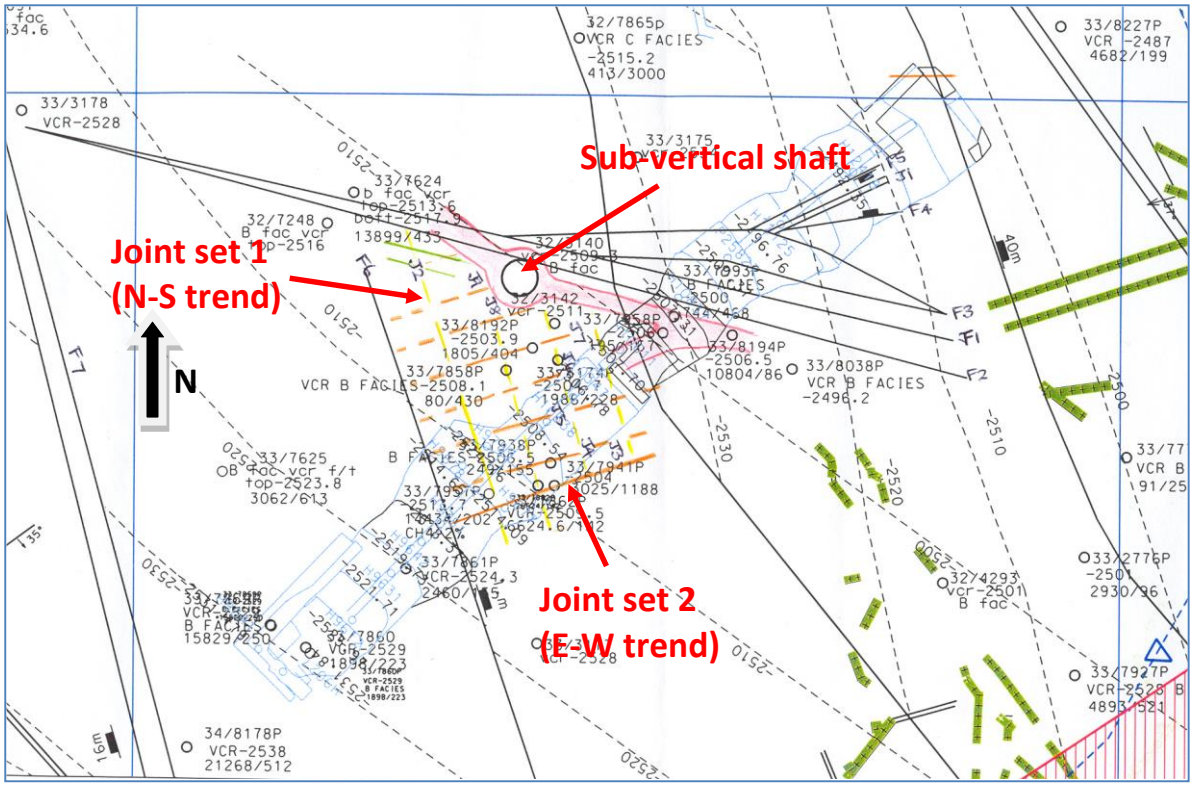


Figure 3-1 N-S (J1) and E-W (J2) joint directions at Ya Rona sub-vertical shaft (Durapraj, 2006b)



Figure 3-2 Photograph, looking east, showing 3rd joint set at Ya Rona sub-vertical shaft (Durapraj, 2006b)

In addition to joint information, for the calculation of RCF, the F-factor has to be determined. Earlier, two extremes in values (Jager and Ryder, 1999) for the F-factor were cited. WAF does not exhibit either of these extremes. In calculation of the RCF for orepasses (Joughin and Stacey, 2005) F = 0.7 was used when the orientation of the orepass to the reef strata dip was less than 80^0. In the Ya Rona example, the vertical shaft is at an angle less than 80^0 to the reef dip. Therefore, the author has used F = 0.7 in the calculation of RCF for the shaft barrel. In terms of the jointing relative to the reef dip, the joint angles are also $<80^0$ to reef dip.

3.3.2. Rockmass rating of WAF

Table 3-1 shows the data available in each of the reports (Ortlepp, et al, 2008; van der Heever, 2007; Durapraj, 2006b; Leach, 2006; and Petho, et al, 2004). The properties of the rockmass are then substituted into the selected rockmass rating systems (Appendix A) to produce a final rating. From Table 3-1, it is evident that the rating range is fairly large, which is indicative of a variable rockmass. Therefore, in the rock engineering design within the Ya Rona Shaft Pillar Extraction, the variability in the WAF, even over short distances, had to be incorporated in the design. Using only absolute values would present one component of strength or failure on a continuum of possibilities, and a single value will not reflect the variability that exists in the WAF rockmass.

Location	**South Deep SV1 (a)**	**Ya Rona Shaft (b)**	**Ezulwini Main Shaft (c)**	**Kloof Main Shaft (d)**	**Range of values prior to 2012 (averages)**	**Calculation of rockmass ratings - 2012**	**Final**
Q	-	-	0.27-2.0	0.6-0.95	0.27 – 2.0	0.10-0.14	0.1-2.0
Qc	-	-	-	-	-	0.058-0.081	-
RMR	-	50	33-45	-	33-50	50	33-50
GSI	-	45	-	-	-	35-50	35-50
MRMR	-	-	-	-	-	32-34	32-34
RCF (shaft barrel)	-	-	-	-	-	4.66	-
Jointing/ metre	4-6	3	-	1-2	1-6		
Number of Joint directions	3	4	-	3-6	3-6		

Table 3-1 Summary of ratings for WAF from different sources ((a) Petho, et al, 2004; (b) Durapraj, 2006; Leach, 2006; (c) Ortlepp, et al, 2008; (d) van der Heever, 2007)

Although the point has been made that there is variability in the WAF across the sites that have been monitored, and for which observations have been made, paradoxically, the rockmass rating values for each of the sites, are very similar to each other.

3.4. Selection of the most appropriate system/s for the WAF

To determine which rockmass rating systems are best suited to WAF, a summary of the learning points, established in chapter 2, are presented. These are that WAF is a weak rock that is:

- Susceptible to oxidation and water,
- Visco-plastic in flow characteristics,
- Prone to time dependent deterioration, and,
- Chemically as well as mechanically altered.

The author has selected five rockmass rating systems for discussion. These are RMR, the Q-system, GSI, MRMR and RCF. These have proven their applicability to several geotechnical environments in shallow, moderate and deep-level mining. For the purposes of this research report, the use of RMR, MRMR and RCF is advocated for the rock engineering design. These have been chosen on the grounds that:

1. Case studies, presented in chapter 2 (Leach, 2003) of this report, use RMR to characterise the WAF rockmass,
2. Although RMR does not take into account the confining stress in the WAF rockmass, it does take into account the excavation relative to joint direction on a more local scale. This is important in the rock engineering excavation design as additional exposure to WAF will require additional support strategies,
3. Q was developed for shallower mines and although Q uses the stress reduction factor (SRF) to articulate the stress field component, more significance is placed on joint information and rock block geometries. The downgrading may also be applicable to shallower environments. The low, medium and high stress factors do not allow enough detail for WAF quantification. Q_c places more weight on the rockmass strength than the prevailing conditions. Furthermore, this rating system may also be too sensitive to minor variations in rock properties. This may impact the rock engineering design significantly,

4. GSI is susceptible to the practitioner's subjective interpretation of the specimen or the rockmass. Two rock engineers may differ vastly for the same rockmass and therefore, the impact of this "incorrect" interpretation on the design may be significant,
5. Although MRMR establishes a base rating value similar to RMR in that it uses joint and groundwater conditions, it also applies suitable adjustments for prevailing local conditions, including stress, blasting effects and weathering. Weathering of WAF is crucial for the rock engineering design,
6. RCF takes the strength of the rock, the prevailing stress condition and to a limiting extent rockmass condition (F) to provide a rockmass rating. It allows the inclusion of jointing in the F-factor. For the purposes of rock engineering design, the WAF rockmass response to stress is of overriding importance, and,
7. Each rating system provides aspects within which WAF can be quantified in different ways.

However, even though there are inherent difficulties when utilising rockmass rating systems, it is an important tool for design. By not using such methods, designs may be flawed in that empirical standards are not met. Therefore, a more rigorous approach may be to subject the same data to a number of classification systems. This would produce a range of values that could be used in design. However, the drawback of such an exercise is that a large range of designs may be produced, which will inherently make the decision-making process more complicated and costly.

Therefore, the selection of an appropriate empirical method, based on sound rock engineering principles, is crucial in the characterisation of the WAF. If this selection is not done correctly, support design may be flawed. This could lead to excavations that are inadequately supported which are susceptible to damage and failure.

4. Consolidation of the WAF rockmass data and the selection of input parameters for numerical modelling

4.1. Introduction

Input parameters are crucial to a numerical model as they determine the deformations and stresses obtained from the output data. Therefore, the objective of this chapter is to provide acceptable input parameters for the numerical modeling exercise that will result in rational information for the design analyses of the Ya Rona Shaft Pillar Extraction.

In this chapter:

- All the data available on the WAF, is consolidated. This process comprises the use of information in chapter 2 of this research report, stress measurements carried out at Ya Rona shaft, geomechanical data, underground observations, small scale rock testing and geologic data;
- By comparing the actual measured data underground, the numerical model can be calibrated to enhance the model accuracy;
- The calibration process will allow for the downgrading of the rockmass where the most appropriate input parameters are selected; and,
- The KDCWest C2012 Life of Mine (LOM12) Extraction Sequence is then numerically modeled using the BesolMS suite of programs.

4.2. The consolidation of WAF data for use in the numerical modelling

Figure 4-1 shows a numerical modeling simulation process (Karabin, et al, 1999) which shows the steps a design team should take when attempting to select the best alternative of a design. The process, outlined within the dotted red line of Figure 4-1, indicates the work done to date with the inelastic models.

The “re-calibration” exercise, referred to in Figure 4-1 (blue dotted line), will compare (Chapter 2, Section 4.2.2.) underground closure measurements and results from numerical modeling using different Young’s Moduli.

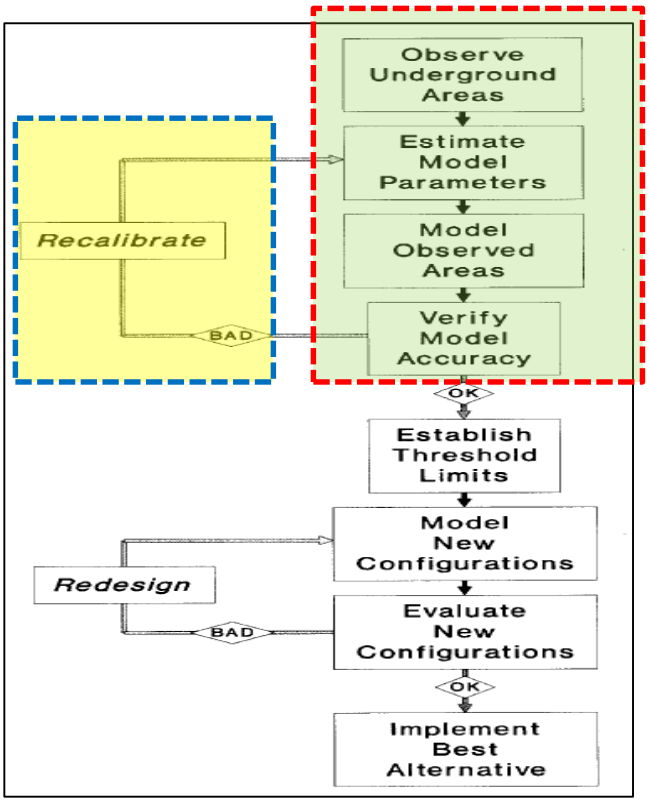


Figure 4-1 Simulation process in numerical modelling (Karabin, et al, 1999)

At the onset of the report, the objective was to ascertain what aspects could contribute to WAF deformation and which components could reasonably be measured for the rock engineering design process. Therefore, the consolidation of the available WAF data for the Ya Rona shaft pillar extraction included:

- Stress measurements,
- Geomechanical data from other WAF exposures,
- Underground observations, including closure measurements,
- Rock testing data, and,
- Geological data.

4.2.1. Stress regime at Ya Rona Shaft Pillar

From the case studies, regional effects on WAF are largely driven by the stress regime, and the large dislocation geological structures. Figure 4-2 shows the measured directions and magnitude (Coetzer, 2003) of the stress at 2500m below surface. These measurements resulted in an increase in the k-ratio from 0.5 to 1.15. Figure 4-3 shows the stress vectors in relation to the shaft barrel steelwork and reef dip. Both the k-ratio and the stress orientations

represented a fundamental shift in data and was, therefore, a major contributor to the rock engineering design.

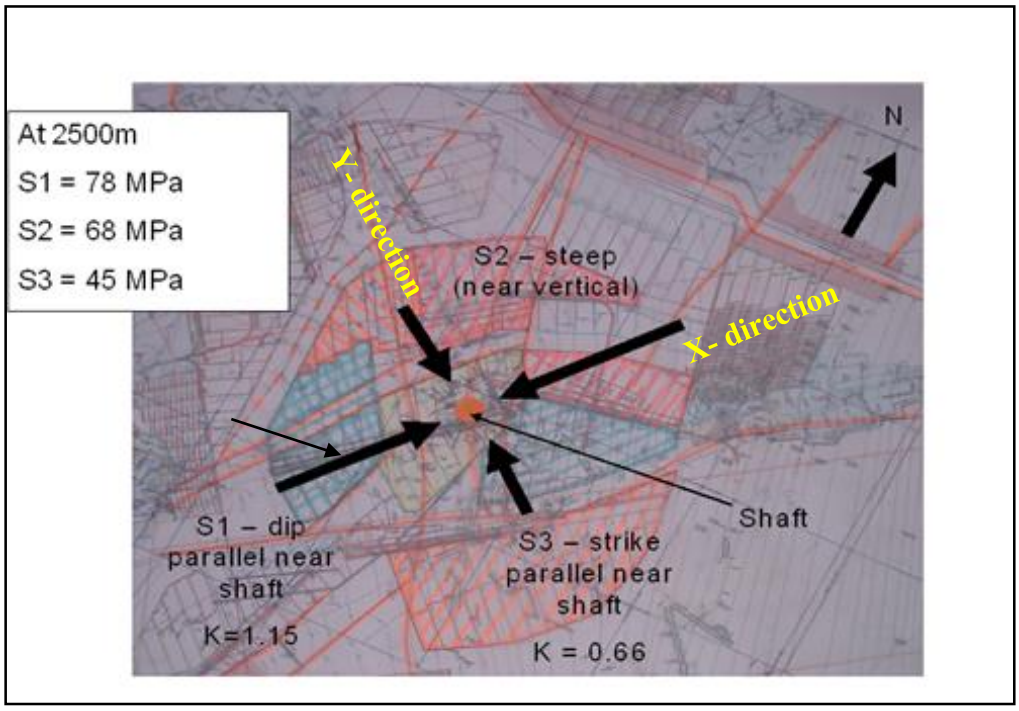


Figure 4-2 Measured in-situ stress profile at Ya Rona shaft showing k-ratio profile (Leach, 2006)

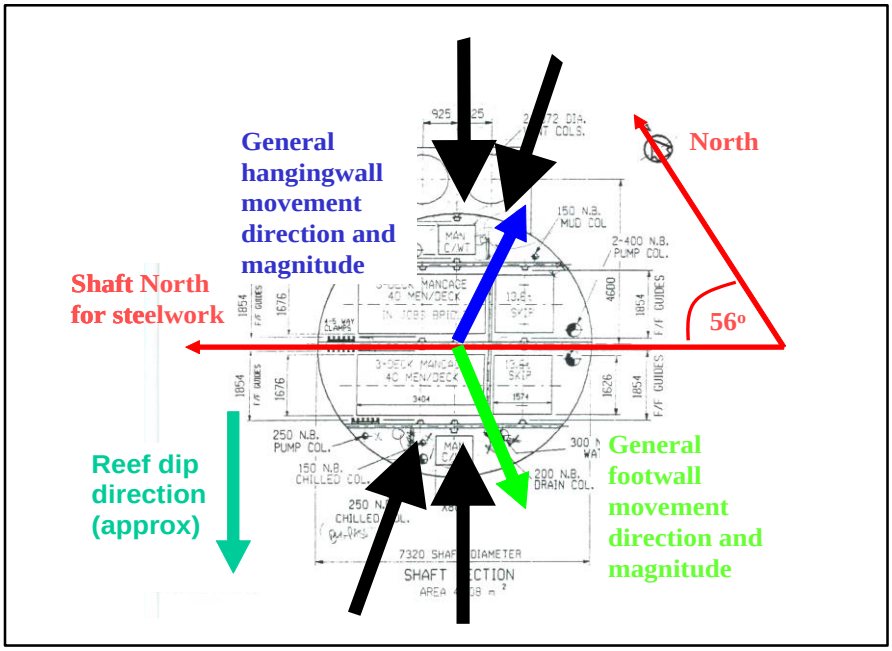


Figure 4-3 Orientation of stresses relative to the Ya Rona shaft barrel and reef dip (Leach, 2006)

4.2.2. WAF strength data

From the available literature and underground observations, there is overwhelming evidence that WAF is a weak rock type. A summary of the material's characteristics is, therefore, invaluable in the calibration exercise of the rock engineering design process when WAF is encountered. Table 4-1 is a revision of the original WAF geotechnical summary compiled by Van der Heever (2007) for use at the Kloof Main Shaft operation (Chapter 2, section 2.3.3). Although the table shows data with some degree of variability, the table provides a valuable basis for the understanding of the geomechanical and geophysical properties of the WAF.

In order to assess behaviour of rockmasses, small scale rock testing must be conducted. To ensure the accuracy of the numerical model, appropriate input data for the numerical model must be established. However, in the case of WAF, there are inherent problems. To illustrate this, photographs of core runs (Figures 4-4 and 4-5), from Ya Rona shaft, are provided. Figure 4-4 shows good quality Alberton Lava drill core, whereas figure 4-5 shows the much poorer quality WAF core. Although these photographs were taken on surface, both had been exposed to time dependant deterioration and could have also been exposed to water. Therefore, rock testing would already use poorer quality material and will yield biased results. In case of the WAF, the degradation is significant and only the "better" quality core, without imperfection, could be used for testing. The bias, therefore, in the WAF case, will be toward 'higher' strength values. However, it can be argued that this bias can be negated using downgrading techniques (Laubscher, 1990).

Although WAF is a weak rock type, it can be "strengthened" using confinement methods. Figure 4-6 shows a graphical representation of the values extruded from laboratory work cited by Van der Heever (Appendix B, Table B-1 and Table 4-1), a well as laboratory results (Yilmaz, 2006). From the scatter-plot graph, the WAF samples exhibited an increase in load bearing ability when subjecting them to increasing levels of confinement. The impact of the load carrying ability to the increasing confinement ability of the WAF was invaluable to the rock engineering design. It meant that if the WAF rockmass is constrained sufficiently, deformation may not be significant as it would withstand the increasing loads placed on it as a result of mining.

	Units	South Deep SV1 (a)	Ya Rona Shaft (b)	South Deep (c)	Ezulwini Main Shaft (d)	Kloof Main Shaft (e)	Range of values (average)	Aspect
Height of WAF zone	**m**	18	19 (3 zones)	18	37 (3 zones)	9	**9-37 (23)**	**1**
Uniaxial Compressive Strength (UCS)	**MPa**	20-80	57-121 (89)	20-80	-	49-107	**20-121 (71)**	**2**
Triaxial Compressive Strength @ 4MPa confinement	**MPa**	-	68-107	-	-	-	**68-107 (88)**	**3**
Triaxial Compressive Strength @ 8MPa confinement	**MPa**	-	95-129	-	-	-	**95-129 (112)**	**4**
Triaxial Compressive Strength @ 15MPa confinement	**MPa**	-	127-152	-	-	-	**127-152 (140)**	**5**
Triaxial Compressive Strength @ 20MPa confinement	**MPa**	92	-	-	-	121	**92-121 (107)**	**6**
Brazilian Indirect Tensile Strength	**MPa**	-	10-14	0.1	-	7-21	**0.1-21 (10.6)**	**7**
Angle of friction		28		17	-	-	**17-28 (23)**	**8**
Shear Strength	**MPa**	-	-	-	-	8.4	**8.4**	**9**
Young's Modulus (E) (downgrade for elastic models)	**GPa**	68	56-74 (3)	68	68	50 (20)	**50-74 (62)**	**10**
Bulk Modulus	**GPa**	40	40	40	-	-	**40**	**11**
Shear Modulus	**GPa**	-	28	28	-	-	**28**	**12**
Density	**kg/m^3**	-	2693-2829	-	-	-	**2693-2829 (2761)**	**13**
Poisson's ratio (v)		0.2	0.14-0.33	0.2	-	0.17-0.33	**0.14-0.33 (0.24)**	**14**
Cohesion	**MPa**	4.3	3.7	2.2	-	-	**2.2-4.3 (3.25)**	**15**
Dilation		-	22	22	-		**22**	**16**
Average RQD		30 (6-40)	31	50	-	40	**6-50 (28)**	**17**
In situ strength	**MPa**	12	12	6	-	-	**6-12 (9)**	**18**

Table 4-1 Summary of WAF raw geotechnical data from different sources (edited from van der Heever, 2007 - (a & c) Petho, et al, 2004; (b) Durapraj, 2006; Leach, 2006; (d) Ortlepp, et al, 2008; (e) van der Heever, 2007)



Figure 4-4 Drill core from Alberton Lava hangingwall geotechnical hole at Ya Rona



Figure 4-5 Drill core from WAF hangingwall geotechnical hole at Ya Rona shaft

For the purposes of understanding the WAF rockmass characteristics (Table 4-1), their limitations are discussed in Table 4-2.

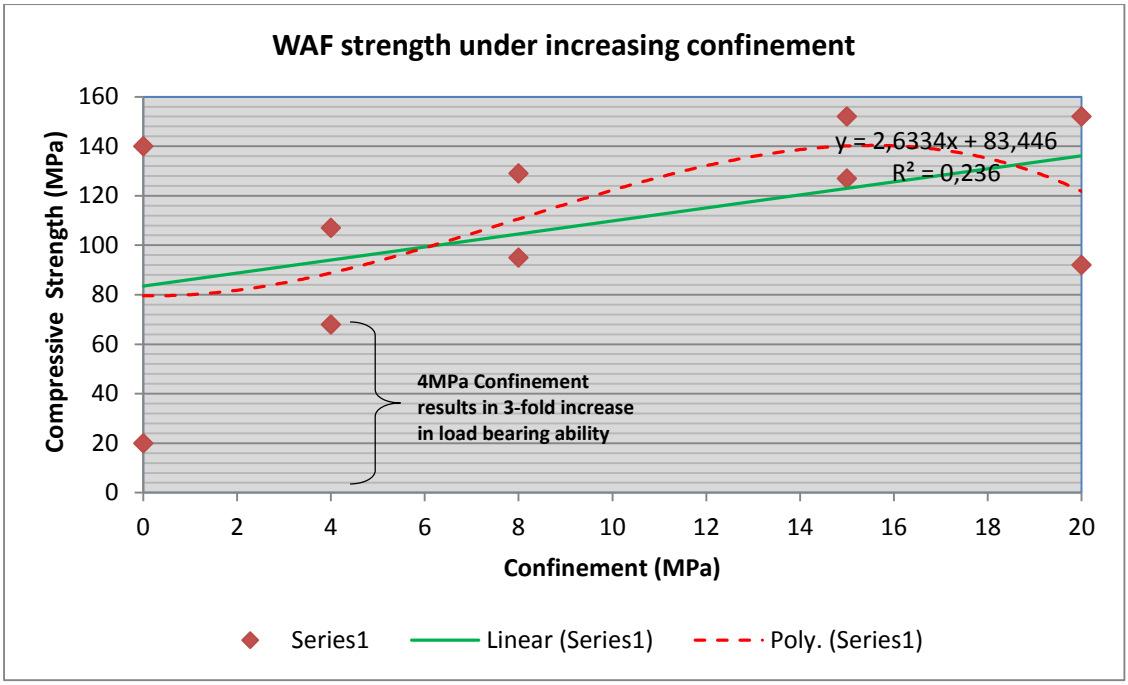


Figure 4-6 Graphical representation of WAF strength under increasing confinement at Ya Rona shaft (compilation of data from Appendix B, Table B-1 (Yilmaz, 2006); and Table 4-1 (Van der Heever, 2007))

Aspect	Parameter	Comment
1	Height of the WAF zone	Variable, but less than 38m, with an average of 23m. Extreme variations in components may be possible within that height.
2	Uniaxial Compressive Strength (UCS)	The data indicates a very large range of values (difference of 120MPa between best and worst), with an average of 71MPa. This would need to be downgraded to 80% of the original UCS for the scale effect (Laubscher, 1990).
3-6	Triaxial Compressive Strength (TCS)	The data indicates a smaller range of values (difference of 32 MPa) as compared to UCS above, with the average ranging from 88 to140MPa, and that under increasing confinement, WAF has the ability to sustain higher loads (Figure 4-6).
7	Brazilian Indirect Tensile Strength	The data indicates a very large range of values (0.1-21MPa), which is indicative of the varied nature of the rockmass at different sites.
8	Angle of friction	The angles measured for WAF represent values indicative of clays with high plasticity to clayey poorly graded gravels (Angle of friction, 2011).
9	Shear Strength	One shear strength test conducted at Kloof Main Shaft (Van der Heever, 2007).
10	Young's Modulus	Small range of values indicating consistency in rockmass characteristics. Significantly wider range of values is observed when downgrading of the laboratory results occurs.
14	Poisson's ratio	The range of value (0.14-0.33) indicates that intrinsic properties of WAF dictate how the rockmass will deform.

Table 4-2 Comment on input parameters for WAF as summarised in table 4-1

4.2.3. The calibration of Young's Modulus for use in the elastic modelling

It is important to note that the numerical modeling packages used at the time (Leach, 2003), could not replicate the anomalous deformation recorded, without significantly downgrading the input parameters. In an attempt to use the available numerical modelling (elastic) software, to replicate the observed deformations, the back analysis approach (Durapraj, 2006a) of selecting input parameters based on observed deformations, was adopted. The Young's Modulus (E) parameter was selected as the variable which would be manipulated in order to produce the elastic equivalent of the observed underground closure. This closure profile was replicated in the elastic MINSIM numerical model using a value for Young's Modulus of 3GPa (Durapraj, 2006a). The back analysis, and resultant Young's Modulus downgrading technique, was also later used at the Kloof Gold Mine (Van der Heever, 2007) to produce similar results for the WAF rockmass. In the Kloof example, the Young's Modulus value of 20 GPa (Figure 2-10) was used to replicate the measured underground closure profile.

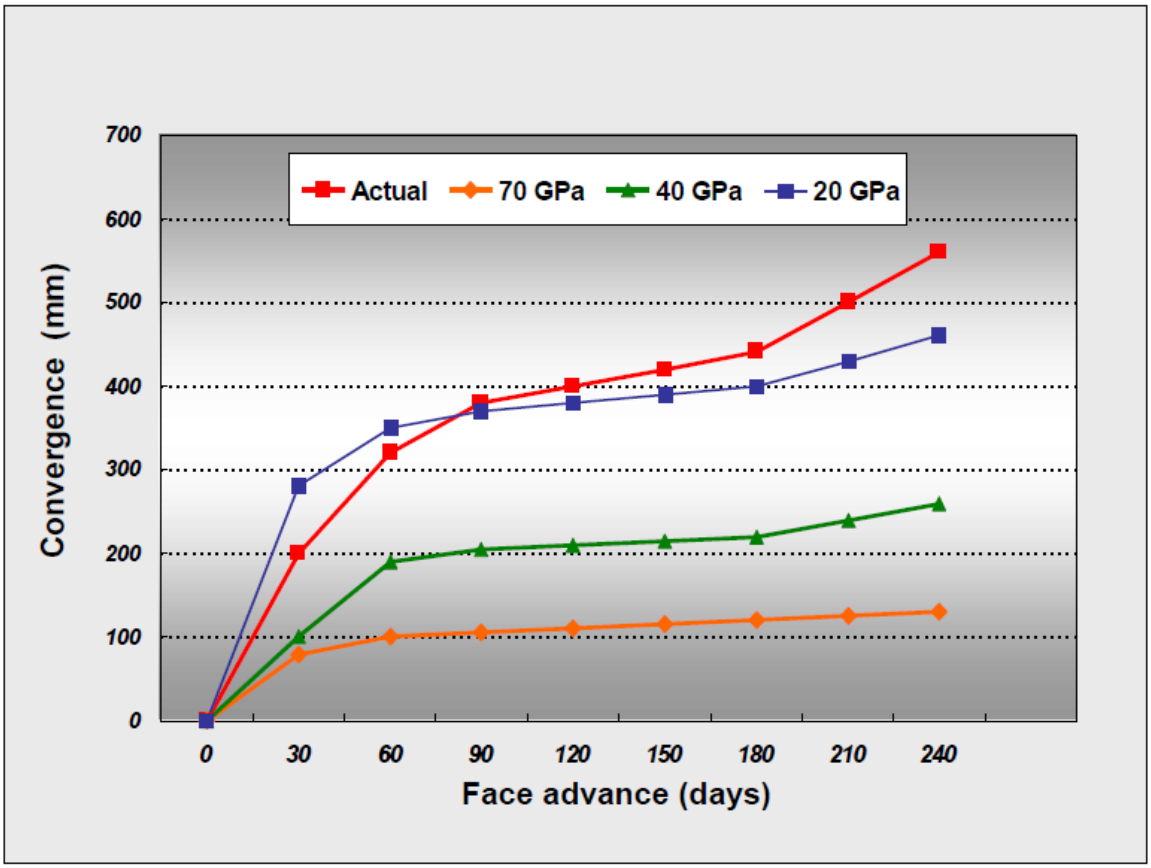


Figure 4-7 Comparison between actual and modelled convergences for different values of Young's Modulus (after Van der Heever, 2007)

The question as why only Young's Modulus was manipulated to achieve the result will result in two answers. Firstly, from numerical modelling experience one should only change a single variable and then observe the impact on the result. Obviously if many variables are changed, the combined effect may produce the desired result, but the modeler would not be able to ascertain which variable had the largest impact. Secondly, in elastic theory, radial and tangential displacement of any point in the rockmass is calculated using the radius of the excavation as well as the point of concern, the depth below surface at which the point exists, the k-ratio impacting on the excavation, the Poisson's Ratio and the Shear Modulus (G) of the rock (derived from the Young's Modulus – Chapter 4, Equation 8). In the Ya Rona example, as the k-ratio is known and the depth of the point being investigated is fixed, the only two factors that can be manipulated are the Young's Modulus and the Poisson's ratio. However, the manipulation of the Young's Modulus produces a more significant change in the result than the manipulation of the Poisson's ratio. Therefore, the Young's Modulus was used to calibrate the numerical model.

In order to select the appropriate value for the Young's Modulus (E) numerical modelling input parameter, a sensitivity analysis was carried out. Different values for E values (3GPa, 20GPa, 50GPa and 70GPa) were used as input parameters in the elastic numerical model. Thereafter, the results were compared (Figure 4-8) to the underground measurements (Durapraj, 2006a).

Figure 4-8 shows that the range in which an appropriate value for E, for use as an input parameter for WAF in an elastic numerical model, could be found between 3GPa and 20GPa, the former being cited by Durapraj (2006a), the latter by Van der Heever (2007). However, in the opinion of the author, the value for E cited in the Kloof example (Van der Heever, 2007), contained more data on convergences than those contained in the Durapraj (2006a) case study. Furthermore, good correlation was obtained between the modelled and actual convergences in the Kloof case study to warrant the use of E=20GPa as the input parameter in the elastic numerical model for this research report.

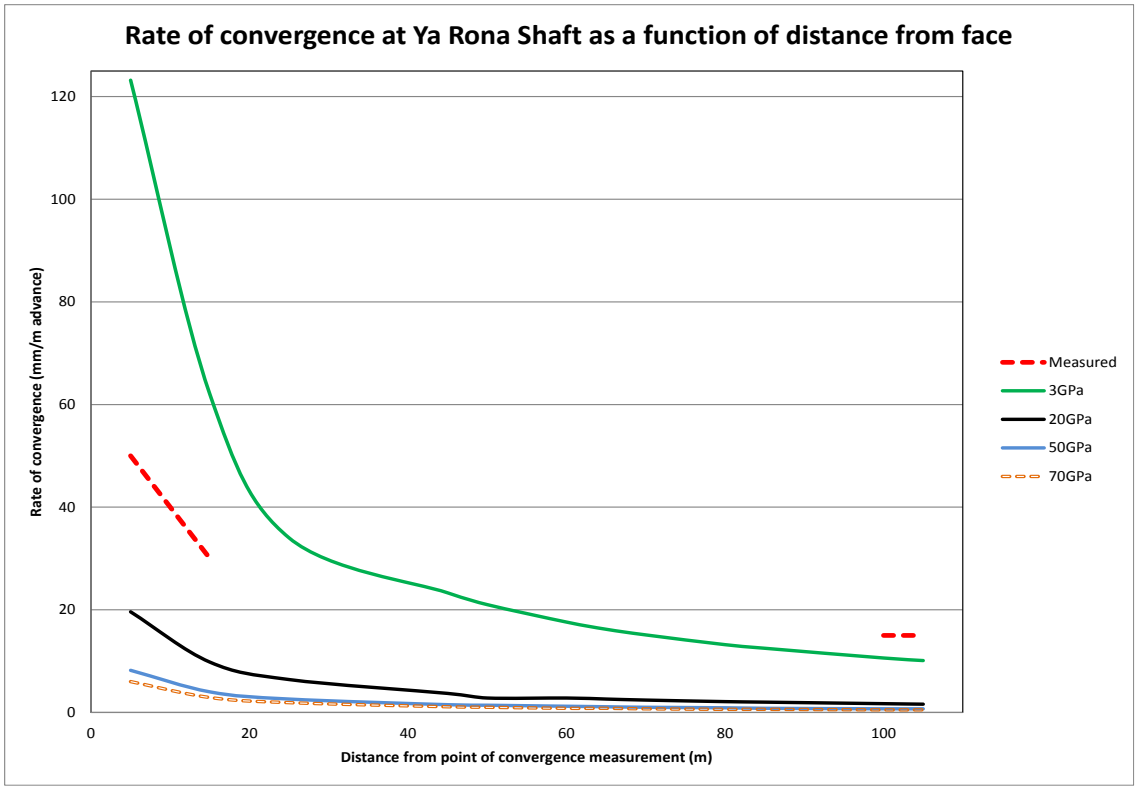


Figure 4-8 Comparison between measured closure and modelled convergences for different values of Young's Modulus (after Van der Heever, 2007)

4.2.4. Rock test data

Apart from the 2006 numerical model calibration using the downgraded UCS, the values for RMR and m_i (Chapter 2, table 2-1) were also adjusted to cater for the observed conditions. It is postulated that the generalized Hoek-Brown failure criteria was used in the 2003 model as it was difficult to procure values for WAF from literature sources. The Hoek-Brown equation (Martin, et al, 1999) is given by Equation 3:

$$\sigma_1 = \sigma_3 + \sigma_{ci}\left(m_b \frac{\sigma_3}{\sigma_{ci}} + s\right)^a \qquad \text{(Eqn. 3)}$$

and the empirically determined parameters are given by equations 4-6 (Martin, et al, 1999):

$$m_b = m_i \exp\left(\frac{GSI - 100}{28}\right) \qquad \text{(Eqn. 4)}$$

$$s = \exp\left(\frac{GSI - 100}{9}\right) \qquad \text{(Eqn. 5)}$$

$$a = 0.5 \qquad \text{(Eqn. 6)}$$

In 2006 WAF rock samples were tested (Yilmaz, 2006). This yielded a low m_b (Hoek-Brown constant m for the rockmass) value of 3 (Appendix B – table B.5.), which is indicative of core with significant fracturing. Good quality lava m_b values (Hoek, 2006), using a GSI value of 75 in equation 4, are approximately 12. Low quality Tuff (Hoek, 2006), indicate values of approximately 2, using a GSI value of 55 in equation 4.

The WAF rock testing (Yilmaz, 2006) also yielded a strengthening parameter β value range of between 4.0 to 4.67. The typical range for β, in equation 7 (Ryder & Jager, 2002), is 3 to10.

$$\sigma_1 = \sigma_c + \beta\sigma_3 \qquad \text{(Eqn. 7)}$$

Therefore, the WAF β value is closer to the lower end of the typical β value range, which is typical of the low strength WAF rockmass.

4.2.5. Geological structures

As is the case in most mining scenarios, geological structures play a vital role in determining how the rockmass will respond to mining-induced stress changes. Mining close to these structures may result in increased levels of dynamic ground motions or seismicity. Therefore, in most deep mines, bracket pillars are designed to reduce exposure to these structures. At the Ya Rona example, WAF is an inherent part of these planes of weakness. A plane of weakness made of weak host rock material will contribute significantly to instability and therefore it is imperative that the numerical model accounts for this.

Table 4-3 shows the list of known seismically active structures (KDCWest, 2012). Figure 4-9 is a plan view of the Ya Rona shaft pillar area, showing the known seismically active features, as well as other faults that have WAF elements within them.

Reference (from Figure 4-9)	**Name Of Structure**	**Dip**	**Reef plane LOI** (Line of Intersection**) Strike**	**Type / infilling / width / thickness / etc** (down-throw in brackets)	**Mmax Recorded / expected**	**Relative seismic potential**
1	Kate's Flt			Normal (30m)	3.3 / 3.5	Moderate
2	R10 Flt	75°W	320°	Normal (15m)	3.0 / 3.2	Low
3	NE/SW Flt (6m fault)			Normal (7m)	3.5 / 3.7	Moderate
5	Syncline axis		Reef syncline	Reef syncline	3.5 / 3.7	High

Table 4-3 List of major geological structures within the Ya Rona shaft pillar (KDCWest, 2012)

The Syncline Axis (Figure 4-9; 5-Syncline Axis), a fold feature (Figure 4-11), changes the strike of the reef as one proceeds east. Therefore the reef dip direction changes from a north-south (N-S) one to an east-west (E-W) direction (Figure 4-10). Located approximately 250m west of the shaft, the Syncline Axis has been the source of many seismic incidents which have damaged both reef workings, as well as the Ya Rona shaft. Due to the geometry, it is often difficult to replicate in an elastic code, but an attempt has been made in this research report. Wilson (2010) indicates that the syncline axis results in ductile folding of the rockmass feature at the base of the feature and brittle failure above (Figure 4-12).

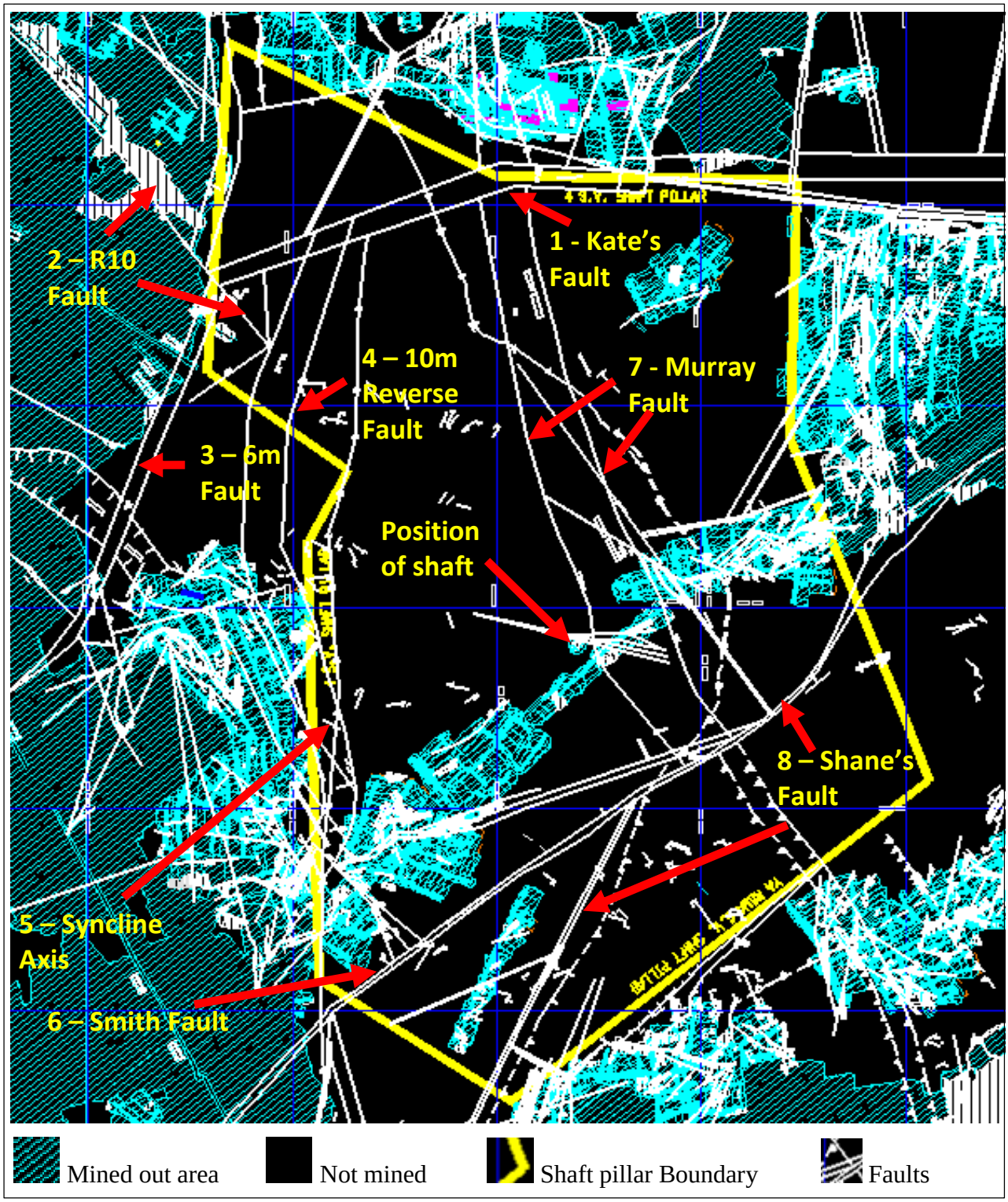


Figure 4-9 CadsMine plan showing location of geological structures within the shaft pillar at Ya Rona and shaft pillar boundary (yellow solid line)

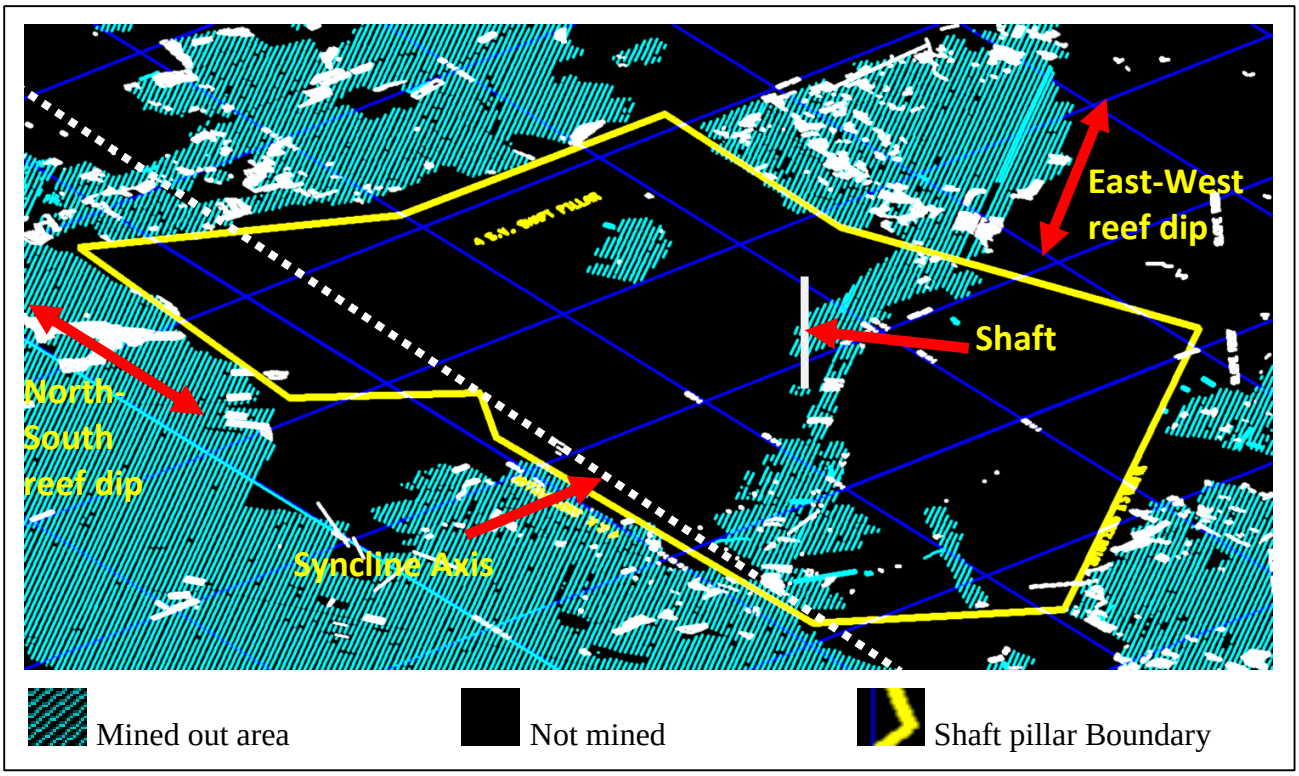


Figure 4-10 CADSMine isometric view of Ya Rona shaft pillar area (yellow border) showing location of shaft, reef dip and the Syncline Axis

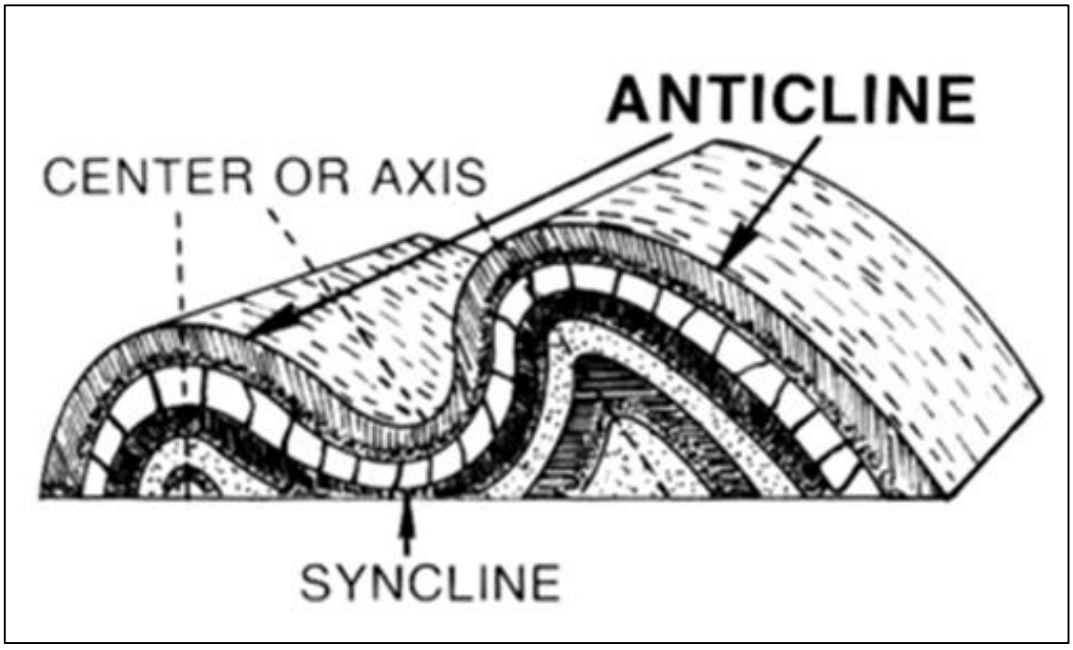


Figure 4-11 Sketch showing folded nature of Syncline Axis (Wilson, 2010)

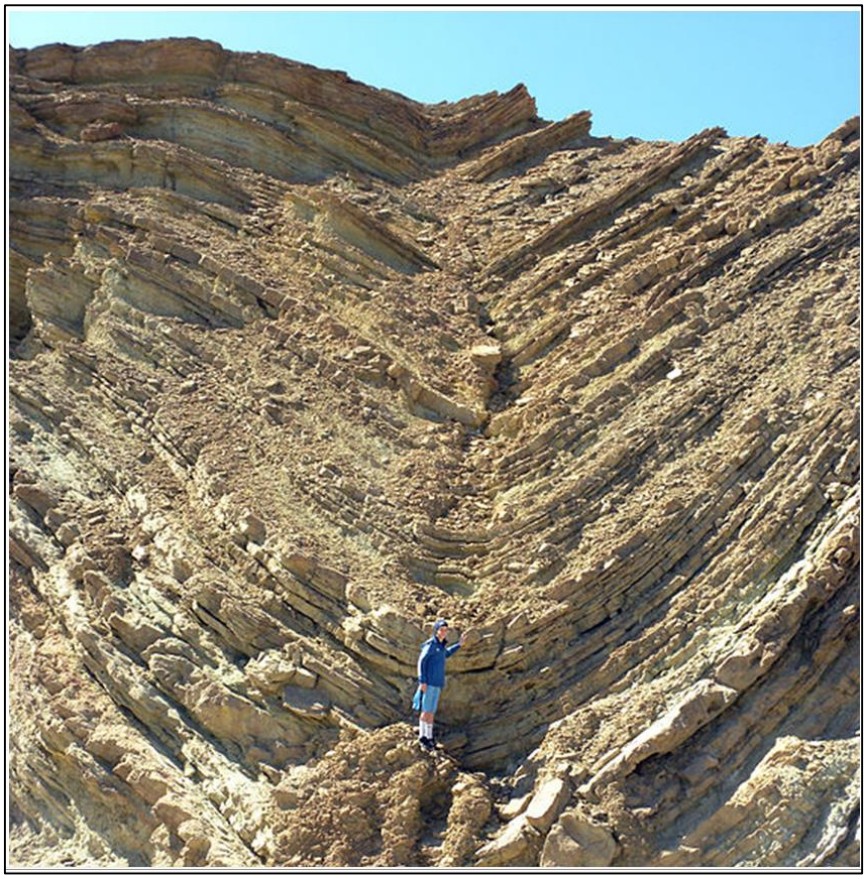


Figure 4-12 Photograph of the Syncline exposed in the lower parking lot of Calico Ghost Town near Barstow, California (Wilson, 2010)

4.3. Selection of input parameters for the numerical modeling

This section focused on verifying the information that would be used in the numerical model. The process is critical as incorrect input data could result in flawed information which will translate into inaccurate designs that could lead to poor decision-making. Poor designs could affect excavation stability and ultimately safety of people.

Table 4-4 is a synthesis of information provided in Table 3-1 and 4-1, and provides a list of rockmass stress and material properties that were used in the execution of the numerical models in this research report.

Although much of the data was available in current literature, a significant constraint was to procure values for the Hoek-Brown failure criterion constants (m, m_i and s). These were especially difficult to procure in light of the fact that much of the rock engineering work has been done in soil mechanics and very little is written on soft rock materials at depth.

Parameter	Value	Comment
Young's Modulus (E)	20 GPa	Van der Heever (2007) – downgraded value for E to be used in elastic modeling to account for inelastic components of closure due to WAF.
Shear Modulus (G)	8 GPa	Single value of 28MPa (Table 4-1) cited, therefore data set inadequate. Relationship between Young's Modulus (E) and Shear Modulus (G) is given by the equation 8: $G = \frac{E}{2(1+\nu)}$ (Eqn. 8) Therefore, calculated value is used.
Poisson's Ratio (υ)	0.24	Average value used in table 4-1, correlates with the equation 9 value of 0.25, using E and G above. $\nu = E/2G - 1$ (Eqn. 9)
Stoping Width	1.8m	Numerically modeled average
Co-ordinate system		Left-handed LO
Z	27.2 MPa/km	Measured stress gradient (Figure 4-2)
Y	18 MPa/km	Measured horizontal stress gradient (Figure 4-2)
X	31.5 MPa/km	Measured horizontal stress gradient in X-direction (Figure 4-2), perpendicular to Y direction
Tensile strength	10.6 MPa	Average value given by table 4-1
Cohesion	3.25 MPa	Average value given by table 4-1
Angle of friction	23^0	Average value given by table 4-1
Uniaxial Compressive Strength (UCS)	57-121 MPa	Current UCS strength value used for support design at Ya Rona to give the worst-case scenario = 57MPa. (Appendix B – table B.3.)
m	3	Value assigned is 5 (Table 2-1); (Martin, et al, 1999) - tunnels in massive to moderately fractured rock, m=0; Yilmaz, (2006) tested WAF and found $m_b = 3$ (Appendix B – table B.5.) m_i value for Tuff (similar to WAF) between 5-20 ((OHMS, 2011)
s	0.11	Martin, et al (1999) found that for tunnels in massive to moderately fractured rock, s = 0.11
β	4.34	4 to 4.67 (Appendix B – table B.4.); average used
F	0.7	See notes on equation 1, chapter 3

Table 4-4 List of rockmass stress and material properties used as input parameters in the Ya Rona shaft pillar numerical model

5. The effect of WAF in the numerical modeling

5.1. Introduction

In the last chapter input parameters were described, calibrated and a sensitivity analysis conducted to ascertain what input data was required for the numerical models. Although numerical models have their limitations, the method is easy, reliable and replicable at producing information for use in rock engineering design. Different scenarios can be easily manipulated so that areas susceptible to damage can be identified with a view to optimizing layouts, before mining has occurred, so that hazards are reduced. The process also subjects the information generated from the analyses to a set of failure criteria that can be used to determine whether a particular layout will be hazardous or not.

Based on the discussions in the previous chapters, it is likely that the WAF rockmass environment will take on an increased hazard profile. Therefore, within this context, the numerical model is a critical component in the rock engineering design process, in that the additional loads and deformations that excavations will be subjected to, will need to be identified and appropriate mitigation measures be enforced. However, the scope of the research report is not large enough to cover the entire project and therefore, only stability analyses of the three most important aspects (Chapter 2, Section 2.5), from a rock engineering design perspective, are concluded. These are the:

1. Ya Rona Sub-Vertical Shaft,
2. Large displacement regional geological structures, and,
3. Life of Mine (KDCWest, 2012) mining plan.

These aspects were also selected because the WAF rockmass is either in direct contact with the aspect, directly overlays it, is part of, or contributes in some way to the instability of the excavation or structure at the Ya Rona Shaft Pillar Extraction.

In this chapter, the numerical modeling used for the analyses is described. The results from the models are interrogated against the set of failure criteria described in Chapter 2 of this research report. The objective is to compare the impact of the lower strength WAF input parameters in the elastic numerical model and the higher strength properties used in the

inelastic numerical modeling conducted by Leach (2003), thereby showing what impact the WAF has on the rock engineering design at the Ya Rona shaft pillar extraction.

5.2. Objectives of the numerical models

The stability analyses will attempt to answer the following questions:

- Within the WAF environment, will the shaft be unstable during the mining phases?
- If instability is noted, what mechanism/s will drive the deformation?
- Under the lower strength conditions, at which stage of the mining process is the shaft most susceptible to failure and/or damage?
- What impact will stress have on the shaft?
- If the strength of the fault planes are lower due to the WAF, are they likely to be more or less stable than if they were made of higher strength material?
- Which faults are more susceptible to rupture?
- Are the regional stability pillars adequate to promote stability, taking cognizance that the pillar material is weaker?
- Can the WAF rockmass promote the future mining layout?

5.3. Overview of the numerical models

Two numerical modeling codes were used to simulate the mining layout:

- BesolMS
- 3DEC (Leach, 2003)

BesolMS is an elastic code, used for solving rock engineering problems based on boundary-element displacement discontinuity methods of analysis. The model illustrates a tabular orebody that is homogenous, isotropic and linearly elastic (Karabin, et al, 1999). BesolMS was selected because it has 3-D, multi-seam, and off-seam stress/strain capabilities.

Backfill was not used in the elastic models. In chapter 4 of this report, the rate of convergence was compared to the actual underground measured closure. Although backfill was placed underground, no backfill was used in all the iterations of the elastic numerical

model. Despite the lack of backfill in the model, the actual underground measured rate of closure compared favourably with the numerical model's rate of convergence. Furthermore, in terms of the rock engineering design, the use of backfill in the numerical model would produce a less conservative result. Moreover, backfill was excluded from the numerical models because far less than the industry norm of 60% of the area mined, had been filled. Therefore, based on the reasons presented above, the author chose to exclude backfill from successive iterations of the elastic numerical modeling.

The three-dimensional code, 3DEC model, allows explicit representation of structures (Leach, 2006), *"which can "day light" in stopes, a feature that is not possible with more conventional modelling codes such as the boundary element codes MinSim and Besol-MS. The 3DEC model comprises a series of elastic blocks, which are cut through by planar partings, which define the various stratigraphic units, as well as the geologic structures"*.

5.3.1. The BesolMS model

The Life of Mine plan for the calendar year 2012 (LOM12) was simulated using a 15 mining step sequence representing 15 years of mining. As the Besol package can only simulate 12 mining steps, two numerical models (Figures 5-1 and 5-2) were used to model the mining sequence.

A brief description of the mining plan shows:

1. The mining of a 30m long (in the X-direction) x 30m wide (in the Y-direction) around the shaft, termed the inner-inner pillar (Figure 5-1). As WAF is known to have a high closure rate, the rock engineering design required that this step be mined in the higher strength quartzite footwall rock so that vertical convergence of the shaft is minimized.
2. The rock engineering design also required that steps 3-5 occur in a sequenced manner (termed 'opening of the eye') so that when ride and tilt of the shaft occur, it will be in a geometrically uniform manner, that is, it will occur equally on the eastern and western flank of the shaft.
3. Stoping will, thereafter, continue in a sequenced manner allowing for symmetry along the shaft axis until the designed pillars are reached.

Note that for purposes of clarity when viewing Figures 5-1 and 5-2, the BesolMS numerical model representing the LOM12 mining sequence, step 11 in Figure 5-2 is the same as step 1 in Figure 5-1, and step 12 in Figure 5-2 represents steps 2-12 in Figure 5-1.

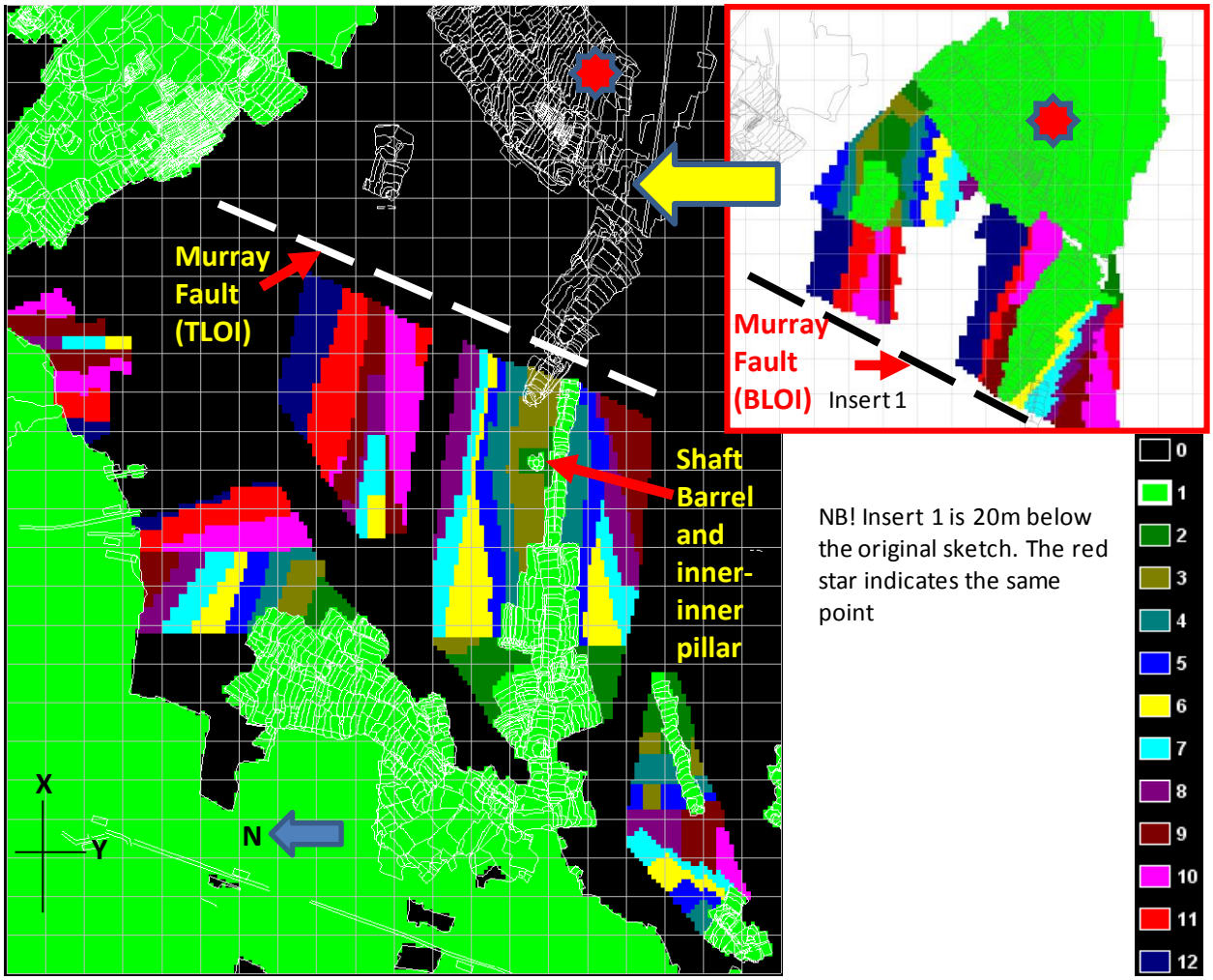


Figure 5-1 Besol simulation of mining plan showing the mining steps 1-12

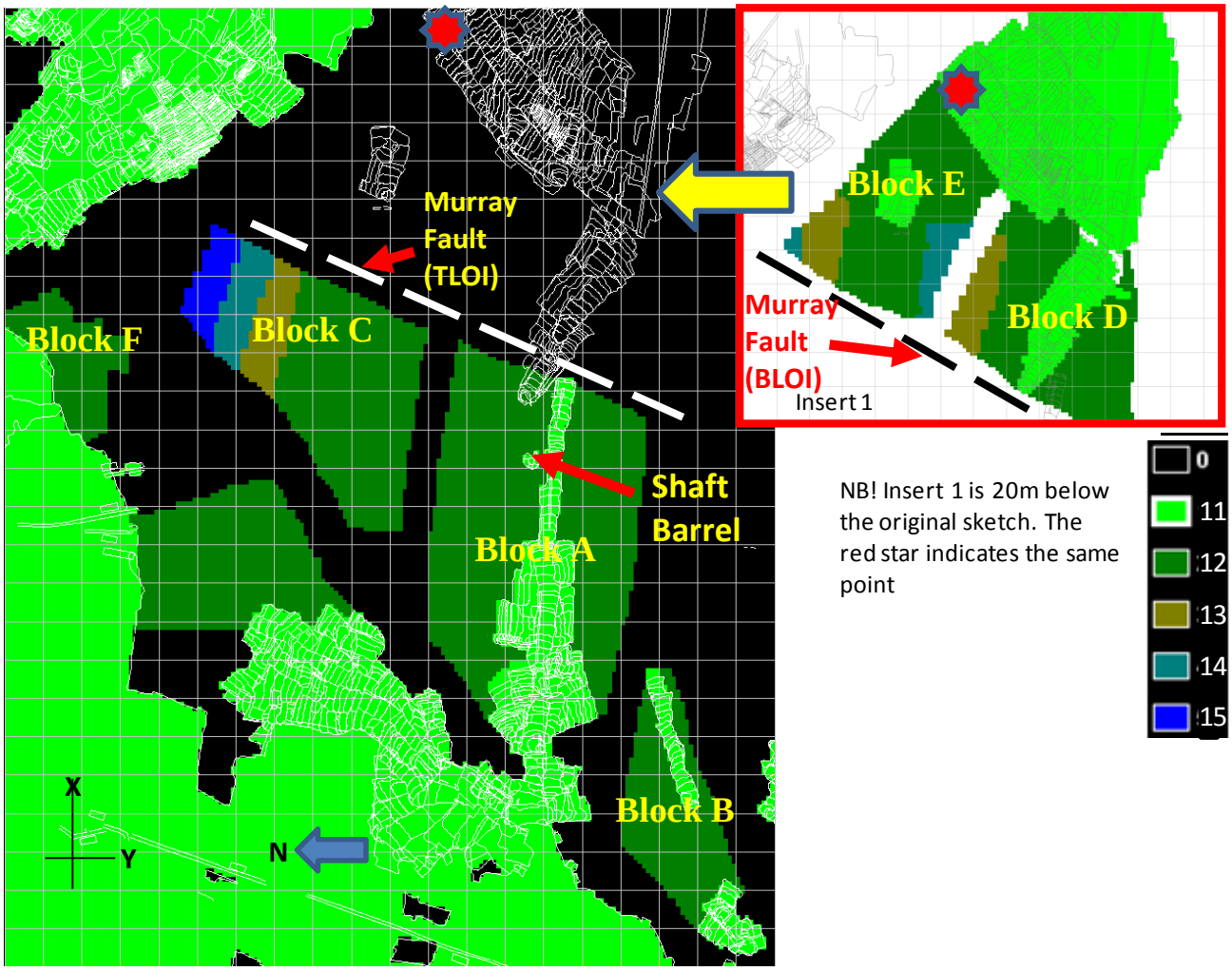


Figure 5-2 Besol simulation of mining plan showing the mining steps 11-15

Figure 5-3 shows the 20m reverse throw Murray Fault which results in an overlap of mining when the reef plane intersects the feature. For the purposes of orientation to figures 5-1 and 5-2, this fault is represented by the white dotted line on the main plan as the top line of intersection (TLOI) of the reef, and on the insert, the same feature is represented by the black dotted line on the bottom line of intersection (BLOI). The Murray fault intersects the shaft (Figure 5-3) at approximately 2525m below surface. The red star on both the main plan and the insert, represent the same point in the horizontal plane, but 20m apart vertically.

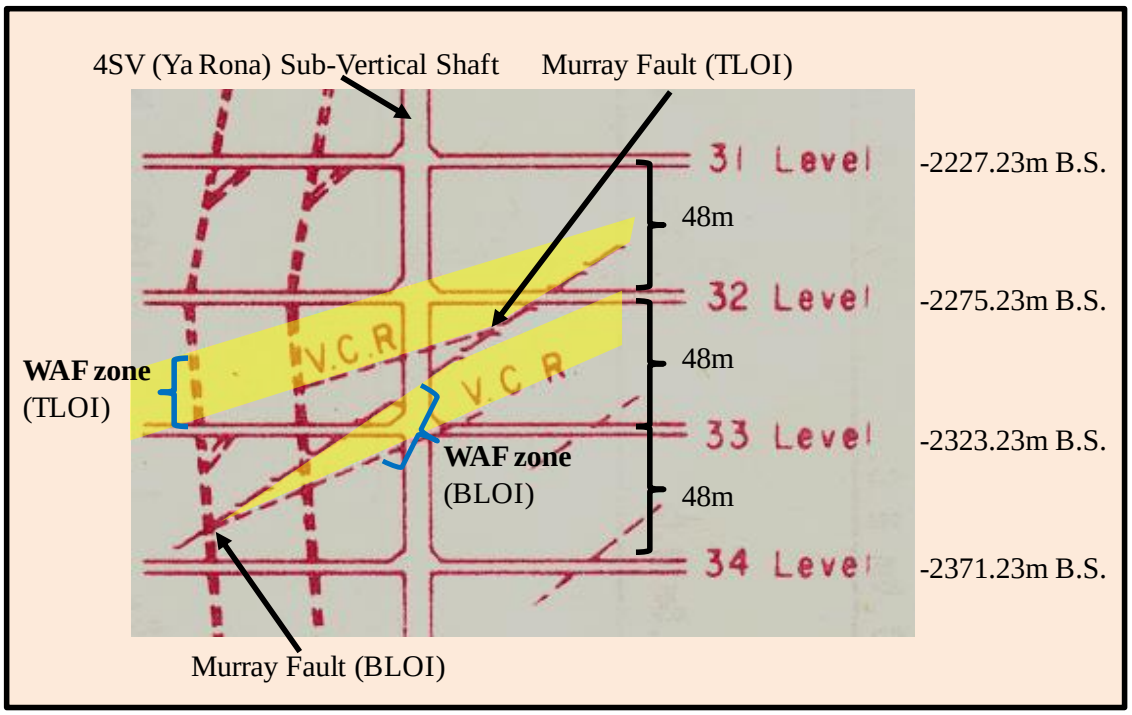


Figure 5-3 Section, looking north, of 4SV (Ya Rona) shaft excavation showing WAF zones above reef contacts and Murray Fault through shaft barrel

5.3.2. The 3DEC model

The 3DEC numerical model (Leach, 2003) was undertaken using good quality rockmass characteristics and then revised (Leach, 2006) using poorer quality WAF rockmass estimates. Table 2-1 shows the different input parameters used in the two iterations and the output data is reflected in Figures 2-6 and 2-7. Leach (2006) concluded that neither the 2003, nor the 2006 input parameters, were correct for the WAF rockmass. The models were used for comparative purposes which would serve as the potential range in which the WAF rockmass behaviour could be placed. The rock engineering design team could therefore base their designs within that range.

In this research report, the output information from the 2003 numerical is used, as more of an in-depth analysis of shaft barrel stability was conducted. Figure 5-4 shows the 3DEC, 2003 numerical model (3km cube) representing the mining sequence and the geologic data available at the time. Figure 5-5 shows the plan view of the 3DEC mining simulation. Table 5-3 shows the input parameters used in the 2003 model.

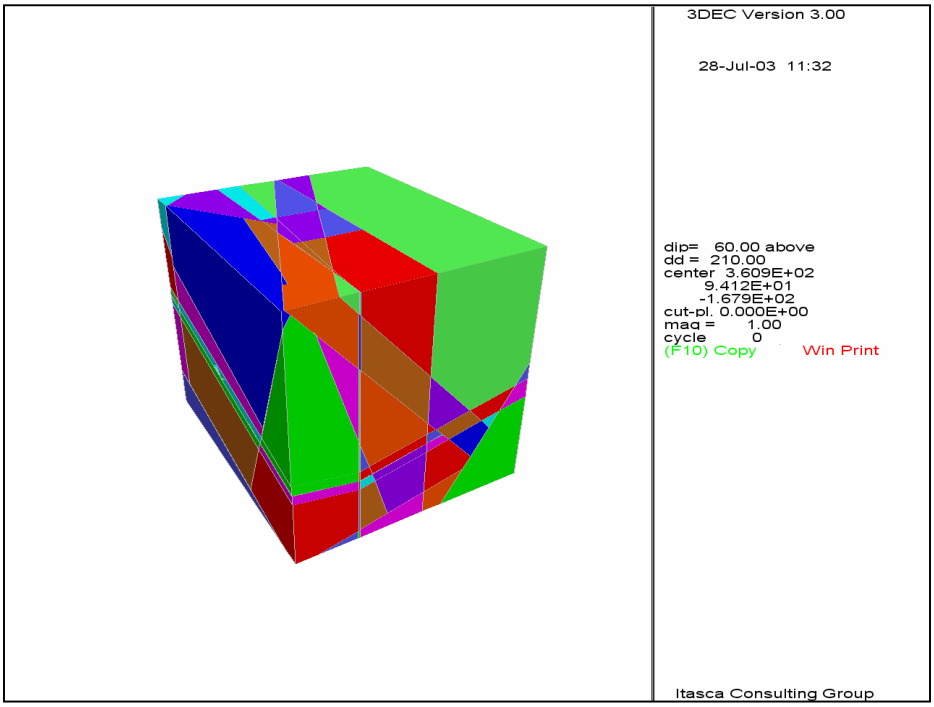


Figure 5-4 Isometric view of the 3DEC numerical modelling showing planes representing geological structures (Leach, 2003)

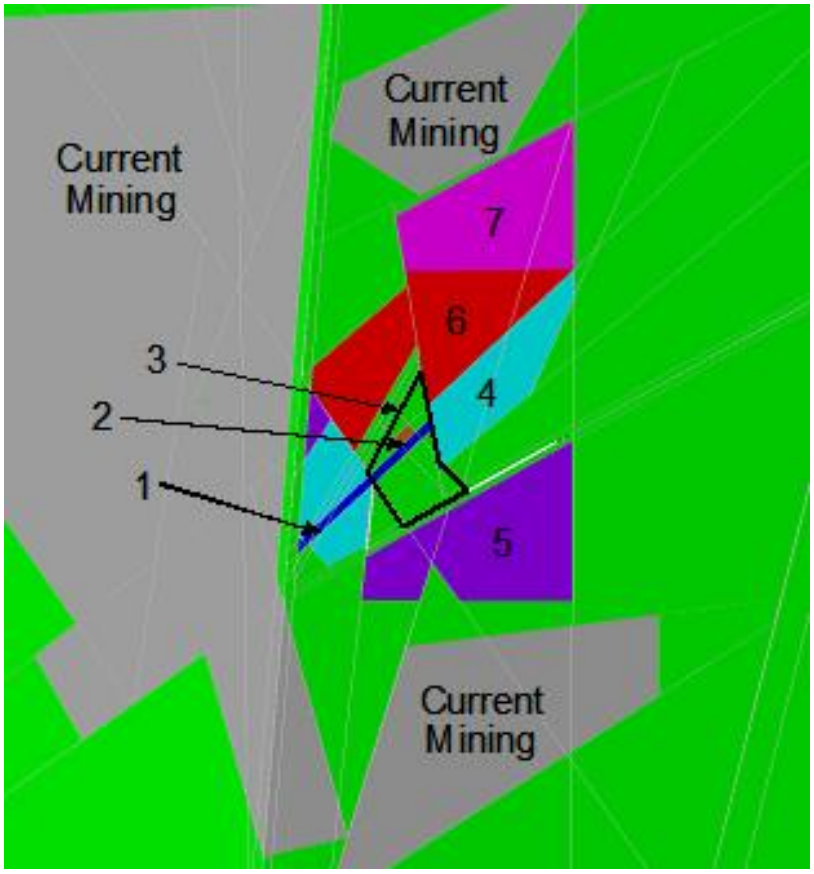


Figure 5-5 Plan view of mining sequence in the 3DEC numerical modelling (Leach, 2003)

Parameter	Value
Young's Modulus (E)	56 GPa
Shear Modulus (G) for Lava hangingwall	33 GPa
Poisson's Ratio (υ)	0.2
RMR	55
TZZ	27 MPa/km
TYY	13.5 MPa/km
TXX	13.5 MPa/km
Uniaxial Compressive Strength (UCS)	150 MPa
m_i	10

Table 5-1 Input parameters used in the 3DEC model (Leach, 2003; Tkloweni, 2007)

5.4. Stability assessments

5.4.1. Shaft stability assessment

Chapter 2, Section 2.5 of this research report identified five failure criteria to which the results of the numerical modeling for the Ya Rona shaft would be interrogated against. As a reminder there were previously stated as:

- Stress imposed on the shaft barrel,
- Horizontal and vertical displacement of the shaft as a result of the reef mining,
- The mining-induced vertical strain,
- Tilt of the barrel, and,
- Ride of the stoping excavation next to the shaft that may impact on shaft stability.

However, the BesolMS numerical modeling code, in the current form, is unable to assess tilt. Therefore, no comparison is possible between the low strength WAF and higher strength material used in the Leach (2003) models. Invariably, tilt would be catered for in the engineering design of the suspended steelwork and therefore, is beyond the scope of this report.

Vertical strain will also not be discussed as during the result analysis there seemed to be two orders of magnitude between the results from the Leach (2003) 3DEC numerical models and those of the BesolMS numerical models. No valuable correlation and comparison could be made from the analysis.

However, as stated in Chapter 2, Section 2.5 of this research report, an RCF analysis will be conducted.

For purposes of clarity in the graphs of the shaft that follow, distance from the reef plane will be indicated as negative or positive (Figure 5-6). A negative intercept on the X-axis will imply that that those values occur in the hangingwall of the reef whereas a positive intercept on the X-axis will imply that those values occur in the footwall of the reef.

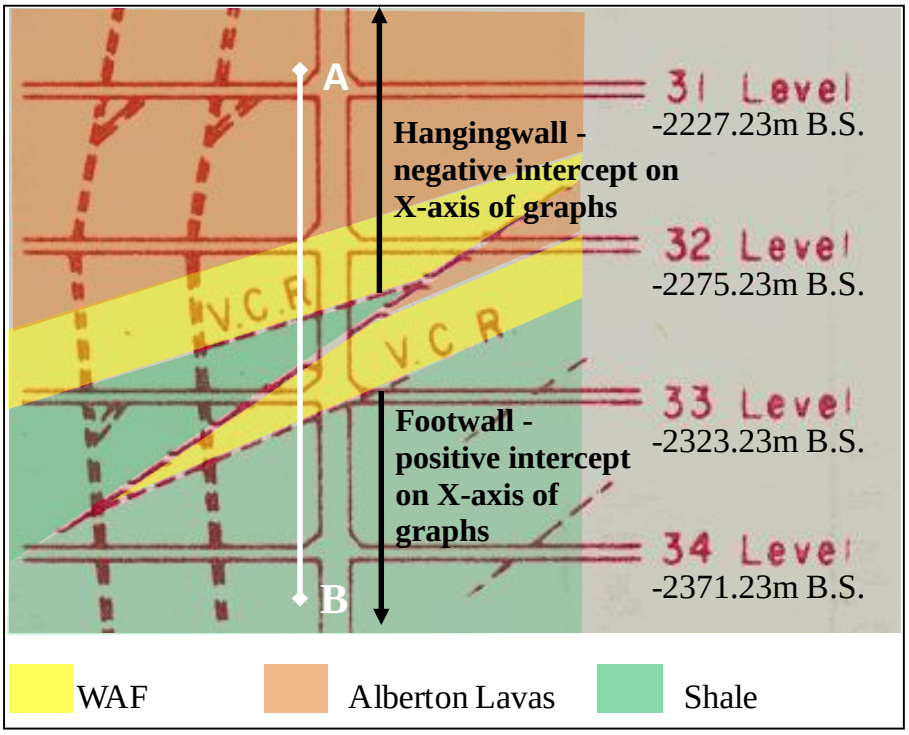


Figure 5-6 Sketch indicating hangingwall and footwall of reef at Ya Rona, as well as Section A-B showing line of analysis for RCF, Vertical and Horizontal displacements at Ya Rona Shaft

5.5.1.1. Stress imposed on the shaft

Figure 5-7 shows the graph of the modelled vertical stress in relation to distance from the reef plane. The graph shows that during Step 1 of the mining plan, both the 65m hangingwall section, including the 19m WAF zone and the 75m footwall section exceeds the 29MPa failure criterion, as set out in Chapter 2, Table 2-3. This continues till step 5, when the entire

section under investigation, fall below the failure criterion. Stress relaxation of the shaft is then deemed to have occurred.

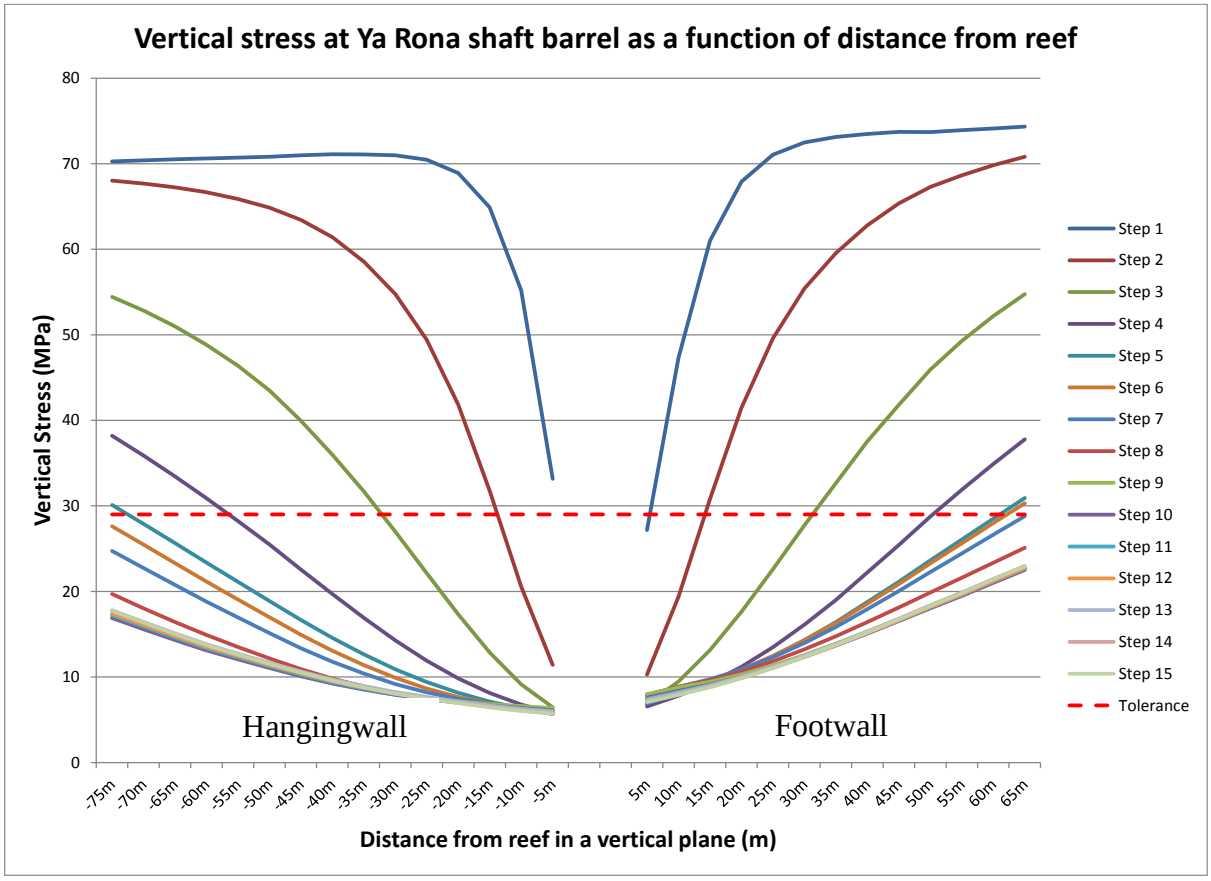


Figure 5-7 Vertical stress along the Ya Rona shaft for the unfilled BESOL model

Figure 5-8 shows the 3DEC vertical stress results of a 1km section of the Ya Rona shaft. The yellow highlighted portion in the graph shows the same zone that was analysed for the BesolMS model in Figure 5-7. The effect of backfill is also indicated in this graph. Leach (2003) reports that *"the backfill results in regeneration of compressive stresses close to reef with locally very high values…thought to result from thrust on the reverse fault driving stope closure and backfill compression….Backfill placement limits fault slip, which in turn maintains the load-bearing capabilities of the pillar between the up thrown and down thrown reef blocks. This results in stress concentration around stope abutments that increase stress on the shaft below reef."* From this discussion, the 3DEC model infers that the footwall below reef will be more susceptible to damage than the hangingwall due to the "punching" effect of the pillar between reef sections. The BesolMS model concurs with this result showing higher stresses in the footwall (Figure 5-7).

Figure 5-8 shows the 3DEC numerical model which shows that the shaft is in compression (3DEC negative sign convention is compression) in the both filled and unfilled cases.

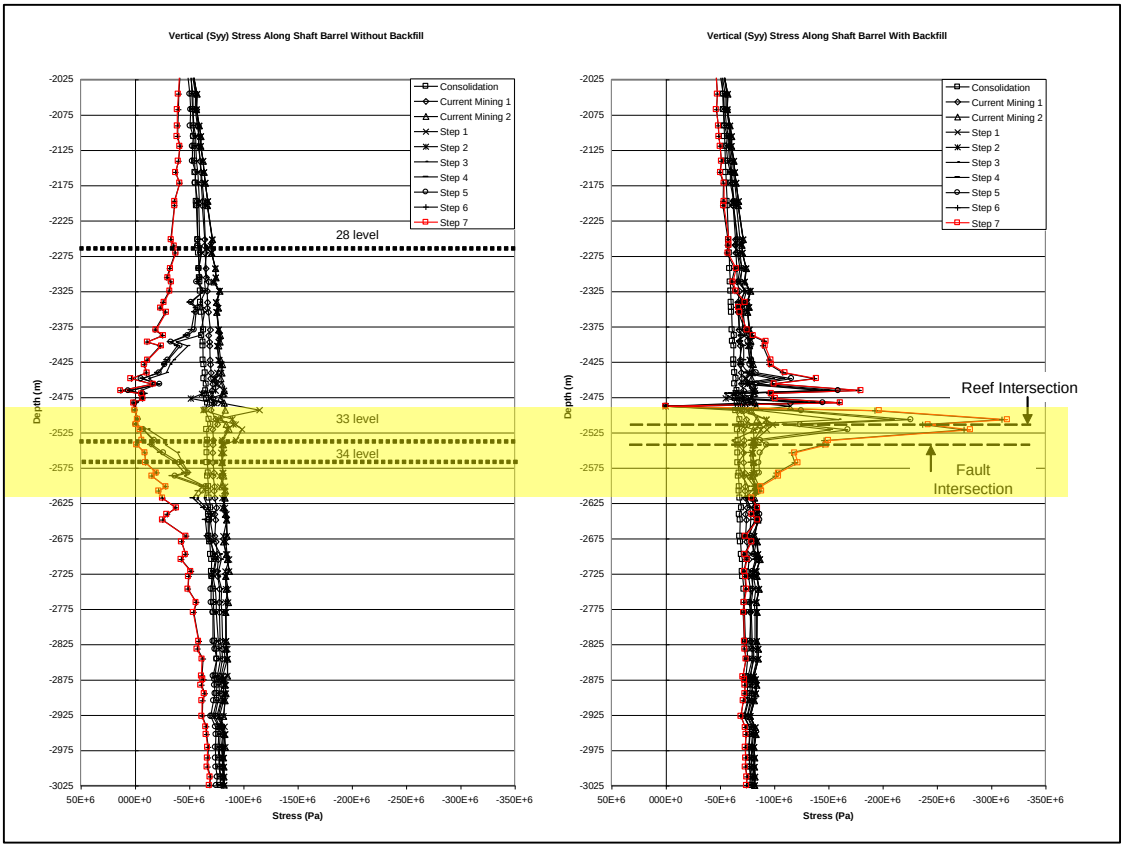


Figure 5-8 Vertical stress along the Ya Rona barrel for unfilled and filled 3DEC models (after Leach, 2003)

5.5.1.2. Vertical and horizontal displacement of the shaft

Although it is generally important to consider shaft dislocations (different off-setting of shaft sidewalls from their original positions) as primary considerations during shaft analyses, greater focus was placed on vertical and horizontal displacements of the sidewalls of the shaft. This shift in focus was mainly due to large measured deformations (Durapraj, 2006b) occurring in the stope horizon, as well as additional moiling of the shaft sidewall (Durapraj, 2007) in the WAF zone (Chapter 2, Figure 2-10), in response to radial displacement (reduction in the shaft diameter) of the shaft concrete lining. Therefore, for the rock engineering design, vertical and radial displacement of the shaft sidewalls assumed greater importance.

5.5.1.2.1. Vertical displacement

Leach (2006) showed that the modeled cumulative displacement along the vertical axis of the shaft barrel was 1.0m, with a 0.2m displacement in the horizontal axis. By using a Factor of Safety (FOS) of 1.5, the rock engineering design team established that the allowable tolerance for the shaft suspended steelwork be 1.5m to accommodate the vertical modeled shortening of the steelwork. However, if the displacements exceeded this tolerance, the steel sections would be cut and replaced.

Figure 5-8 shows the Section A-B along the vertical axis of the Ya Rona shaft along which the analyses for RCF, vertical and horizontal displacements were taken using the BesolMS model. Figure 5-9 provides an indication of direction (X, Y and North) and the 7.3m wide Ya Rona shaft diameter the Ya Rona shaft. Figure 5-10 shows the plot of vertical displacement as a function of distance to reef.

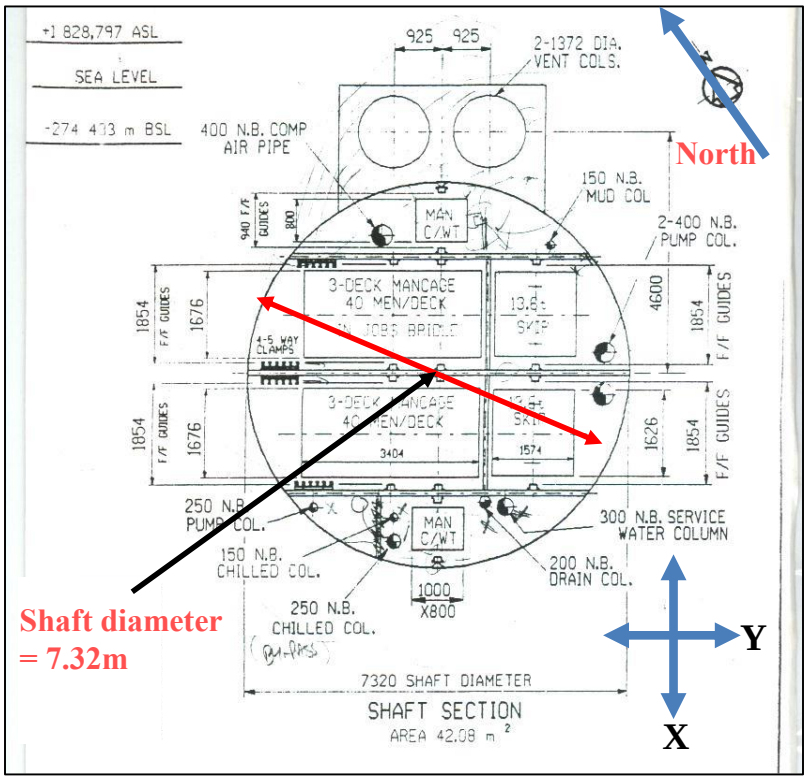


Figure 5-9 Plan section of Ya Rona Sub-Vertical Shaft showing true north, X and Y directions (after Leach, 2006)

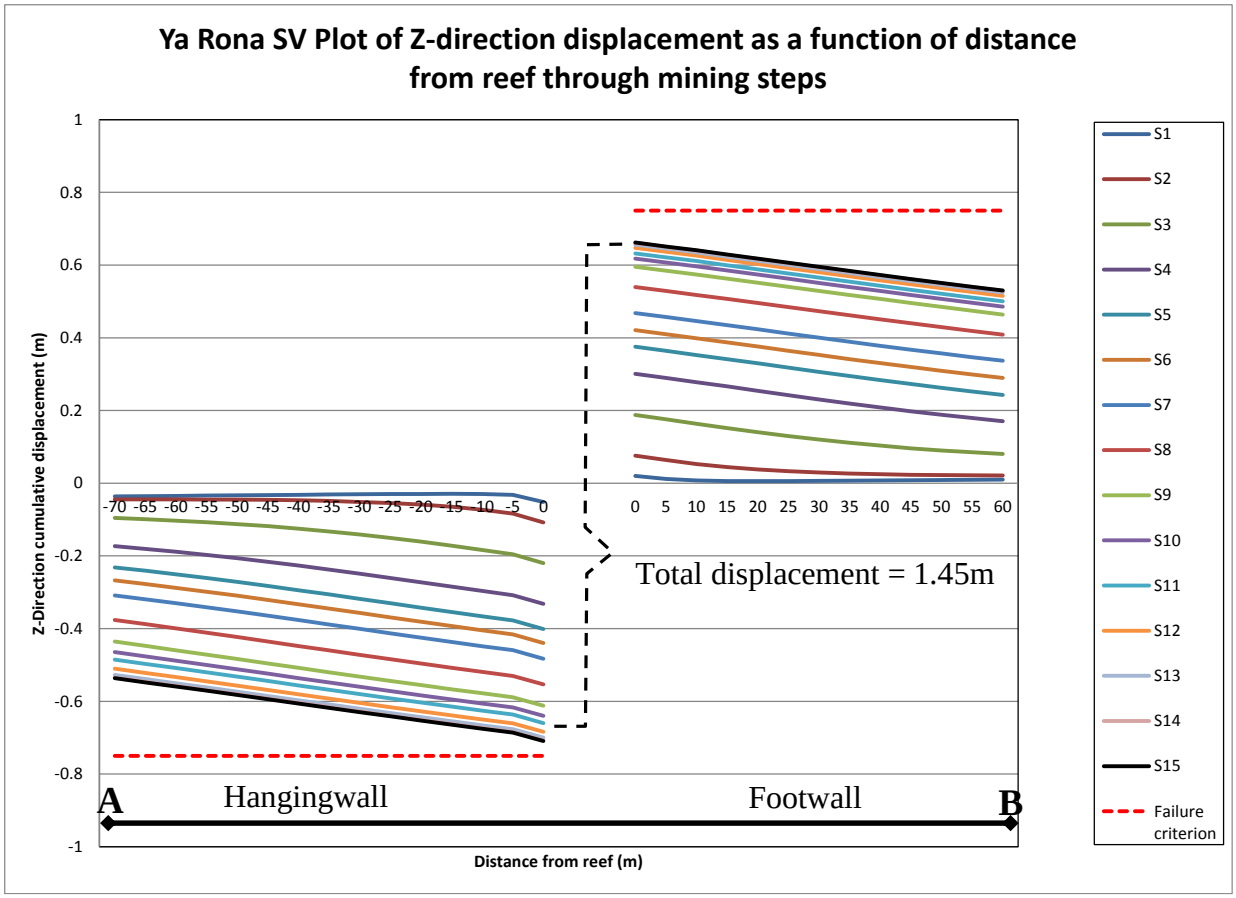


Figure 5-10 Cumulative displacement in the Z-direction as a function of distance to reef through 15 mining steps at Ya Rona shaft

Figure 5-10 shows that:

- Using the WAF rockmass, vertical displacement increases by 45% increase as opposed to the Leach (2006) 3DEC displacement results. The BesolMS model indicates a cumulative displacement of 1.45m;
- The failure criterion is met, except that no FOS is available. Chapter 2, Table 2-3 sets the total vertical tolerance at 1.5m;
- Whereas the good rockmass data in Leach (2003) shows that most of the displacement occurs in the last stages of mining, the lower strength WAF model indicates that almost 25% of the total vertical displacement occurs in the initial steps 1 to 3. Step 3 is the removal of the 30m x 30m inner-inner pillar closest to the shaft;
- Steps 4 to 5 show a further 25% (0.1-0.4m) deformation when the 'opening of the eye' is in progress; and,
- Thereafter, the rate of vertical displaceemnt reduces from step 8 to 15.

5.5.1.2.2. Horizontal displacement

As described previously, the rock engineering design team focused on the consequences of the pseudo-plastic behaviour that the WAF exhibited. Leach (2006) established that the radial displacement (Figure 5-11) could theoretically be as much as 4.5m (Chapter 2, Figure 2-7). The result was presented within the context that the low WAF rock strength of 30MPa was used in the numerical model. Furthermore, backfill or any other restraining forces (support and concrete lining) were not computed in the numerical model. For the purposes of this research report, only X and Y displacements could be determined from the elastic models.

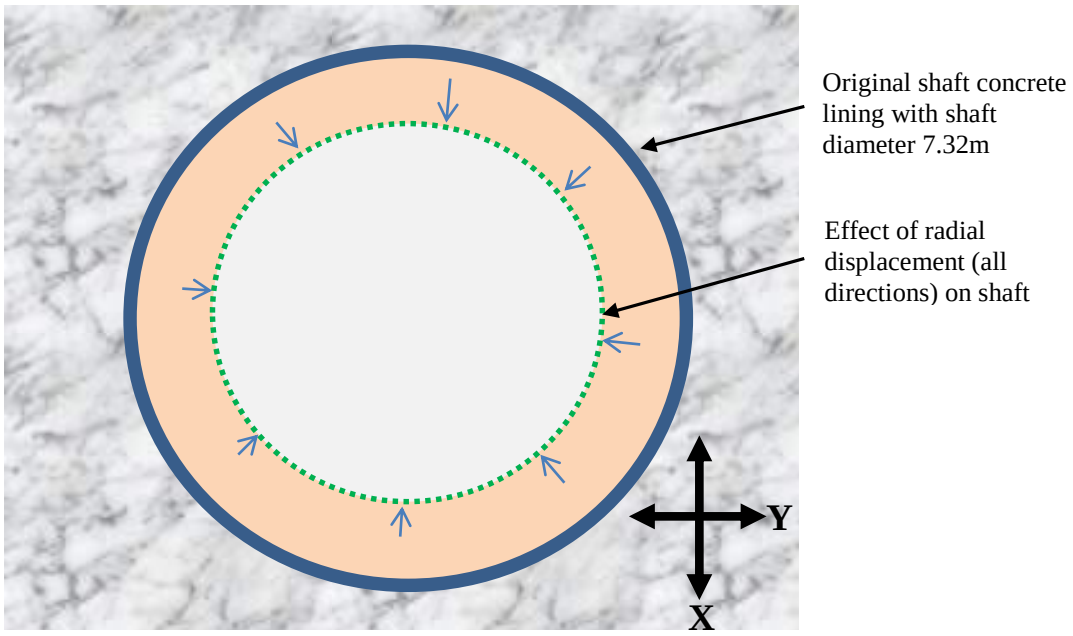


Figure 5-11 Sketch showing exaggerated radial displacement of Ya Rona shaft

Figure 5-12 and 5-13 show the cumulative displacement in the horizontal Y-direction and X-direction respectively. The radial displacement tolerance (Chapter 2, Table 2-3) was set at 0.15m. Therefore, across the shaft diameter, a total of 0.3m displacement could be tolerated. Using a FOS of 1.5, this tolerance would be reduced to 0.2m. However, this displacement could not be tolerated as the shaft steelwork was only 0.15m from the concrete lining. Therefore, from an engineering perspective, only 0.15m of radial displacement could be allowed.

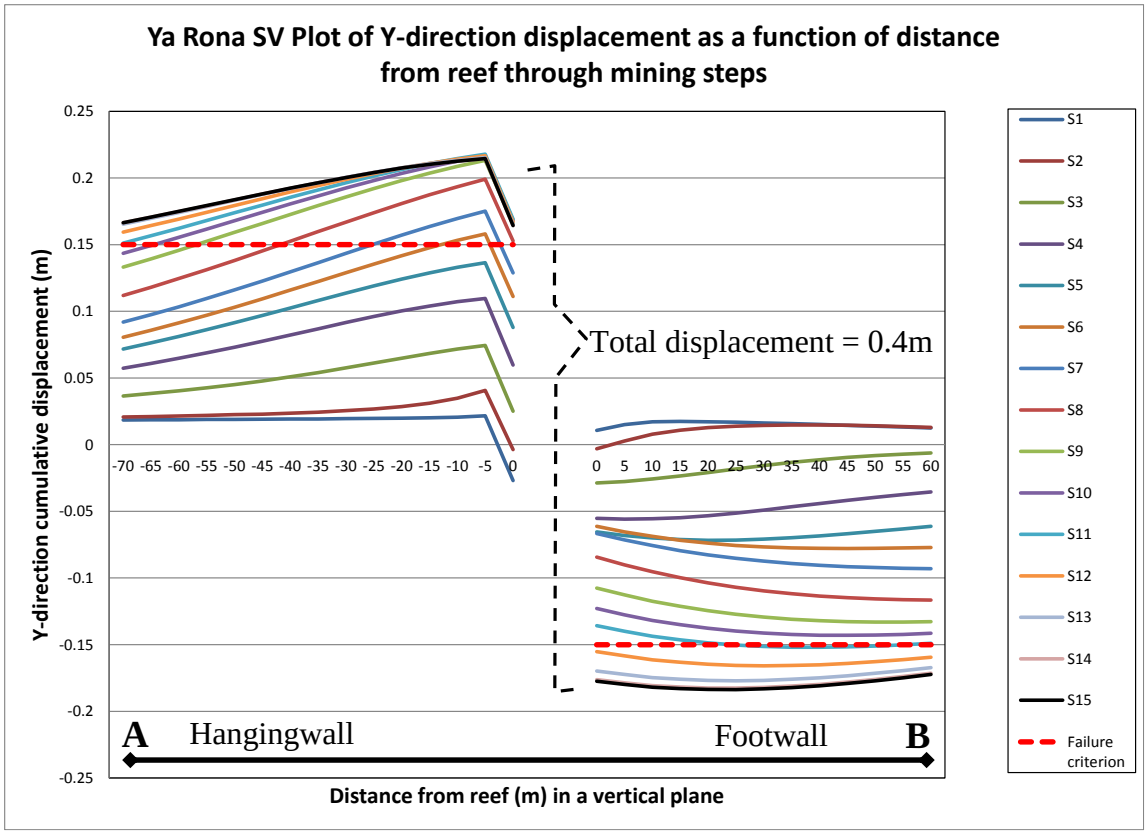


Figure 5-12 Cumulative diplacement in the Y-direction as a function of distance to reef

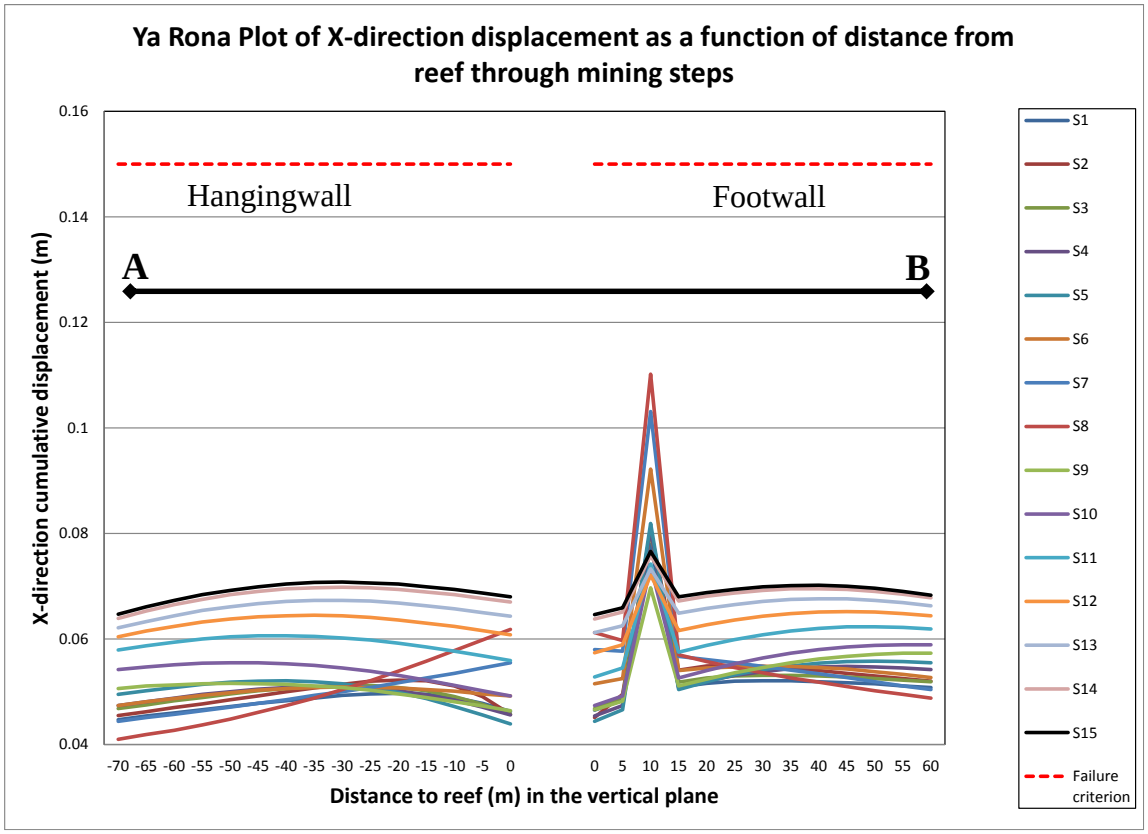


Figure 5-13 Cumulative displacement in the X-direction as a function of distance to reef

Figure 5-12 shows the cumulative displacement in the Y-direction. Key points of note are that:

- The cumulative displacement in the horizontal direction is approximately 0.4m. The tolerance was set (Chapter 2, Table 2-3) at 0.3m. Therefore displacement is 33% more than the tolerance;
- As with the vertical displacement, 25% of the total Y-direction displacement occurs up to step 2, which is the removal of the 30m x 30m inner-inner pillar;
- Steps 3 to 5 represent another 25% of the total Y-direction displacement, when the 'opening of the eye' is in progress;
- The failure criterion is exceeded at step 7 in the WAF hangingwall. The footwall only exceeds the criterion at step 8; and,
- Of note is that during step 1 and 2 positive displacement is exhibited, particularly in the footwall. This means that the hangingwall and footwall are moving in the same direction at the Murray Fault area (Figure 5-3).

Figure 5-13 show the cumulative displacement in the X-direction. Key points of note are that:

- The failure criterion is not exceeded in this direction (maximum displacement is 0.11m at Murray Fault zone in footwall), hence noticeable dog-earing will occur in the shaft as the Y-direction displacement is 0.4m;
- As with the vertical displacement, the largest changes occur up to step 5, when the 'opening of the eye' is in progress; and,
- The spike in the graph represents displacement at the position where the Murray Fault (Figure 5-3) intersects the shaft.

5.5.1.3. Ride in stoping excavations near the shaft

Although much emphasis was placed on shaft displacement, it is still important from a rock engineering design point of view, to assess the modeled ride. Figure 5-14 shows approximately 190mm of ride occurring in the Y-direction, driven by the high horizontal stress gradient (k-ratio = 1.15) and the low strength WAF material. Insignificant ride occurs in the X-direction. High ride magnitudes are observed up to step 9 when mining reaches the stabilizing pillars. No criteria for ride is stipulated.

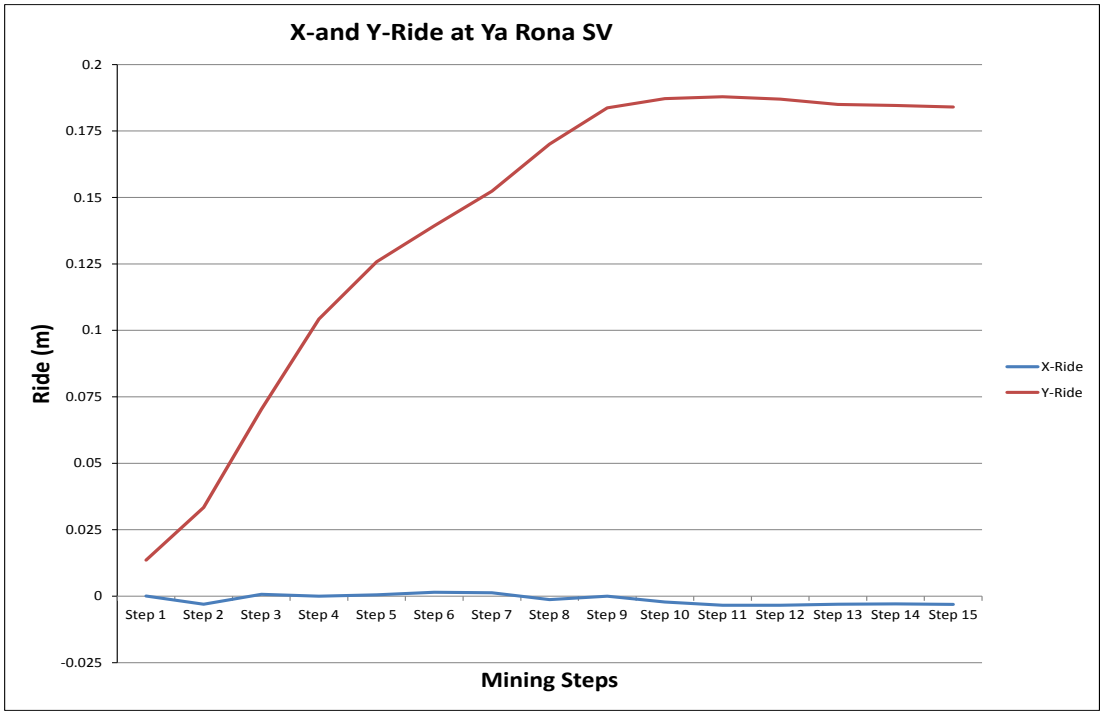


Figure 5-14 X-and-Y-Ride at the Ya Rona Shaft

In the 3DEC modeling, Leach (2003) highlighted similar potential displacements (Figures 5-15 to 5-18). Note that the scales in these figures are exaggerated. The numerical models included a k-ratio of 0.5 with relatively stronger WAF rockmass properties combined with not backfilled and backfilled stopes. The backfilled stopes resulted in a 15mm reduction in displacement in the X-direction, and 60mm in the Y- direction at the last stage of mining.

Figures 5-15 and 5-17 indicate maximum values of approximately 80mm in Y-direction and 100mm in X-direction, respectively, in the 3DEC models for ride at the Ya Rona shaft using stronger WAF rockmass properties and a 0.5 k-ratio. Using the lower strength WAF properties and the correct k-ratio, approximately 190mm of ride in the Y-direction is observed. This represents more than a two-fold increase in ride at the last stage of mining in the WAF environment.

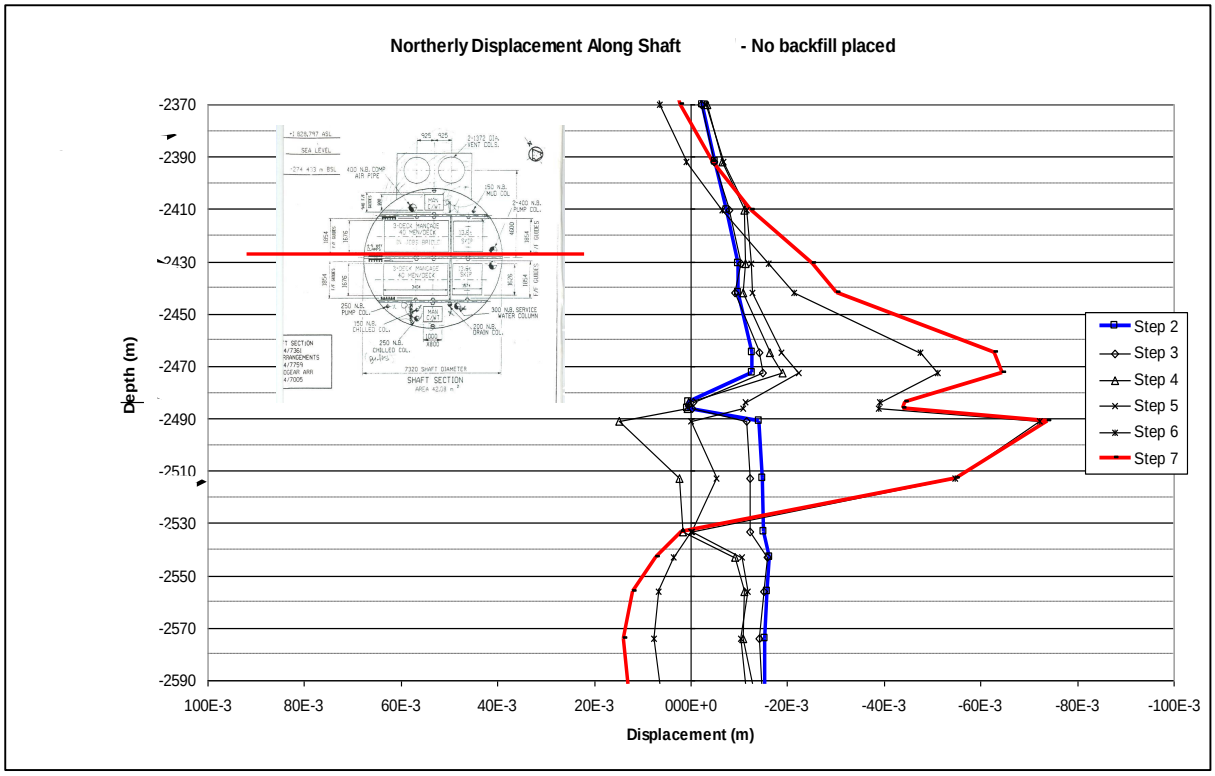


Figure 5-15 Displacement in the Y-direction of the Ya Rona shaft for unfilled models (after Leach, 2003)

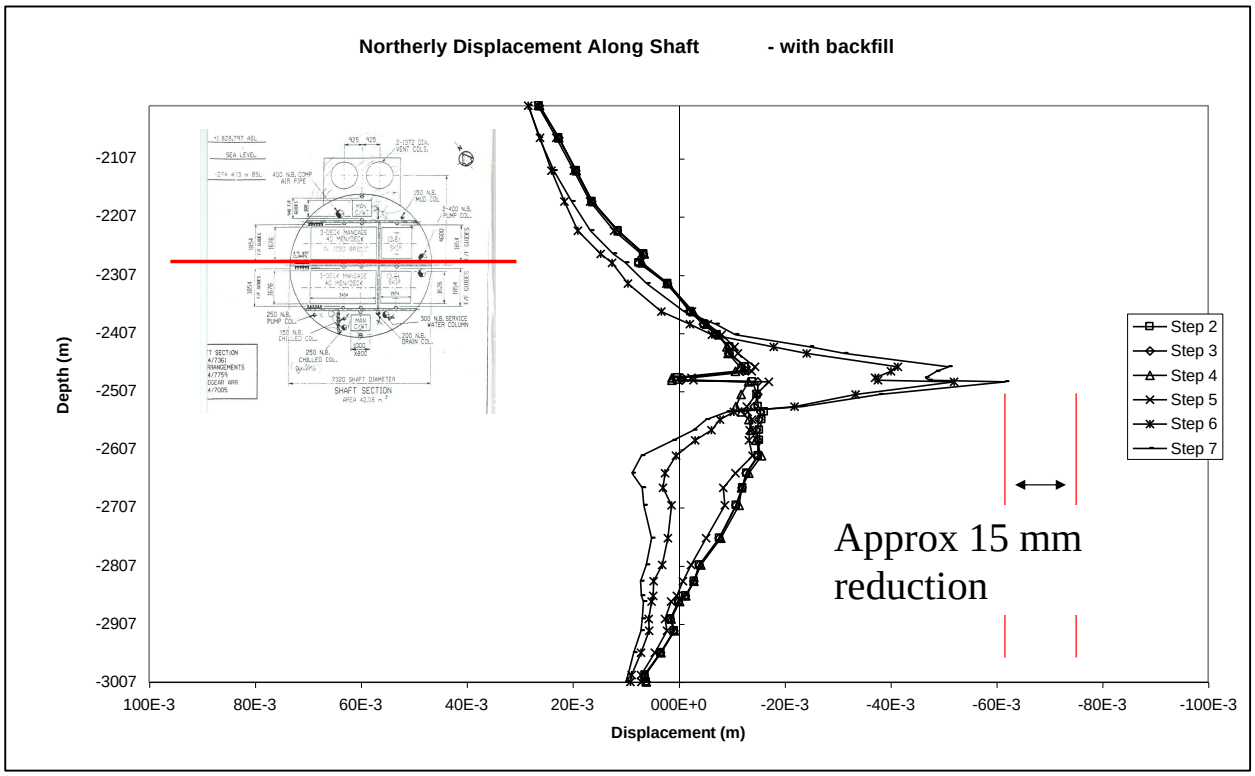


Figure 5-16 Displacement in the Y-direction of the Ya Rona shaft for filled models (after Leach, 2003)

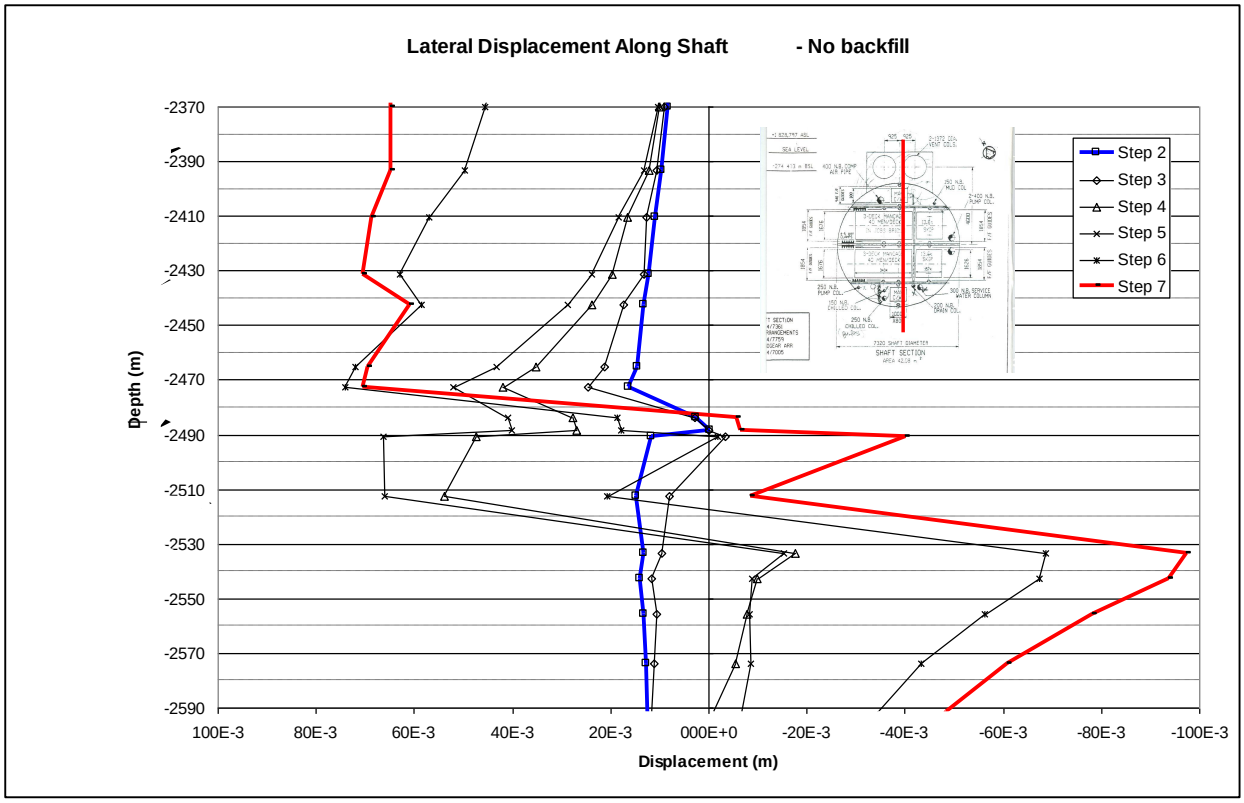


Figure 5-17 Displacement in the X-direction of the Ya Rona shaft for unfilled models (after Leach, 2003)

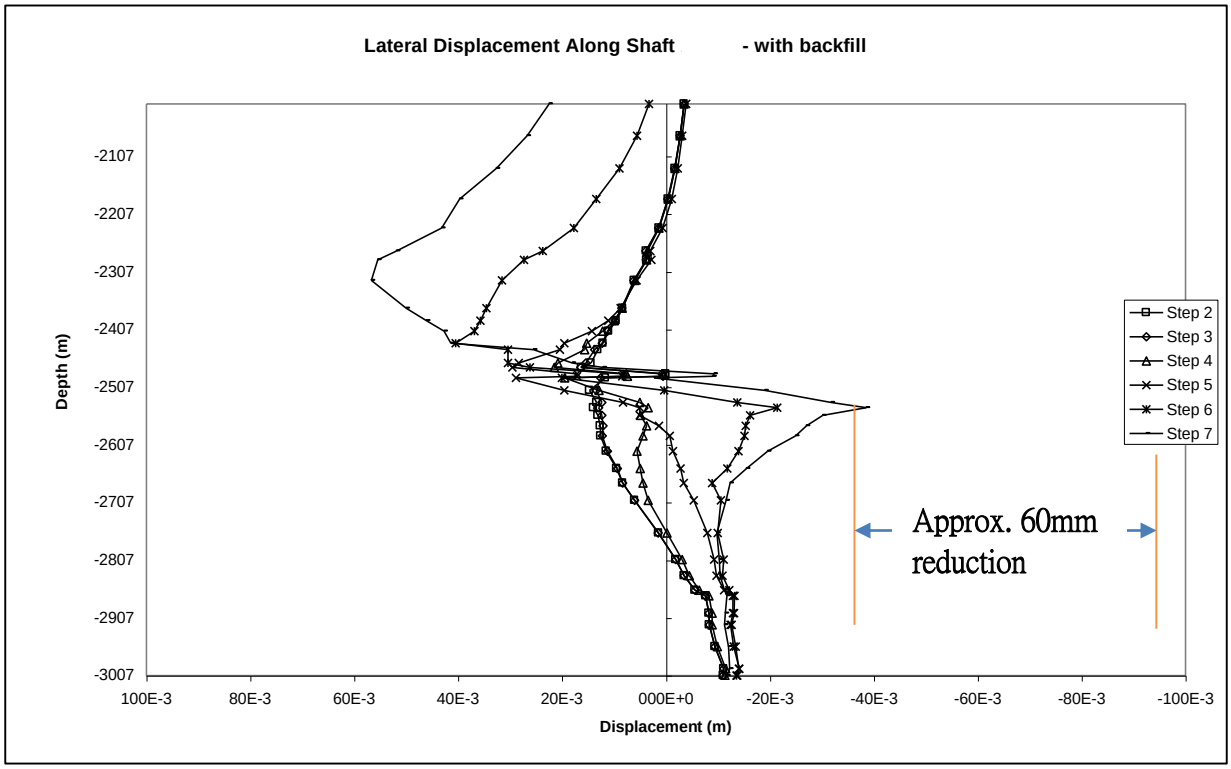


Figure 5-18 Displacement in the X-direction of the Ya Rona shaft for filled models (after Leach, 2003)

5.5.1.4. Rockwall Condition Factor (RCF)

Up to this point, the impact of WAF on the numerical model has been displayed in terms of displacement. Rockwall Condition Factor (RCF) employs a stress profile combined with rock material strength properties to provide a *"recommended design criterion for expressing and controlling tunnel condition…"* and that for *"RCF>1 conditions rapidly deteriorate and increased levels of support resistance and areal coverage are required."* (Jager & Ryder, 1999).

In Chapter 3 of this report, Table 3-1 showed a calculated RCF of 4.66 when using the RCF rockmass rating system. Figure 5-24 shows the analyses of the Besol model using the low strength WAF rockmass. For purposes of comparison, using Equation 2, a good quality rockmass (200MPa) at the same depth and stress gradient (k=1.15) would yield an RCF of 0.3 as a failure criteria.

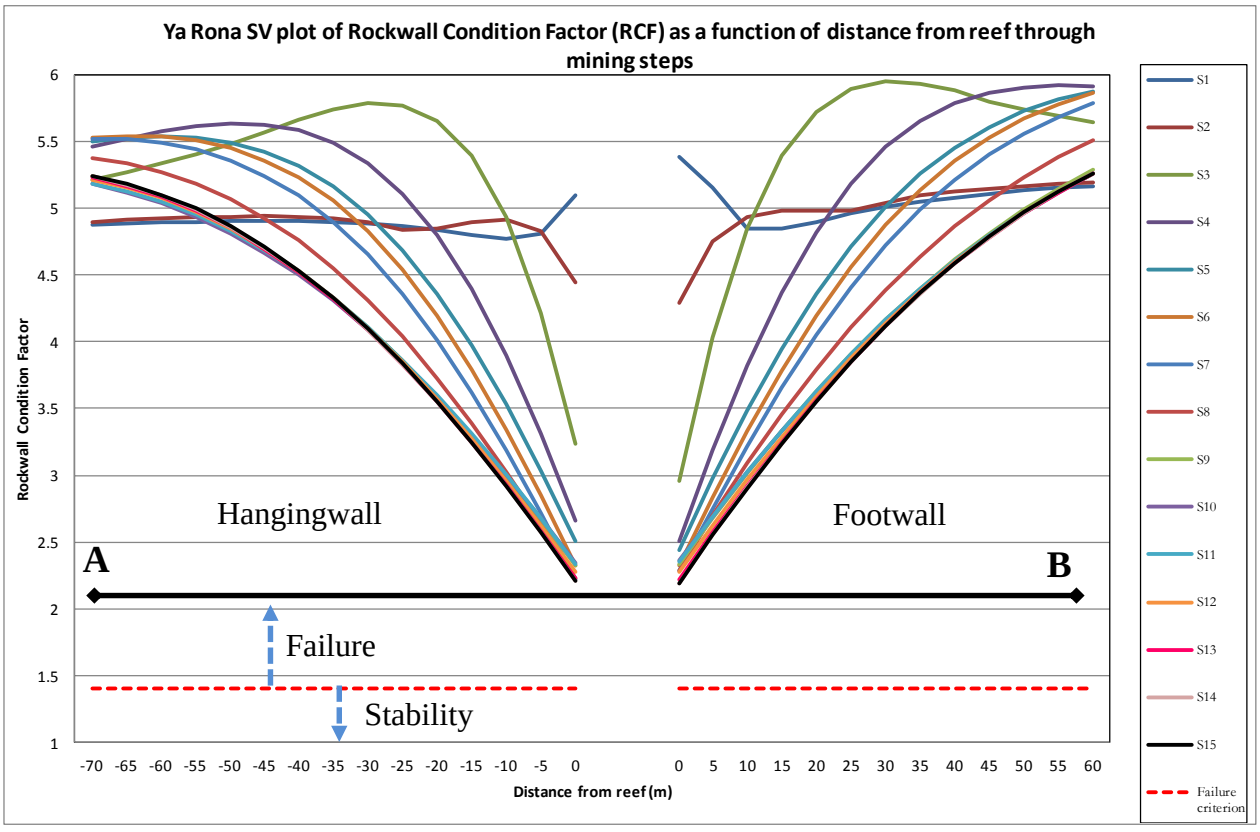


Figure 5-19 Plot of RCF as a function of distance from reef at the Ya Rona Sub-vertical shaft through 15 mining steps

From the graph (Figure 5-19), key points of note include:

- The failure criterion is exceeded through all phases of mining and that instability can be expected in both the hangingwall and footwall of the reef,
- 5m into the hangingwall and 10m into the footwall, large changes in RCF occur during mining step 2. This step is the mining of the 30m x 30m inner pillar,
- Between mining steps 2 and 3 (the 'opening of the eye'), the largest change in RCF is noted. It is expected that during this mining step, the largest deformation will occur in the sidewalls of the shaft. The area most susceptible to damage will be within a zone, 25m above the reef (in the WAF zone) to 30m below the bottom reef band (in shale rockmass), and,
- Thereafter, a gradual reduction in RCF occurs. This is viewed as stress relaxation where dilation of the fractures could occur and additional support measures may have to be employed to deal with the *"lack of resilience in conventional support systems"* (Jager & Ryder, 1999).

5.5.1.5. Concluding remarks on the shaft stability

From the analyses in this section, the low strength WAF contributes significantly to the stability of the shaft. Where comparisons are made between the inelastic and the elastic model, all criteria are exceeded in the low strength elastic BesolMS numerical model. Moreover, all models show a propensity for instability of the shaft in the first five mining steps. However, after step 1 of the mining plan, moiling of the shaft concrete lining had to occur after it had cracked (Durapraj, 2007). This allowed the strength of the concrete lining to be compromised with the result that radial displacement increased. The numerical models did not account for this increase and is the reason why the modeled convergences do not mimic the measured data.

5.5.2. Large displacement regional geological structures' assessment

Within the Ya Rona shaft pillar extraction many of the large displacement geological structures have been highlighted in Chapter 4 of this report. Although, the structures have been modeled in the 3DEC code by Leach (2003), no explicit Excess Shear Stress (ESS) analyses had been completed for these structures. For the purposes of this research report, the

impact on the low strength rockmass on the susceptibility to slip of some of the listed features (Chapter 4, Table 4-3, Figure 4-9) are critical as it would indicate where additional clamping/bracket pillars may be necessary or where mine designs would have to change to reduce the ESS.

This section initially deals with calibration of ESS with regard to WAF. Thereafter, each of the significant geological features is interrogated along the ESS failure criteria (Chapter 2, Table 2-3).

5.5.2.1. Calibration of ESS with respect to different Young's Moduli

Figure 5-20 shows the comparison of ESS value at the Syncline Axis between numerical models using a Young's Modulus of 70GPa (high strength rockmass) and 20MPa Young's Modulus (lower strength WAF rockmass).

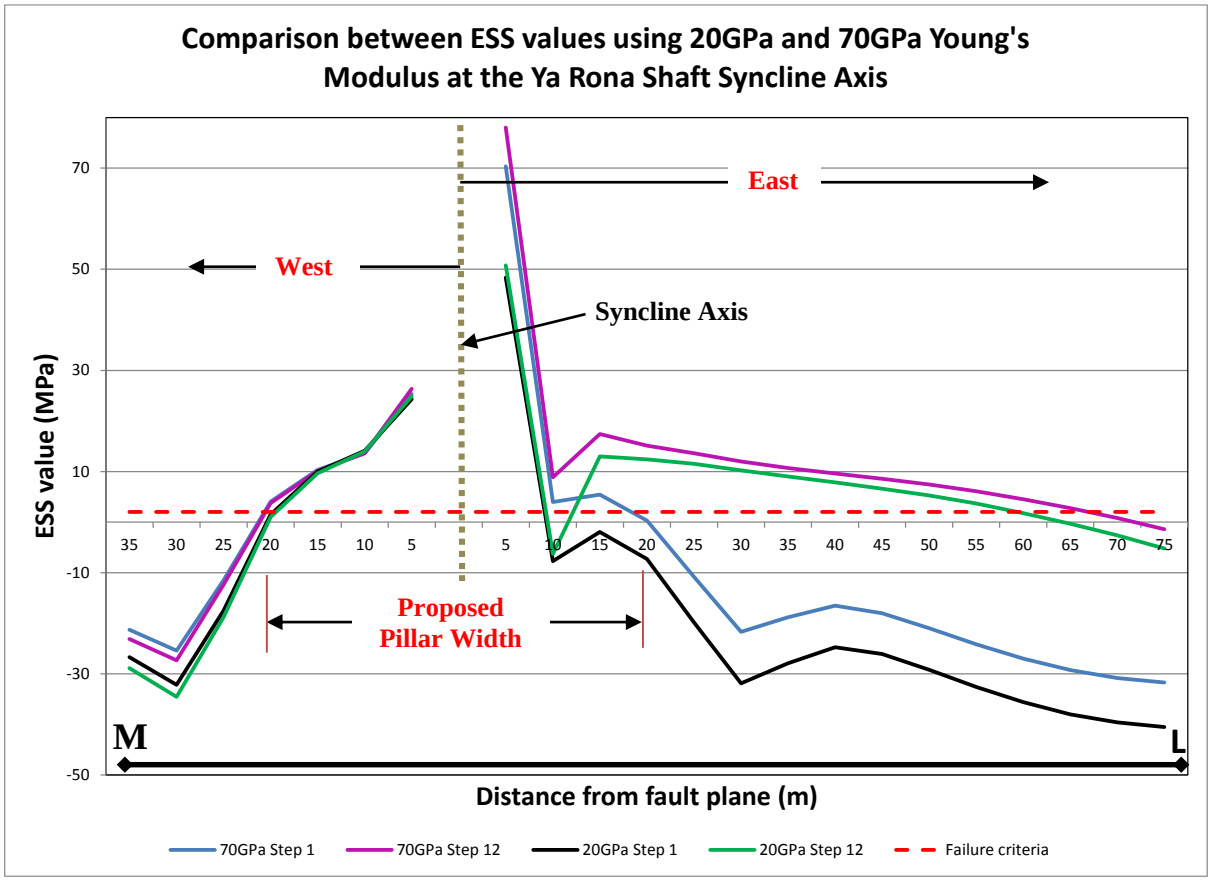


Figure 5-20 Comparison of ESS value using 70GPa and 20GPa Young's Modulus at steps 1 and 12 of the BesolMS numerical model at the Syncline Axis

In Figure 5-20, the Syncline Axis is represented by the grey dotted line. The analysis of the first and last step of each elastic model, using the different Young's Moduli, was used for comparative purposes. The graph (Figure 5-20) shows that:

- In the two models, values to the west of the Syncline axis do not exhibit large differences as no mining has been replicated in the numerical model on that side of the feature, and,
- To the east of the feature, using the 20GPa Young's Modulus, ESS values are low, whereas the 70GPa Young's Modulus numerical model produces higher ESS values. Intuitively higher strength rock material, with a high Young's Modulus, is more brittle and will fail more violently and therefore, higher ESS values are expected.

As the WAF rockmass exhibits the lower strength properties, all the analyses of the geological structures in this section, will use the 20GPa Young's Modulus numerical modeling data.

5.5.2.2. ESS analyses of the geological structures

Figure 5-21 is a plan of the modeled mining sequence showing the location of the major geological structures, and the sections that were used for analyses. An isometric plan of the Figure 5-21 showing the sections in three dimensions is provided in Figure 5-22. The sections were chosen for ESS analyses as they contained the highest value set. Therefore, the bias was set to ensure that if those particular value sets exceeded the criterion, the feature was susceptible to slip. These structures and sections are indicated on the figures as:

1. Kate's Fault (section C-D)
2. Murray Fault (section E-F)
3. Smith Fault (section G-H)
4. Shane's Fault (section J-K)
5. Syncline Axis (section L-M)

The numerical modeling has incorporated clamping or bracket pillars on the structures. Therefore, should the results not meet the ESS failure criteria (Chapter 2, Table 2-4), the mining layout or additional clamping on the structures may be necessary.

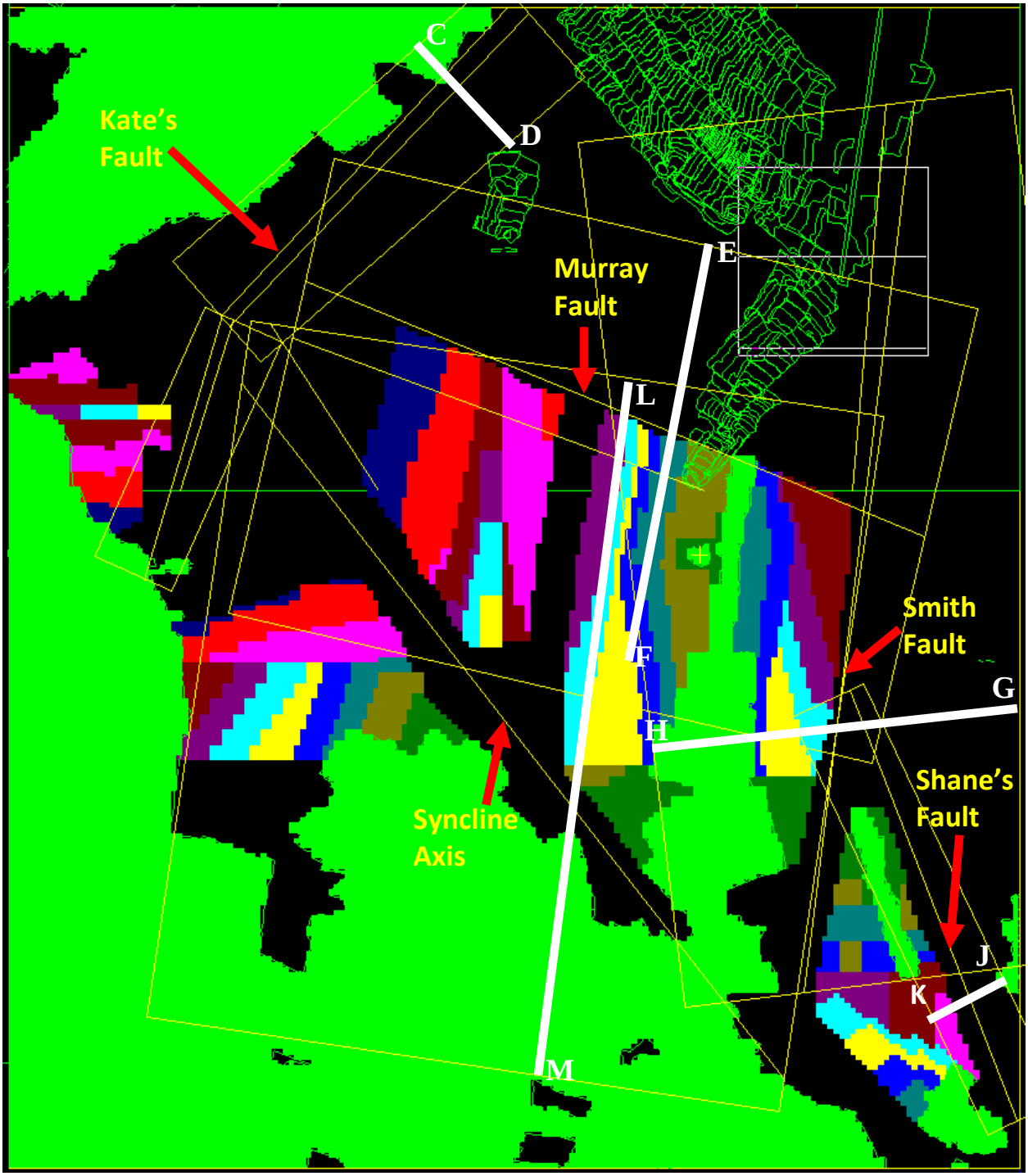


Figure 5-21 Plan view of the modelled geological features showing positions at which ESS data of faulting was analysed for the Ya Rona SV Pillar Extraction

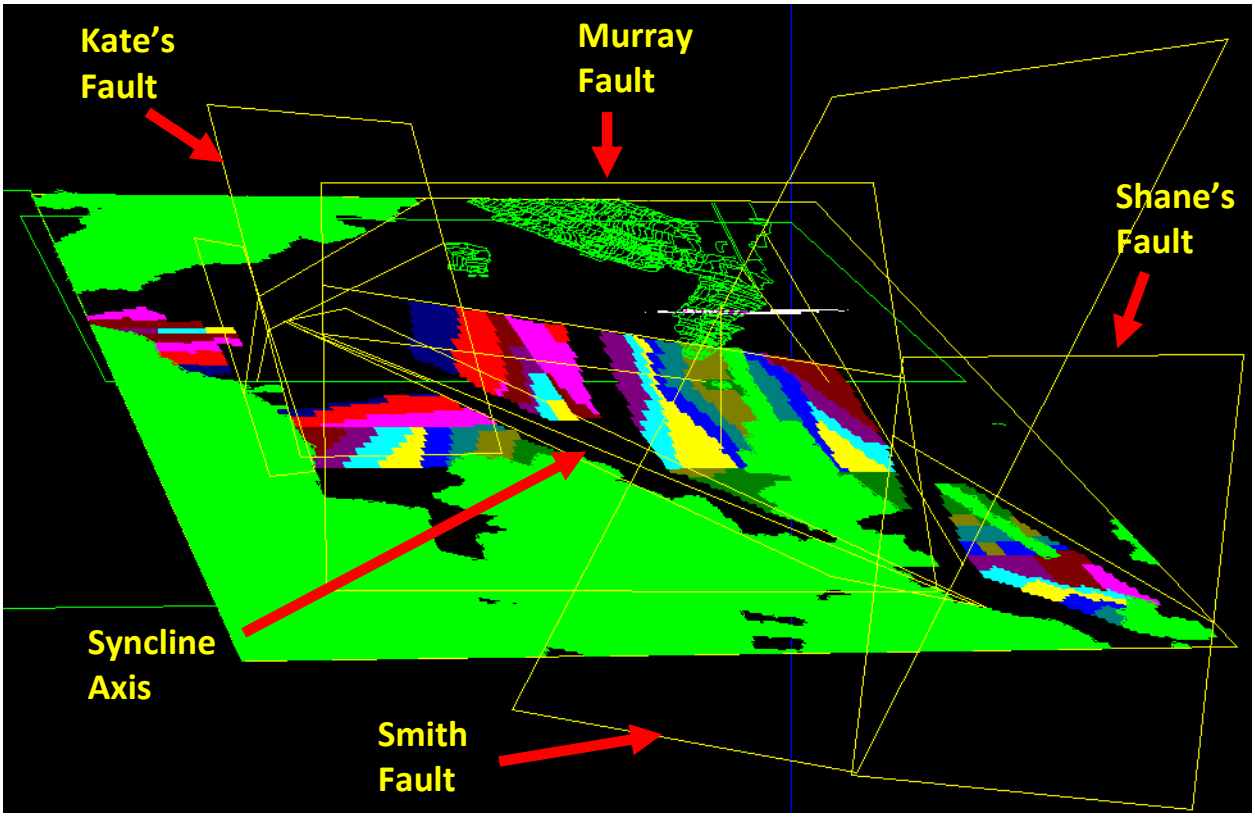


Figure 5-22 Isometric view of the modelled plane views of geological features at the Ya Rona SV Pillar Extraction

5.5.2.2.1. ESS assessment of the Syncline Axis

The Syncline Axis structural nature has been discussed in Chapter 4 of this report. It is a known seismically active feature, and has been bracketed with a suitably sized pillar, which also satisfies the regional stability pillar requirement.

Apart from the analyses provided in Section 5.5.2.1, the plot of ESS values obtained for Section L-M in Figure 5-20 also shows that:

- The failure criterion (Chapter 2, Table 2-4) is exceeded where the high strength material constitutes the plane of weakness. For 20m to the west and 65m to the east of the Syncline Axis, the ESS values exceed the limit;
- When comparing the 70GPa and 20GPa cases, ESS value reductions are realized with the 20GPa model at both steps in the model; and,
- For both models, large ESS values are observed in both steps for a distance of 20m on either side of the Syncline Axis.

From a rock engineering design perspective, in theory, a 40m bracket pillar (Figure 5-20) would be the optimal width to clamp the Syncline Axis.

5.5.2.2.2. ESS assessment of Kate's Fault

The Kate's Fault has a throw of 72m throw (Chapter 4, Table 4-3) and is known to be a seismically active feature. Previously bracket pillars were designed to clamp this fault. Geometrically, the design provides the opportunity to not only clamp the fault but serve as a regional stability pillar (Figure 5-2, Block E) within the shaft pillar extraction.

Figure 5-23 shows a plot of the ESS values obtained for Section C-D in Figure 5-21. The graph highlights the change in ESS value as mining occurs. Note that the fault plane is split into three parts; the hangingwall, the reef packages and the footwall of the feature.

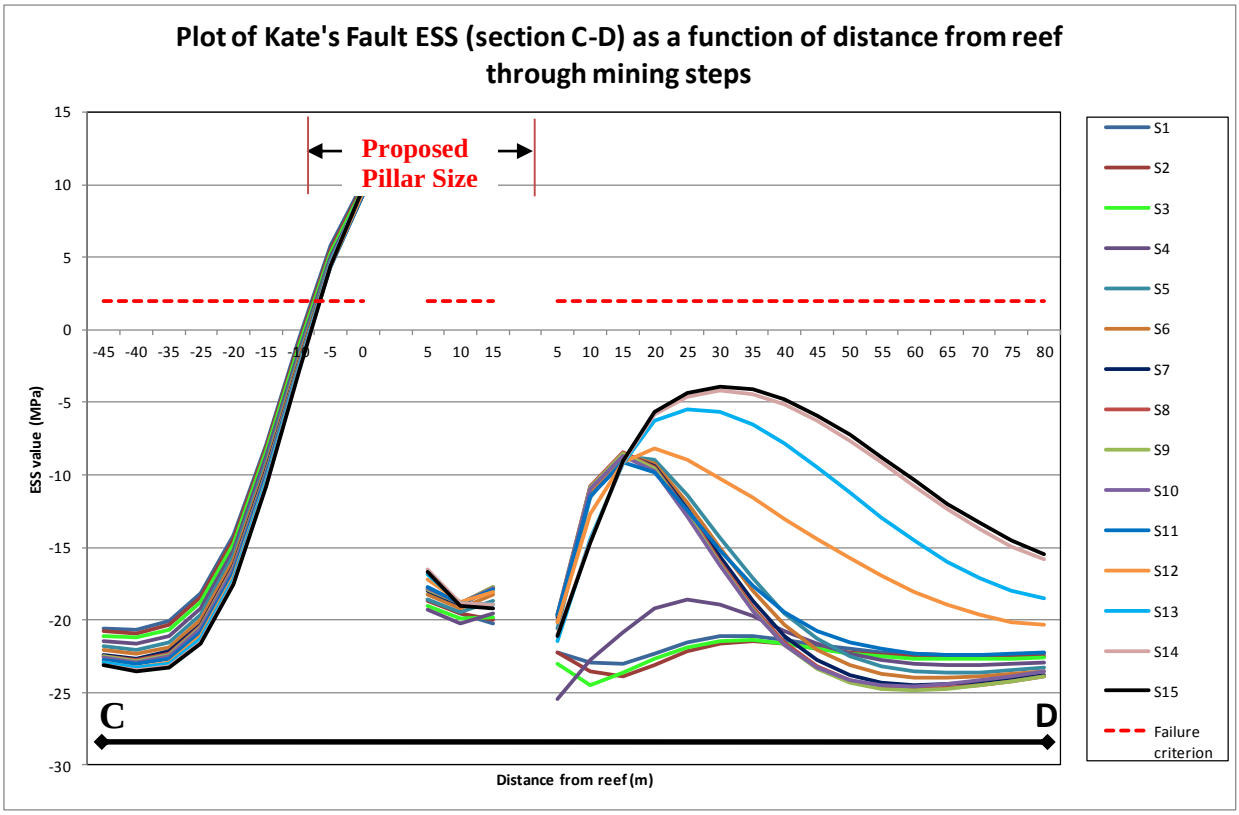


Figure 5-23 Plot of Kate's Fault ESS value (section C-D) as a function of distance from reef over 15 mining steps

Analysis of Figure 5-23 shows that:

- The failure criterion (Chapter 2, Table 2-4) is exceeded in all mining steps in the first 10m of hangingwall above the upper reef band;
- All other ESS values and changes thereto, fall below the failure criterion;
- A large change in ESS value occurs from step 4 to 5 in the footwall of the fault plane; and,
- From steps 6 to 12, large changes in the footwall data do not occur, but large changes in the ESS values occur on the bottom reef extraction from step 12 to 15 as mining gets closer to the feature. However, this is still below the failure criterion.

From a rock engineering design perspective, the data suggests that a bracket pillar is not required on the footwall portion of the fault plane, but one is suggested for the hangingwall side (Figure 5-23). Therefore, mining may occur up to the feature on the footwall side of the fault plane.

5.5.2.2.3. ESS assessment of Murray Fault

The Murray fault is a reverse fault with a throw of 20m and is not known to be seismically active feature. However, for safety reasons, the structure has been bracketed with a pillar.

Figure 5-24 shows a plot of the ESS values obtained for Section E-F in Figure 5-21. Analysis shows that:

- The ESS failure criterion (Table 5.3) is exceeded where the reef planes overlap,
- ESS values exceed the criterion in the overlap from step 5. This continues to the end of mining with significant ESS values, of greater than 70 MPa, being recorded;
- Large changes in ESS value occur in the overlapped reef packages between steps 8 and 9;
- After step 11, in the 15m hangingwall portion of the fault on the upthrown reef plane exceeds the ESS value failure criterion; and,
- Although there are some large changes in ESS value on the lower, downthrown reef plane, the value does not exceed the criterion.

From the rock engineering design perspective, the data suggests that a 20m bracket pillar (Figure 5-24) be left on the upthrow side of the fault, and a 5m pillar be left on the downthrown side.

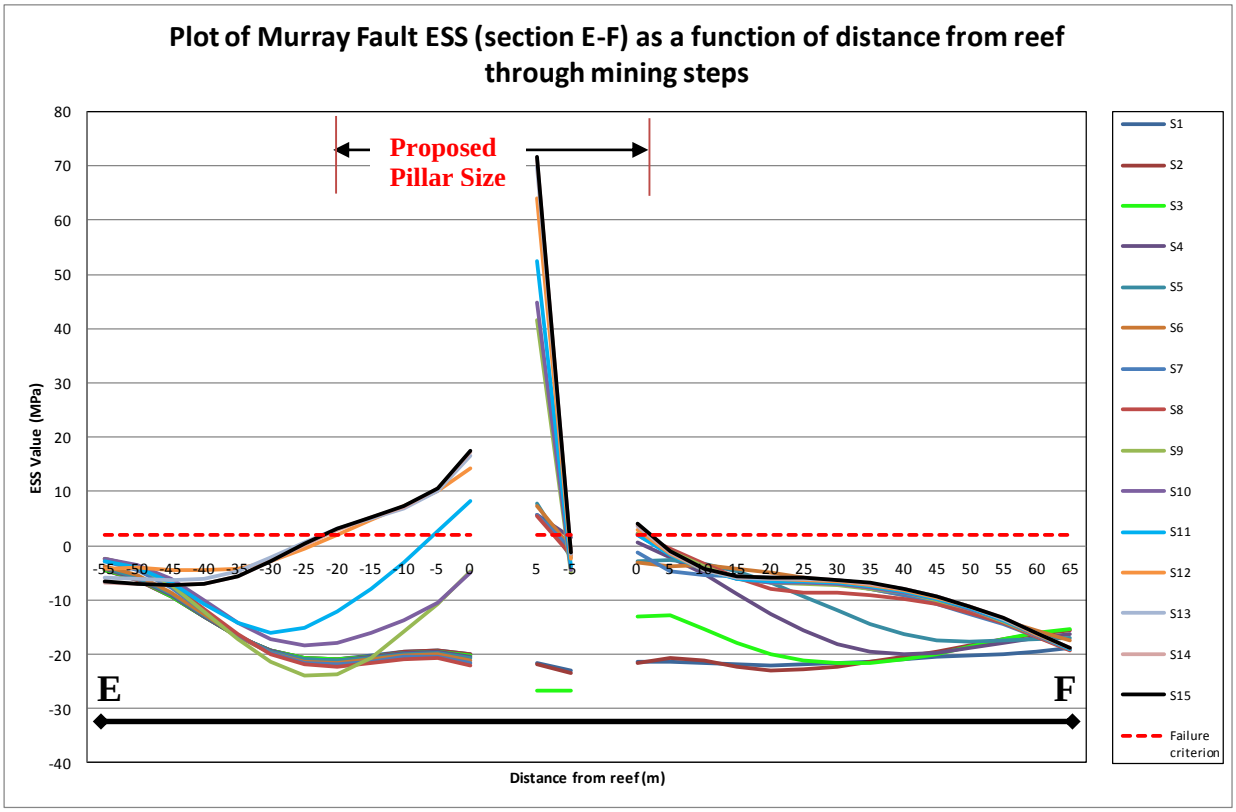


Figure 5-24 Plot of Murray Fault ESS value (section E-F) as a function of distance from reef over 15 mining steps

5.5.2.2.4. ESS assessment of Smith Fault

Smith Fault is a 10m throw, normal fault, which is a known seismically active feature, bracketed with a suitably sized pillar which satisfies both the regional stability pillar requirement, as well as the clamping force.

Figure 5-25 shows a plot of ESS values obtained for Section G-H in Figure 5-21. Analysis shows that:

- ESS values, throughout all mining steps, do not exceed the failure criterion;
- The largest change in ESS value occurs at steps 13-15 when the mining is closest to the structure. However, the values are still within the criterion; and,

- The data suggests that no bracket pillar needs to be left on the feature.

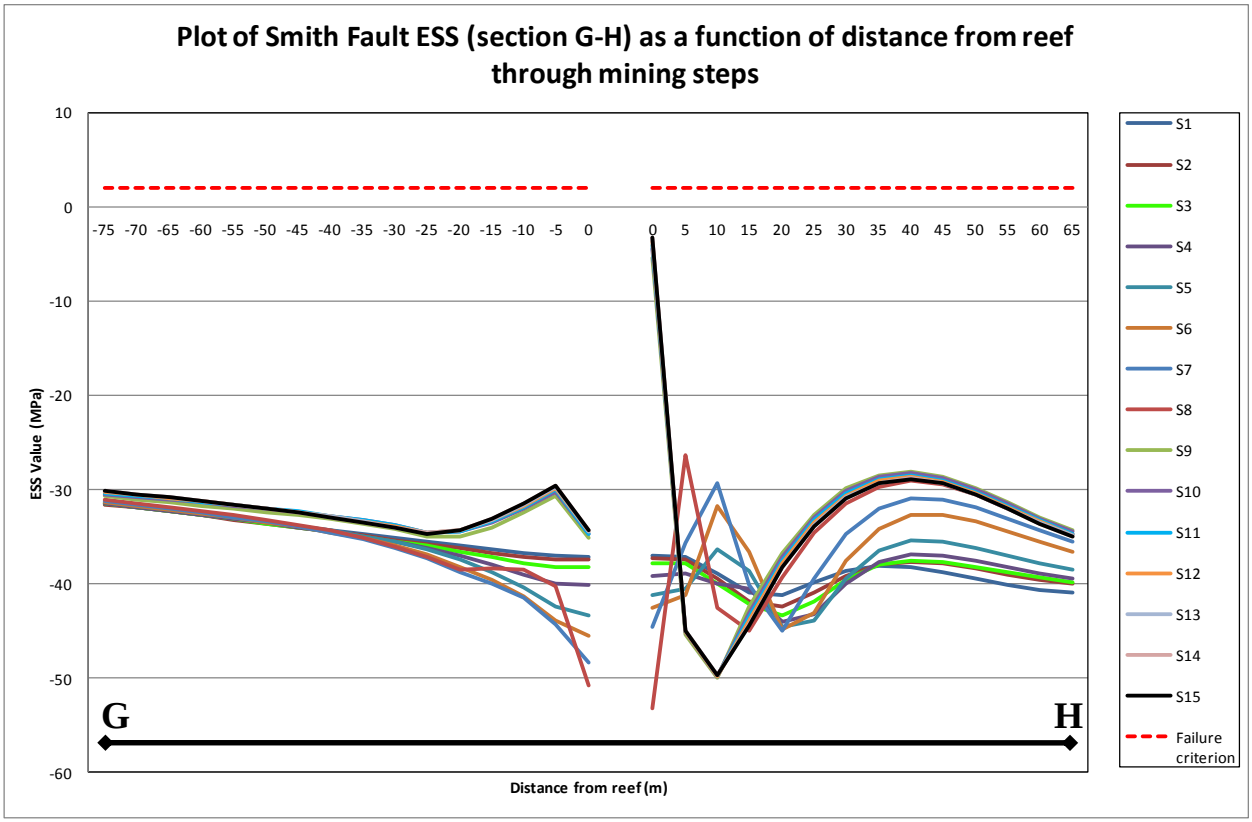


Figure 5-25 Plot of Smith Fault ESS value (section G-H) as a function of distance from reef over 15 mining steps

5.5.2.2.5. ESS assessment of Shane's Fault

Shane's Fault is a 20m throw, reverse fault, which is not a known seismically active feature, but has been bracketed with a suitably sized pillar, which also satisfies the regional stability pillar requirement.

Figure 5-26 shows a plot of ESS values obtained for Section J-K in Figure 5-21. The data is recorded at a position where the pillar dimension is the smallest at the end of mining. Analysis indicates that ESS values remain below the failure criterion for the duration of mining. The data suggests that no bracket pillar is required on the feature.

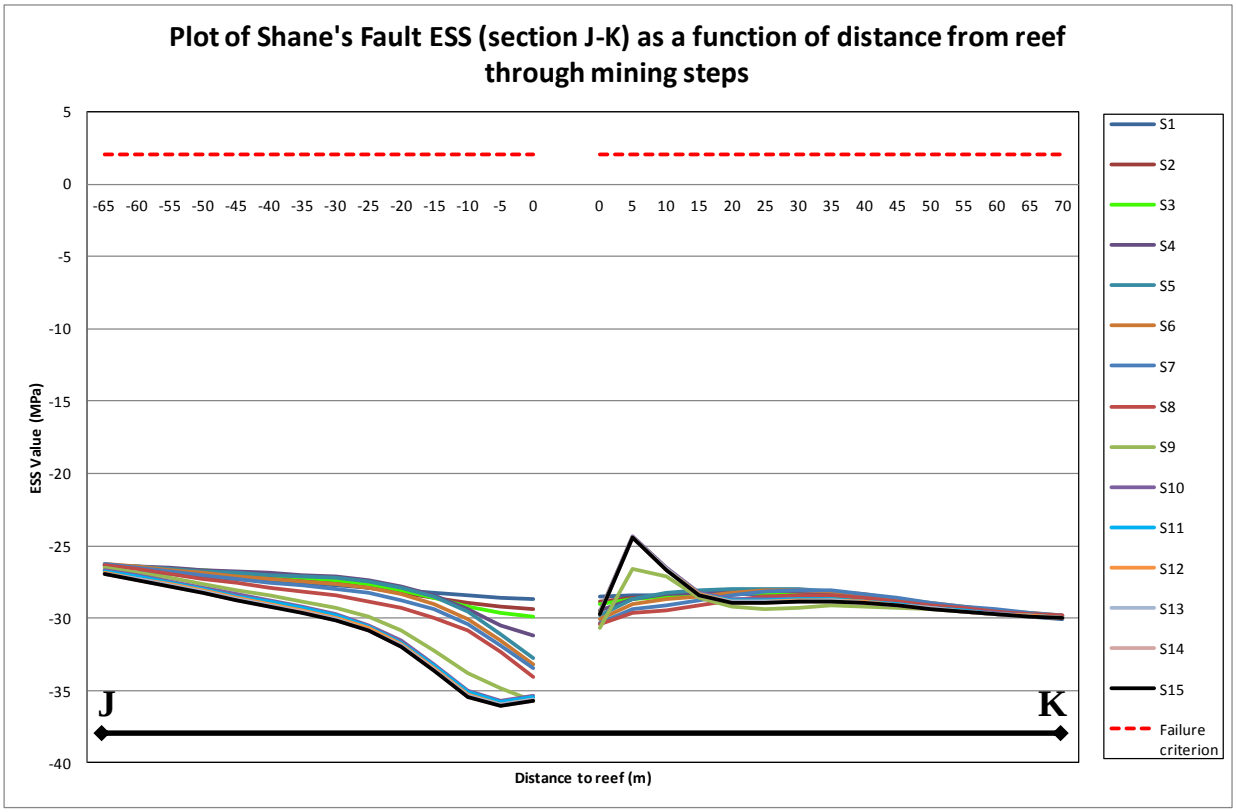


Figure 5-26 Plot of Shane's Fault ESS value (section J-K) as a function of distance from reef over 15 mining steps

5.5.3. LOM12 mining plan assessment

Stability pillars are an integral part of a mining sequence in that they allow the dissection of a larger block of ground into smaller manageable units. These units or mining blocks are designed under a specific set of criteria (Chapter 2, Table 2-4) which would include the Average Pillar Stress (APS) and Energy Release Rate (ERR). In the Ya Rona example, the mining sequence incorporated two additional regional stability pillars (Figure 5-27, pillar XX and ZZ). The bracket pillars fulfilled unique roles in that they firstly clamped the geological structures and secondly, by leaving blocks of ground, additional regional stability was created.

However, the strength of the pillars, in relation to the stress imposed on them is crucial in terms of understanding whether they would provide the regional effect that is required. The effect of the WAF gains increasing importance in this section of the report.

A calibration exercise (Figure 5-28) using the low and high strength materials in the models will be followed by the analyses of the two pillars.

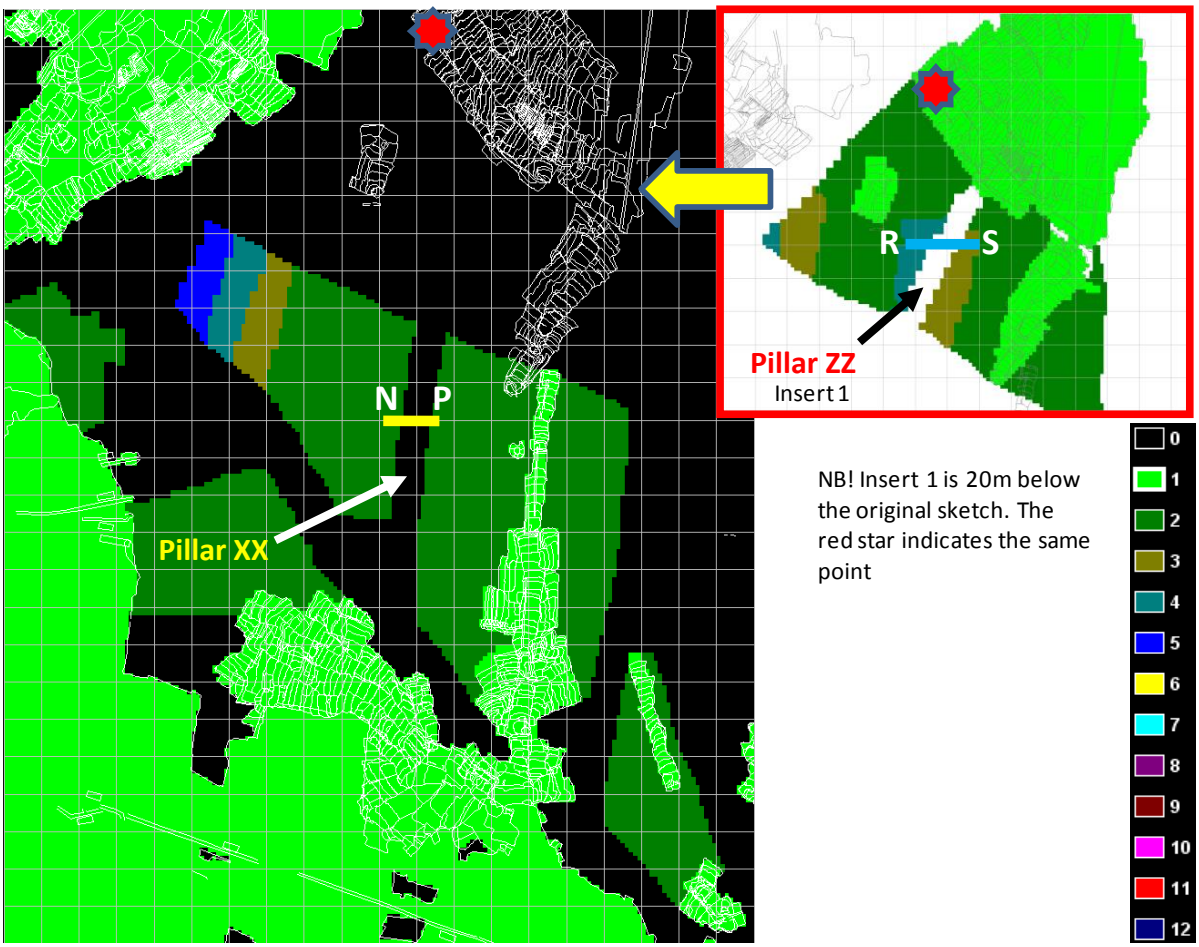


Figure 5-27 Besol MSPrep model showing the regional stability pillars (XX and ZZ) with the sections N-P and R-S used for pillar analysis

5.5.3.1. Regional Stability Pillar assessment

5.5.3.1.1. Calibration of the model to show the effect that WAF has on APS

To illustrate the effect that the low strength WAF has on APS, the APS results of Pillar XX, are interrogated against the failure criteria (Chapter 2, Table2-4) and high strength (200MPa) quartzite. Figure 5-28 shows that:

- The average APS is 255MPa;

- If the pillar is comprised of 57MPa WAF material, the APS of the pillar will be need to be <143MPa (APS = 2.5 x σ_c). The APS of the pillar in the current mining sequence is higher than the criterion;
- If the pillar is comprised of 89MPa (average WAF UCS at Ya Rona) WAF material, the APS of the pillar will be need to be <223MPa (APS = 2.5 x σ_c). The APS of the pillar in the current mining sequence is higher than the criterion; and,
- If the pillar is comprised of 200MPa quartzite material, the APS of the pillar will be need to be <500MPa (APS = 2.5 x σ_c). The APS of the pillar in the current mining sequence is the lower than the criterion.

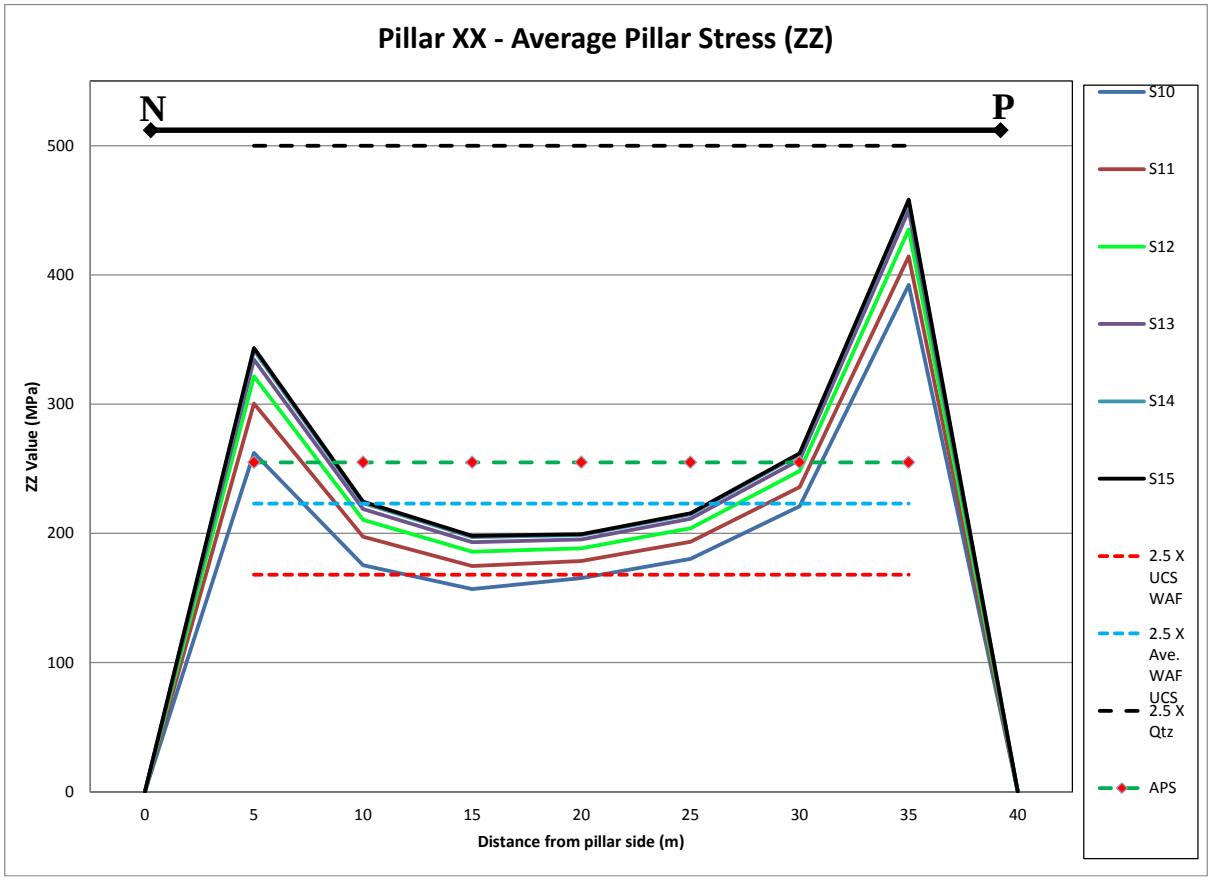


Figure 5-28 Graph showing APS of Pillar XX (Figure 5-27, section N-P)

5.5.3.1.2. Pillar XX APS assessment

Average pillar stress (APS), normal (ZZ orientation) to the reef plane, for pillar XX is shown in figure 5-28. The analysis of section N-P reveals:

- The APS of the pillar at step 15 is approximately 255 MPa; and,

- This is 78% more than the WAF <143MPa failure criterion (Chapter 2, Table 2-4), and 14% higher than the average WAF <223MPa failure criterion (Chapter 2, Table 2-4).

5.5.3.1.3. Pillar ZZ assessment

Similarly, Figure 5-29 shows APS data at Step 15 of the mining sequence of Pillar ZZ:

- The APS of the pillar at step 15 is approximately 349 MPa; and,
- This is 144% more than the WAF <143MPa failure criterion (Chapter 2, Table 2-4), and 42% higher than the average WAF <223MPa failure criterion (Chapter 2, Table 2-4).

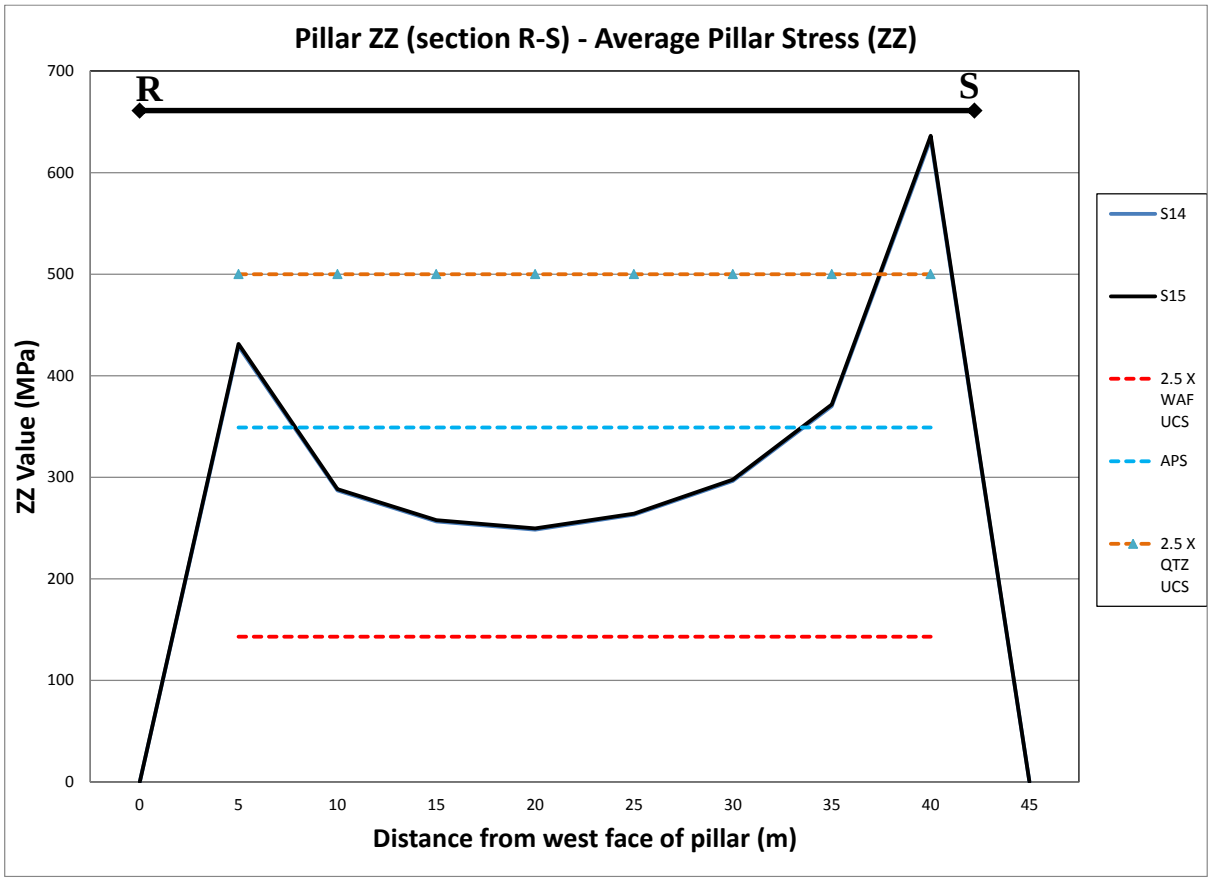


Figure 5-29 Graph showing APS of Pillar ZZ (figure 5-27, section R-S)

5.5.3.2. Energy Release Rate (ERR)

Table 5-4 shows the average ERR values for each of the Block A-F mining blocks (Figure 5-2). Note that each of the values presented are the averages for each mining step. Values exceeding 30 MJ/m^2 are highlighted in yellow. The scatterplot (Figure 5-35) of the ERR values show that mining in every block exceeds the failure criterion (Chapter 2, Table 2-4) at some stage of mining. Note that in both Table 5-4 (red dotted block) and Figure 5-30 (light blue line), Block E 'appears' to reduce in ERR value at Step 9. The reason for this is that Block E is made up of two mining areas (Figure 5-2). Therefore, the ERR data set is taken from steps 2-8 to represent the first, upper stage of mining, whereas from step 9 onwards, the ERR data (red dotted block in Table 5-4) represents the second, lower stage of mining in the same block.

	Block A (MJ/m^2)	**Block B** (MJ/m^2)	**Block C** (MJ/m^2)	**Block D** (MJ/m^2)	**Block E** (MJ/m^2)	**Block F** (MJ/m^2)
Step 1	No values computed as no change in mining occurred					
Step 2	9.7	12	-	9.6	11.8	
Step 3	18.4	11.2	-	-	19	
Step 4	28.9	17.5	-	-	24.3	
Step 5	39.7	18.3	-	-	31.2	
Step 6	58.2	13.1	5.5	24.3	55.1	4.7
Step 7	54	15.1	8.8	29	76.1	7.9
Step 8	53.3	30.8	9.2	34.3	71.9	42.5
Step 9	52.6	39.8	15.9	40.5	5	48.4
Step 10	-	36.4	28.6	52.9	13.4	62
Step 11	-	-	35.9	56.5	30.8	125.1
Step 12	-	-	39.6	72.5	43.7	210.2
Step 13	-	-	41.7	69.1	43.4	-
Step 14	-	-	41	-	75.9	-
Step 15	-	-	39.4	-	-	-

Table 5-4 LOM12 ERR values for mining blocks over the 15 mining steps

As equation 1 (Chapter 2) suggests, ERR is calculated using stress, volume and area. Therefore, the WAF rockmass properties will not impact on the results. However, from a rock engineering design perspective, the only manner in which ERR can be reduced is by manipulating the volume or area, as depth is fixed. Volume can be reduced through

reducing stoping width and area can be curtailed with the introduction of additional stability pillars.

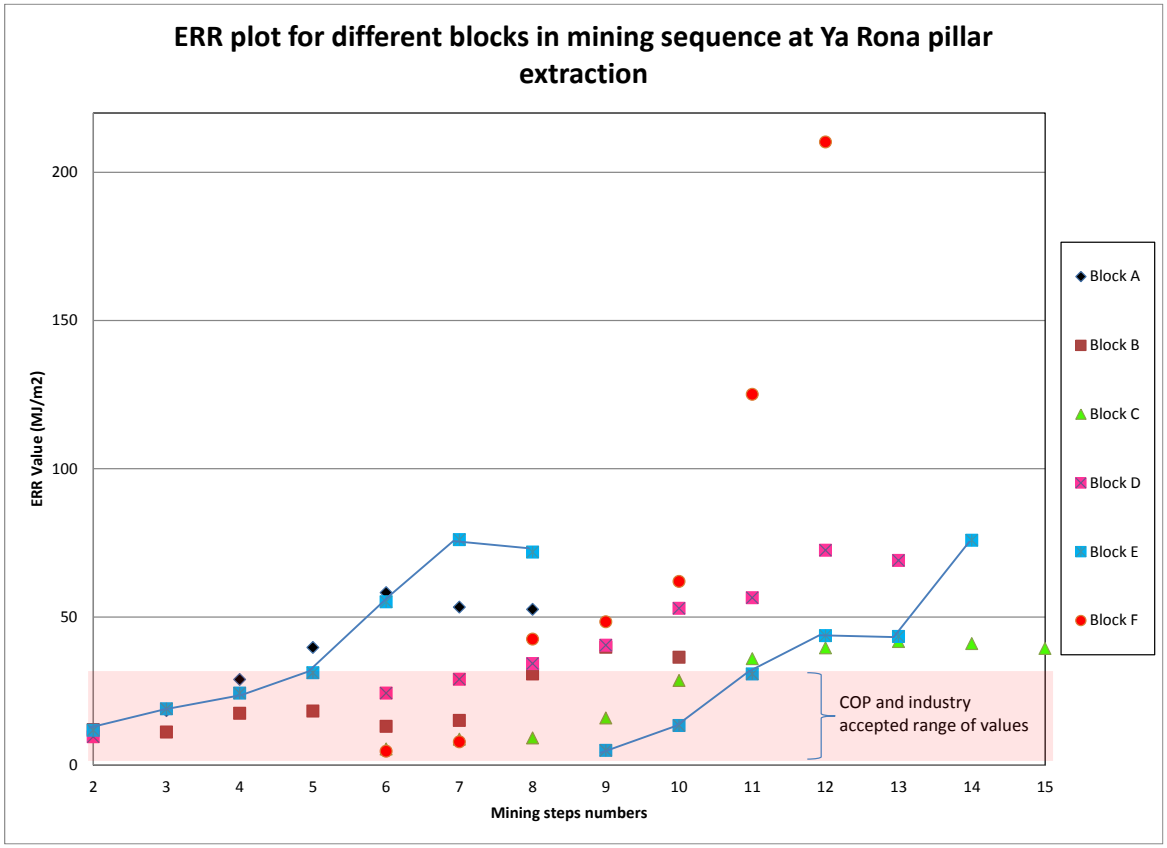


Figure 5-30 ERR Plot of mining blocks over time at Ya Rona pillar extraction

Figure 5-30 shows that:

- Of the 56 data points, 24 points fall below the 30MJ/m^2 failure criterion (Chapter 2, Table 2-4); and that,
- This indicates that 57% of the mining will occur above the ERR failure criterion, indicating that to keep ERR to acceptable criterion levels, the strike spans in each block would need to be reviewed.

5.6. Conclusions with regard to the WAF influence in the numerical models

The salient features of the WAF contribution to the numerical modeling analyses shows that:

- The indicated cumulative vertical displacement of 1.45m, at the shaft, will mean that there is no FOS available for the shaft suspended steelwork should this displacement increase. The engineering design only caters for a 1.5m vertical displacement;

- The cumulative Y direction horizontal displacement is 0.4m which is higher than the 0.3m failure criterion;
- 190mm of ride is possible in the Y-direction (across the reef strike);
- RCF is exceeded at all stages of mining;
- The Syncline Axis and Murray Fault show that slip on the features are likely;
- The Smith and Shane's Fault do not suggest slip in the model;
- The regional stability pillars' APS exceed the failure criterion; and,
- ERR values exceed the failure criterion at every block at or after step 4.

5.7. Revised mining layout using WAF properties

Section 5.6 of this report showed areas within the current mining sequence that did not meet the failure criterion (Chapter 2, Tables 2-3 and 2-4). In an effort to produce results that show an improvement and attempt to meet the failure criterion, as set out in Chapter 2 of this research report, Figures 5-31 and 5-32 show a revised mining sequence for the Ya Rona Shaft Pillar Extraction. The difference between the LOM12 mining sequence and the revised sequence is that:

- Instead of using 30-40m wide regional stability pillars, 50m wide regional stability pillars are modeled, and,
- A maximum mining span of 110m is used for each mining block.

The modeling results will still be subjected to the failure criteria, as set in Chapter 2 of the research report. The 20GPa Young's Modulus will be used in the BesolMS numerical model.

5.7.1. Change in Vertical and Horizontal displacement of the Shaft

Figure 5-10 showed cumulative vertical displacement of 1.45m at the Ya Rona shaft. In the revised model, Figure 5-33, the maximum vertical displacement is 0.88m, a 65% improvement, which for a FOS of 1.7.

Figure 5-12 showed 0.4m cumulative Y-direction displacement of the shaft. In the revised model, Figure 5-34, the maximum Y-direction displacement is 0.24m. This is lower than the

failure criterion of 0.3m. As the X-direction cumulative displacement met the failure criterion in the original design, no further analysis was required in the revised layout.

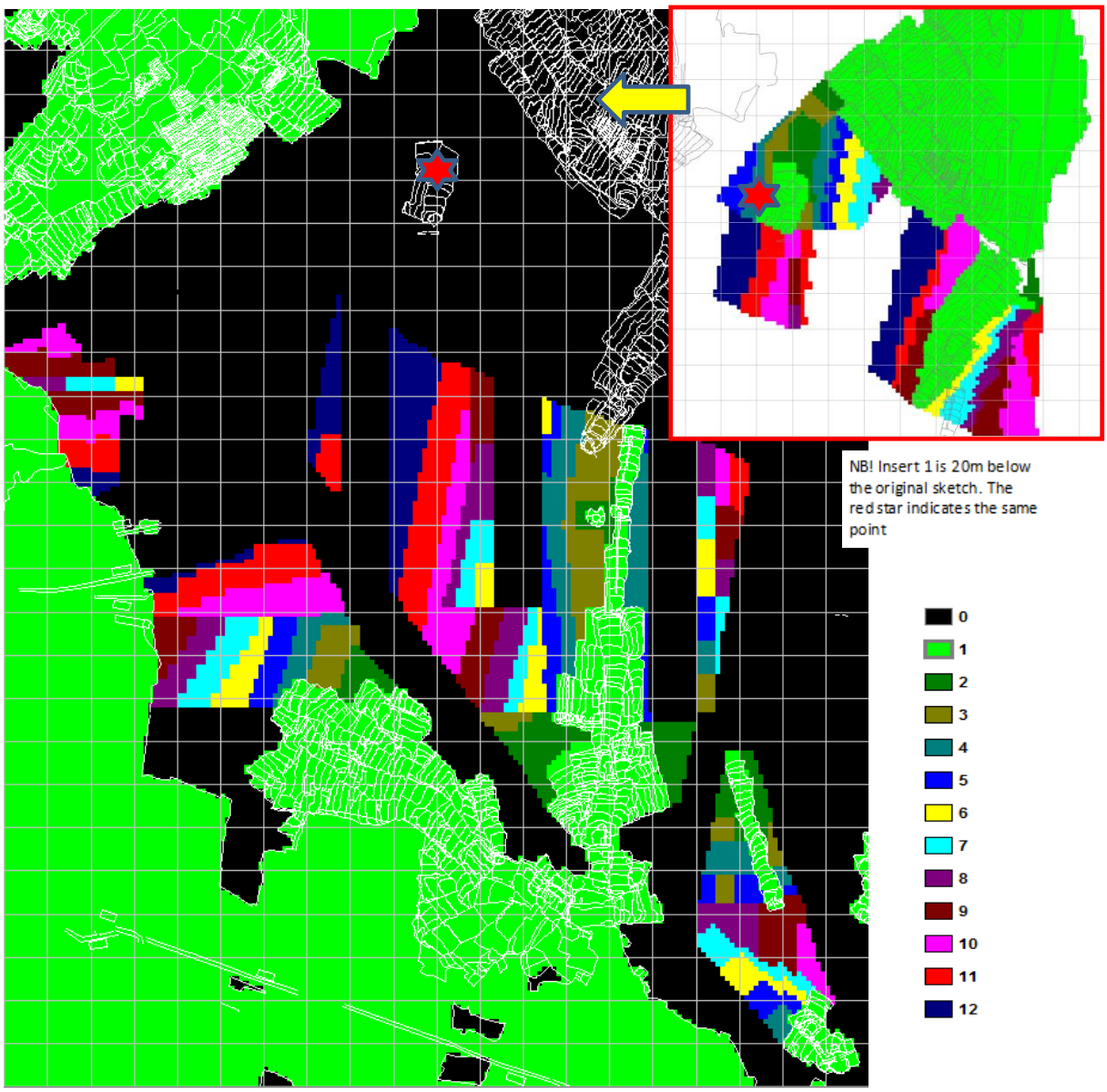


Figure 5-31 Revised Besol simulation of mining plan showing the mining steps 1-12

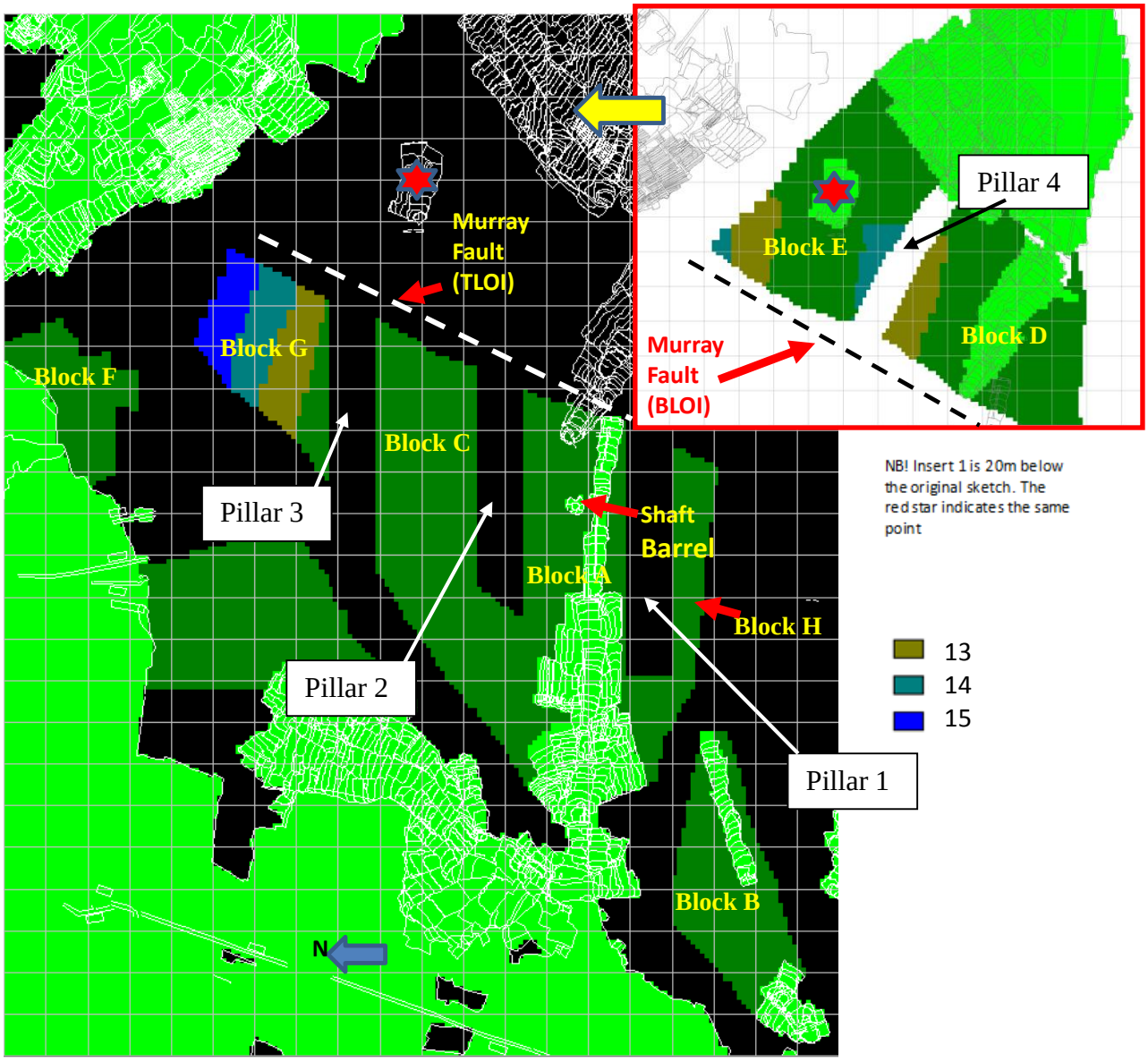


Figure 5-32 Revised Besol simulation of mining plan showing the mining steps 13-15

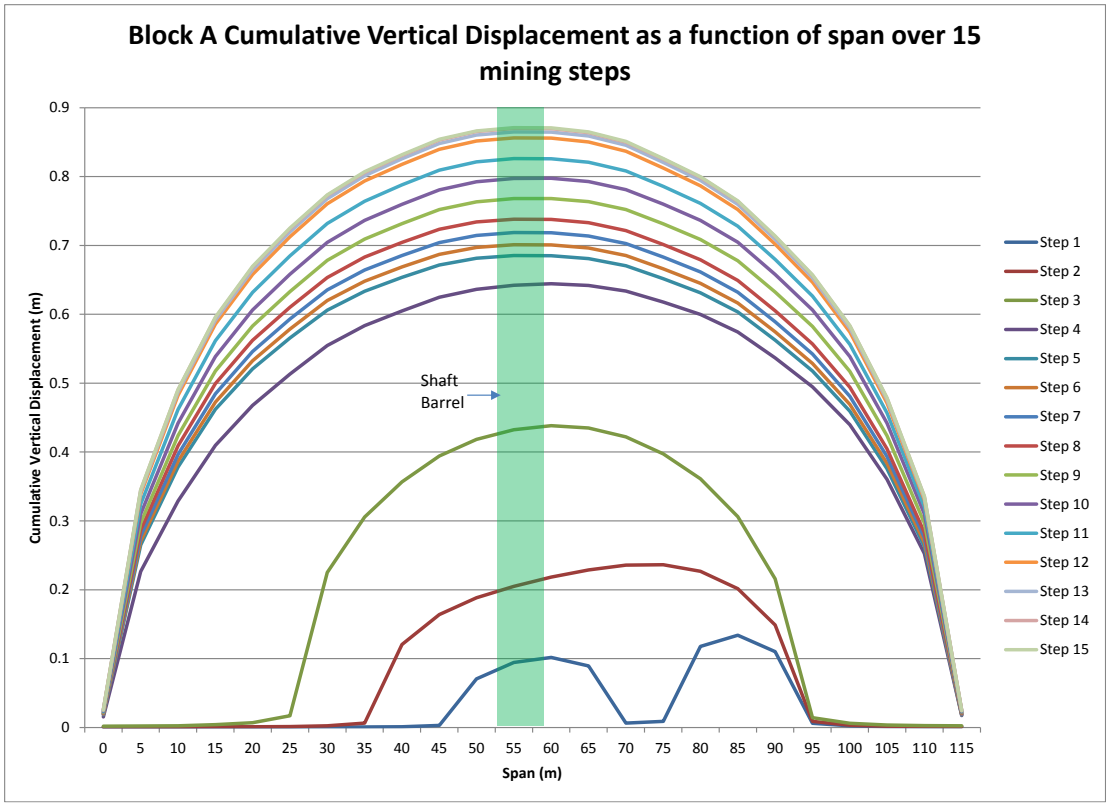


Figure 5-33 Revised Model: Cumulative Vertical Displacement of Block A showing the superimposed shaft

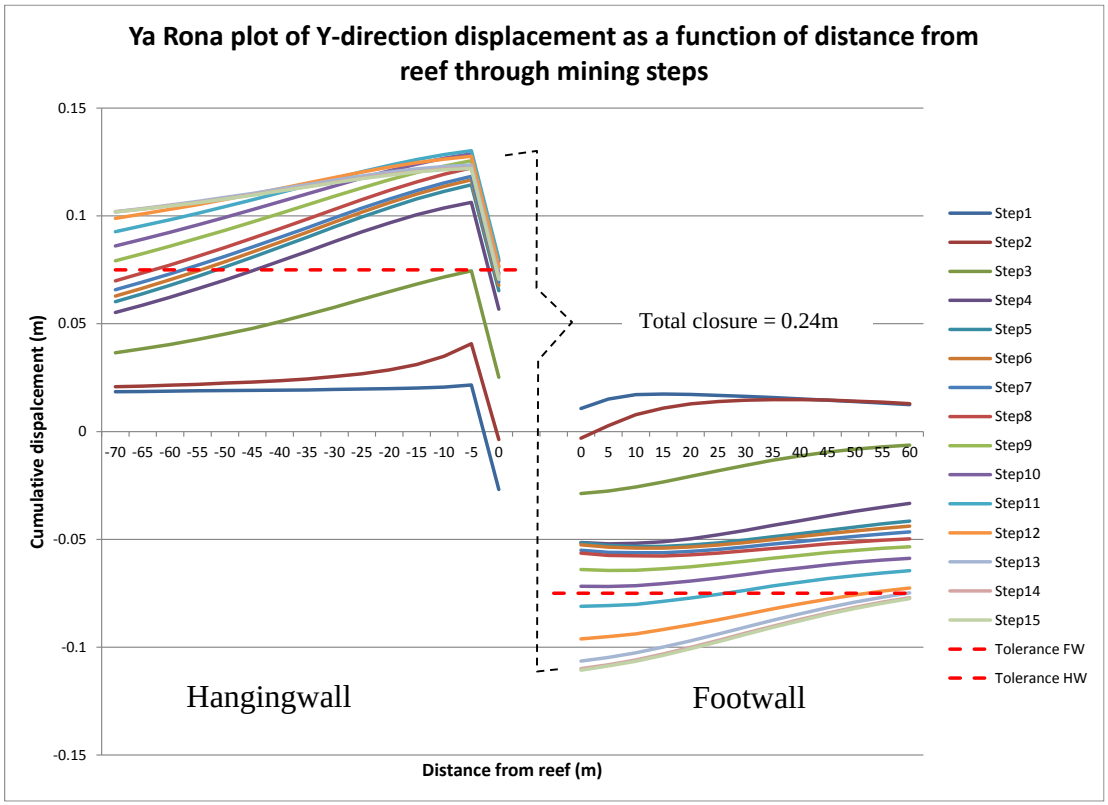


Figure 5-34 Revised Model: Ya Rona Shaft Cumulative Y-Direction displacement

5.7.2 Change in ride at the Shaft

Figure 5-35 is the comparison between the current mining plan modelling data and the optimised simulation for X-and-Y-Ride at the Ya Rona Shaft. The graph shows that with the current mining simulation total ride in the Y-direction is approximately 0.19m, whereas in the revised 110m span, Y-direction ride is 0.12m, a 58% change. As with Section 5.5.1.3, no ride criterion is stipulated.

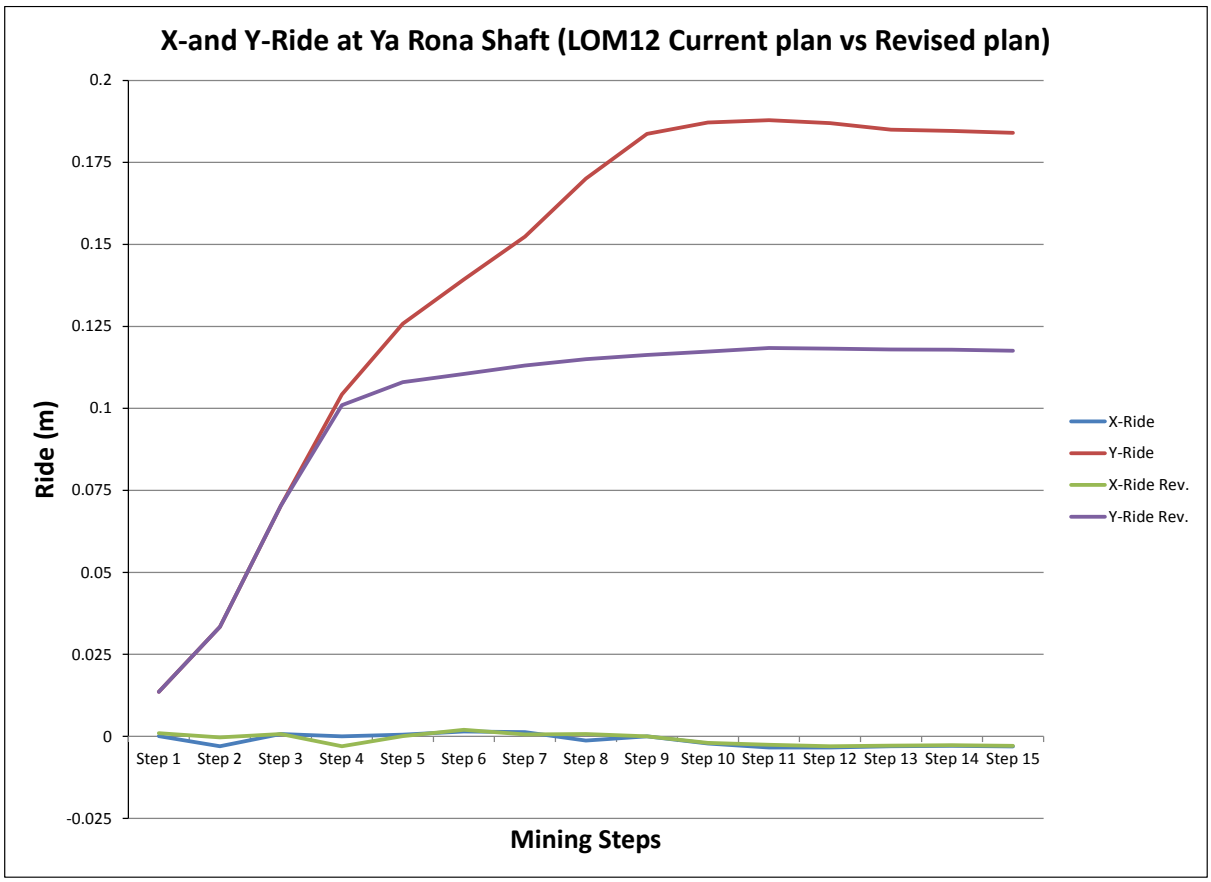


Figure 5-35 Current vs Revised Model: X-and-Y-Ride plot at the Ya Rona Shaft

5.7.3. Change in RCF

No significant change in RCF is realized in the revised model and therefore no analysis thereof is presented in this section. The RCF criterion is exceeded in both models.

5.7.4. Change in ESS of the Syncline Axis and Murray Fault

Figure 5-36 plots ESS as a function of distance from the reef plane for the Syncline Axis, using the Young's Modulus of 20GPa in the revised elastic model. In comparison to Figure 5-20, a significant reduction in ESS is realised, although the criterion is still exceeded for 20m in both hangingwall and footwall of the Syncline Axis.

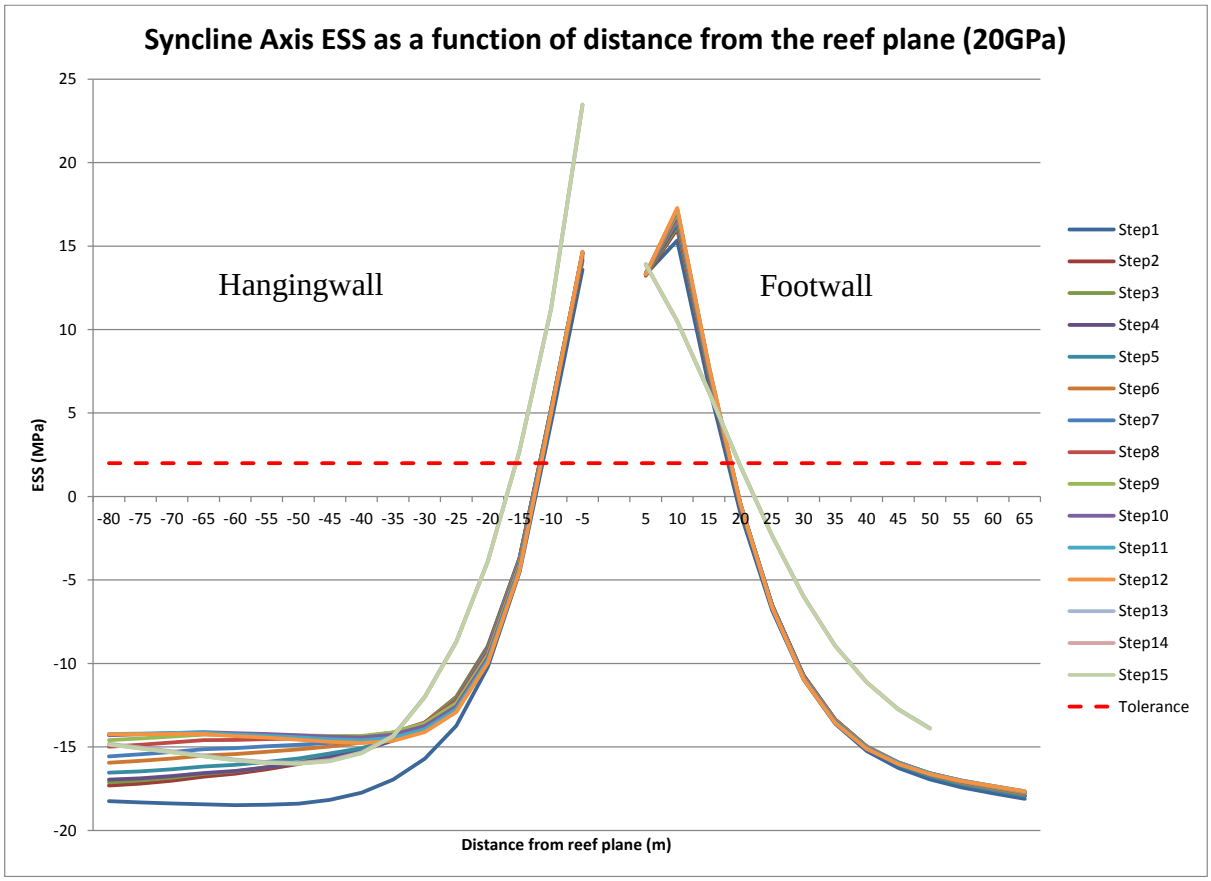


Figure 5-36 Revised Model: Syncline Axis ESS as a function of distance from the reef plane

Figure 5-37 shows ESS of the Murray Fault in the revised plan. In comparison to Figure 5-24, a reduction in ESS is realised, although the failure criterion is still exceeded. Of note is that the footwall the Murray Fault shows higher ESS values in the revised plan than the current LOM12 plan. The overlapped section also shows a higher ESS value in the revised plan.

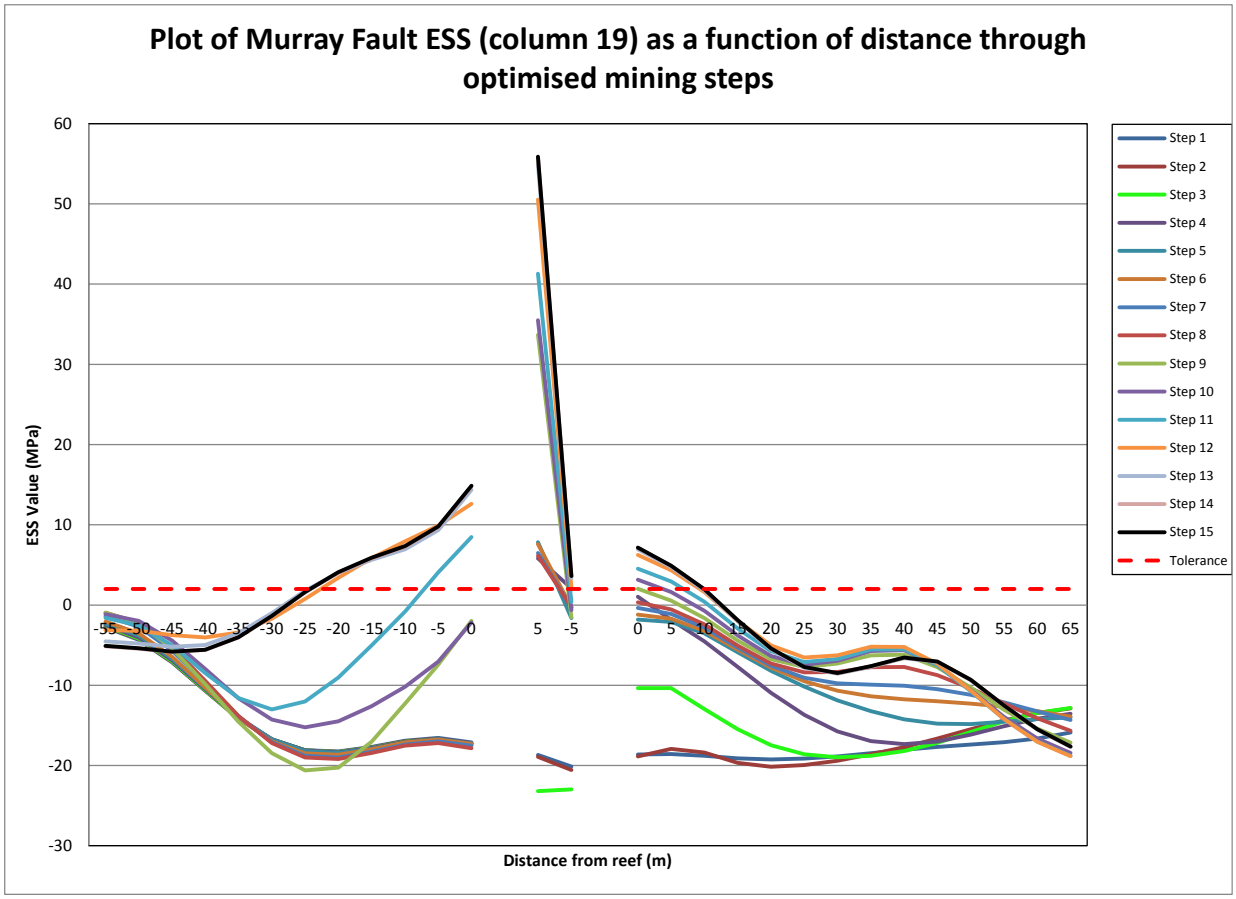


Figure 5-37 Revised Model: Murray Fault ESS as a function of distance from reef plane

5.7.5. Change in Average Pillar Stress

Figure 5-32 show the relative positions of each of the simulated pillars used in the revised mining sequence. Four pillars (Pillars 1-4) were simulated, each with a width of at least 50m. The failure criterion (Chapter 2, Table 2-4) is represented as the transparent yellow block in Figures 5-38 to 5-41. The figures show that

- Pillar 1 – APS falls within the range and marginally above the lower limit;
- Pillar 2 similar to Pillar XX (Figure 5-27) – APS falls within the range but is closer to the upper limit;
- Pillar 3 – APS falls within the range; and,
- Pillar 4 is the widening of the existing Pillar ZZ (Figure 5-27) – APS is still above the range and above the upper limit. However, in terms of the block availability and geometry, additional pillars cannot be designed to reduce this APS.

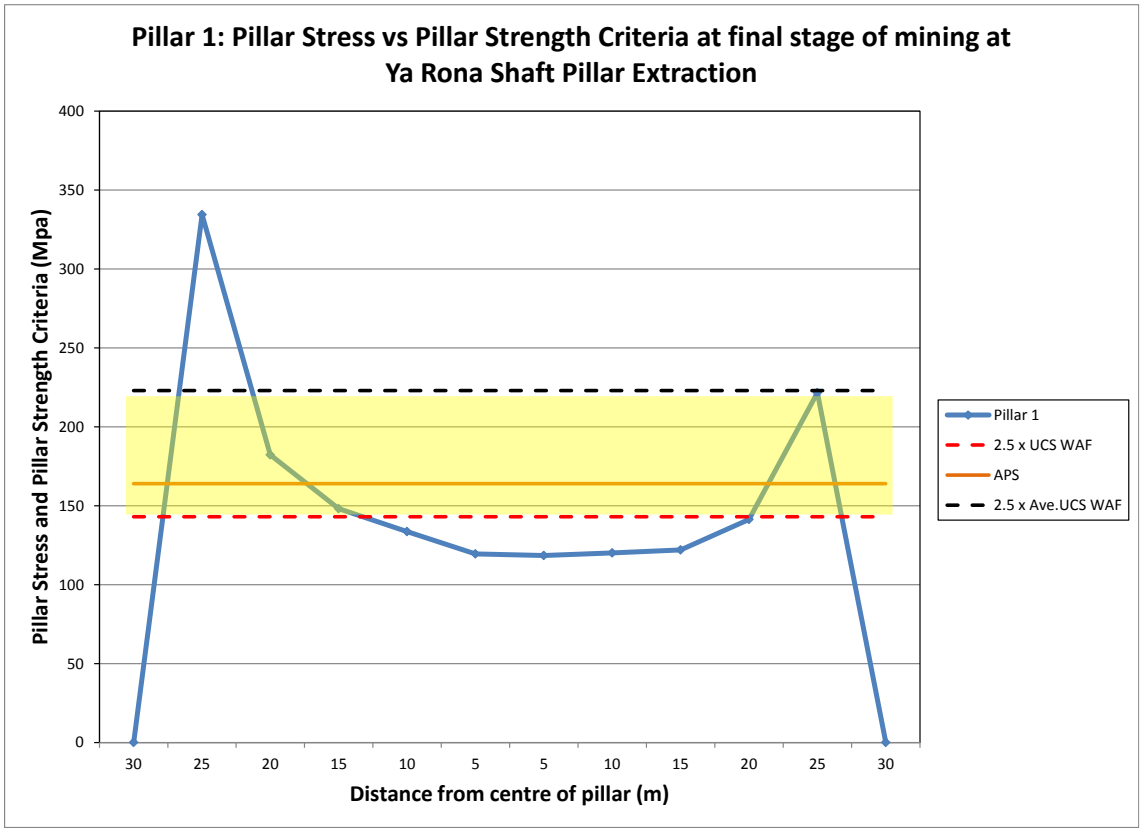


Figure 5-38 Pillar Stress vs Pillar Strength Criteria at final stage of mining of Pillar 1

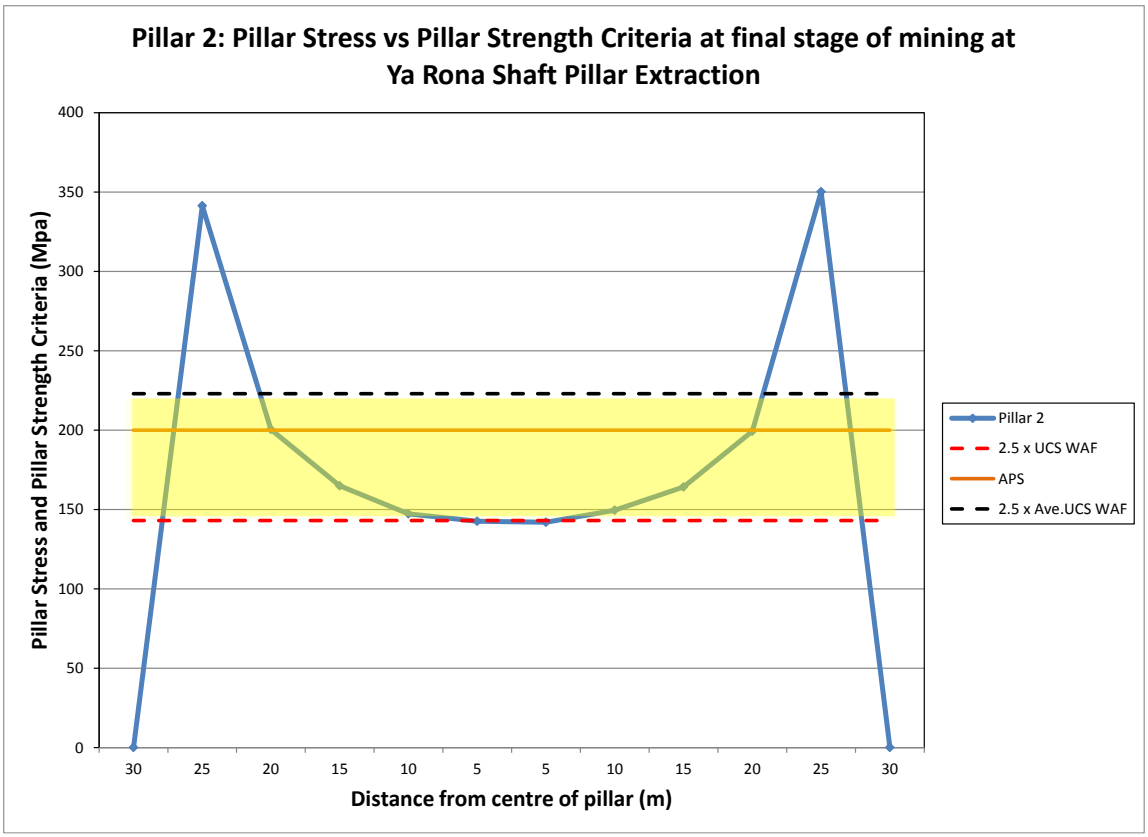


Figure 5-39 Pillar Stress vs Pillar Strength Criteria at final stage of mining of Pillar 2

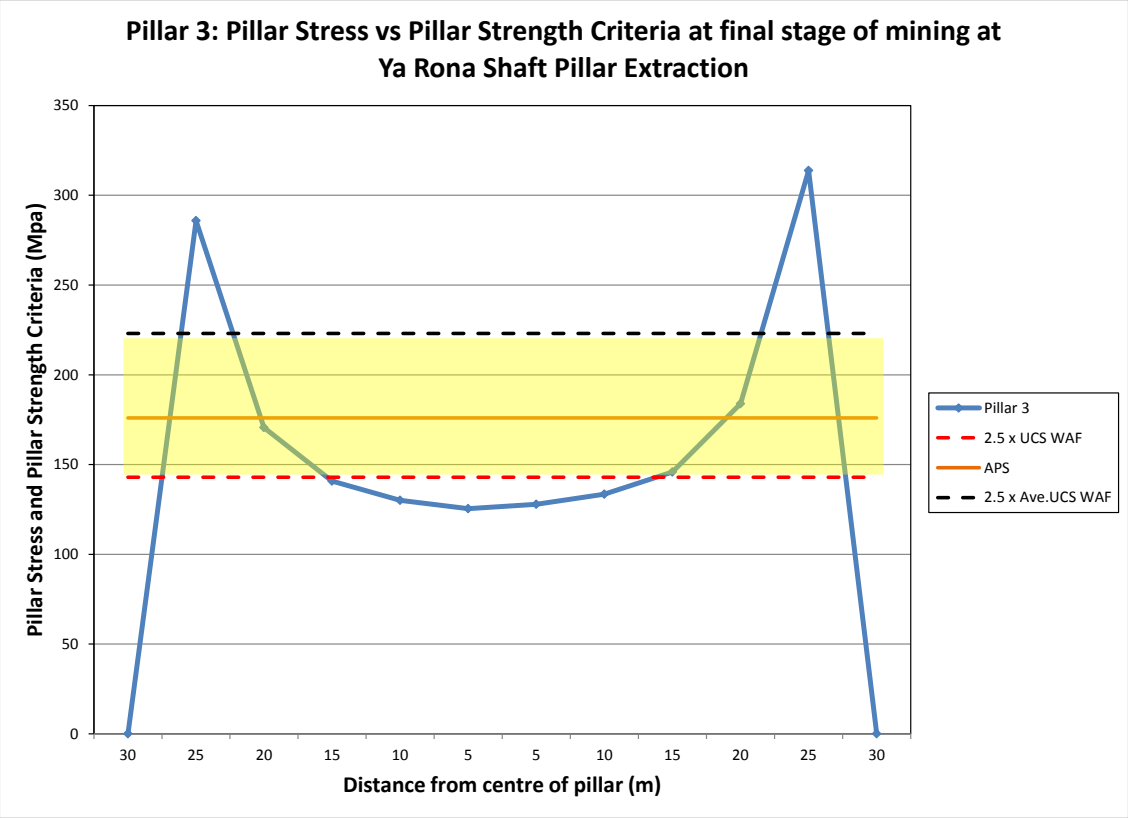


Figure 5-40 Pillar Stress vs Pillar Strength Criteria at final stage of mining of Pillar 3

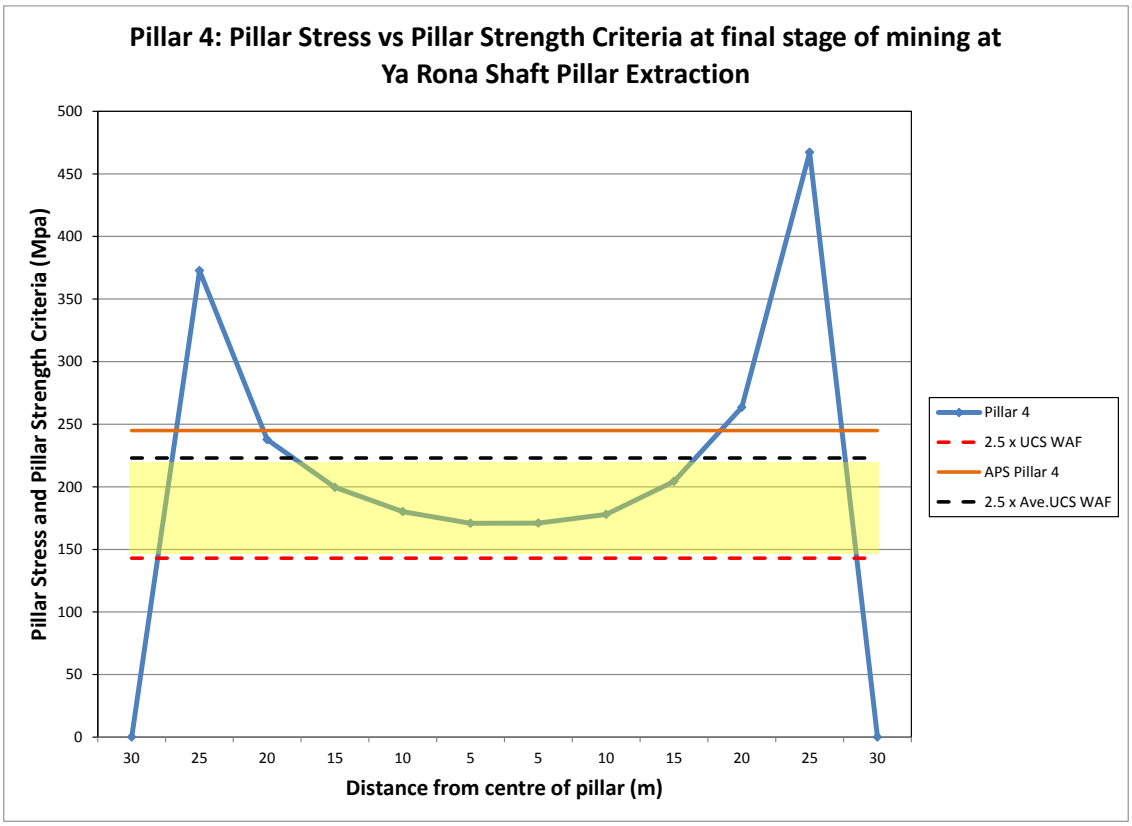


Figure 5-41 Pillar Stress vs Pillar Strength Criteria at final stage of mining of Pillar 4

5.7.6. Change in ERR

From Table 5-5 and Figure 5-42:

- Of the 65 data points, 40 points (62%) fall below the 30MJ/m_2 failure criterion (Chapter 2, Table 2-4). Therefore, 38% are above the failure criterion; and,
- This represents an improved ERR (from 57% to 38%) in the revised mining sequence.

	Block A	**Block B**	**Block C**	**Block D**	**Block E**	**Block F**	**Block G**	**Block H**
	(MJ/m^2)							
Step 1	No values computed as no change in mining occurred							
Step 2	9.7	12	-	9.6	11.1		-	5.1
Step 3	17.9	11.2	-	-	21.2		-	5.9
Step 4	28.9	17.5	-	-	25.5		-	6.0
Step 5	41.9	18.3	-	-	35.7		-	5.9
Step 6	17.8	13.0	5.6	23.0	54.8	4.7	-	8.0
Step 7	-	14.8	9.6	23.7	75.5	7.9	-	8.0
Step 8	-	30.0	10.9	31.1	64.1	42.4	-	8.5
Step 9	-	38.8	7.1	31.7	4.8	47.9	-	14.2
Step 10	-	35.6	34.2	43.7	12.6	61.7	-	16.7
Step 11	-	-	31.1	48.3	28.6	116.6	5.5	21.0
Step 12	-	-	35.1	62.9	39.7	208.5	7.7	-
Step 13	-	-	-	58.9	39.2	-	18.6	-
Step 14	-	-	-	-	68.1	-	28.5	-
Step 15	-	-	-	-	-	-	32.3	-

Table 5-5 ERR values for optimised mining sequence over the 15 mining steps

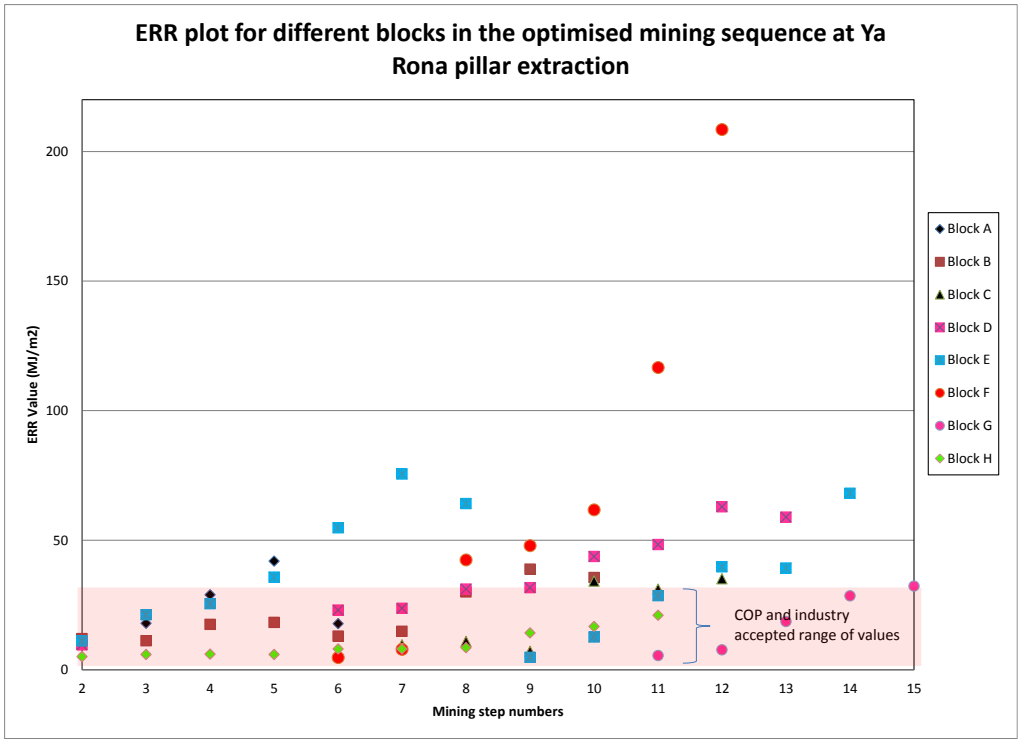


Figure 5-42 ERR Plot of revised mining sequence at Ya Rona pillar extraction

5.8. Conclusions from the optimized mining sequence

The revised mining sequence delivers the following results:

- Mining spans are reduced to a maximum of 110m;
- This results in reduced vertical displacement of the shaft to approximately 60% less than the current LOM12 mining plan;
- The Y-direction displacement in the shaft is lower than the failure criterion;
- Ride is reduced in the Y-direction;
- The change in RCF is insignificant and does not meet the failure criterion in the both mining sequences;
- Reduction in ESS on both the Murray Fault and the Syncline Axis is noted but the failure criteria are still exceeded at some points in the rockmass, most notably 20m above and below the reef planes;
- None of the regional stability pillars meet the APS criteria set out in Chapter 2 if the lower UCS value for WAF is used. However, if the average UCS value is used, 3 or the 4 pillars meet the criteria; and,
- A reduction in ERR is indicated in the revised plan.

6. Mitigation strategies to reduce the impact of WAF

6.1. Introduction

In chapter 5 those areas more susceptible to damage than others were highlighted. The impact of WAF in the design was outlined and additional numerical modelling was undertaken to quantify how changes in the design could show better results. In this chapter, WAF mitigation strategies are tabled to reduce the negative impact of WAF on the mining plan. These show how the:

- Tailored monitoring system can give advance warning of WAF failure, and,
- Current WAF mitigation strategies will reduce the impact of the WAF.

6.2. Instrumentation and monitoring

Instrumentation and routine monitoring of excavations are important tools for design and analyses in rock engineering. There are a number of systems that are used in the industry but the key elements fall into one of two categories. They are either capable of:

- Real-time monitoring, or,
- On-site monitoring.

The latter entails downloading data from instrumentation sited in the monitored excavations. This could mean a delay in retrieving the data and consequently processing of the data may be late. Vital information, required by the rock engineering professional, to may decisions may be compromised. In the real time monitoring system, data is sent up from the monitoring sites through the existing engineering systems to a data capturing computer which is easily accessible to the rock engineering design team. In most cases, the rock engineering practitioner uses a combination of both systems to procure data.

Therefore, when the WAF rockmass showed anomalous behaviour, the selection of the type of system was unanimous. The fact that WAF could fail at any time, based on the case studies presented in chapter 2, dictated that a real-time system be employed to monitor those excavations where WAF stability was imperative. In the case of the shaft, the data needed to be readily available so that conveyances could be stopped if failure was imminent. Therefore, in 2006, a network of geotechnical instruments was installed in the shaft to monitor the WAF. Recorded during this phase was the fact that the drilling proced difficult

due to the fractured and weathered nature of the WAF rockmass. This gave the design team insight into the stress levels and the potential for deformation should failure result. Figure 6-1 shows the planned network which monitored the WAF, the reef stope as well as the Murray Fault.

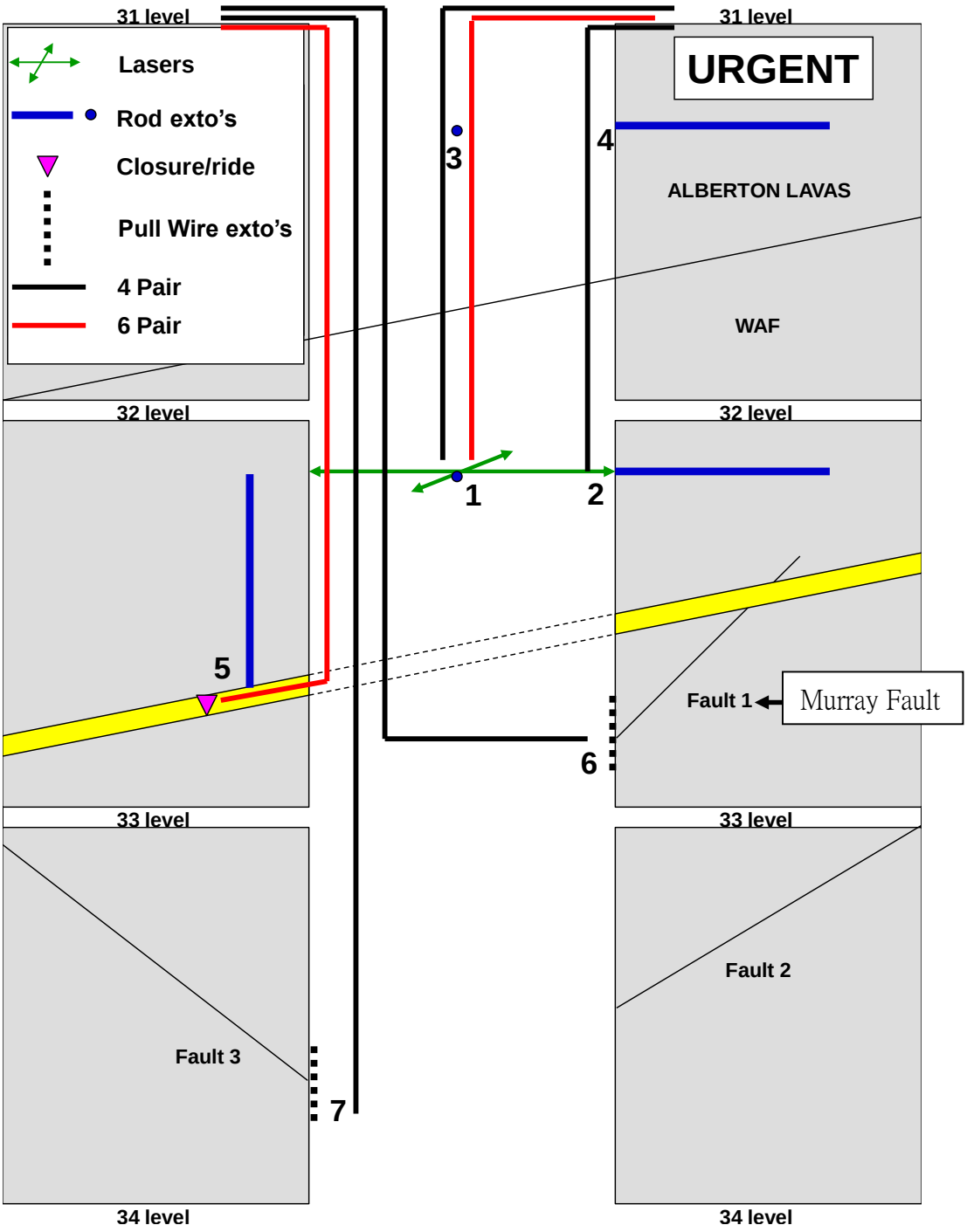


Figure 6-1 Section of Ya Rona shaft showing planned network of geotechnical instruments



Figure 6-2 Collage of photographs (from left – multipoint rod extensometer, calcification of rod extensometer, laser sight, wire extensometer) showing the geotechnical monitoring instruments installed at Ya Rona shaft

The original 2006 system met with limited success as calcification (Figure 6-2) around the geotechnical units occurred. This impacted negatively on the ability of the rock engineering design team to make informed decisions on the WAF. Shaft examinations of the barrel could quantify visible damage whereas the system could not. The upgrade immediately showed that the WAF was in creep mode (Figure 6-3; data after 2009/02/15), with intermittent large deformations. Unfortunately the system relied on point measurements (lasers) and could not quantify large zones of failure. Another upgrade was provided, named the Shaft Barrel Deformation System (SBDS), which is a “real” time survey monitoring system (Figure 6-4) comprising a number of prisms, fixed to different points on the shaft barrel sidewall, which are sighted at regular intervals by two survey theodolites.

The data (Figure 6-5) from the new system showed the creep behaviour of the WAF.

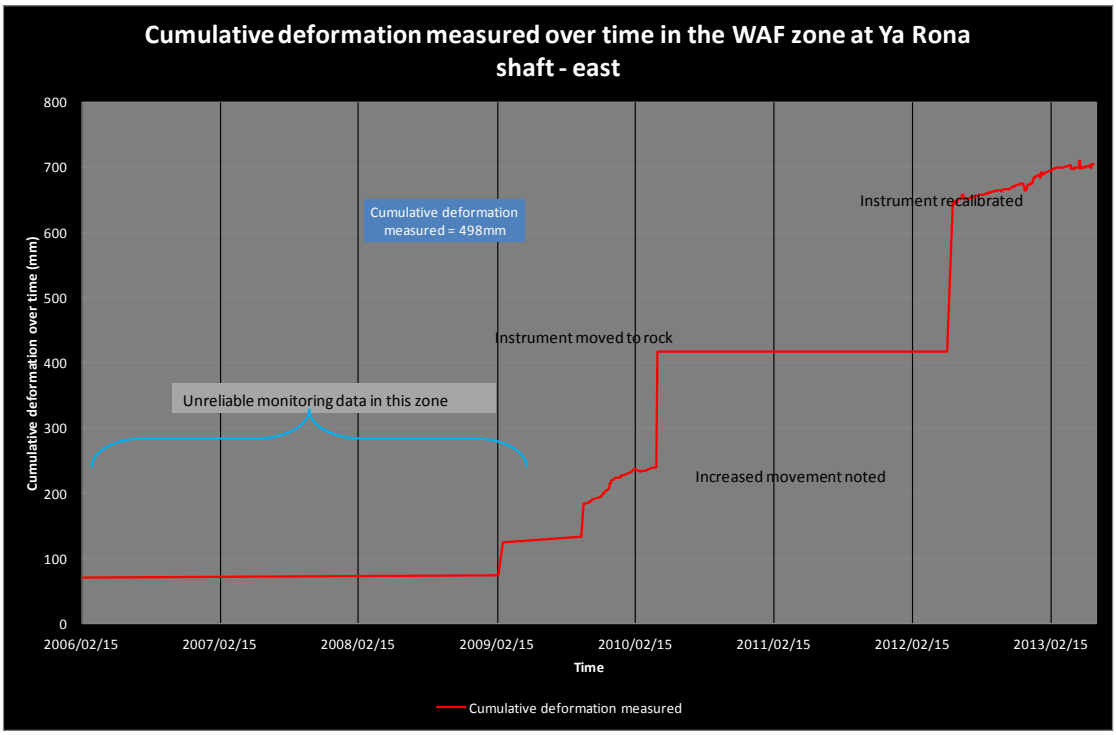


Figure 6-3 East laser plot of cumulative deformation over time (2007-2013) at Ya Rona shaft

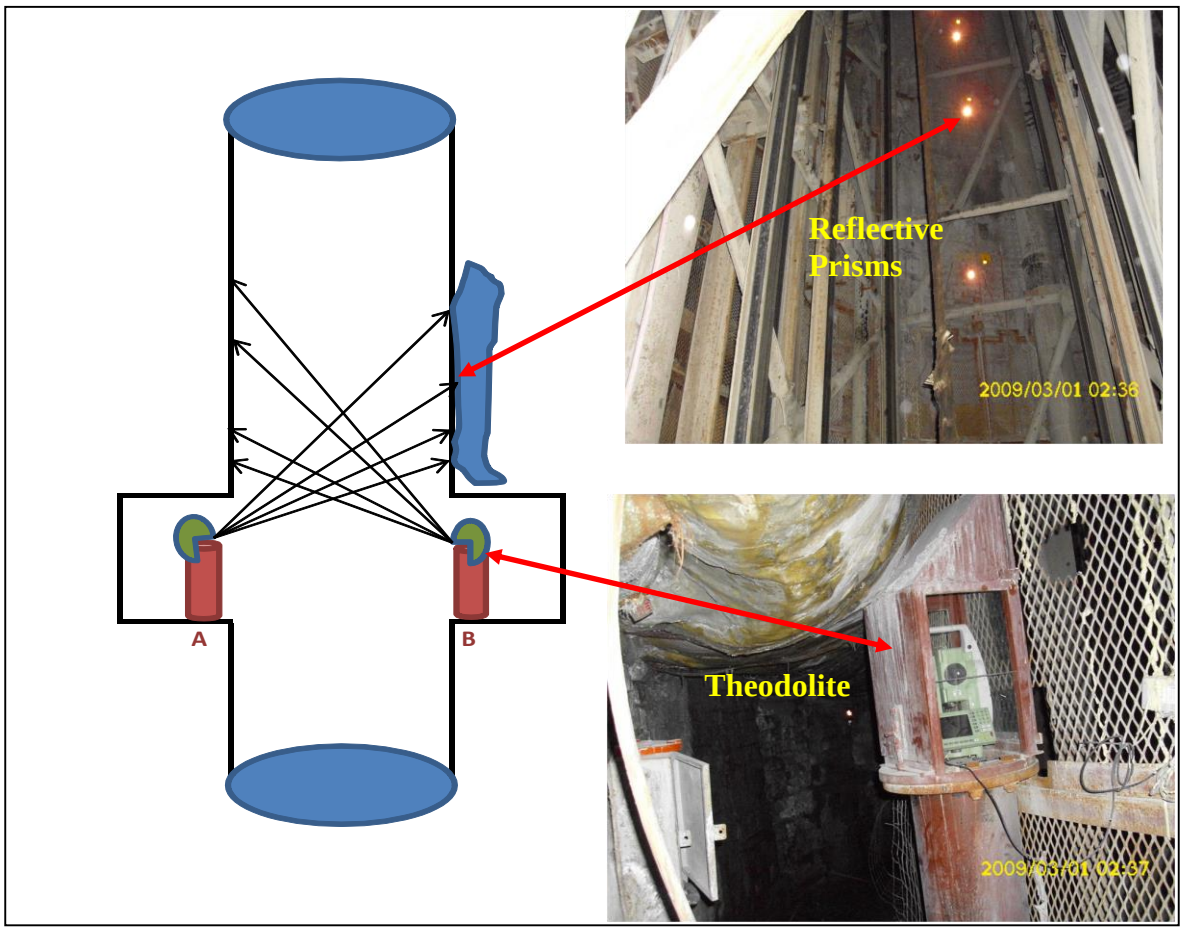


Figure 6-4 Section of Ya Rona shaft barrel and photographs showing theodolite multipoint survey instruments and prisms installed in 2009 at Ya Rona shaft

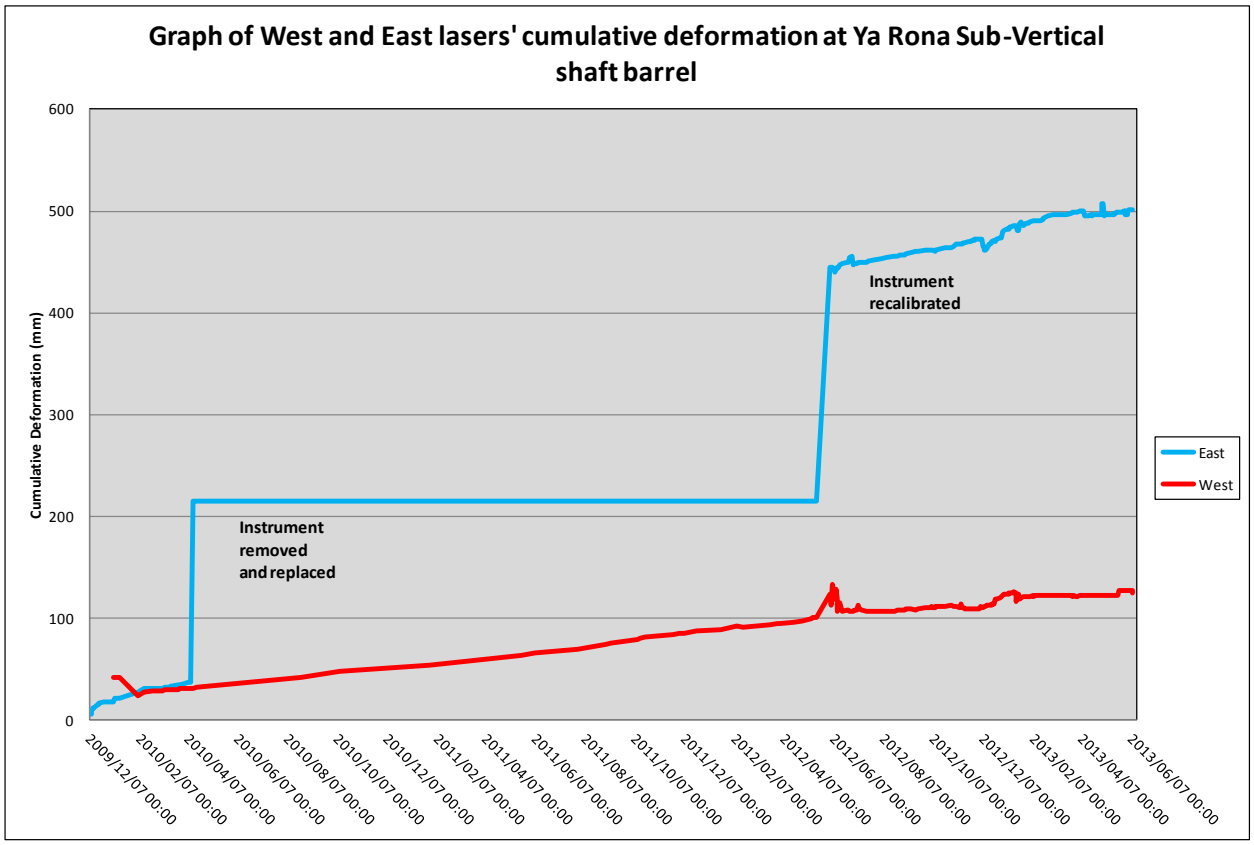


Figure 6-5 East and West lasers' plot of cumulative deformation over time (2009-2013) at the Ya Rona Sub-Vertical shaft showing WAF creep behaviour

6.3. Current WAF mitigation strategies to reduce the impact of WAF

The five main areas, that need WAF mitigation strategies according to the numerical modelling analyses, are:

1. The Ya Rona (4) Sub-Vertical barrel system stability,
2. The Syncline Axis potential for slip,
3. The Murray fault wedge displacement and potential for slip,
4. The stoping areas' susceptibility for damage from WAF, and,
5. Regional stability pillars' not meeting the failure criterion.

Although this chapter will concentrate primarily on the four areas above, other WAF mitigation strategies, within shaft pillar extraction, will also be discussed briefly. The reason for this is that although each excavation may need a particular WAF support strategy, all the strategies should have a common design to ensure that the support system for the Ya Rona shaft pillar extraction is not compromised.

6.3.1. Ya Rona Shaft WAF mitigation strategy

A shaft system is the most important entity in any mining infrastructure, as it is the main point of ingress and egress of men, material and ore. In a typical deep mine, the shaft system would comprise of one or more vertical shaft sections with horizontal tunnelling extending from the vertical sections. The horizontal sections would contain key service excavations; namely, level stations, sub-stations, workshops, hoist rooms, dams, pump chambers, raisebore holes and orepass systems. These excavations function as key elements in the mining process and therefore, protection of these excavations is imperative. Any geotechnical risk to these excavations must be dealt with timeously and appropriately.

It is clear from the numerical modelling analyses, the underground observations and the prevailing stress conditions that WAF poses the largest threat to the shaft - WAF rockmass passes through it at two locations (Figure 6-6). It is, therefore, imperative that a support system be designed that is able to restrain the forces imposed on it. The WAF zone height is measured at 19m (Figure 2-10), but from the numerical modelling, the potential zone of damage could be as much as 70m above and below reef.

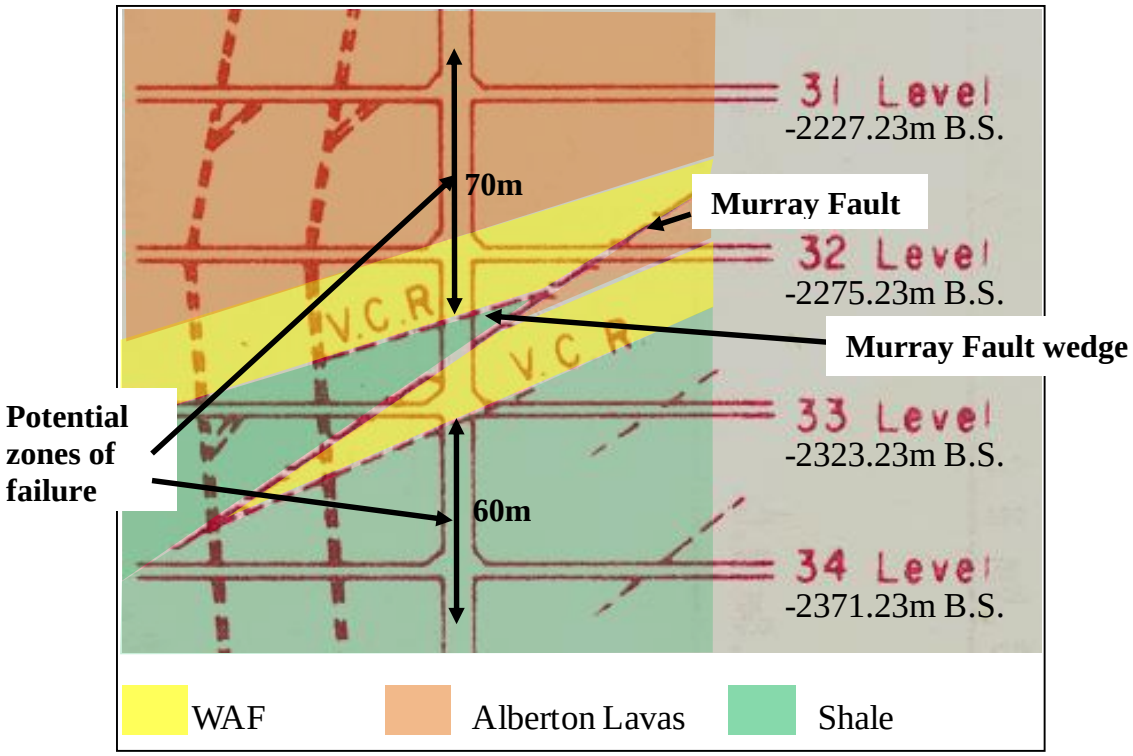


Figure 6-6 Graphical representation showing the Murray Fault wedge, the two WAF intersections and the zones of potential failure in the Ya Rona Shaft

Therefore from a design point of view, four zones (Figure 6-6; Table 6-1) had to be quantified to ameliorate the effect of the WAF and the 70m potential deformation zone. These were selected on the basis of their rockmass characteristics as well as their expected modes of failure.

Zone	Acronym	Characteristics	Failure Mechanism/s	Support Procedure
Alberton Lava Zone	ALZ	Good quality rock, 229-291 MPa (Appendix B – Table b-4)	Brittle, stress-induced, dynamic	SP1
WAF	WZ	Poor quality rockmass above upper conglomerate, visco-plastic, 57-152 MPa (Appendix B – Table b-4)	Creep, Time dependant, stress-induced, dynamic	SP2
Shale WAF	SWZ	In between top reef and bottom reef, area in between top reef and Murray Fault, shale footwall of top reef and WAF of lower reef	Creep, Time dependant, stress-induced, dynamic	SP3
Shale	SZ	Average quality rockmass	Stress-induced, dynamic	SP1

Table 6-1 Zones of weakness at the Ya Rona Sub-Vertical Shaft

6.3.1.1. The Alberton Lava Zone (ALZ)

With an average UCS of 263MPa from the 4 rock core tests conducted (Yilmaz, 2006), Alberton Lavas exhibit the best quality rock at the Ya Rona SV barrel. It is expected that damage will occur in this zone from stress-induced failure or failure from seismic loading. Therefore, all excavations in this area have had to contain support elements that would be able to yield under seismic loading as well as areal coverage to ensure that additional restraint is provided under static conditions. Horizontal excavations included tendons, welded mesh, lacing and site specific mechanical anchors to mitigate the hazard. Although the shaft barrel has a 300mm concrete lining, the support system was upgraded to include 3m yielding tendons (primary criterion), welded mesh and lacing (Figure 6-7). As most of the support was installed in the good quality Alberton Lava rockmass, the decision was taken to install only vertical lacing ropes. However, during mining, if the area showed increased deformation, rehabilitation measures would include diagonal lacing.

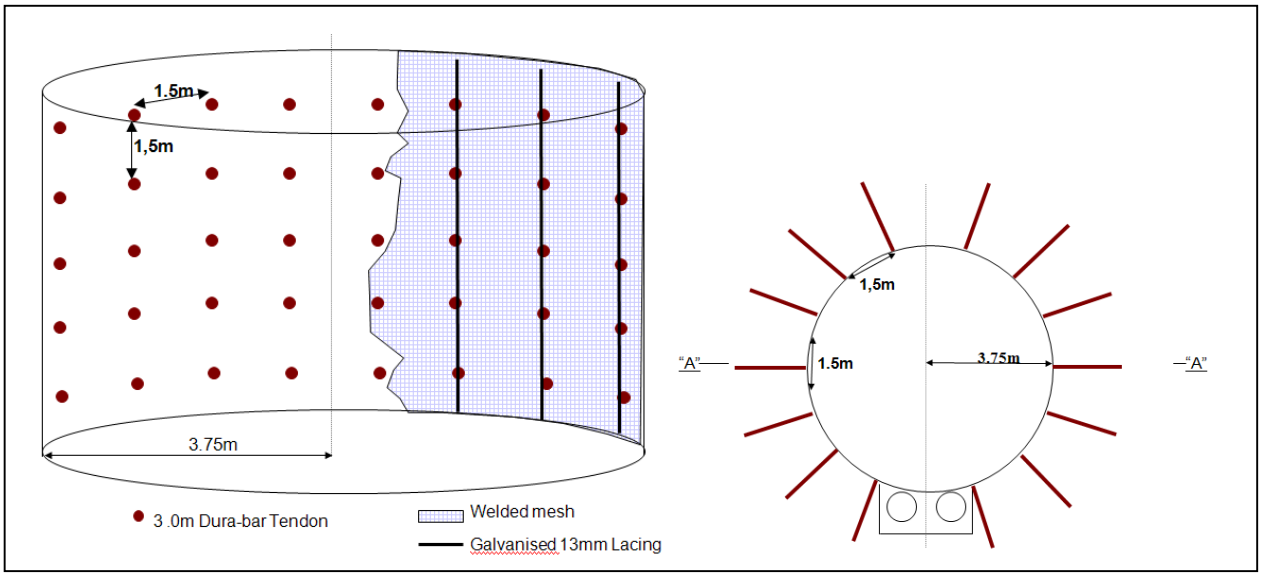


Figure 6-7 Graphical representation of SP1 standard at Ya Rona SV (amended from Durapraj, 2002)

6.3.1.2. The WAF Zone (WZ)

Twelve rock core tests (Yilmaz, 2006) yielded an average UCS of 102MPa. In this zone, the expected modes of failure would include stress-induced failure, damage as a result of seismic loading, time dependant deterioration from creep and chemical alteration through exposure to air and water.

For the horizontal excavations, especially the level stations, site specific support strategies were prescribed. In addition, some of the horizontal excavations had to be re-sited as the potential for deformation exceeded the known capacity of the support system that could have been installed in these excavations.

In the shaft sidewall, the support design required that a combination of 3m yielding tendons, welded mesh, vertical and diagonal lacing ropes, and 4.5m mechanical anchors, be installed. However, after the drill crews reported that holes did not stay open long enough (indicative of high stress conditions or a highly fractured rockmass) to remove the drill steel, insert the mechanical anchors and grout effectively, the design was changed to use resin bolts (Figure 6-8). The drilling regime of a resin bolt is that the drill steel does not have to be removed from the hole – the resin bolt doubles as the drill steel and provides an aperture through which resin can be injected.

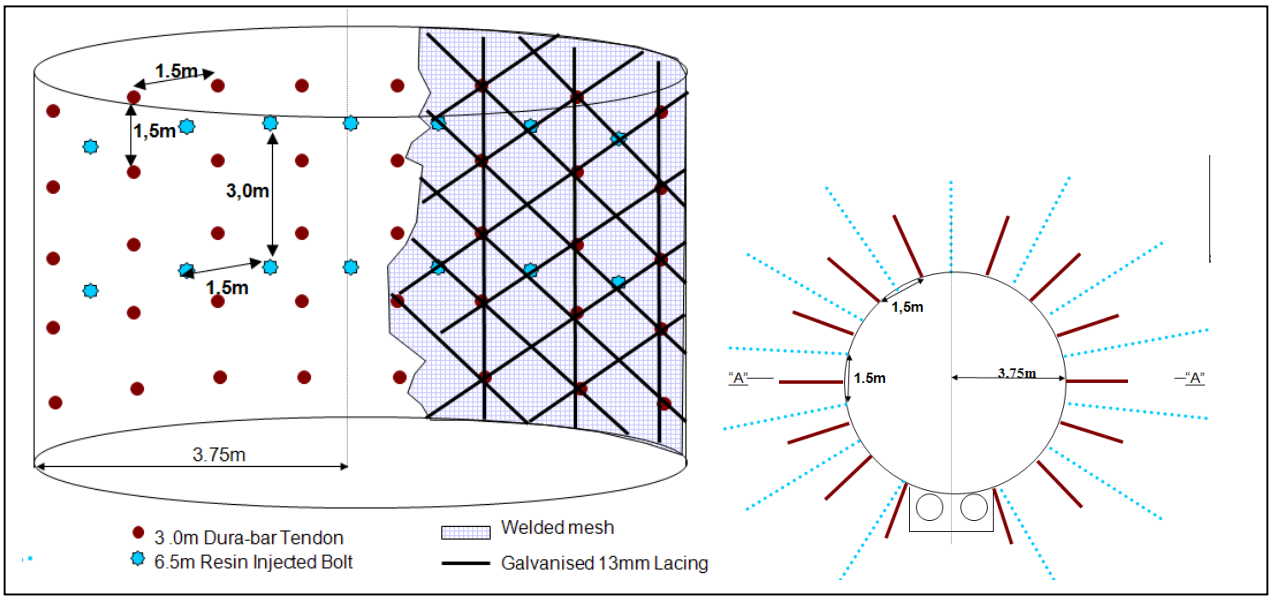


Figure 6-8 Graphical representation of SP2 standard at Ya Rona SV (amended from Durapraj, 2002)

As this zone also showed poor restraint properties, the concrete in this zone was tested (Yilmaz, 2006 - Appendix B - table B-4). UCS values showed that the concrete installed was of a lower strength than the design strength of 30MPa. Moreover, because the lining showed severe deformation in the WAF zone, parts had to moiled out. This process resulted in the the revelation that the thickness of the lining was sub-standard. Some portions exhibited rock in residual strength mode - note the comparison (Figure 6-9) between the shear fracture angle of a rock specimen under uniaxial compression when in residual strength mode and that of the fracture angle of the concrete lining. The angles seem to be the same and therefore, the inference can be made that the concrete was in a residual strength mode.

6.3.1.3. The Shale WAF Zone (SWZ)

This zone is a combination of poor quality WAF, the Murray Fault plane and the shale footwall. Although no testing of the shale has been conducted, underground investigations have indicated that the shale rockmass is of a poor quality. It was expected that damage would occur in this zone from stress-induced failure or from seismic loading. Previously, drilling in this zone did not present any difficulties, as opposed to drilling in the WZ zone. Therefore, 3m yielding tendons 4.5m mechanical anchors, vertical lacing ropes and welded mesh (Figure 6-10), was prescribed for this zone. If required, rehabilitation measures would include the installation of diagonal lacing.

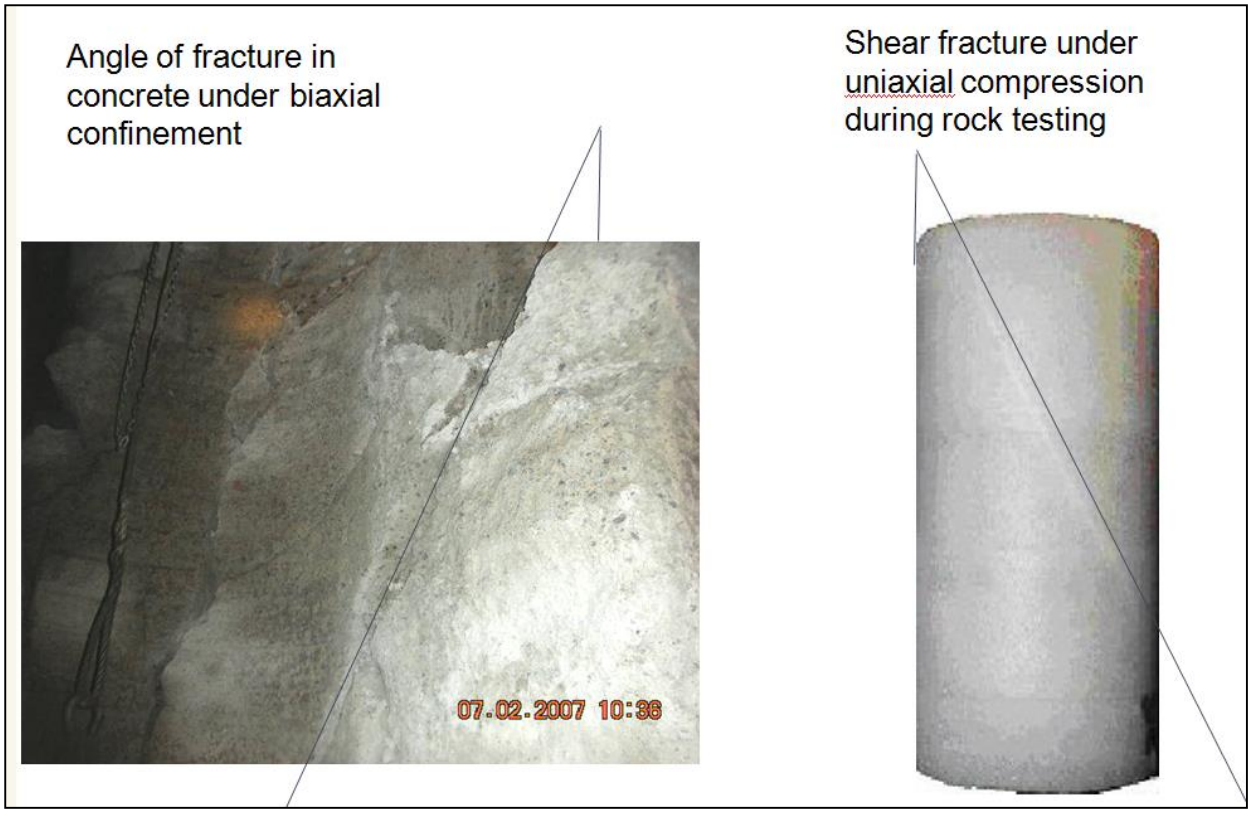


Figure 6-9 Photographs showing comparison of fracture angle for concrete lining and rock specimen (Durapraj, 2007)

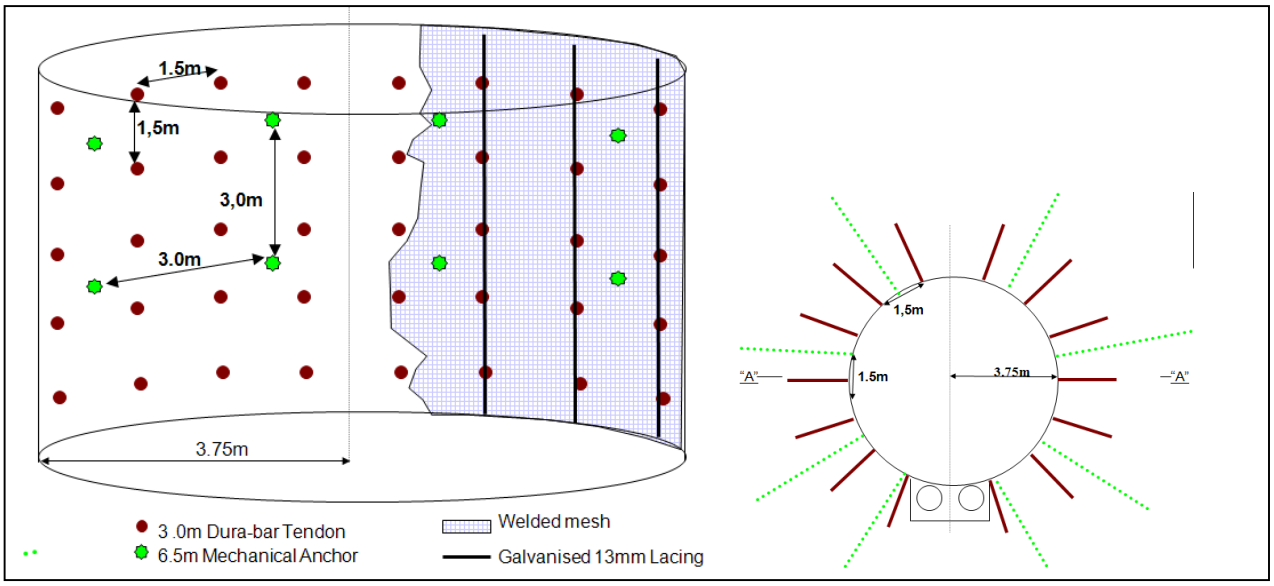


Figure 6-10 Graphical representation of SP3 standard at Ya Rona SV (amended from Durapraj, 2002)

6.3.1.4. The Shale Zone (SZ)

The rockmass in this zone is of average quality. It was expected that damage, in this zone, would occur from stress-induced failure or seismic loading. Therefore, the support regime in Figure 6-7 was prescribed.

6.3.1.5. The siting of the inner pillar extraction in the footwall

In an attempt to reduce the impact of the mining of the inner pillar extraction on the operational shaft, the rock engineering design had to consider alternatives that would limit the WAF impact. The so-called 'de-stressing' (stoping slot) of the shaft was to occur in the footwall of the reef (Figure 6-11). Siting the stoping slot in the footwall allowed the more competent reef (Yilmaz, 2006) to be the hangingwall of the slot. Therefore, the impact of WAF displacement would not impact on the shaft excavation. Figure 6-11 shows the plan (Besol simulation) and section views of the 30m on strike by the 30m on the 'flat' dip inner pillar mining sequence.

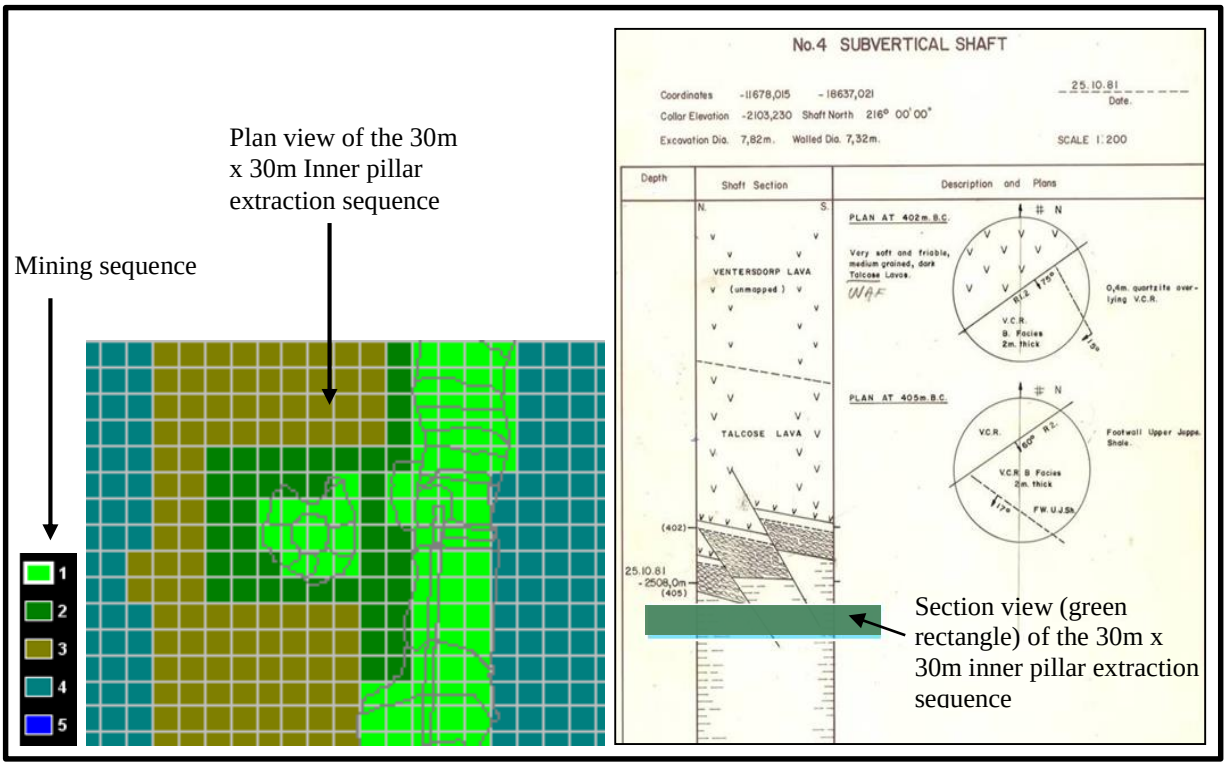


Figure 6-11 Plan (simulation) and section (stoping footwall slot) views of the Inner-inner pillar extraction at the Ya Rona Sub-Vertical shaft

6.3.2. The Syncline Axis mitigation strategy

From the numerical modelling, it was understood that leaving an appropriately sized bracket pillar would negate the effect of the WAF influence on the Syncline Axis. From Figure 5-20, this bracket pillar was designed to be 20m on either side of the fault intersection with the reef.

6.3.3. The Murray Fault mitigation strategy

The Murray fault intersects the shaft (Figure 6-6) and creates a wedge-shaped rock block against the shaft concrete lining. Prior to 2003, the only restraint, provided for this block, was the 300mm thick concrete lining, shown in Figure 6-9, which is purported to be in a residual strength phase. Hence, if this rock block was liberated, only the concrete lining would prevent it from damaging the shaft. However, as part of the support strategy outlined for the SWZ zone, 3m tendons and the 4.5m mechanical anchors with mesh had been prescribed. This, however, would have been able to restrain movement of keyblocks in the immediate periphery or the reinforced shell created by the support system. If the rupture point of the Murray Fault was more deep-seated (>5m) and the resultant effect liberated a larger block of rock (the wedge in Figure 6-6), the support system may not be able to restrain the forces involved in the rupture.

Furthermore, it has been established that the fracture zone in the WAF was significantly larger when drilling of the geotechnical holes occurred. It is also now known that the WAF has the ability to creep, so the support system must be able to arrest the resultant forces. A fit-for-purpose yielding anchor was developed for this application by the rock engineering design team. It consisted and performed in the following manner:

- 25ton, 6 core, single strand, yielding cable anchor,
- 11.5m long anchor (Appendix C, Figures C-1 to C-4) could have a yield range of 135-210mm before breaking. The yield potential was approximately four to seven times more than the ‘normal’ cable anchor,
- Could withstand a maximum load range of between 161-169kN,
- A residual strength of 110kN, and,
- The units could tolerate 250kN and 200mm yield during dynamic testing.

Had the WAF not been part of the rockmass at the Murray Fault, the design team would have not prescribed the designed specific yielding support for this zone.

6.3.4. WAF mitigation strategies in the stoping horizon

Apart from analysing the design in the numerical model, appropriate support strategies in the stoping excavations required consideration. As the hangingwall of the stope would inevitably be WAF, the rock engineering design team had to ensure the continued stability of the mining excavations on the reef horizon. Therefore, a key concern was the closure profile of each block of ground in the mining sequence. Should the expected high closure rates be experienced, the support system must be able to counteract the effect.

This section also talks to the mine design aspects that contribute to stability on the reef horizon and presents the Ya Rona in-house design case data that could be used in future extractions where WAF specific strategies are required.

6.3.4.1. Closure assessments

As opposed to convergence, which is the elastic movement of the entire rockmass, closure takes into account both the elastic and inelastic components of deformation in the rockmass. It is an important measure of stability as well as access. If the back areas, which are usually the access to the workings, are inaccessible, this could impede production. Moreover, if the back area closes at a high rate, additional shear load is placed on the mining front, which may result in a higher strain-burst potential.

Table 6-2 shows the modeled closures for the current LOM12 and the revised mining sequence. The larger mining spans (LOM12) resulted in 0.7m – 1.45m of closure on the reef horizon. Therefore final mining heights were in the range of 0.35m – 1.1m. The revised plan resulted in closures of 0.4m – 1.4m, resulting in final heights of 0.4m – 1.6m. Certain blocks in the sequence produced more favourable closure profiles as their spans had been reduced significantly.

Block	Modelled Stoping Width (m)	LOM12 Modelled Cumulative Closure (m)	Final Access Height (m) for LOM12	Revised Mining Sequence	Final Access Height (m) for optimized sequence
A	1.8	1.45	0.35	0.9	0.9
B	1.8	0.7	1.1	0.7	1.1
C	1.8	1.1	0.7	0.9	0.9
D	1.8	1.38	0.42	1.4	0.4
E	1.8	1.2	0.6	1.1	0.7
F	1.8	1.4	0.4	1.4	0.4
G	1.8	-	-	0.8	1.0
H	1.8	-	-	0.4	1.4

Table 6-2 Comparison of closures modeled in LOM12 and Optimized plan for Ya Rona Shaft Pillar Extraction

The data mirrors the closure profile (Figure 4-8) for the closure measurements undertaken by Durapraj (2006c), where 50% closure was calculated in the WAF environment despite backfill being placed.

6.3.4.2. Backfill selection

Although this research report does not include an in-depth discussion of backfill, it is an important part of the design, especially when considering the high closure rates that have been experienced in the WAF rockmass. Numerical modeling using backfill as a support medium in a shaft pillar extraction (Raffield, et al, 1993), found that:

- Small vertical closures resulted when using backfill, and that,
- The design strain for both the shaft lining and steelwork were not exceeded when backfill was placed.

Therefore, the use of backfill was prescribed in mitigation of the high closures being experienced.

At Ya Rona Shaft, classified tailings have been used since 1995 as large amounts of waste rock and residue are produced in the mining process. Backfill reticulation systems are in place at all the shafts and therefore, the decision to use classified tailings seemed the logical choice at the Ya Rona shaft pillar.

6.3.4.3. Pre-stressed Elongates and Pack considerations

To restrain the high closure rates in WAF, a combination of backfill, pre-stressed elongates and packs have been prescribed. Even though backfill provides a measure of local stability, it still needs a significant amount of closure before the full benefit of backfill can be experienced. Pre-stressed timber chock packs and pre-stressed elongates provide the active, immediate WAF restraint. Appendix C, Figures C-5 to C-9 show test data for the specific products used in the support system.

The information in Chapter 2 showed that WAF has multiple planes of weakness. These rock blocks, therefore, have the ability to rotate if left unsupported. From a design viewpoint, the support system must try to prevent these rotations and therefore minimize the undesired falls of ground (FOGs). Figure 6-12 illustrates block failure as a result of inadequate areal coverage. Mechanical tendons had been installed in the WAF rockmass without the areal (mesh) support. The support system failed because the load imparted by the WAF rockmass was not dispersed over several integrated support elements.



Figure 6-12 Photograph showing multiple failure surfaces of WAF which resulted in a significant fall of ground

6.3.4.4. Rock Consolidation

Figure 6-13 shows the stand-up time for WAF using Q-value information provided in Chapter 3, Table 3-1 (Q = 0.1-2.0). Using a mining span of 1.8m, which is the access gully width, stand-up time for WAF (blue block in Figure 6-13) is plotted on a roof span/stand-up time design chart. Unsupported WAF has a stand-up time of between 2 and 30 days. In a typical mining cycle on a conventional mine blasting a face, backfill is usually installed about 4-6m from the face. To get to this position, the face would have to be blasted 4-6 times which could take anything from 4-14 days depending on cleaning and support cycles. Therefore, at any time in the cycle, some of the WAF could be left unsupported for more than 2 days. From a design perspective, 3m long rock consolidation bolts were prescribed to ensure that more active support was installed in the WAF rockmass. This was in addition to the pre-stressed elongate, pack and backfill WAF mitigation support system.

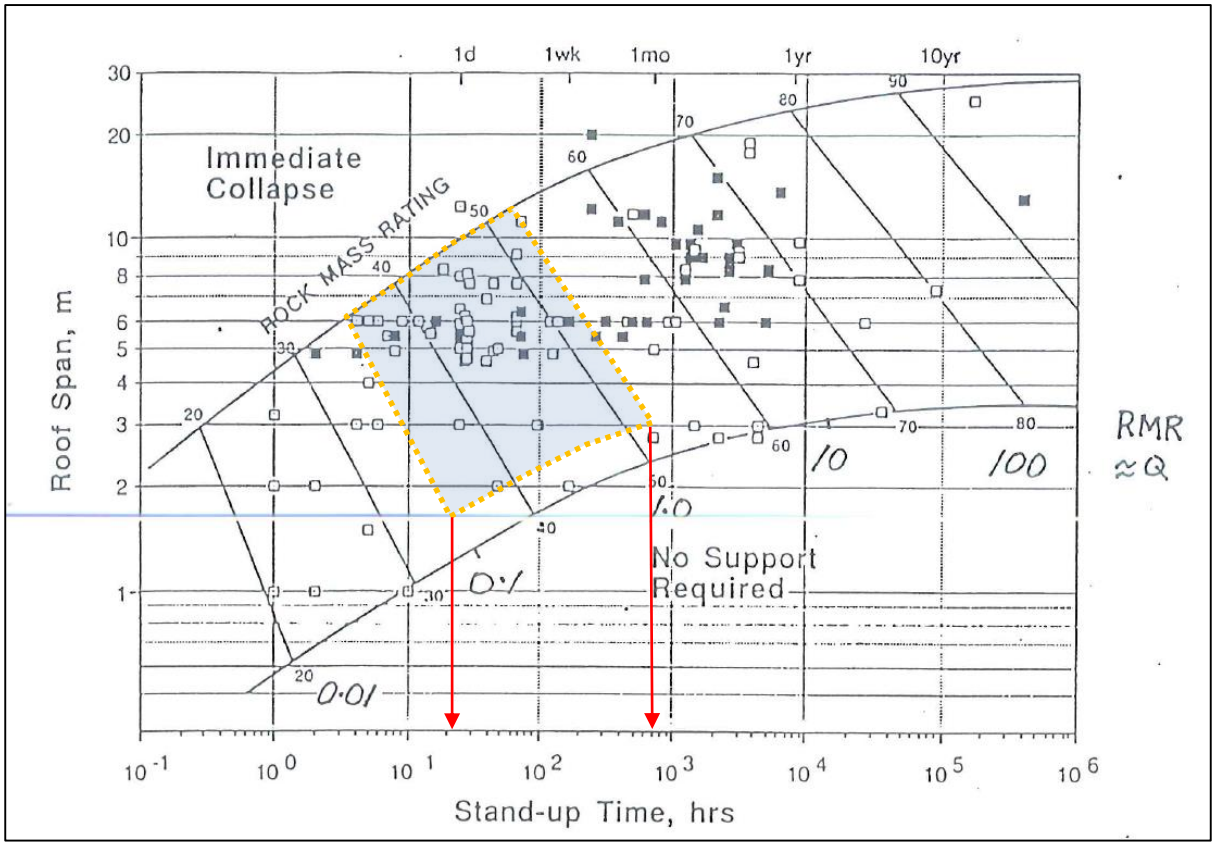


Figure 6-13 Graph of roof span vs Stand-up Time for WAF using Q

The design team also considered the use of temporary safety netting as well as large headboards above the pre-stressed elongate units to assist with areal coverage.

6.3.4.5. Proposed Mining Guidelines in WAF

This section deals primarily with those rock engineering team design aspects that showed success when dealing with the WAF rockmass in the stoping horizon. It is based on underground observations and experiential evidence which cannot be referenced from the known literature as there are no known mines that have tried these WAF mitigation techniques. The data is merely here to provide a platform for further research into the field.

From a design perspective, the impact of WAF had to be considered in the following manner:

- What volumes could be successfully extractedin the mining sequence that would result in sustainable production?, and,
- How would a Wide-Raise instead of a Development Raise in WAF contribute to stability so that sustainable mining rates could be achieved?

6.3.4.5.1. Mining Sequence and Extraction Rate in WAF

Figure 6-14 shows the mining sequence modelled by Tkloweni (2007). The figure illustrates the mining steps where one block is extracted after the other. From a practical mining perspective the sequence is flawed in that a sustainable tonnage profile cannot be maintained. Each block takes approximately 2 years to develop before full-scale mining operations can commence. Once this block is complete, the process continues. From a rock engineering design point of view, research has shown that the WAF rockmass will converge. In the 2 year waiting period, the WAF will deform to the extent that re-development may be necessary for full-scale stoping to occur.

The proposed solution would be to develop each block concurrently whilst permitting limited-scale stoping. This strategy would allow additional support measures to be instituted in areas where WAF showed degradation, whilst maintaining a sustainable mining tonnage profile.

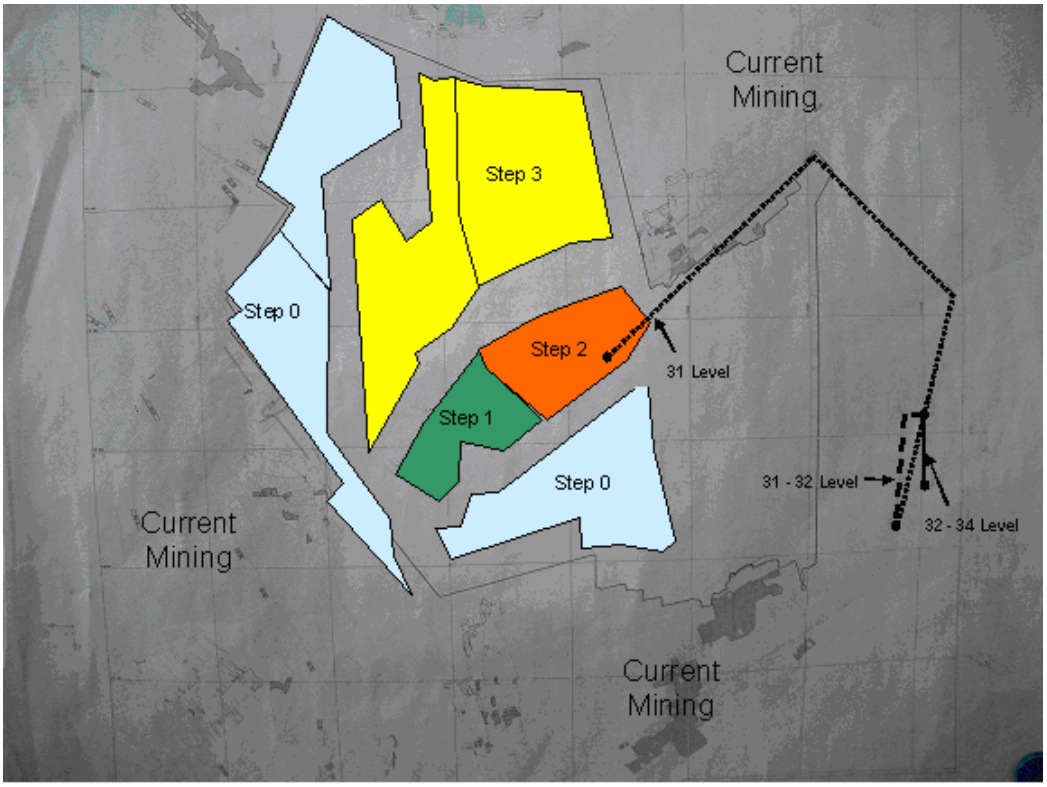


Figure 6-14 Modelled mining sequence at Ya Rona Shaft pillar extraction (Tkloweni, 2007)

6.3.4.5.2. Wide-Raising as opposed to Raise Development

This section deals with the design team's preference for a Wide-Raise excavation instead of a Development Raise excavation to mitigate the effects of WAF. To illustrate the reason for the preference, Figures 6-15 and 6-16 show before and after photographs of a development raise (Chapter 5, Figure 5-5) with WAF hangingwall. The photographs show falls of ground after the blast which highlight the susceptibility of excavation in WAF to damage. Figure 6-17 shows a crack in the WAF hangingwall after a ledging blast was taken on the same excavation after the fall of ground was cleaned.



Figure 6-15 Photograph showing a development raise with WAF hangingwall before the production blast



Figure 6-16 Photograph showing the same development raise in figure 6-15 after the production blast



Figure 6-17 Photograph showing tensile crack failure after the ledging blast in the raise featured in figure 6-15

The rock engineering design team highlighted the tensile failure of the excavation as a result of the high horizontal stress components in the WAF rockmass and proposed that wide-raise designs replaced development raise designs in WAF. The new stoping designs would allow for concurrent ‘development raising’ (gully) and stoping (ledging) to occur. This allowed the WAF rockmass to be supported with both tendons and stope support (packs and pre-stressed elongates).

6.3.5. Regional stability

Regional stability is usually provided by in-situ stope pillars (cut as mining progresses), regional dip or strike pillars (designed pillars to limit mining spans), or large satellite-type pillars (pillars located at the extremities of the mining plan – the last remnants). Hydraulically placed backfill ribs or paddocks are also useful in providing the necessary regional stability. Chapter 5, Section 5-7, showed how the revised mining spans resulted in better regional stability results. Furthermore, the research has shown that some bracket pillars may not be necessary and that many of the designed bracket pillars will be successful at performing the dual role of clamping the structure, as well as providing regional stability.

7. Guidelines and Conclusions

7.1. A guideline for mining under WAF conditions in a Shaft Pillar Extraction

The focus of this report was to understand the rockmass behaviour and characteristics of the WAF and how these elements have or would contribute to rock engineering design at the Ya Rona Shaft Pillar Extraction. Using the knowledge assimilated in this research report, a design guideline or process methodology (Figure 7-1) is advocated for similar mining opportunities in WAF at similar depths. The process is biased in favour of rock engineering and contains four levels, each of which have specific decision-making and design guidelines:

- Level one – the most important stage at which the critical decision-making is articulated. High order risk assessments are conducted to determine the greatest risks to the shaft pillar extraction. The level is underscored by the calculated and perceived risks. In the Ya Rona case study these were:
  - The mining sequence,
  - Seismicity,
  - Geological complexity,
  - Environmental factors, and,
  - Production sustainability.
- Level 2 - using the Ya Rona example, geological complexity was perceived to be the highest risk. Interventions in level two are, therefore, restricted by this fact. The other four risk factors would have their design rationale should they be noted as the highest risk. This level requires that design criteria are set.
- Level 3 – makes provision for measures in mitigation of risk. These can be used as building blocks for more suitable risk mitigation measures.
- Level 4 – when executing (mining) the plan, the rock engineering needs to monitor the hazards, revise standards to address these hazards and focus on the longevity and sustainability of the mine design. Where required, back analyses may be conducted to optimise the plan.

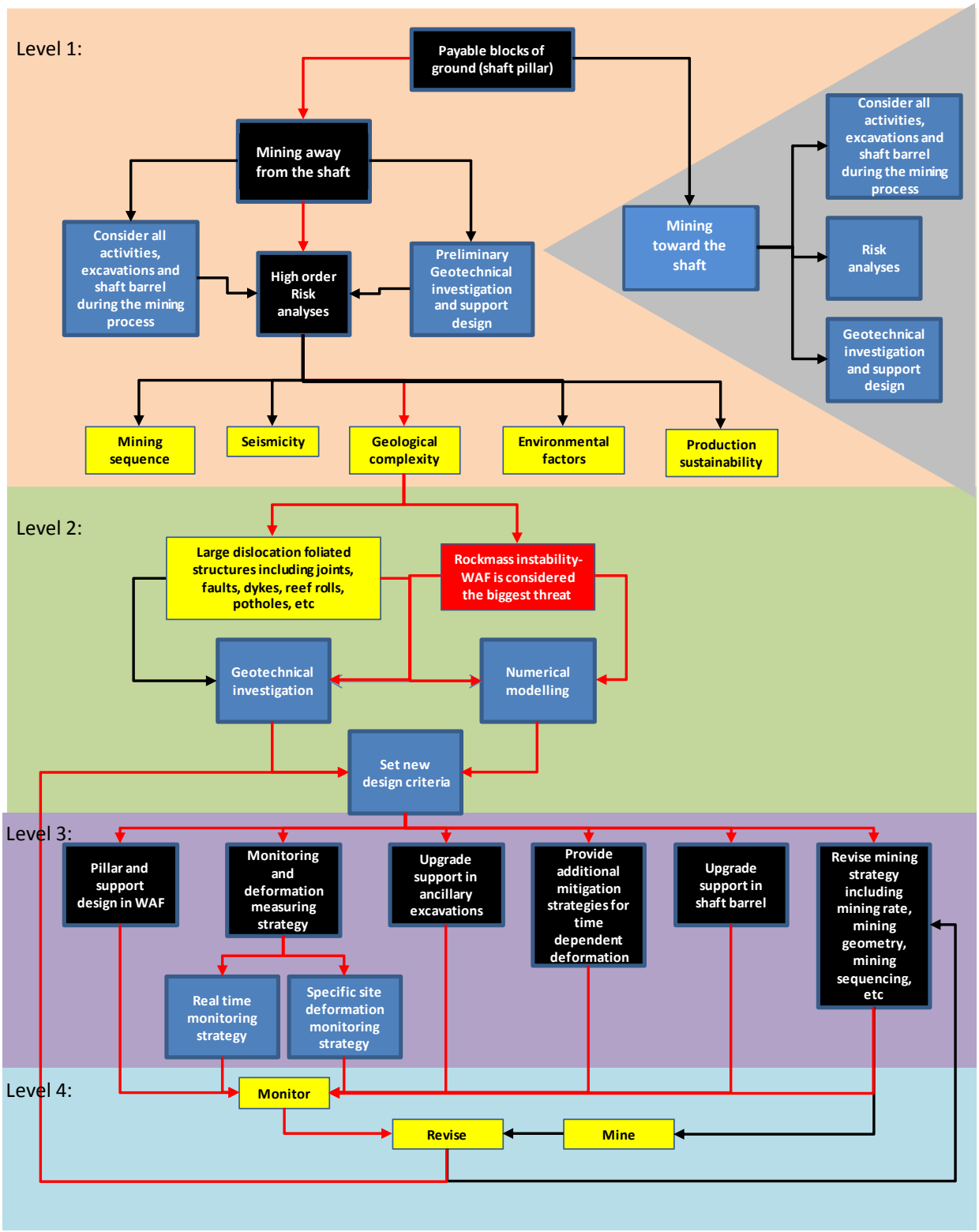


Figure 7-1 Design process methodology when mining WAF in a Shaft Pillar Extraction at depth

7.2. Conclusions from the research

From the onset, the rock engineering design was underscored by four main objectives:

1. The unique geotechnical characteristics and behaviour of the WAF should be highlighted. Using rockmass rating systems to characterise the rockmass, and through literature interrogation, the WAF material could be analysed.
2. Guidance on the input parameters for the numerical model should be gleaned from available literature.
3. The results of the numerical modeling should outline the inherent risks to the infrastructure as well as the mining plan. Where practically possible, mining sequences should be optimized.
4. Mitigation measures should be presented in mitigation of risk when mining in the WAF.

7.2.1. The WAF 'understood'

Both the literature review and the underground observations at the various case study sites have outlined the unique characteristics of WAF. These cases have only been possible as a result of failures of the excavations containing WAF. It is, therefore, important for this information to be readily available to the industry so that future catastrophic events can be averted.

There are several WAF rockmass characteristics that could result in damage and injury. Of significant note is that WAF deteriorates over time (time dependant creep behaviour) and exposure to water and air inevitably results in deterioration of the rockmass. Within the shaft pillar extraction environment, WAF is also subjected to increased loading conditions as a result of blasting, poor mine design and increased volumetric extraction rates which promote the "visco-plastic" behaviour. The research data also shows that failure of the weak WAF rockmass can also be promoted by mining induced stress, stress orientations and changes in stress magnitude.

Rockmass ratings have confirmed that WAF is a very poor rockmass. Though RMR, MRMR and RCF have their inherent limitations, they were chosen as case studies in WAF have used them previously. In this research report, each system can quantify aspects of the WAF in

different ways. Furthermore, they were chosen as they included prevailing stress conditions, rockmass properties and rock block (jointing, faulting) information, all of which are important when characterising the WAF rockmass.

Geotechnically, WAF is a highly altered, volcanic rock with foliation that reduces with increasing distance from the VCR reef. The degree of foliation, in the rock engineering context, would refer to the inherent stability of the rockmass. The higher the foliation, the less stable the rockmass. Moreover, every case study highlighted the variability of the strength of the WAF which is linked to mineralization of the WAF. Elements within the WAF rockmass include talcose, olivine and tremolite, all of which have high hydrogen and oxygen components. Therefore, on a mineral element level, WAF cannot tolerate additional exposure to water and air. The result is that deteriration on a molecular level occurs which plays a large role in the decay of the rockmass.

Rock testing revealed the low inherent strength of the WAF, but also showed under confinement conditions that the WAF rockmass would have the ability to increase its load-bearing abilities. From a rock engineering design point of view, the ability to use appropriate support measures to increase the ability of the WAF to maintain load without failure is hopeful. It is therefore imperative that timeous support measures be enforced so that the onset of WAF degradation is delayed.

7.2.2. Numerical modeling – toward understanding the input parameters for modeling of the WAF rockmass

To ensure that the input parameters used in the numerical model are representative of the rockmass within which mining is occurring, their careful selection for the model is critical. Within this research report, this selection was done through case study analyses, as well as rockmass characterization, coupled with rock test data. Although both elastic (BesolMS) and inelastic (3DEC) numerical modeling data was used to present information on WAF behaviour, the author preferred the use of the downgraded Young's Modulus to represent the rockmass in its current state. Using underground data, calibration and sensitivity analyses showed that the downgraded input parameter could represent the WAF adequately.

7.2.3. Shaft Pillar Extraction Design Revision

From a rock engineering design viewpoint, numerical modelling input parameters are crucial for the design phase of any project. Both elastic and inelastic models showed that some elements of the intended mining sequence did not meet the failure criteria. A revised sequence was provided so that the potential areas of concern could be addressed. However, due to the inherent poor WAF rockmass properties, the data still showed that:

- During mining, the shaft will still sustain damage as a result of radial and vertical displacements;
- Slip on features is still possible, especially where faults intersect the shaft and stoping horizons. These will pose an elevated seismic risk if bracket pillars are not designed properly; and,
- The Average Pillar Strength (APS) and Energy Release Rate (ERR) benefit from the revised sequence.

7.2.4. WAF mitigation

Emerging from the investigations, are two definitive WAF mitigation "schools of thought". On the one hand, some rock engineering practitioners (Ortlepp, et al, 2008) prefer the "belts and braces" approach, where the WAF material is supported to a significantly high degree, only constrained by what is practical and executable, where time and money do not matter. In contrast, the rock engineering design team at Ya Rona, understood the inherent difficulties when mining with WAF. By using the results from the numerical model, the mitigation approach undertaken entailed the:

1. Use of a systematic monitoring regime to alert personnel about the deformation trends in WAF;
2. Where data can be interrogated and decisions executed in a timeous manner, these should be articulated;
3. Provision of mitigation strategies to maintain the Ya Rona Shaft stability during the extraction process. These measures are to be enforced as this excavation is an operational entity where damage and injury could prevent sustainable production;
4. Monitoring of the Syncline Axis and the Murray Fault so that slip on these features could be prevented, or at least the consequences of failure could be managed;

5. Revision of mining sequences in WAF, so that better results could be obtained from the numerical modelling. Such results may or may not meet the stated failure criteria but can serve as input data to the risk assessment and mitigation strategies proposed by the rock engineering design team; and,
6. Provision of a fit-for-purpose support system that will have the ability to restrain the deformation potential of WAF. The system must be installed in a timeous manner to inhibit the time dependant behaviour of WAF.

Although there are numerous other WAF mitigation measures in place at the Ya Rona shaft pillar extraction, the scope of this research report had to be constrained.

7.3. Concluding remarks

To end this research report by suggesting that the WAF rockmass is clearly understood would be an over-indulgence. To conclude by stating that the extensive work in the industry on WAF is worth merit, is an understatement. This research report enables aspects of many of the WAF case studies to become published work. Furthermore, the author has suggested that with the application of rockmass rating systems, rock testing and numerical modelling, the rock engineering design within the WAF rockmass can be substantially improved.

In conclusion, it is the view of the author that the techniques employed, within this research report, to classify and numerically model the WAF, combined with the methodologies presented in WAF mitigation within the Ya Rona Shaft Pillar Extraction project, can be used for rock engineering design purposes, as well as featuring as a guideline for future extractions, of a similar nature, in WAF.

8. Recommendations for further research

As there are not many case studies on WAF, opportunities may exist within the rock engineering and mining fraternity to present aspects alluded to but not explored in this research report.

From the author's viewpoint, in-depth analyses on dynamic ground motions within the WAF environment could be quantified. This research could explore seismic response to production within the 'soft' WAF environment. In addition, the dynamics of blast loading on the WAF rockmass could also be investigated. At Ya Rona Shaft, a lack of strain bursting of the faces in the WAF environment relative to the stronger Alberton Lava faces, was experienced. The data could optimise both blast design as well as explosive types that could be used in the WAF rockmass.

Designs based for shaft pillar extractions in WAF could be improved with the use of inelastic techniques. An example of a modelling code that could explicitly model all the factors, variables and mechanisms of failure within the WAF rockmass environment is ABAQUS. Moreover, kinematic UNWEDGE analyses could be used to determine areas of potential pseudo-static instability using the available joint information and fracture patterns in WAF. This could be coupled to an optimal backfill design in the WAF rockmass.

Furthermore, exploration on the mechanisms of failure of WAF in response to differing stress regimes needs to be quantified. The explicit impact of deviatoric stress on the WAF could show the visco-plastic behaviour of the material.

References

Angle of friction. (2011, April 29). Retrieved June 2, 2013, from www.geotechdata.info: http://www.geotechdata.info/parameter/angle-of-friction

Barton, N., Lien, R., & Lunde, J. (1974). Engineering Classification of Rock Masses for the Design of Tunnel Support. Rock Mechanics 6. 6/4, pp. 189-236. Springer-Verlag.

Bieniawski, Z. (1989). Engineering rock mass classifications. New York: Wiley.

Castelyn, F.C. & Durapraj, S. (May 2007). 4 Sub-Vertical Shaft Pillar Extraction. The Association of Mine Managers of South Africa, AMMSA, Johannesburg.

Coetzer, S. (2003). Measurement of rock stress at Driefontein Mine, 4 shaft East. CSIR-Miningtek. Unpublished report.

CSIR-Miningtek. (2003). Yielding Anchor Load-Deformation Tests. Unpublished tests .

Deere, D.U. (1989). Rock quality designation (RQD) after 20 years. U.S. Army Corps Contract report, Vicksburg.

Deere, D.U, & Deere, D.W. (1988). The Rock Quality Designation (RQD) index in practice. (L. Kirkaldie, Ed.) Rock Classification Systems for Engineering Purposes (Special Publication 984), 91-101.

Deere, D.U., & Deere, D. W. (1998). The Rock Quality Index in Practice: Rock Classification Systems for Engineering Purposes. In L. Kirkaldie (Ed.), ASTM STP 984, (pp. 91-101).

Driefontein Consolidated Propriety Limited. (2006). Code of Practice to combat rock fall and rock burst accidents in tabular metalliferrous mines (4th ed.). (GroundworkConsulting, Ed.)

Durapraj, S. (2002). Support Standards in WAF. Unpublished support standards.

Durapraj, S., & Lindeque, T. (2005). Geological Complexity and it's influence on Rock Engineering Design of the extraction of the 4 Sub-vertical Shaft Pillar at Driefontein Gold Mine. Annual Goldfields Mining and Rock Engineering Seminar (p. 12). Unpublished presentation.

Durapraj, S. (2005, November). Ya Rona Shaft Visit. Unpublished presentation.

Durapraj, S. (2006a). Manipulation of a numerical model to back analyse underground in-situ rockmass behaviour on an atypical gold mine in the Witwatersrand basin. Graduate Diploma in Engineering: Coursework assignment, University of the Witwatersrand, Johannesburg.

Durapraj, S. (2006b). Manipulation of a number of models and analyses to understand the geological instabilities in a specific rockmass to predict the potential for large scale failure of a shaft on an atypical gold mine in the Witwatersrand basin. Graduate Diploma in Engineering: Coursework assignment, University of the Witwatersrand, Johannesburg.

Durapraj, S. (2006c). Driefontein 4 Sub-Vertical shaft pillar extraction: Vailidation of the mining as per Scenario 1 in the event of the loss of the shaft barrel. Carletonville: Unpublished report.

Durapraj, S. (2007). (4SV) Ya Rona Shaft Pillar- the Extraction of the Chase. Annual Goldfields Mining and Rock Engineering Seminar (pp. 1-32). Unpublished presentation.

Durapraj, S. (2008). Ya Rona Sub-vertical Slot mining investigation. Goldfields: KDCWest. Unpublished report.

Durapraj, S. (2010). Driefontein 4 Sub-vertical shaft pillar extraction: Mining extraction profile, shaft barrel and shaft pillar analysis for BFP2011. Goldfields: KDCWest. Unpublished report.

Evert, H. (2006, November 20). Rockbolts and cables. Retrieved June 2, 2013, from www.rocscience.com: http://www.rocscience.com/hoek/corner/14_Rockbolts_and_cables.pdf

Hoek, E. (2006, November 20). Rockmass properties. Retrieved June 5, 2013, from www.rocscience.com: http://www.rocscience.com/hoek/corner/11_Rock_mass_properties.pdf

Hoek, E. (2008, March 17). Rockmass Classification. Retrieved June 2, 2013, from www.rocscience.com: http://www.rocscience.com/hoek/corner/3_Rock_mass_classification.pdf

Jager, A.J., & Ryder, J.A. (1999). A handbook on rock engineering practice for tabular hard rock mines. Johannesburg, South Africa: The Safety in Mines Research Advisory Committee (SIMRAC).

Joughin, W.C. (2009). Note on the examination of damage in the Driefontein 4 shaft (Ya Rona) sub-shaft, Goldfields Limited. Unpublished report, SRK Consulting Engineers and Scientists.

Joughin, W.C., Stacey, T.R. (2005). Risks associated with rockpasses in deep level tabular mines based on historical pass performance. The Journal of the South African Institute of Mining and Metallurgy, Volume 105 Refereed paper, Johannesburg.

Karabin, G.J & Evanto, M.A. (1999, June). Experience with the boundary-element method of numerical modeling to resolve complex ground control problems . Proceedings of the Second International Workshop on Coal Pillar Mechanics and Design (pp. 99-114). Pittsburgh: U.S.Department of Health and Human Services.

KDCWest. (2012). Code of Practice to combat rock fall and rock burst accidents in tabular metalliferous mines (5th ed.). (S. Mulder, Ed.) Goldfields KDCWest Driefontein Consolidated Propriety Limited.

Kloof, South Africa. (1997). Retrieved June 2, 2013, from www.mining-technology.com: http://www.mining-technology.com/projects/kloof/kloof1.html

Laubscher, D. (1990). A geomechanics classification system for the rating of rock mass in mine design. Journal of the South African Institute of Mining and Metallurgy , 90 (10), 257-273.

Leach, A. R., Dlokweni, T. & Lightfoot, N. (2003, September). Driefontein 4 Shaft Pillar Extraction: Analysis based on 2003 revised geological structure. Driefontein Gold Mine. Unpublished report.

Leach, A. (2006, October). Driefontein 4 Shaft Pillar Extraction: Re-assessment of hazards due to WAF intersection in 4 Sub-vertical Shaft barrel. Driefontein Gold Mine. Unpublished report.

Malan, D. F., Napier, J.J.A.L. & Grave, M. (2003, September). Experiments on stope closure as a diagnostic measure of rock behaviour. ISRM-10CONGRESS-2003-133. Johannesburg: International Society of Rock Mechanics, SAIMM .

Martin, C., Kaiser, P., & McCreath, D. (1999). Hoek-Brown parameters for predicting depth of brittle failure around tunnels. (pp. 136-149). NRC Canada.

Modulus of Rigidity. (n.d.). Retrieved June 2, 2013, from www. EngineeringToolBox.com: http://www.engineeringtoolbox.com/modulus-rigidity-d_946.html

OHMS. (2011). Introduction to Numerical Modelling Exam Preparation Course. Open House Mangement Services.

Olivier, A. (2002). Recommendations on the Shaft Pillar Extraction. Driefontein Gold Mine. Unpublished report.

Ortlepp, W.D, Joughin, W.C., Ward, A.K., & Thompson, J. (2008). Reinforcement support of the Concrete Shaft Lining in Westonaria Formation Lava in Ezulwini Vertical Shaft System. 6th International Symposium on Ground Support in Mining and Civil Engineering Construction (pp. 561-580). Cape Town: SAIMM, SANIRE and ISRM.

Palmstrom, A., & Broch, E. (2006). Use and Misuse of Rock Mass Classification Systems with particular reference to the Q-system. Tunnels and Underground Space Technology , 21, 575-593.

Parker, S. (1994). Dictionary of Geology and Minerology (5th ed.). United States of America: McGraw-Hill.

Pells, P.J.N. (2008). What happened to the mechanics in rock mechanics and the geology in engineering geology? 6th International Symposium on Ground Support in Mining and Civil Engineering Construction (p. 30=32). Cape Town: SAIMM, SANIRE and ISRM.

Pells, P.J.N., & Bertuzzi, R. (2011, June 11). Limitations of Rock Mass Classification Systems for Tunnel Support Systems. Retrieved June 7, 2013, from www.pellsconsulting.com.au: http://www.pellsconsulting.com.au/downloads/limitationsOfRockMassClassificationSystems.pdf

Petho, S.Z., Badenhorst, C., Rangasamy, T., Obermeyer, P., & Arnold, T. (2004). Preliminary results of the rock engineering, geotechnical and geological evaluation of the collapse of a section of the SV1 shaft sidewall. Goldfields South Deep Gold Mine. Unpublished report.

Raffield, M.P., James, J.V., & Isaac, A.K. (1993). Computer Modeling of the Shaft Movements Induced by the Pre-extraction and Backfilling of the Shaft-reef Area on South Deep Mine. Minefill 93 (pp. 65-72). Johannesburg: SAIMM.

Rangasamy, T., Oelofse, J., Sellers, E., & Linzer, L. (2003). An intergrated, simplistic approach for determining the viability of extracting threee associated remnants in a scattered, deep level gold mine. ISRM 2003 - Technology roadmap for rock mechanics. Johannesburg, SAIMM, 2003.

Rangasamy, T., & James, J. (June, 2006). Shaft instabilities directly/indirectly related to the Westonaria Formation Lavas (WAF). Driefontein 4SV# Pillar Extraction: Westonaria Formation Lavas (WAF) Workshop. Unpublished presentation.

Ryder, J.A. (1988). Excess shear stress in the assessment of geologically hazrdous situations. Journal of The South African Institute for Mining and Metallurgy , 88 (1), 27-37.

Ryder, J.A., & Jager, A.J. (2002). A textbook on Rock Mechanics for tabular hard rock mines. Johannesburg: The Safety in Mines Research Advisory Committee (SIMRAC).

Sappi Mining Timber. (2002). Saturn Prop Load Deformation Tests. Unpublished tests.

Sappi Mining Timber. (2002). Spud 3 Test Summary Report. Unpublished report.

Schweitzer, J.K. & Johnson, R.A., (January 1997) Geotechnical classification of Deep and Ultra-deep Witwatersrand Mining Areas, South Africa. 1997. Retrieved May 06, 2014, from http://researchspace.csir.co.za/dspace/bitstream/10204/1528/1/schweitzer_1997.pdf.txt

Spearing, A.J.S. (1995). Handbook on Hard-rock Strata Control (Special Publication Series SP6 ed.). Johannesburg, South Africa: SAIMM.

Tkloweni, H. (2007). Vent hole stability. Driefontein Gold Mine. Unpublished report.

University of the Witwatersrand. (2008). Graduate Diploma in Engineering: Rockmass Classification. (D. H. Yilmaz, Compiler) Johannesburg, South Africa: Unpublished notes.

Van der Heever, P.K. (2007). Characterisation of the Westonaria Formation at Main Shaft, Kloof Gold Mine. Confidential document to Kloof Gold Mine, Groundwork Consulting, Johannesburg.

Van der Heever, P.K. (2009). A summary of the geotechnical investigations at Kloof Main Shaft for the period February 2007 to April 2009. Confidential document to Kloof Gold Mine, Groundwork Consulting, Johannesburg.

Watson, B.P. (2004). A rock mass rating system for evaluating stope stability on the Bushveld Platinum mines. The Journal of The South African Institute of Mining and Metallurgy , 229-238.

Wilson, M. A. (2010, March 9). SynclineCalico. Retrieved May 11, 2014, from http://en.wikipedia/wiki/synclineaxis.

Yilmaz, H. (2006, May). Driefontein 4Shaft WAF Rock test results. (H. Yilmaz, Compiler), University of Witwatersrand, Rock Engineering Laboratory, Johannesburg: Unpublished test results.

Appendices

Appendix A

Rockmass Rating

A.1 The Q-system of rock mass classification (after Barton, Lien and Lunde – 1974)

The numeral value of the Q-rating can vary from 0.001 for extremely poor rock to 1000 for excellent rock. Q is defined by the following equation 1.

$$Q = \left(\frac{RQD}{Jn} \cdot \frac{Jr}{Ja} \cdot \frac{Jw}{SRF}\right) \qquad \text{(Eqn. A1)}$$

RQD is the Rock Quality Designation
Jn is the joint set number
Jr is the joint roughness number
Ja is the joint alteration number
Jw is the joint water reduction factor
SRF is the stress reduction factor

RQD/*Jn* reflects block size; *Jr*/*Ja* reflects the joint shear strength; *Jw*/*SRF* reflects the confining stress conditions.

If RQD <10, use 10.

Parameter 1: Rock Quality Designation

Rock Quality Designation (RQD) is determined as the percentage of the sum of the length of drill core segments > 10 cm over the total mapped length of drill core (figure A-1).

Description	**Value**
Very poor	0 to 25
Poor	25 to 50
Fair	50 to 75
Good	75 to 90
Excellent	90 to 100

Table A-1 RQD value (Barton, 1989)

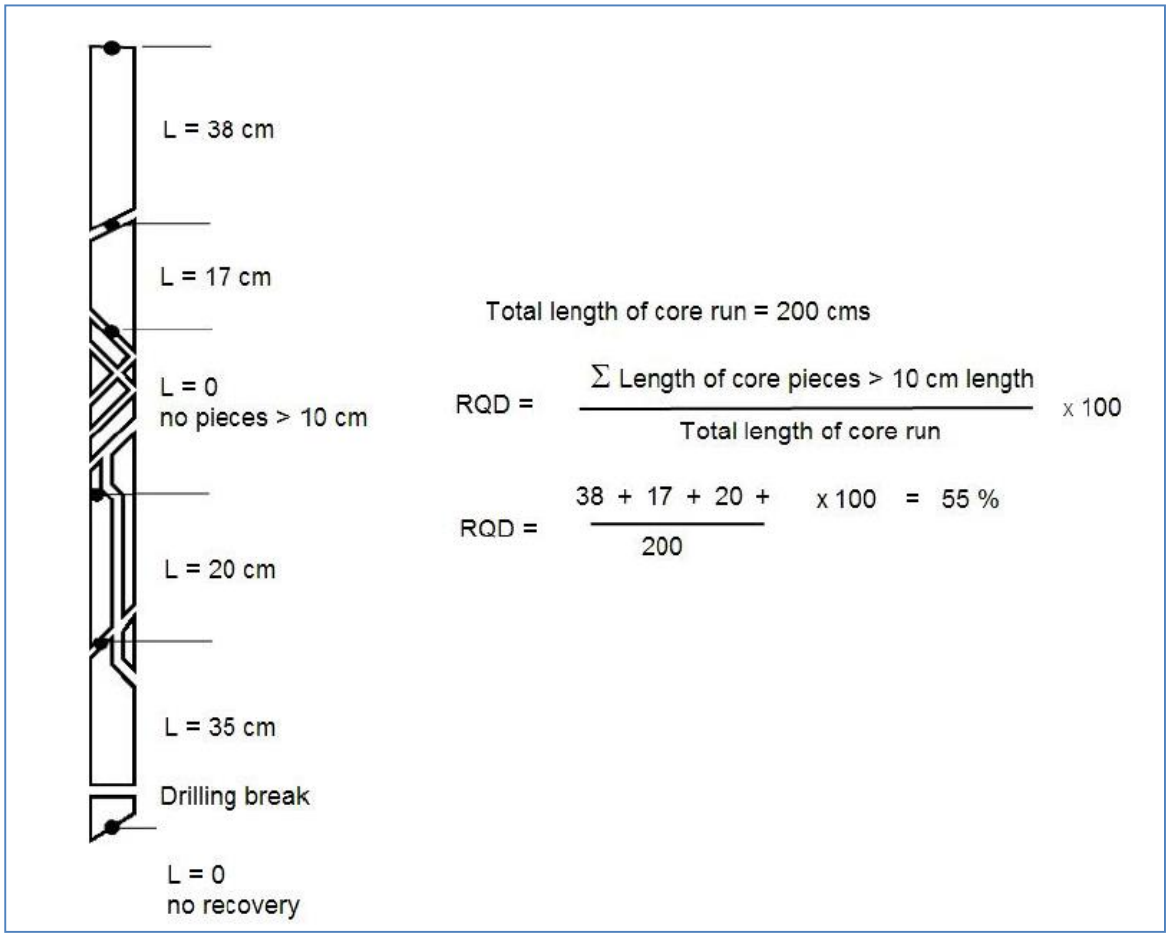


Figure A-1 Procedure for measurement and calculation of RQD (Deere, 1989)

Parameter 2: Joint set parameter (Jn)

Description	Value
Massive, no or few joints	0,5 to 1
One joint set	2
Two joint sets	4
Three joint sets	9
Three joint sets plus random joints	12
Four or more joint sets, heavily jointed	15
Cubed, blocky, crushed appearance	20

Table A-2 Joint sets parameter (Barton, 1989)

Parameter 3: Joint roughness parameter (Jr)

Description	Value
Discontinuous	4
Rough, irregular, undulating	3
Smooth, undulating	2
Slickensided, undulating	1.5
Rough or irregular, planar	1.5
Smooth, planar	1
Slickensided, planar	0.5

Table A-3 Joint roughness parameter (Barton, 1989)

3) Description of joint surface Roughness	Undulating	Planar
Discontinuous	4	4
Rough	3,0	1,5
Smooth	2,0	1,0
Slickensided	1,5	0,5
Planes containing gouge or gravel, thick enough to prevent rock wall contact	1,0	1,0

Table A-4 Joint roughness parameter (Barton, 2002)

Parameter 4: Joint alteration parameter (Ja)

Description	Value
Tight, healed, impermeable filling\welded	0.75
Unaltered surfaces, staining only	1.0
Slightly altered filling, clay-free	2.0
Silty or sandy-clay fillings	3.0
Low-friction, kaolinite, chlorite, talc filling	4.0
Consolidated, softening filling (< 5mm)	6.0
Swelling clay fillings	12

Table A-5 Joint alteration parameter (Barton, 1989)

Description of gouge	**J_a for joint separation (mm)**		
4) Joint alteration	**<1,0[1]**		
a) Tightly healed, hard, non-softening impermeable rock mineral filling	0,75		
b) Unaltered joint walls, surface staining only	1,0		
c) Slightly altered, non-softening mineral coatings, sandy particles, clay free disintegrated rock.	2,0		
d) Silty or sandy-clay coatings, small clay fraction (Non-softening)	3,0		
e) Softening or low friction clay mineral coatings (e.g. chlorite) and small quantities of swelling clays	4,0		
	1,0-5,0[2]	**>5,0[3]**	**>5,0[4]**
f) Sandy particles, clay-free disintegrated rock, etc	4	5	
g) Strongly over-consolidated non-softening clay mineral fillings	6	6	10
h) Medium or low over-consolidation, softening, clay mineral fillings	8	8	13
i) Swelling clay fillings i.e. montmorillonite. J_a depends on per cent of swelling particles	8 - 12	8 - 12	13 - 20

Figure A-2 Joint alteration parameter (Barton, 2002)

Note (after Watson, 2004):

1 Joint walls effectively in contact.

2 Joint walls come into contact before 100 mm shear (thin mineral coatings).

3 Joint walls do not come into contact at all upon shear (Zones or bands of disintegrated or crushed rock and clay).

4 Joint walls do not come into contact at all upon shear (Thick, continuous zones or bands of clay).

Parameter 5: Joint water parameter (Jw)

Description	**Value**
Dry or minor inflow	1
Medium inflow	0.6
Large inflow	0.5
Outwashing of fillings	0.3

Table A-7 Joint water parameter (Barton, 1989)

Condition of groundwater	Head of water (m)	J_w
a) Dry excavation or minor inflow 5l/min locally	<10	1,0
b) Medium inflow, occasional outwash of joint/fissure fillings	10-25	0,66
c) Large inflow in competent ground with unfilled joints/fissures	25-100	0,5
d) Large inflow with considerable outwash of joint/fissure fillings	25-100	0,33
e) Exceptionally high inflow upon excavation, decaying with time	>100	0,2-0,1
f) Exceptionally high inflow continuing without noticeable decay	>100	0,1-0,05

Table A-8 Joint water parameter (Barton, 2002)

Description	*SRF* value
a) Multiple occurrences of weakness zones containing clay or chemically disintegrated rock, very loose surrounding rock (any depth).	10
b) Single weakness zones containing clay or chemically disintegrated rock (depth of excavation < 50 m)	5
c) Single shear zones in competent rock (clay-free), loose surrounding rock (any depth)	2,5
d) Multiple shear zones in competent rock (clay-free), loose surrounding rock (any depth)	7,5
e) Single shear zones in competent rock (clay-free), (depth of excavation <50 m)	5,0
f) Single shear zones in competent rock (clay-free), (depth of excavation >50 m)	2,5
g) Loose open joints, heavily jointed or "sugar-cube" etc (any depth).	5,0

Table A-9 Stress reduction factor for weakness zones (Barton, 2002)

Description	UCS/σ_1	s_t/σ_1	*SRF* value
h) Low stress, near surface	>200	>13	2,5
i) Medium stress, favourable	200-10	13-0,66	1,0
j) High stress, very tight structure (usually favourable to stability, may be unfavourable for wall stability)	10-5	0,66-0,33	0,5-2
k) Moderate slabbing after > 1 hour in massive rock	5-3	0,5-0,65	5-50
l) Slabbing and rock burst after a few minutes in massive rock	3-2	0,65-1	50-200
m) Heavy rock burst (strain-burst) and immediate dynamic deformations in massive rock)	<2	>1	200-400

Note: This table generally applies in hard dry rock conditions.

Table A-10 Stress reduction factor for competent rock and rock stress problems (Barton, 2002)

Description	s_t/σ_1	*SRF* value
n) Mild squeezing stress	1 - 5	5 - 10
o) Heavy squeezing stress	> 5	10 - 20

Table A-11 Stress reduction factor for squeezing rock: plastic flow of incompetent rock under influence of high stress (Barton, 2002)

Description	*SRF* value
p) Mild swelling stress	5 - 10
q) Heavy swelling stress	10 - 15

Table A-12 Stress reduction factor for swelling rock: chemical swelling activity depending on presence of water (Barton, 2002)

A.1.1. Calculation of Q-rating range for the Ya Rona example

Table A-13 shows the calculation of Q for WAF at Ya Rona shaft.

Parameter	*Rating*	*Comment*
Rock quality Designation (RQD):	25-50	Poor – measured 31
Joint set parameter (Jn):	9	3 sets observed
Joint roughness parameter (Jr):	1.5	Slicken-sided, undulating
Joint alteration number (Ja):	8	Talcose and clay mineral infilling, no crushed rock, but apertures >1mm, joint walls do not come in contact upon shear
Joint water parameter (Jw):	1.0	Dry, no in-flows or wash-outs
Stress reduction parameter (SRF):	5 – 7.5	(For weakness zones) – loose open joints, mild swelling rock pressure

Table A-13 Calculation of Q for WAF at Ya Rona shaft

Final Q rating of WAF at Ya Rona: 0.10 - 0.14

A.2 The Qc normalized value

Qc is a value of Q normalized with respect to intact rock strength.

$$Qc = Q \times UCS/100 \qquad \text{(Eqn. A2)}$$

Final Qc rating of WAF at Ya Rona: 0.058 - 0.081

A.3 Bieniawski's Geomechanics Classification (RMR)

Bieniawski (1973) published a rock mass classification called the Geomechanics Classification System or the Rock Mass Rating (*RMR*) system. Since it's inception, there have been several refinements (1973-1998) particularly to the values assigned to the parameters. The RMR rating is derived by summing the following 5 parameters (Table A-14):

1. Rock material strength (UCS),
2. RQD,
3. Joint Spacing,
4. Joint Roughness and separation, and,
5. Groundwater.

The RMR value can range between 0 (very poor quality rock) and 100 (excellent quality).Where there are less than 3 joints, the value can be increased by 30%. The 6th parameter (table A-15) applies to a modification for discontinuities relative to an excavation.

Aspects to note are that:

- RMR does not take into account the confining stress in the rockmass,
- More weight is given to both RQD and joint spacing,
- *"RMR is insensitive to minor variations in rockmass"* – Watson, 2010, and,
- The support strategies have not been revised to accommodate new support units.

Parameter			Range of values						
1	Strength of intact rock material	Point load index	>10 MPa	4 – 10 MPa	2 – 4 MPa	1 – 2 MPa	For this low range – *UCS* is preferred		
		UCS	>250 MPa	100-250 MPa	50-100 MPa	25-50 MPa	5-25 MPa	1-5 MPa	<1 MPa
	Rating		**15**	**12**	**7**	**4**	**2**	**1**	**0**
2	Drill core quality *RQD*		90% - 100%	75% - 90%	50% - 75%	25% - 50%	<25%		
	Rating		**20**	**17**	**13**	**8**	**3**		
3	Spacing of joints		>2 m	0,6 – 2 m	0,2 – 0,6 m	0,06–0,2 m	<0,06 m		
	Rating		**20**	**15**	**10**	**8**	**5**		
4	Condition of joints		Very rough surface, not continuous, no separation, no weathered wall	Slightly rough surfaces, Separation <1 mm, Slightly weathered walls	Slightly rough surfaces, Separation <1 mm, Highly weathered walls	Slickensided surfaces or gouge<5 mm thick or separation 1-5 mm continuous.	Soft gouge>5 mm thick or separation >5 mm continuous.		
	Rating		**30**	**25**	**20**	**10**	**0**		
5	Groundwater	Inflow per 10 m tunnel length	None	10 l/min	10-25 l/min	25-125l/min	>125 l/min		
		Joint water pressure/Major principal stress	0	0 – 0,1	0,1 – 0,2	0,2 – 0,5	> 0,5		
		General conditions	Completely dry	Damp	Wet	Dripping	Flowing		
	Rating		**15**	**10**	**7**	**4**	**0**		
6	Strike and dip of joints (see Table A2)		Very favourable	Favourable	Fair	Unfavourable	Very Unfavourable		
	Rating		**0**	**-2**	**-5**	**-10**	**-12**		

Figure A-3 Geomechanics classification parameters (Bienawski, 1989)

Strike perpendicular to excavation axis				Strike parallel to excavation axis		Dip 0^0-20^0 irrespective of strike
Drive with dip		Drive against dip				
45^0-90^0	20^0-45^0	45^0-90^0	20^0-45^0	45^0-90^0	20^0-45^0	
Very favourable	**Favourable**	**Fair**	**Unfavourable**	**Very favourable**	**Fair**	**Fair**

Figure A-4 The effect of joint strike and dip orientation in tunneling (Bieniawski, 1989)

A. CLASSIFICATION PARAMETERS AND THEIR RATINGS

Parameter			Range of values						
1	Strength of intact rock material	Point-load strength index	>10 MPa	4 - 10 MPa	2 - 4 MPa	1 - 2 MPa	For this low range - uniaxial compressive test is preferred		
		Uniaxial comp. strength	>250 MPa	100 - 250 MPa	50 - 100 MPa	25 - 50 MPa	5 - 25 MPa	1 - 5 MPa	< 1 MPa
	Rating		15	12	7	4	2	1	0
2	Drill core Quality RQD		90% - 100%	75% - 90%	50% - 75%	25% - 50%	< 25%		
	Rating		20	17	13	8	3		
3	Spacing of discontinuities		> 2 m	0.6 - 2 . m	200 - 600 mm	60 - 200 mm	< 60 mm		
	Rating		20	15	10	8	5		
4	Condition of discontinuities (See E)		Very rough surfaces Not continuous No separation Unweathered wall rock	Slightly rough surfaces Separation < 1 mm Slightly weathered walls	Slightly rough surfaces Separation < 1 mm Highly weathered walls	Slickensided surfaces or Gouge < 5 mm thick or Separation 1-5 mm Continuous	Soft gouge >5 mm thick or Separation > 5 mm Continuous		
	Rating		30	25	20	10	0		
5	Groundwater	Inflow per 10 m tunnel length (l/m)	None	< 10	10 - 25	25 - 125	> 125		
		(Joint water press)/ (Major principal σ)	0	< 0.1	0.1, - 0.2	0.2 - 0.5	> 0.5		
		General conditions	Completely dry	Damp	Wet	Dripping	Flowing		
	Rating		15	10	7	4	0		

B. RATING ADJUSTMENT FOR DISCONTINUITY ORIENTATIONS (See F)

Strike and dip orientations		Very favourable	Favourable	Fair	Unfavourable	Very Unfavourable
Ratings	Tunnels & mines	0	-2	-5	-10	-12
	Foundations	0	-2	-7	-15	-25
	Slopes	0	-5	-25	-50	

C. ROCK MASS CLASSES DETERMINED FROM TOTAL RATINGS

Rating	100 ← 81	80 ← 61	60 ← 41	40 ← 21	< 21
Class number	I	II	III	IV	V
Description	Very good rock	Good rock	Fair rock	Poor rock	Very poor rock

D. MEANING OF ROCK CLASSES

Class number	I	II	III	IV	V
Average stand-up time	20 yrs for 15 m span	1 year for 10 m span	1 week for 5 m span	10 hrs for 2.5 m span	30 min for 1 m span
Cohesion of rock mass (kPa)	> 400	300 - 400	200 - 300	100 - 200	< 100
Friction angle of rock mass (deg)	> 45	35 - 45	25 - 35	15 - 25	< 15

E. GUIDELINES FOR CLASSIFICATION OF DISCONTINUITY conditions

Discontinuity length (persistence)	< 1 m	1 - 3 m	3 - 10 m	10 - 20 m	> 20 m
Rating	6	4	2	1	0
Separation (aperture)	None	< 0.1 mm	0.1 - 1.0 mm	1 - 5 mm	> 5 mm
Rating	6	5	4	1	0
Roughness	Very rough	Rough	Slightly rough	Smooth	Slickensided
Rating	6	5	3	1	0
Infilling (gouge)	None	Hard filling < 5 mm	Hard filling > 5 mm	Soft filling < 5 mm	Soft filling > 5 mm
Rating	6	4	2	2	0
Weathering	Unweathered	Slightly weathered	Moderately weathered	Highly weathered	Decomposed
Ratings	6	5	3	1	0

F. EFFECT OF DISCONTINUITY STRIKE AND DIP ORIENTATION IN TUNNELLING**

Strike perpendicular to tunnel axis		Strike parallel to tunnel axis	
Drive with dip - Dip 45 - 90°	Drive with dip - Dip 20 - 45°	Dip 45 - 90°	Dip 20 - 45°
Very favourable	Favourable	Very unfavourable	Fair
Drive against dip - Dip 45-90°	Drive against dip - Dip 20-45°	Dip 0-20 - irrespective of strike°	
Fair	Unfavourable	Fair	

* Some conditions are mutually exclusive . For example, if infilling is present, the roughness of the surface will be overshadowed by the influence of the gouge. In such cases use A.4 directly.

** Modified after Wickham et al (1972).

Figure A-5 Rockmass rating system (Bieniawski, 1989)

A.3.1. Calculation of RMR-rating range for the Ya Rona example

Table A-16 shows the calculation of RMR for WAF at Ya Rona shaft.

Parameter	***Rating***	***Comment***
Strength of intact material:	7	UCS of 58-92MPa
Drill core quality (RQD):	8	31%
Spacing of joints:	15	2 joints + 1 flat joint per 3 metres
Condition of joints:	10	Slickesided surfaces, separation 1-5mm
Groundwater:	15	Completely dry
Strike and dip orientations of joints:	-5	Fair – in combination with faults in vertical excavations, stability of blocks are fair

Table A-14 Calculation of RMR for WAF at Ya Rona shaft

Final RMR rating of WAF at Ya Rona: 55 (Rock class III - Fair).

A.4 Geological strength index (GSI)

GSI provides a simple visual method of quantifying the rockmass in different geological conditions. The system is in a form of a chart (figure A-6) which shows a range of rockmass structures and a range of joint surface conditions. Correlation between the X and Y axes description of a particular rockmass, provides a GSI value. For repeatability, a single value for GSI should not be chosen. A range of GSI values are recommended for a particular case. Correlation to RMR is given by equation 3.

GSI= RMR-5 (Eqn. A3)

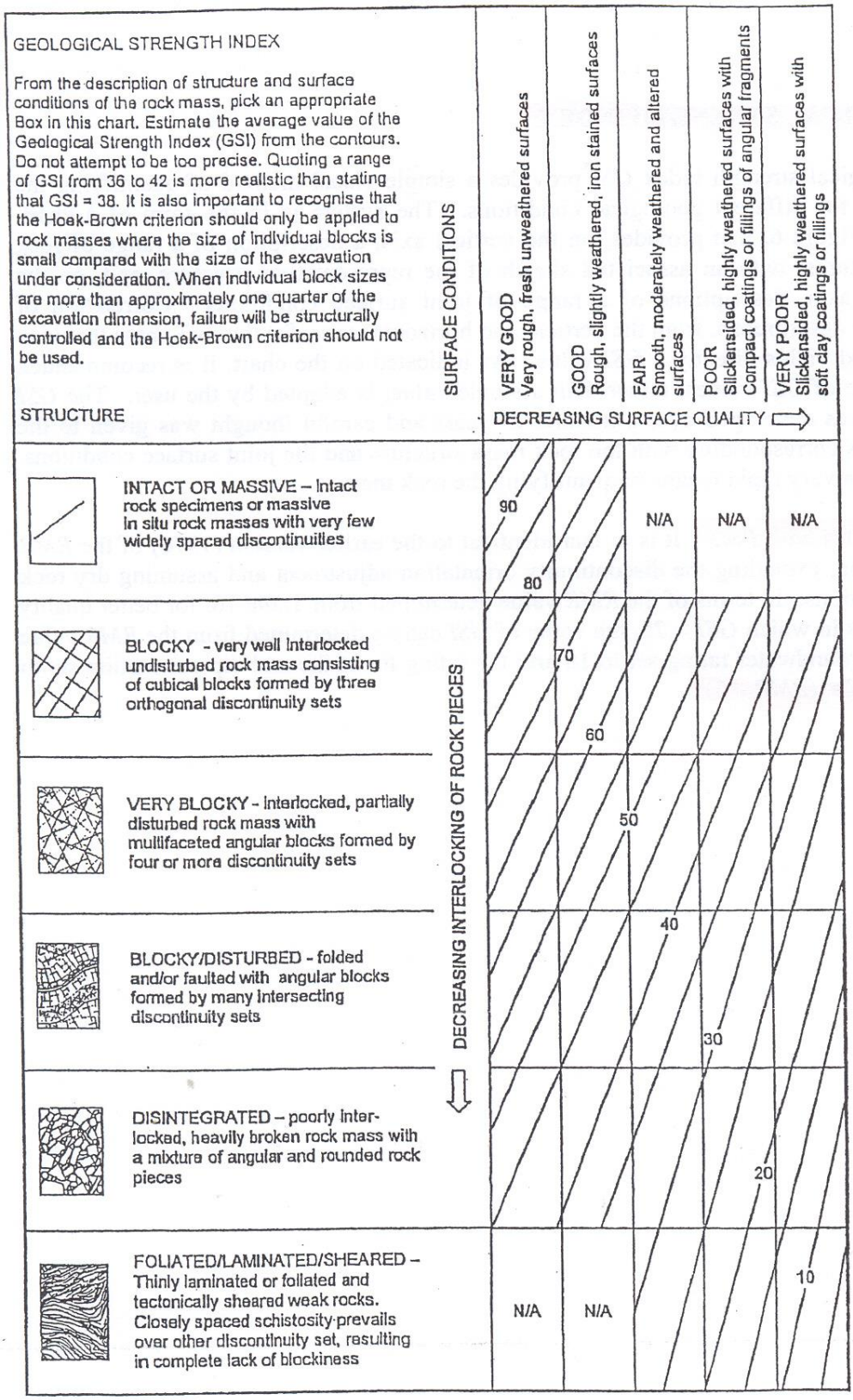


Figure A-6 GSI correlated with geological descriptions (University of the Witwatersrand, 2008)

A.4.1. Calculation of GSI-rating range for the Ya Rona example

From equation A3, GSI is calculated at 45-50. However, from figure A-6, the POOR, slickensided, highly weathered surfaces with compact fillings with BLOCKY/DISTURBED, folded and faulted formed from intersecting discontinuity sets yields a value range 35-40.

Final GSI rating of WAF at Ya Rona: 35-45

A.5 Mining Rockmass Classification (MRMR)

MRMR is a modification of RMR developed by Laubscher and Taylor, 1974. It uses the same parameters as RMR but combines groundwater and joint condition. Refinement of the system (Laubscher, 1990) to include more aspects of mining accounted for much of the work done after 1974. Laubscher also introduced the DRMS (Design Rock Mass Strength) concept during this time, where the intact rock strength (IRS) was downgraded to take into account scale effects (sample size relative to population).

The MRMR is obtained by summing up the following 4 parameters:

1. Rock material strength (UCS),
2. RQD,
3. Joint Spacing, and,
4. Joint Condition and Groundwater.

MRMR value can range between 0 and 100. MRMR is usually about 5 points lower than RMR.

The MRMR rating is adjusted in the following manner:

- No of joint sets and spacing (figure A-7),
- Table A-16 showing the joint condition and groundwater,
- Weathering (figure A-8),
- Joint orientation (figure A-9), and,
- Blasting effects (table A-17).

	Parameter	Range of values										
1	*RQD*	100 - 97		96 - 84	83 - 71	70 - 56	55 - 44	43 - 31	30-17	16 - 4	3 - 0	
	Rating (*RQD*x15/100)	**15**		**14**	**12**	**10**	**8**	**6**	**4**	**2**	**0**	
2	*UCS* (MPa)	185	184 - 175	174 - 165	164-145	144-125	124-105	104-85	84-65	44-25	24-5	4-0
	Rating	**20**	**18**	**16**	**14**	**12**	**10**	**8**	**6**	**4**	**2**	**0**
3	Joint spacing	Refer to Figure A 7										
	Rating	Maximum rating = 25										
4	Joint condition + groundwater	Refer to Table A 16										
	Rating	Maximum rating = 40										

Table A-15 Mining Rock Mass Rating (Laubscher, 1990)

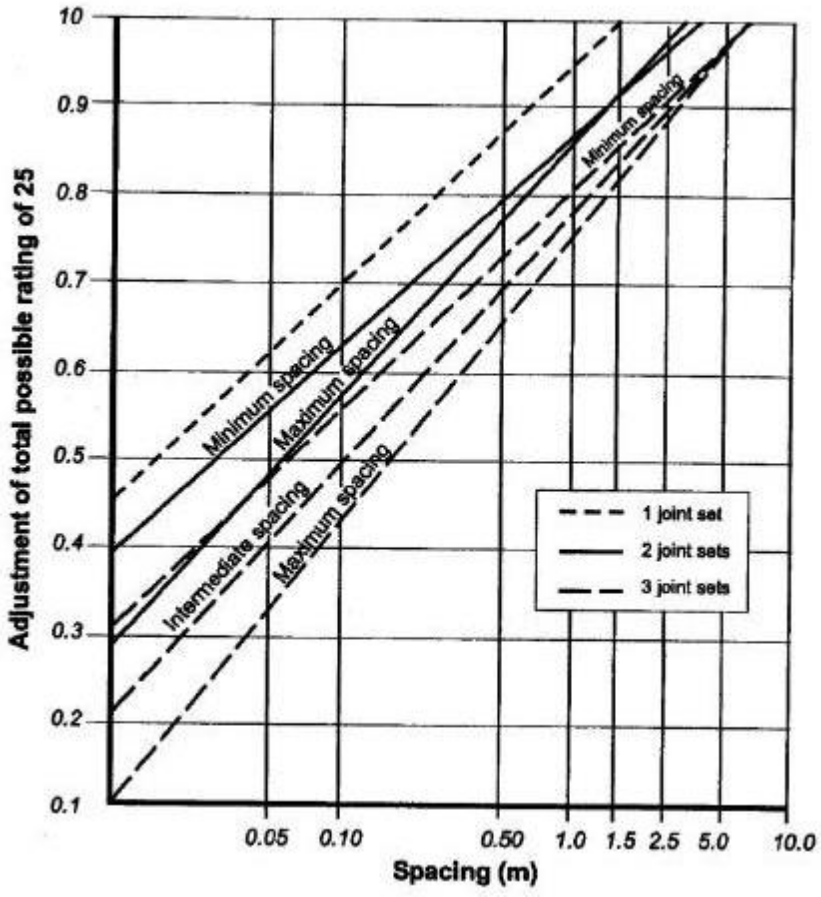


Figure A-7 Adjustment of MRMR as a factor of number of joints and spacing (Laubscher, 1990)

Parameter	Description		Dry conditions	Wet conditions		
				Moist	Moderate pressure (25-125 l/min)	Severe pressure (>125 l/min)
A Joint expression (large scale irregularities)	Wavy	Multi-directional	100	100	100	95
		Uni-directional	90 - 95	90 - 95	85 - 90	75 - 80
	Curved		80 - 89	75 - 85	70 - 80	60 – 70
	Straight		70 - 79	65 - 74	60	40
B Joint expression (small scale irregularities or roughness)	Very rough		100	100	95	90
	Striated or rough		85 - 99	85 - 99	80	70
	Smooth		60 - 84	55 - 80	60	50
	Polished		50 - 59	40 - 50	30	20
C Joint wall alteration zone	Stronger than wall rock		100	100	100	100
	No alteration		100	100	100	100
	Weaker than wall rock		75	70	65	60
D Joint filling	No fill – surface staining only		100	100	100	100
	Non softening and sheared material (clay or talc free)	Coarse sheared	95	90	70	50
		Medium sheared	90	85	65	45
		Fine sheared	85	80	60	40
	Soft sheared material (e.g. talc)	Coarse sheared	70	65	40	20
		Medium sheared	65	60	35	15
		Fine sheared	60	55	30	10
	Gouge thickness <amplitude of irregularity		40	30	10	
	Gouge thickness >amplitude of irregularity		20	10	5 (Flowing material)	

Table A-16 Adjustment of MRMR for joint condition and groundwater (Laubscher, 1990)

Rate of weathering and adjustments (%)					
Description of weathering extent	**6 months**	**1 year**	**2 years**	**3 years**	**4+ years**
Fresh	100	100	100	100	100
Slightly	88	90	92	94	96
Moderately	82	84	86	88	90
Highly	70	72	74	76	78
Completely	54	56	58	60	62
Residual soil	30	32	34	36	38

Figure A-8 Adjustment of MRMR for weathering (Laubscher, 1990)

Number of joint defining the block	**Adjustments (%)** **Number of faces inclined away from the vertical**				
	70	75	80	85	90
3	3	-	2	-	-
4	4	3	-	2	-
5	5	4	3	2	1
6	6	5	4	3	2 or 1

Figure A-9 Adjustment of MRMR for joint orientation (Laubscher, 1990)

Excavation or blasting technique	Adjustment (%)
Boring	100
Smooth wall blasting	97
Good conventional blasting	94
Poor blasting	80

Table A-17 Adjustment of MRMR for blasting effects (Laubscher, 1990)

A.5.1. Calculation of MRMR-rating range for the Ya Rona example

Table A-18 shows the calculation of MRMR for WAF at Ya Rona shaft.

Parameter	*Rating*	*Comment*
Strength of intact material:	6-10	UCS of 58-92MPa
Drill core quality (RQD):	4.65	31%
Spacing of joints:	20.5	0.82 x 25
Condition of joints and groundwater:	60-70	Dry conditions, Soft sheared material - talcose
Weathering adjustment	96%	Slightly weathered after 4 years from time of exposure (based on Petho, et al, 2004)
Joint inclination adjustment	70%	3 joint sets incline away from vertical
Stress adjustment	60%	Poor confinement
Blasting adjustment	80%	Poor blasting

Table A-18 Calculation of MRMR for Ya Rona shaft

Final MRMR rating of WAF at Ya Rona: 32 - 34

A.6 Rockwall Condition Factor (RCF)

In deep mining environments, excavations are subjected to high and changing stress regimes. Damage from strainbursts and rockbursts are often noted. The design method should recommend applicable support systems.

$$RCF = \frac{3\sigma_1 - \sigma_3}{F\sigma_c} \qquad \text{(Eqn. A4)}$$

Where σ_1 and σ_3 are the major and minor principal stresses within the plane of the excavation, and,
F is a factor to represent the downgrading of σ_C (UCS) for the rockmass coupled to the excavation size.

(Jager & Ryder, 1999) In good quality rock, F = 1; in poor discontinuous rock, F = 0.5
Field tests were conducted in 3m x 3m quartzite tunnels, so if the excavation is larger (>6m x 6m), then F may be downgraded by 10-20%.

For RCF <0.7, good ground conditions existed,
For 0.7< RCF<1.4, average conditions prevailed, with moderate support installed, and,
For RCF>1.4, poor ground conditions were observed.

A.6.1. Calculation of RCF for the Ya Rona example (Shaft barrel)

For the calculation of RCF, Figure A-10 represents the stress regime. F = 0.7 is used based on experiential evidence in that WAF exposed to air and water at the shaft barrel. Moreover, the WAF unrestrained has suffered from a high horizontal stress gradient. Therefore, for the purposes of this report, the WAF will be treated as if is in the secondary creep phase.

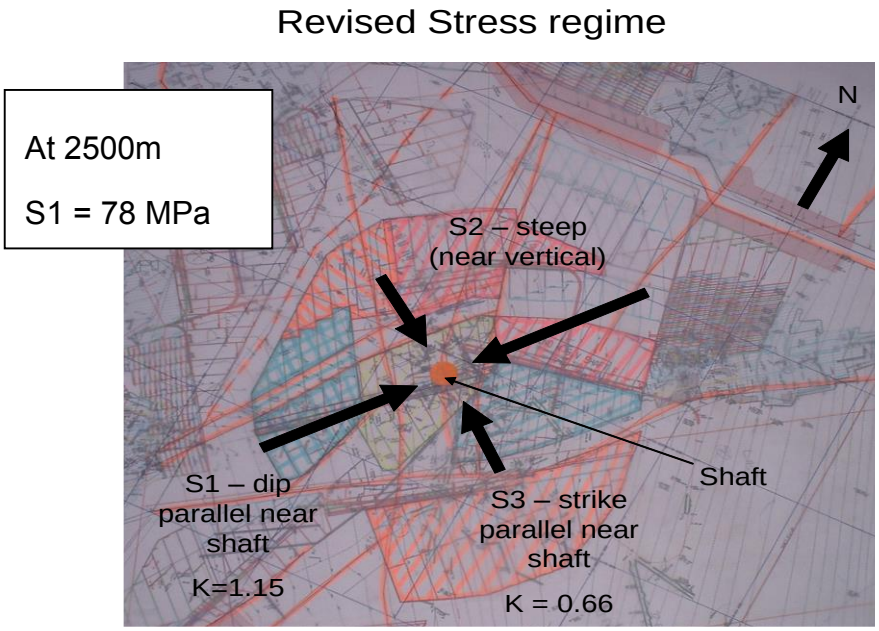


Figure A-10 Modelled stress regime (Leach, 2006)

Therefore, although not totally discontinuous, the WAF has suffered deformation. Using the UCS of 57MPa, the:

Final RCF rating of WAF at Ya Rona = 4.66

A.6 Stability Graph Method (N)

The stability graph method or the revised N' (Watson, 2004) is not considered for this report, as it was developed especially for shallower Bushveld mines and incorporated the size and shape of excavations.

It may be necessary to revisit this when mitigation strategies are discussed.

Appendix B

WAF Rock Test and Rock Fracture Data

Properties	Units	GAP 102 2003	WAGM 2005	Drief'tein 2006	S. Deep 2006	Main # 2007	Realistic averages
Uniaxial CS	MPa	100 to 140	20 to 80	50 to 100	20 to 80	49 to 107	30 to 50
Triaxial CS (σ2 in MPa)	MPa	-	92 (20)	139 (16)	-	121 (20)	120 (20)
Young's modulus	GPa	68	68-	53 to 74	68	50	50 to 65
Bulk modulus	GPa	40	40	40	40		40
Shear modulus	GPa	28	-	28	28		28
Poisson's ratio		0,18 to 0,27	0,2	0,14 to 0,33	0,2	0,17 to 0,33	0,25
Cohesion	MPa	6	4,3	3,7	2,2		4,0
Angle of friction	°	34	28	27	17		24
Dilation	°	22	-	22	22		25
Tensile strength	MPa	0,7	-	12	0,1	7 to 21	13
Shear strength	MPa					8,4	8
Average RQD		62	*30*	52	50	40	45
In situ strength	MPa	23	12	12	6		11

Table B-1 Compilation of WAF strength data from different sources (Van den Heever, 2007)

9.5.2006				
Brazilian Tensile Strength (UTS)				
Specimen Ref No	Diameter (mm)	Length (mm)	Failure Load (kN)	UTS (MPa)
WAF1	41.0	21.2	14.2	**10.40**
WAF2	40.0	21.1	17.4	**13.12**
WAF3	40.0	20.5	18.6	**14.44**
WAF4	41.2	21.2	15.2	**11.08**
REEF5	41.6	21.1	15	**10.88**

Table B-2 WAF and conglomerate UTS results for Driefontein Gold Mine Ya Rona shaft (Yilmaz, 2006)

19.4.2006									
Uniaxial Compressive Strength (UCS), Elastic Modulus (E), Poisson's Ratio (ν)									
Specimen Ref No	**Diameter (mm)**	**Length (mm)**	**L/D**	**Mass (g)**	**Density (kg/m^3)**	**Failure Load (kN)**	**E (GPa)**	**ν**	**UCS (MPa)**
1-WAF(3)	41.7	84.3	2.0	310	2693	165.0	74.02	0.14	**120.82**
2-LAVA(6)	60.0	135.8	2.3	1056	2750	460.0	146.98	0.31	**162.69**
3-Concr(4)	143.8	332.0	2.3	11528	2138	420.0	39.32	0.39	**25.86**
VCR 1	41.6	103.2	2.5	388.0	2766	176.0	70.58	0.28	**129.49**
VCR 2*	41.6	103.0	2.5	404.0	2886	220.0	53.17	0.16	**161.86**
5-WAF	40.2	101.0	2.5	360	2808	72.0	55.62	0.25	**56.73**
6-WAF*	41.2	101.8	2.5	384	2829	138.0	56.28	0.33	**103.51**
7-WAF*	40.0	101.0	2.5	356	2805	73.0	UCS only		**58.09**
8-WAF	41.2	101.2	2.5	380	2817	136.0	UCS only		**102.01**
	Length 1 (mm)	Length 2 (mm)	Length 3 (mm)	Mass (g)	Density (kg/m^3)	Failure Load (kN)			**UCS (MPa)**
Resin 1	79.8	79.9	80.5	676	1317	368.0	UCS only		**57.72**
Resin 2	80.8	79.4	80.1	682	1327	379.0	UCS only		**59.08**
* specimen contained fracture									

Table B-3 WAF, concrete and Alberton Lava results for Driefontein Gold Mine Ya Rona shaft (Yilmaz, 2006)

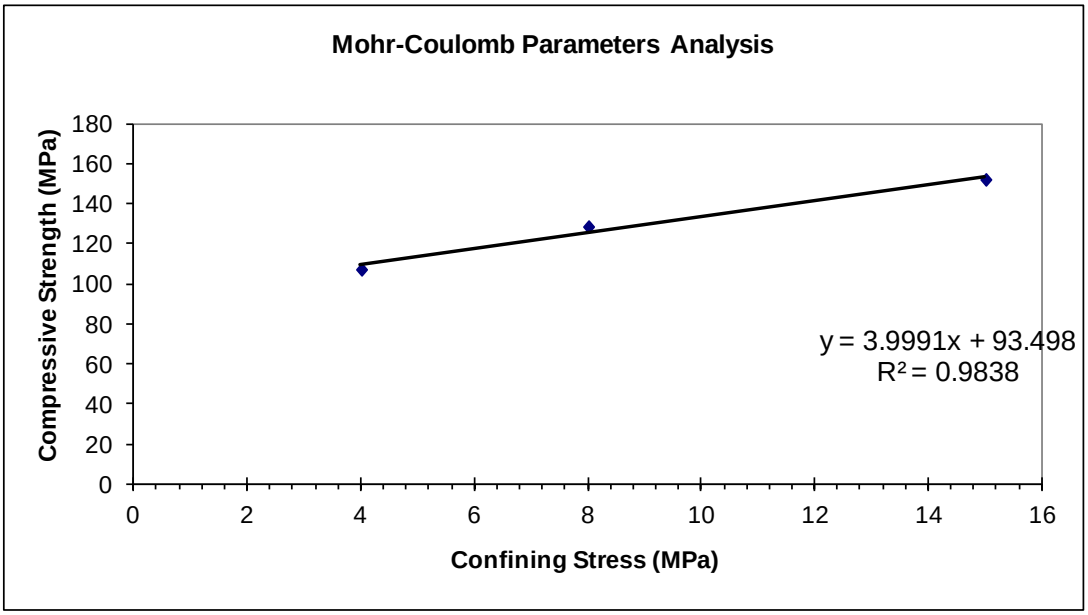


Figure B-4 Graph showing increasing WAF strength as a function of confinement for Driefontein Gold Mine Ya Rona shaft (Yilmaz, 2006)

Core Test Results

19.04.2006

								Mohr-Coulomb Parameters				
Specimen Ref No	**Wits Ref No**	**Diameter (mm)**	**Length (mm)**	**Mass (g)**	**Failure Load (kN)**	**Confinement (MPa)**	**Strength (MPa)**	**UCS (MPa)**	**β**	**C_o**	**ϕ**	**R^2**
(1) WAF	1A	41.7	80.3	301.0	93.0	4	**68.10**	**51.99**	**4.67**	**12.0**	**40.3**	**0.98**
	1A	41.7	80.3	301.0	129.0	8	**94.46**					
	1A	41.7	80.3	301.0	144.0	12	**105.44**					
	1A	41.7	80.3	301.0	173.0	16	**126.67**					
(5)LAVA	2A	59.6	122.5	962.0	640.0	4	**229.40**	**213.27**	**4.99**	**47.7**	**41.8**	**0.98**
	2A	59.6	122.5	962.0	721.0	8	**258.44**					
	2A	59.6	122.5	962.0	765.0	12	**274.21**					
	2A	59.6	122.5	962.0	811.0	16	**290.70**					
VCR	3A	41.6	87.2	332.0	180.0	4	**132.43**	**98.06**	**11.28**	**14.6**	**56.8**	**0.95**
	3A	41.6	87.2	332.0	279.0	8	**205.27**					
	3A	41.6	87.2	332.0	355.0	15	**261.19**					
(1B)WAF	4A	41.6	85.0	322.0	146.0	4	**107.42**	**93.50**	**4.00**	**23.4**	**36.9**	**0.98**
	4A	41.6	85.0	322.0	175.0	8	**128.75**					
	4A	41.6	85.0	322.0	207.0	15	**152.30**					

	Mohr-Coulomb Parameters
	UCS (MPa)
β	Strengthening Parameter
C_o	Cohesion (MPa)
ϕ	Internal Friction Angle (^{o})

Table B-5 WAF, Alberton Lava and conglomerate test results for Driefontein Gold Mine Ya Rona shaft (Yilmaz, 2006)

Table for calculation of σ_{ci} and m_i from triaxial test data

σ_1 (MPa) (Input)	σ_3 (MPa) (Input)	x	$(\sigma_1-\sigma_3)^2$ y	xy	x²	y²
68.1	4		4108.3	16433.1	16.0	16877999.5
94.5	8		7474.6	59796.6	64.0	55869212.7
105.4	12		8730.8	104769.7	144.0	76227068.4
126.7	16		12248.5	195976.3	256.0	150026157.1
n	$\sum x$		$\sum y$	$\sum xy$	$\sum x^2$	$\sum y^2$
4.0	**40.0**		**32562.2**	**376975.7**	**480.0**	**299000437.8**

$$\sigma_{ci} = \sqrt{\frac{\sum y}{n} - \frac{\sum x}{n}\left[\frac{\sum xy - \frac{(\sum x \sum y)}{n}}{\sum x^2 - \frac{(\sum x)^2}{n}}\right]}$$

$$m_i = \frac{1}{\sigma_{ci}}\left[\frac{\sum xy - \frac{(\sum x \sum y)}{n}}{\sum x^2 - \frac{(\sum x)^2}{n}}\right]$$

σ_{ci}	**41.49**	
m_i	**15.47**	
s	**1.00**	(Intact Rock)

Table B-6 WAF test results for Driefontein Gold Mine Ya Rona shaft (Yilmaz, 2006) showing the m_i and s values

Borehole	Depth	Type	Description	Orientatio	Thickness
1	0.10	Fracture	Open	Flat	0.10
	0.35	Fracture	Closed	Flat	0.25
	0.80	Fracture	Open	Flat	0.45
	1.20	Fracture	Open	Flat	0.40
	1.33	Fault	1 cm gouge	Flat	0.13
	1.65	Fault	1 cm gouge	Flat	0.32
	2.50	Blocked	Broken rock		0.85
Location	2.14m to gully center				
	4.0m to gully peg H10350				
	8.39m to Abutment				
	3.86m to face on 06-08-04				
Hole Diameter	45mm	Hole Inclination		60deg	
Base Reading	223mm				

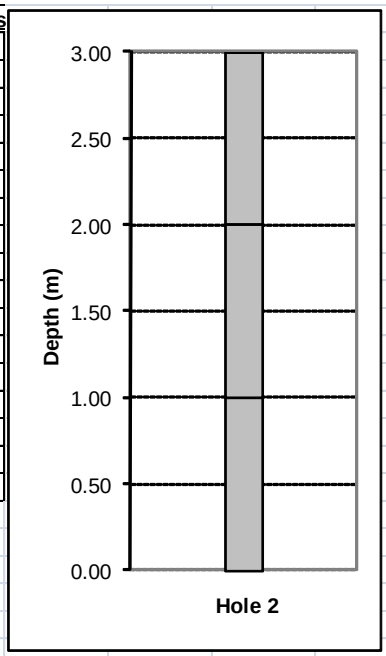


Figure B-7 Excel worksheet showing fracturing in WAF in Hole 1 in stope at Ya Rona

Borehole 2	Depth	Type	Description	Orientatio	Thickness
	0.01	Fracture	Open	Flat	0.01
	0.80	Fracture	Open	Flat	0.79
	0.81	Fault	Yellow gouge	Flat	0.01
	0.90	Fracture	Closed	Flat	0.09
	1.10	Fracture	Closed	Oblique	0.20
	1.55	Fracture	Closed	Oblique	0.45
	2.00	Fracture	Open	Flat	0.45
	2.10	Fracture	Closed	Flat	0.10
	2.15	Fracture	Closed	Oblique	0.05
	2.53	Fault	Shear	Flat	0.38
	2.60	Fracture	Open	Flat	0.07
	2.95	Fracture	Open	Flat	0.35
	3.48	Fracture	Open	Flat	0.53
	3.79	Fracture	Closed	Flat	0.31
	4.00	Fracture	Open	Steep	0.21
	4.10	EOH			0.10
Location	6.93m to gully center				
	4m to gully peg H10350				
	5.80m to Abutment				
	3.90m to face on 06-08-04				
Hole Diameter	45mm	Hole Inclination		58deg	
Base Reading	805mm				

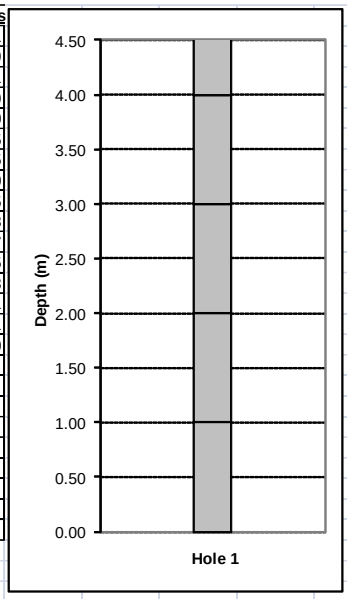


Figure B-8 Excel worksheet showing fracturing in WAF in Hole 2 in stope at Ya Rona

Borehole3	Depth	Type	Description	Orientatio	Thickness
	0.41	Fracture	Closed	Flat	0.41
	0.52	Fracture	Closed	Flat	0.11
	0.60	Fracture	Open	Oblique	0.08
	0.68	Fracture	Closed	Flat	0.08
	0.77	Fault	Shear	Oblique	0.09
	0.88	Fracture	Closed	Flat	0.11
	0.91	Fracture	Closed	Flat	0.03
	0.97	Fracture	Closed	Oblique	0.06
	0.93	Fracture	Open	Flat	-0.04
	1.12	Fracture	Closed	Flat	0.19
	1.18	Fault	Shear	Flat	0.06
	1.25	Fracture	Closed	Flat	0.07
	1.33	Fracture	Open	Flat	0.08
	1.35	Fracture	Open	Steep	0.02
	1.37	Fracture	Open	Steep	0.02
	1.40	Fracture	Open	Steep	0.03
	1.56	Fault	Gouge	Oblique	0.16
	1.60	Fracture	Open	Flat	0.04
	1.90	Fracture	Open	Flat	0.30
	1.92	Fault	Yellow gouge	Flat	0.02
	2.10	Fracture	Closed	Flat	0.18
	2.20	Fracture	Open	Flat	0.10
	2.25	Fracture	Closed	Flat	0.05
	2.30	Fracture	Closed	Flat	0.05
	2.81	Fracture	Closed	Flat	0.51
	3.10	Fault	Open	Flat	0.29
	3.20	Fracture	Open	Flat	0.10
	3.25	Fracture	Open	Flat	0.05
	3.31	Fracture	Open	Flat	0.06
	3.40	Fracture	Open	Flat	0.09
	3.90	Fracture	Open	Oblique	0.50
	4.60	EOH			0.70
Location	8.07m to gully center				
	1m to gully peg H10350				
	2.87m to Abutment				
	6.39m to face on 06-08-04				
Hole Diameter	45mm	Hole Inclination		62deg	
Base Reading	758mm				

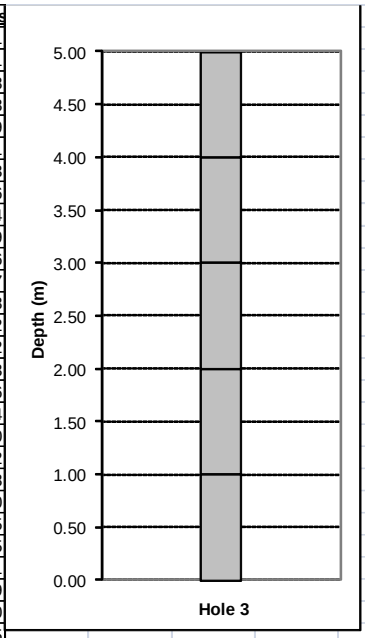


Figure B-9 Excel worksheet showing fracturing in WAF in Hole 3 in stope at Ya Rona

Appendix C

Support Units' Data

C.1. Yielding Anchor Test Data

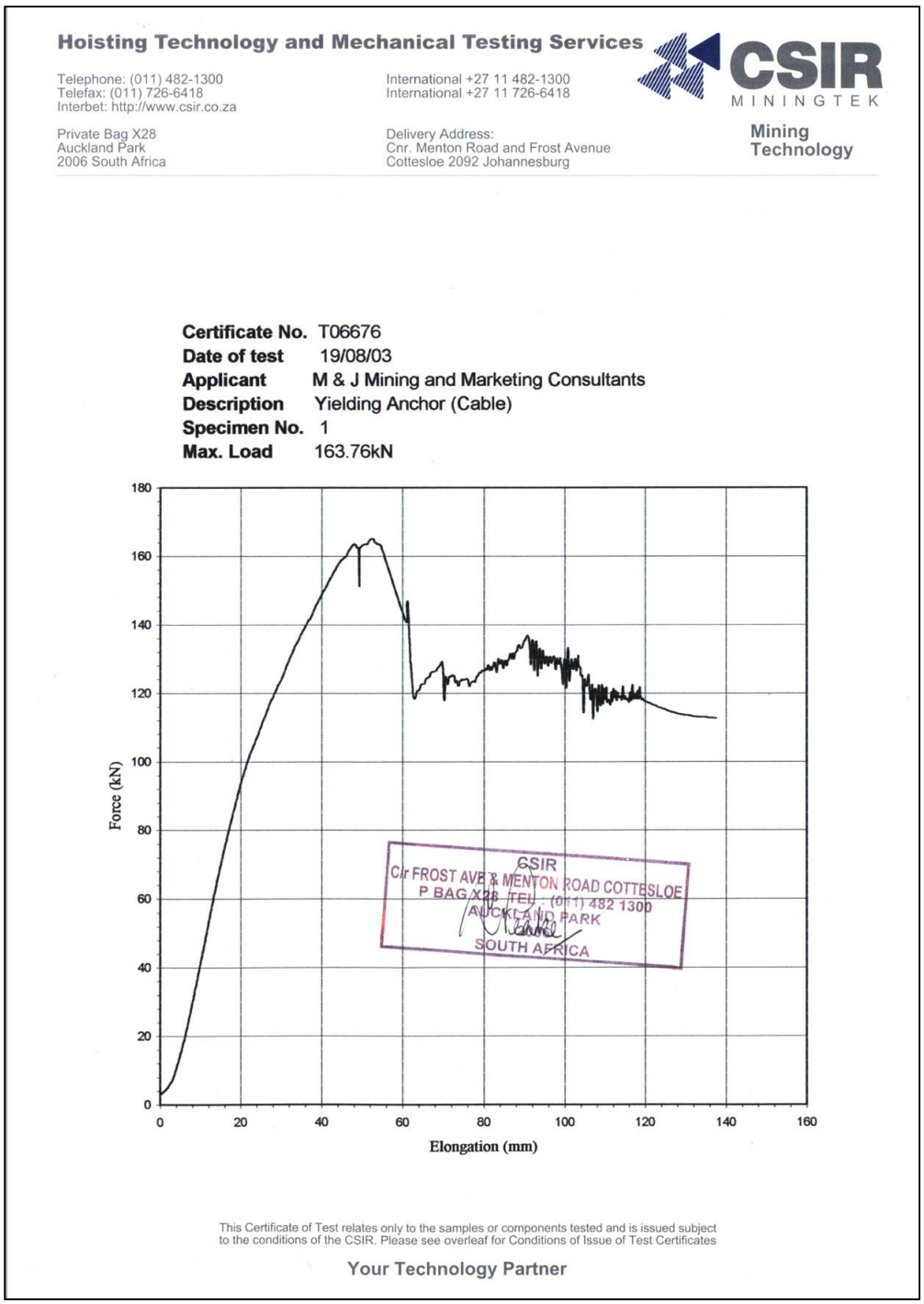


Figure C-1. M&J Mining Yielding Anchor (1) Load-Deformation curve

Hoisting Technology and Mechanical Testing Services

Telephone: (011) 482-1300
Telefax: (011) 726-6418
Interbet: http://www.csir.co.za

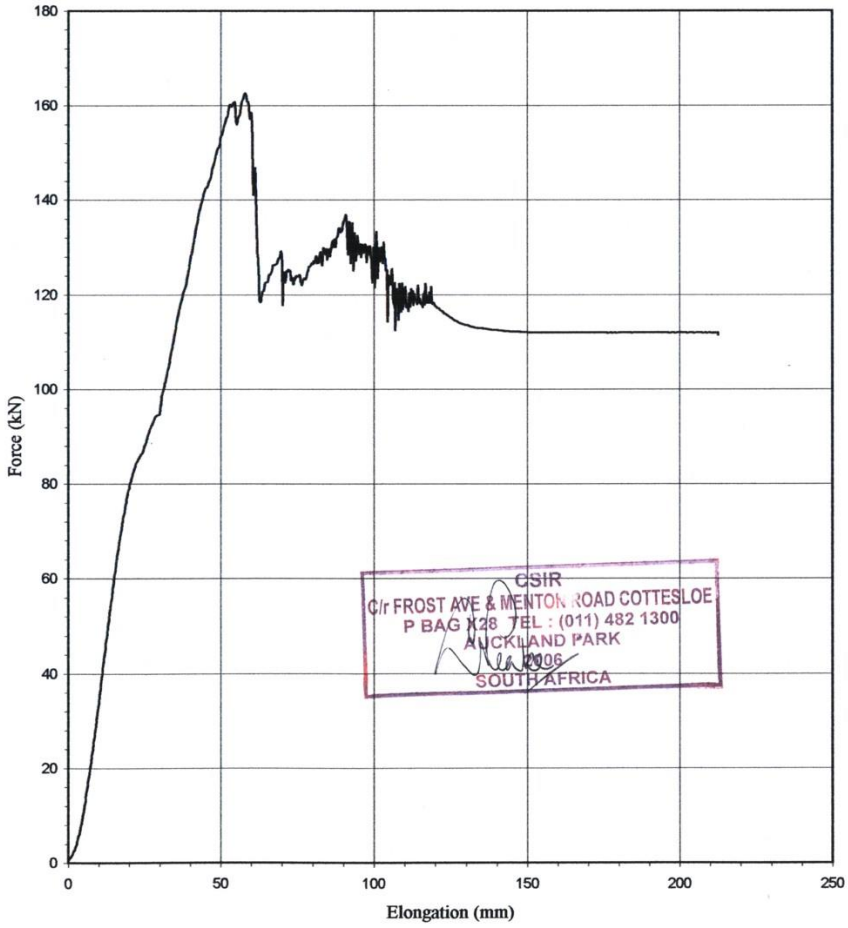
International +27 11 482-1300
International +27 11 726-6418

Private Bag X28
Auckland Park
2006 South Africa

Delivery Address:
Cnr. Menton Road and Frost Avenue
Cottesloe 2092 Johannesburg

CSIR MININGTEK
Mining Technology

Certificate No. T06676
Date of test 19/08/03
Applicant M & J Mining and Marketing Consultants
Description Yielding Anchor (Cable)
Specimen No. 2
Max. Load 160.76kN



CSIR
C/r FROST AVE & MENTON ROAD COTTESLOE
P BAG X28 TEL : (011) 482 1300
AUCKLAND PARK
2006
SOUTH AFRICA

This Certificate of Test relates only to the samples or components tested and is issued subject to the conditions of the CSIR. Please see overleaf for Conditions of Issue of Test Certificates

Your Technology Partner

Figure C-2. M&J Mining Yielding Anchor (2) Load-Deformation curve

Hoisting Technology and Mechanical Testing Services

Telephone: (011) 482-1300
Telefax: (011) 726-6418
Interbet: http://www.csir.co.za

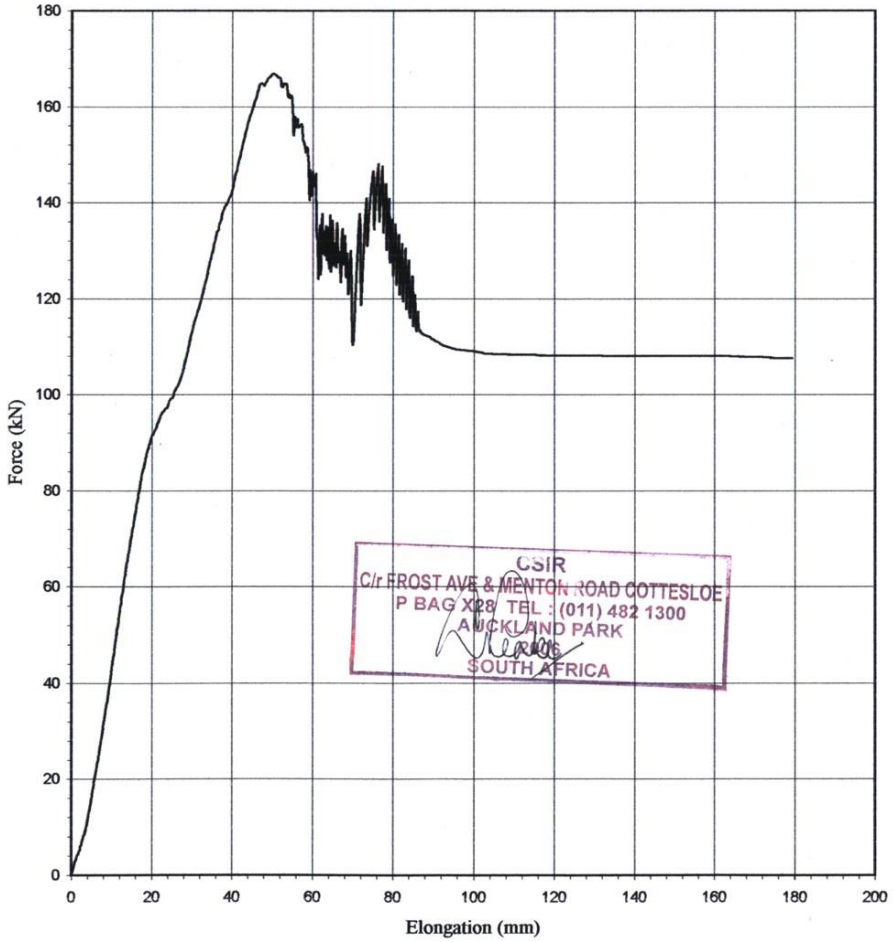
International +27 11 482-1300
International +27 11 726-6418

Private Bag X28
Auckland Park
2006 South Africa

Delivery Address:
Cnr. Menton Road and Frost Avenue
Cottesloe 2092 Johannesburg

CSIR MININGTEK
Mining Technology

Certificate No. T06676
Date of test 19/08/03
Applicant M & J Mining and Marketing Consultants
Description Yielding Anchor (Cable)
Specimen No. 3
Max. Load 166.84kN



This Certificate of Test relates only to the samples or components tested and is issued subject to the conditions of the CSIR. Please see overleaf for Conditions of Issue of Test Certificates

Your Technology Partner

Figure C-3. M&J Mining Yielding Anchor (3) Load-Deformation curve

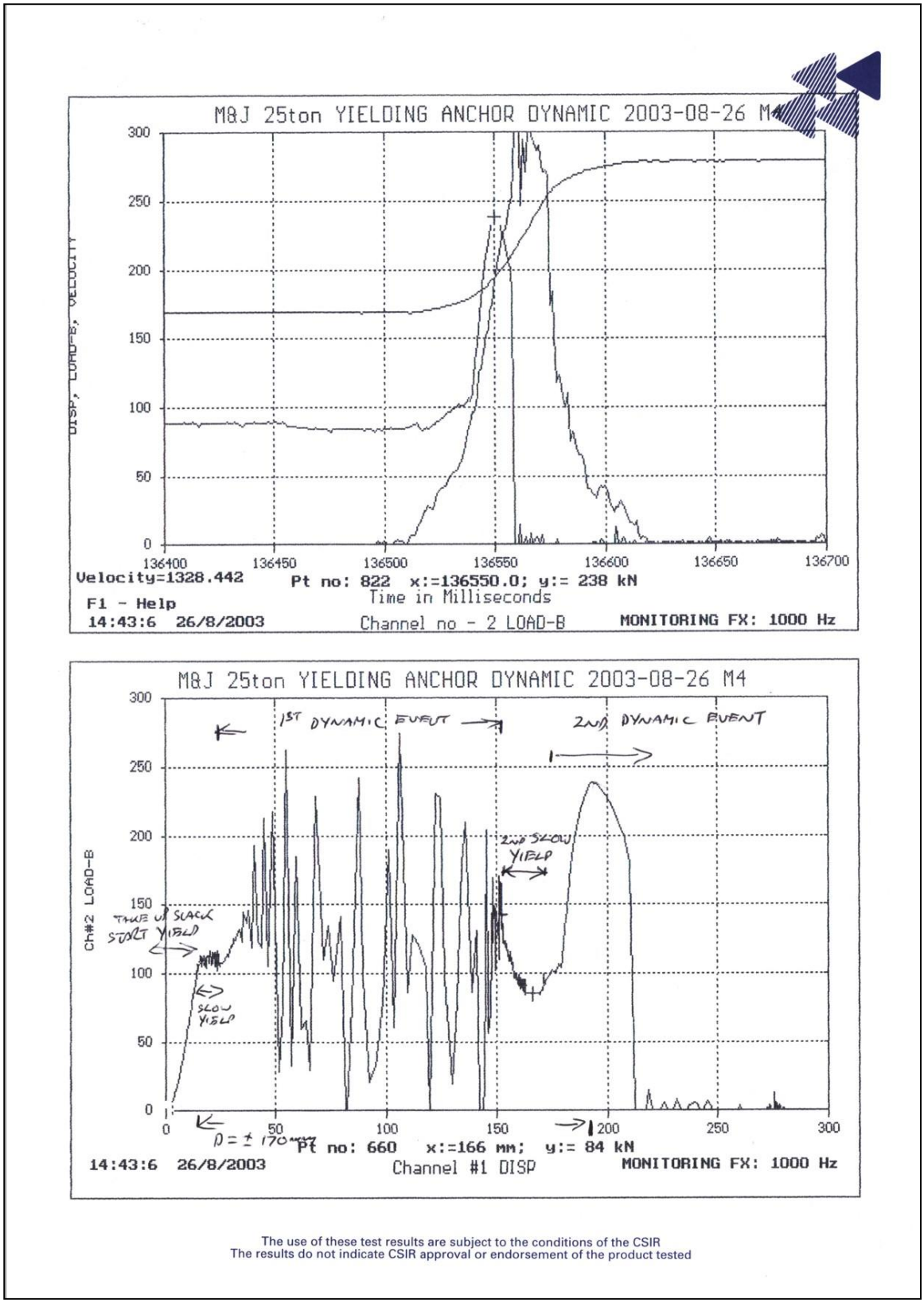
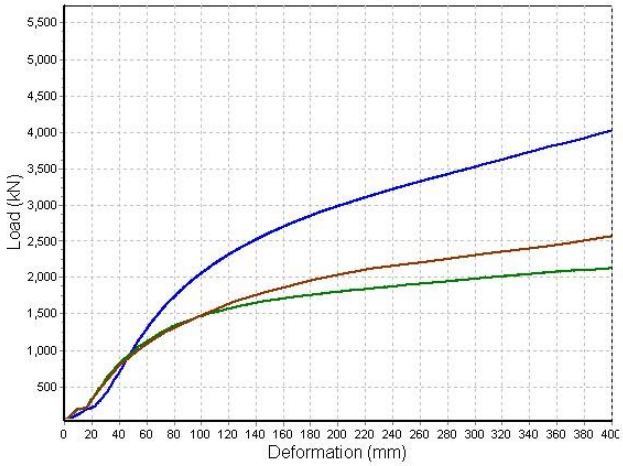


Figure C-4. M&J Mining Yielding Anchor Dynamic Load-Deformation and Load – Time curves

C.2. Timber Chock Test Data

SPUD 3 Test Summary Report. (Current)

Product Name	**1**	SPACED CHOCKS	**2**	CHOCK MAT	**3**	CHOCK MAT
Other Specifications						
Slab Material; Specs		<None Selected>;		SALIGNA; CONVENTIONAL SLABS (RIS		SALIGNA; CONVENTIONAL SLABS (RISE
Block Material; Specs		<None Selected>;		NONE;		NONE;
SMT Test Ref. Number		18.T.2.1		13.A.2.1		13.A.2.2
Product Comments						



	1	2	3
Test Height (cm)	217	223	225
Pack Length (cm)	110	110	110
Pack Width (cm)	110	110	110
Loading Rate (mm/min)	16	30	30
Unit Length/Height (cm)		110	110
Unit Width/Thin Dia. (cm)		14.5	14.5
Unit Rise/Thick Dia. (cm)	13	13	13
Unit Weight (kg)	18	13	13
Block Length (cm)	110		
Block Width (cm)	15.6		
Block Rise (cm)	13		
Test Date	2002/09/17	1998/11/16	1998/11/16

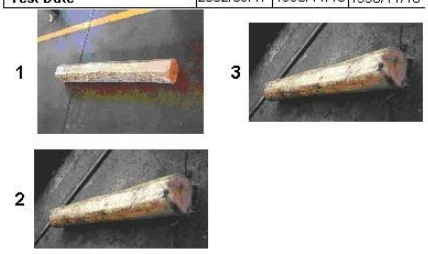


Figure C-5. SMT 110mm timber chock Load-Deformation curve

C.3. Pre-stressed Elongate Test Data

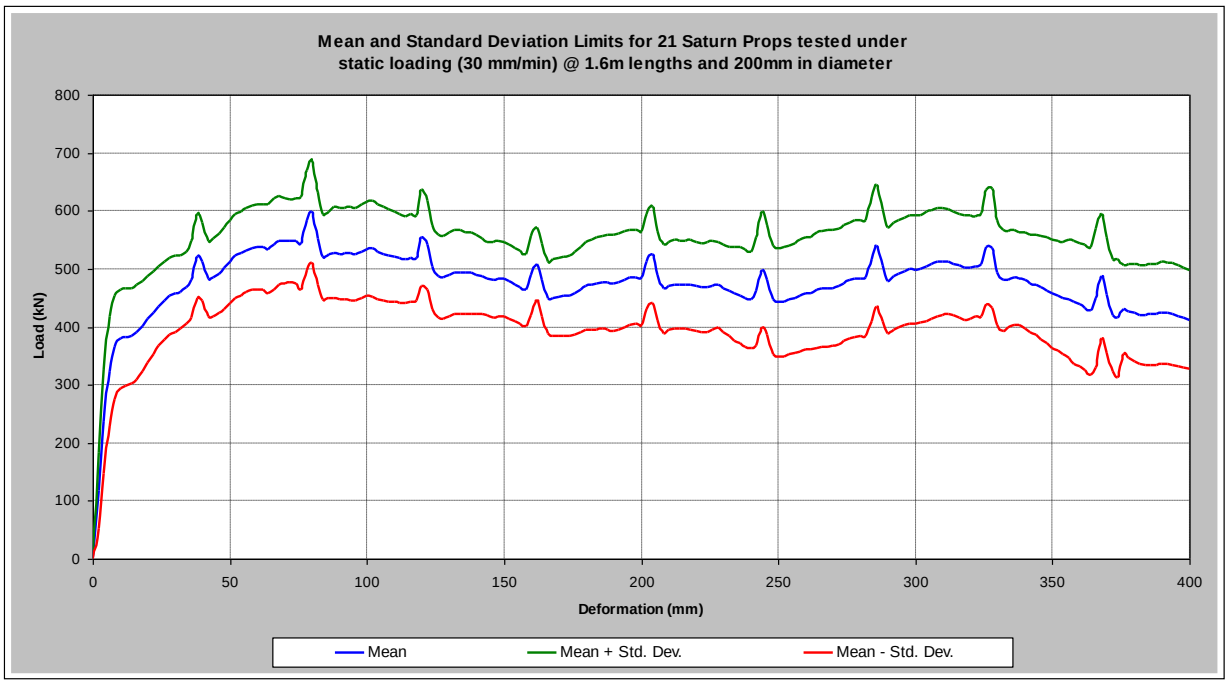


Figure C-6. SMT Saturn Prop Load-Deformation curve (pseudo-static)

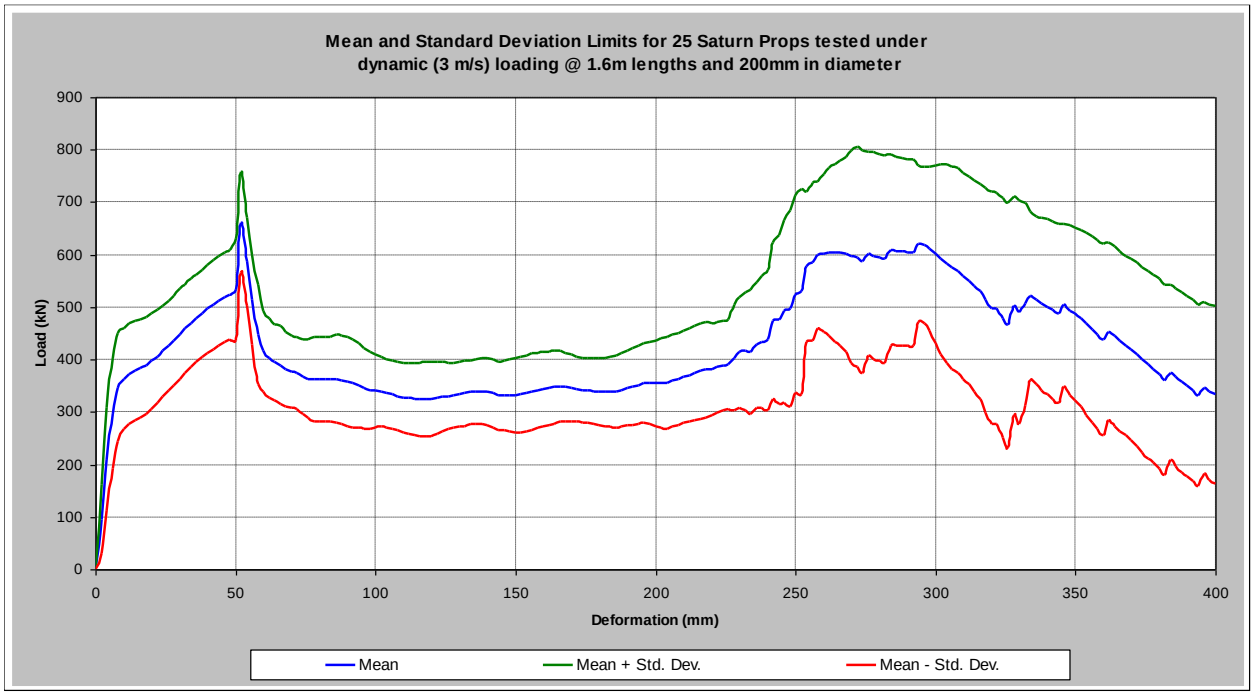


Figure C-7. SMT Saturn Prop Load-Deformation curve (dynamic)

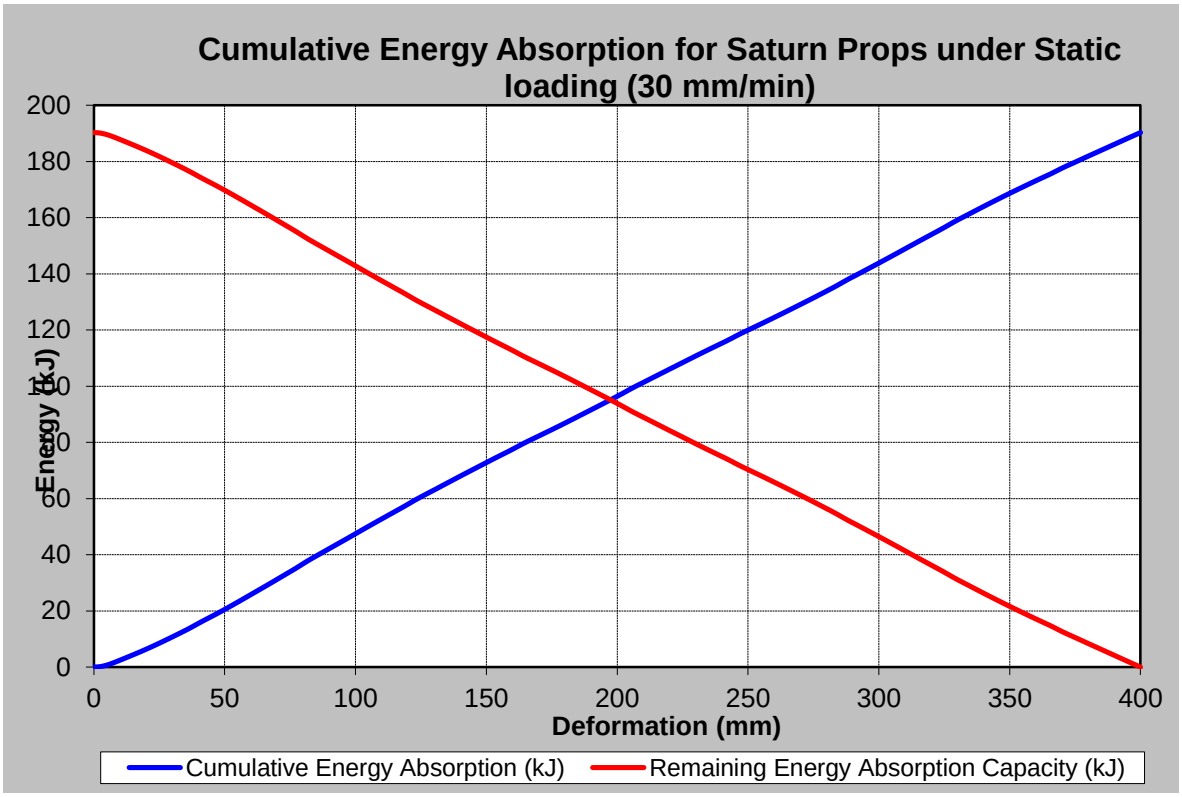


Figure C-8. SMT Saturn Prop Energy Absorption under pseudo-static loading conditions

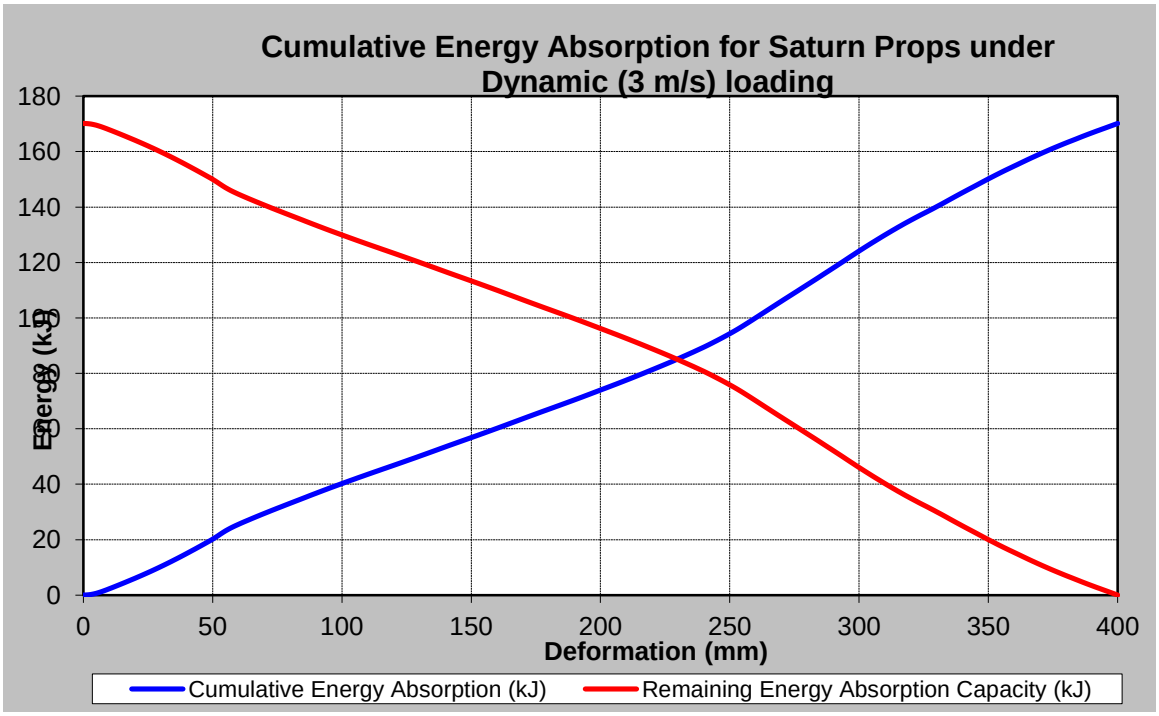


Figure C-9. SMT Saturn Prop Energy Absorption under dynamic conditions